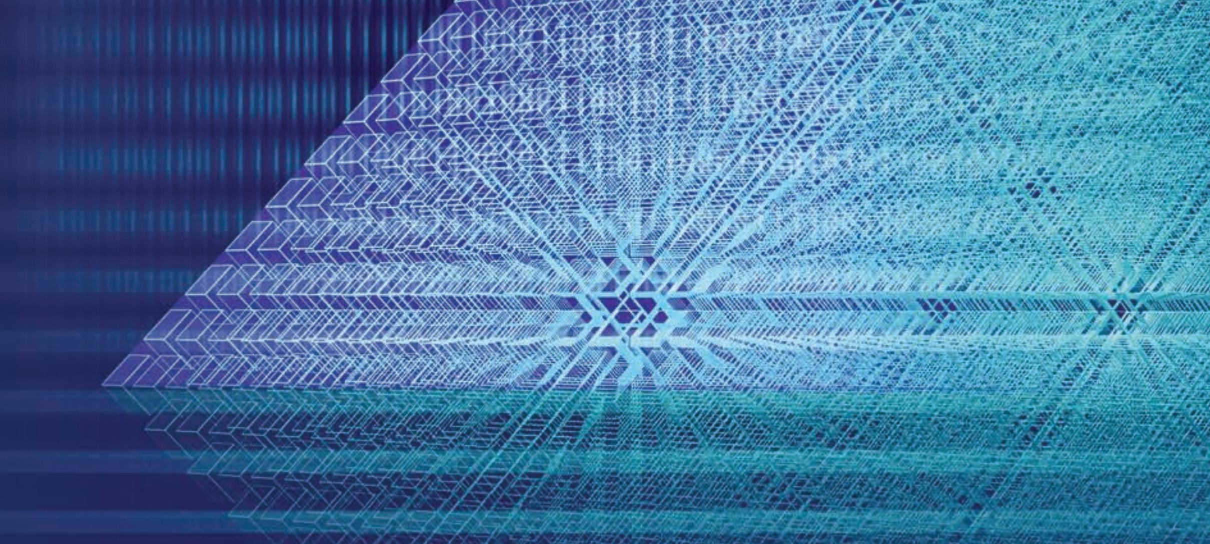

TECHNICAL REPORTS SERIES NO. 465

Cyclotron Produced Radionuclides: Principles and Practice

IAEA
International Atomic Energy Agency

CYCLOTRON PRODUCED RADIONUCLIDES: PRINCIPLES AND PRACTICE

The following States are Members of the International Atomic Energy Agency:

AFGHANISTAN
ALBANIA
ALGERIA
ANGOLA
ARGENTINA
ARMENIA
AUSTRALIA
AUSTRIA
AZERBAIJAN
BANGLADESH
BELARUS
BELGIUM
BELIZE
BENIN
BOLIVIA
BOSNIA AND HERZEGOVINA
BOTSWANA
BRAZIL
BULGARIA
BURKINA FASO
CAMEROON
CANADA
CENTRAL AFRICAN REPUBLIC
CHAD
CHILE
CHINA
COLOMBIA
COSTA RICA
CÔTE D'IVOIRE
CROATIA
CUBA
CYPRUS
CZECH REPUBLIC
DEMOCRATIC REPUBLIC OF THE CONGO
DENMARK
DOMINICAN REPUBLIC
ECUADOR
EGYPT
EL SALVADOR
ERITREA
ESTONIA
ETHIOPIA
FINLAND
FRANCE
GABON
GEORGIA
GERMANY
GHANA
GREECE
GUATEMALA
HAITI
HOLY SEE
HONDURAS
HUNGARY
ICELAND
INDIA
INDONESIA
IRAN, ISLAMIC REPUBLIC OF
IRAQ
IRELAND
ISRAEL
ITALY
JAMAICA
JAPAN
JORDAN
KAZAKHSTAN
KENYA
KOREA, REPUBLIC OF
KUWAIT
KYRGYZSTAN
LATVIA
LEBANON
LIBERIA
LIBYAN ARAB JAMAHIRIYA
LIECHTENSTEIN
LITHUANIA
LUXEMBOURG
MADAGASCAR
MALAWI
MALAYSIA
MALI
MALTA
MARSHALL ISLANDS
MAURITANIA
MAURITIUS
MEXICO
MONACO
MONGOLIA
MONTENEGRO
MOROCCO
MOZAMBIQUE
MYANMAR
NAMIBIA
NEPAL
NETHERLANDS
NEW ZEALAND
NICARAGUA
NIGER
NIGERIA
NORWAY
PAKISTAN
PALAU
PANAMA
PARAGUAY
PERU
PHILIPPINES
POLAND
PORTUGAL
QATAR
REPUBLIC OF MOLDOVA
ROMANIA
RUSSIAN FEDERATION
SAUDI ARABIA
SENEGAL
SERBIA
SEYCHELLES
SIERRA LEONE
SINGAPORE
SLOVAKIA
SLOVENIA
SOUTH AFRICA
SPAIN
SRI LANKA
SUDAN
SWEDEN
SWITZERLAND
SYRIAN ARAB REPUBLIC
TAJIKISTAN
THAILAND
THE FORMER YUGOSLAV REPUBLIC OF MACEDONIA
TUNISIA
TURKEY
UGANDA
UKRAINE
UNITED ARAB EMIRATES
UNITED KINGDOM OF GREAT BRITAIN AND NORTHERN IRELAND
UNITED REPUBLIC OF TANZANIA
UNITED STATES OF AMERICA
URUGUAY
UZBEKISTAN
VENEZUELA
VIETNAM
YEMEN
ZAMBIA
ZIMBABWE

The Agency's Statute was approved on 23 October 1956 by the Conference on the Statute of the IAEA held at United Nations Headquarters, New York; it entered into force on 29 July 1957. The Headquarters of the Agency are situated in Vienna. Its principal objective is "to accelerate and enlarge the contribution of atomic energy to peace, health and prosperity throughout the world".

TECHNICAL REPORTS SERIES No. 465

CYCLOTRON PRODUCED RADIONUCLIDES: PRINCIPLES AND PRACTICE

INTERNATIONAL ATOMIC ENERGY AGENCY
VIENNA, 2008

COPYRIGHT NOTICE

Sales and Promotion, Publishing Section
International Atomic Energy Agency
Wagramer Strasse 5
P.O. Box 100
1400 Vienna, Austria
fax: +43 1 2600 29302
tel.: +43 1 2600 22417
email: sales.publications@iaea.org
http://www.iaea.org/books

Printed by the IAEA in Austria
December 2008
STI/DOC/010/465

IAEA Library Cataloguing in Publication Data

Cyclotron produced radionuclides : principles and practice. — Vienna : International Atomic Energy Agency, 2008.
p. ; 24 cm. — (Technical reports series, ISSN 0074–1914; no. 465)
STI/DOC/010/465
ISBN 978–92–0–100208–2
Includes bibliographical references.

1. Radioisotopes in medical diagnosis. 2. Radioisotopes — Therapeutic use. 3. Cyclotrons. 4. Targets (Nuclear physics) I. International Atomic Energy Agency. II. Series: Technical reports series (International Atomic Energy Agency) ; 465.

IAEAL 08–00529

FOREWORD

Application of radioisotopes has shown a significant growth in the last decade, and one of the major factors contributing towards this increased growth has been the availability of a large number of cyclotrons exclusively dedicated to the production of radioisotopes for medical applications. A recent IAEA survey (Directory of Cyclotrons Used for Radionuclide Production in Member States, IAEA-DCRP/2006) estimated that there are more than 350 cyclotrons available in Member States. Many of these cyclotrons are dedicated to the production of isotopes for positron emission tomography (PET), more specifically, ^{18}F for the production of fluorodeoxyglucose (^{18}FDG). Although production of isotopes other than ^{18}F using these cyclotrons is limited, their use could be augmented for the production of the large number of isotopes useful in medicine and industry.

The IAEA has been extending support in various forms to Member States to acquire as well as to enhance the technology for production of isotopes using cyclotrons. Publications covering different aspects of radioisotope production using cyclotrons are one such means of support identified by Member States needing IAEA input. A Consultants Meeting organized during 2004 identified the necessity for publications on different aspects of cyclotron produced isotopes.

During the preparation of the above publication, as well as during the deliberations of an international symposium on Trends in Radiopharmaceuticals (ISTR-2005) held in Vienna during November 2005, the need for a comprehensive book on cyclotrons with a special emphasis on production of isotopes was identified. The main reason was the lack of a single source of up to date information on this topic, despite the availability of a large number of related publications in the scientific literature. Work towards the preparation of such a publication was initiated during a Consultants Meeting held in Vienna during April 2006. The consultants suggested that the book should incorporate the basic science behind the accelerator technology, in addition to providing all relevant information regarding radioisotope production. Consequently, this publication contains chapters on, for example, accelerator technology, theoretical considerations about nuclear reactions, the technology behind targetry, techniques on preparation of targets, irradiation of targets under high beam currents, target processing and target recovery. Chapters highlighting the uses of cyclotron produced isotopes, as well as future trends in this field, are included. The intended readership of this publication is scientists interested in translating this technology into practice, technologists already working in Member States with cyclotrons who wish to enhance the utility of existing machines, and managers who are in the process of setting up facilities. In addition, students working towards higher degrees in related fields will also greatly benefit from reading this book.

The manuscript for this publication was prepared by the following consultants: D.J. Schlyer, Brookhaven National Laboratory, United States of America; P. Van den Winkel, Cyclotron Laboratory, Vrije Universiteit Brussel (VUB), Belgium; T.J. Ruth, TRIUMF, Canada; and M.M. Vora, King Faisal Specialist Hospital and Research Centre, Saudi Arabia. The IAEA thanks the consultants for their valuable contributions and is also grateful to those scientists who reviewed the manuscript for this book. The IAEA officers responsible for this publication were M.R.A. Pillai and M. Haji-Saeid of the Division of Physical and Chemical Sciences.

CONTENTS

CHAPTER 7: TARGET PROCESSING AND MATERIAL RECOVERY 155

Chapter 1

INTRODUCTION

1.1. SCOPE OF THE BOOK

The building of cyclotrons in the 1930s ushered in the beginning of the production of radioisotopes and their subsequent use in medicine, industry, agriculture and research. With the high energy charged particles and the high beam current available in cyclotrons, it is possible to produce abundant quantities of a wide variety of radioisotopes.

Immediately after World War II, almost all the radioisotopes in use were made in reactors. The production of radioisotopes in cyclotrons for medical applications revived in the 1950s, after the discovery that ^{201}Tl could be used as an ideal tracer for detecting myocardial perfusion. Thallous chloride labelled with ^{201}Tl remains the gold standard for measuring cardiac blood flow despite the availability of ^{99m}Tc myocardial perfusion agents. The preparation of fluorodeoxyglucose (^{18}FDG) in the mid-1970s and its use for studying glucose metabolism was a major breakthrough, leading to the development of the now widely used imaging modality called positron emission tomography (PET). The use of ^{18}FDG along with a PET camera yields excellent quality images of the brain (for studying functional abnormalities), heart (for studying viability function) and tumours (for detection of metastases). A large number of other ^{18}F and ^{11}C labelled radiopharmaceuticals were developed subsequently, and the quest for newer and more effective ones continues at present.

Apart from the PET and single photon emission computed tomography (SPECT) isotopes for diagnostic imaging studies, cyclotron produced isotopes are also finding extensive therapeutic applications. An example is the use of cyclotrons with large beam currents for the production of ^{103}Pd for brachytherapy applications. Another example of the cyclotron produced isotopes being used for treatment is the production of alpha particle emitting isotopes, notably ^{211}At and ^{213}Bi, for targeted therapy of cancer.

The applications of cyclotron produced isotopes have been expanding at a much faster pace in the last 15 years, as seen by the large number of new machines being installed for isotope production. Some cyclotrons are dedicated to the production of a single isotope such as ^{18}F or ^{103}Pd. The IAEA published a directory on cyclotrons used for isotope production [1.1] in 1998, with a revised version of it being published in 2006 [1.2] that documents the cyclotrons available in Member States.

The present publication is aimed at providing information on the various aspects of production of radioisotopes by the use of cyclotrons and provides some of the collective experience on the installation and operation of radioisotope production facilities. Issues such as principles of operation, descriptions of linear accelerators (linacs) and cyclotrons, choice of accelerator, types of facilities and potential uses, theory of radioisotope production, accelerator targetry, enriched isotopes and radiochemistry are discussed. Sections 1.2–1.8 outline the contents of each chapter. The heading for each section of this chapter is the same as that for the corresponding chapter number in the book. Each section describes some of the highlights of the corresponding chapter.

1.2. USES OF ACCELERATOR PRODUCED RADIOISOTOPES

Chapter 2 describes the basic uses of radioisotopes for medical and non-medical applications. The tracer principle forms the basis for most experiments with radioisotopes, with the concept of the tracer principle and how specific activity (SA) relates to this concept being described in detail. Factors influencing SA are also discussed.

Medical applications represent the vast majority of the uses of radiotracers. A number of examples of how radiotracers are used in clinical medicine, as well as in basic research, are given. The use of radioisotopes in industry and other research arenas is growing rapidly. While many of the examples provided are of the use of reactor produced radioisotopes, the source of the radioisotope is not important, and the reader is encouraged to find the radioisotope that meets their own criteria for a particular application. One should keep in mind that the half-life should not exceed that required to gain the desired information.

There is also an extensive use of radionuclides in basic chemical and biological research. Using the radioactive atoms as a tracer to determine where atoms migrate during chemical reactions and biological pathways is a common and very useful method of investigation.

1.3. ACCELERATORS

Chapter 3 provides a description of how cyclotrons and linacs work, and of the important characteristics of these accelerators for the production of radioisotopes. A general description of the operating characteristics of linacs is provided, along with the basic equations that govern the energy of the acceleration. A description is included of the linacs that are commercially available as of the time of writing of this book.

Next, a general description of the operating characteristics of cyclotrons is provided, and the basic equations that govern the energy of an accelerator are explained. Included are descriptions of the basic components of cyclotrons such as the radiofrequency (RF) system, the ion source, the vacuum system and the extraction system. A description is included of the cyclotrons that are commercially available as of the time of writing of this book, as well as a table of the operating characteristics of these cyclotrons. A brief description of the other accelerators that have been used for the production of radioisotopes is also given.

Choosing an accelerator can be a daunting task. Thus, a brief outline of issues that should be considered is given. While this is not an exhaustive exploration of this complex topic, the issues described will help users to understand the variety of problems and to identify which ones are of greatest importance in their circumstances.

Details of the characteristics of the commercial cyclotrons designed for radionuclide production are compiled and are listed in tables at the end of the chapter. The purpose of these tables is to give people a starting point for asking questions concerning the characteristics of cyclotrons and how one cyclotron would be preferable to another for a particular application.

1.4. THEORY OF RADIOISOTOPE PRODUCTION

Chapter 4 explains, at a basic level, the nuclear processes that occur in the transmutation of one element to another. There is a wide variety of nuclear reactions that are used in an accelerator to produce artificial radioactivity. The bombarding particles are usually protons, deuterons or helium particles. The energies used range from a few megaelectronvolts (MeVs) to hundreds of MeVs. This chapter explains the compound nucleus model and gives some of the common terminology of nuclear reactions. The nuclear reaction cross-section represents the total probability that a compound nucleus will be formed and that it will decompose in a particular channel. There is a minimum energy below which a nuclear reaction will not occur, except by tunnelling effects. This section describes the energetics of nuclear reactions and explores some aspects of the compound nucleus model.

The production rate of a radionuclide is described, including the calculation of the thick target yield and how to obtain and use literature cross-section data.

References to the SRIM (Stopping and Range of Ions in Matter) code for estimating energy loss in compounds on the basis of elemental composition are also given. The concept of the saturation factor (SF) is described and why it usually takes a long time to produce long lived radionuclides.

1.5. TARGETRY

Chapter 5 provides a brief description of the phenomena associated with accelerator targets and explains, at a basic level, some of the practical considerations in the use of cyclotron targets. All cyclotron targets share many characteristics in the basic physics, chemistry and engineering that go into the design of a target. The problems in the design and construction of cyclotron targets need to be defined. Some practical examples from the literature are included of how the sometimes mutually exclusive solutions to the numerous problems encountered in the optimal design of a cyclotron target have been arrived at. An attempt has also been made to present some simple formulas and ‘rules of thumb’ that may be used in the design of cyclotron targetry. In this vein, simple equations have been used, and the reader may decide whether simple approximations are sufficiently accurate in the particular application under consideration.

In addition to these basic principles, there are practical questions related to transport of the beam from the accelerator to the target, as well as the important matter of dealing with enriched target material and the ensuing recycling concerns.

1.6. TARGET PREPARATION AND IRRADIATION

Chapter 6 explains how cyclotron targets are prepared and irradiated. There is some information on how targets should be manufactured in order to maintain high SA for certain radioisotopes. Transport of materials from the target to the hot cell is also covered. Cleaning and routine maintenance of gas and liquid targets are discussed, along with some polishing techniques for target surfaces. There is a significant section on the preparation of solid targets by electrodeposition. A specific example using ^{201}Tl is given. Practical information such as spreadsheets for planning the plating of targets is also provided. Issues, such as cooling and dealing with beam density and distribution, associated with irradiating targets are discussed.

1.7. TARGET PROCESSING AND MATERIAL RECOVERY

Chapter 7 deals with the processing of targets including those of the solid, gas and liquid varieties. Continuing with the ^{201}Tl example from Chapter 6, it is explained how to process this target and recover the enriched material, and the necessity of following quality control (QC) procedures. Two different techniques for the recovery of enriched target material are described. Examples of ^{11}C and ^{18}F precursors are included as examples of radioisotopes produced in gas and liquid targets, respectively.

1.8. FUTURE TRENDS

Chapter 8 describes some possible trends for the future of radioisotope production. In this chapter, the growth of the field is discussed, as well as what are seen as the real needs of the community and the IAEA in the future.

REFERENCES TO CHAPTER 1

[1.1] INTERNATIONAL ATOMIC ENERGY AGENCY, Directory of Cyclotrons Used for Radionuclide Production in Member States, IAEA-TECDOC-1007, IAEA, Vienna (1998).

[1.2] INTERNATIONAL ATOMIC ENERGY AGENCY, Directory of Cyclotrons Used for Radionuclide Production in Member States, IAEA-DCRP/2006, IAEA, Vienna (2006).

Chapter 2

USES OF ACCELERATOR PRODUCED RADIOISOTOPES

2.1. INTRODUCTION

The development of nuclear technology is one of the most significant achievements of the twentieth century. Nuclear technology is currently used in nearly every field and aspect of our lives from medicine, to manufacturing and construction, to powering common household items, and to producing electricity for over 16% of worldwide needs. A list of some of these common uses can be found in Table 2.7 at the end of this chapter.

The first practical application of a radioisotope was made by G. de Hevesy in 1911. At the time, de Hevesy was a young Hungarian student working with naturally radioactive materials in Manchester in the United Kingdom. Having little in the way of financial means, he lived in a boarding house and took his meals there with his fellow boarders. He began to suspect that some of the meals might be made from leftovers from the preceding days or even weeks, but he could never be sure. To try and confirm his suspicions, de Hevesy placed a small amount of radioactive material into the remains of a meal. Several days later when the same dish was served again he used a simple radiation detection instrument (a gold leaf electroscope) to check if the food was radioactive. It was, and de Hevesy's suspicions were confirmed.

The use of radionuclides in the physical and biological sciences can be broken down into three general categories; imaging, radiotherapy and radiotracers. Imaging can be further divided into PET and SPECT. These topics are beyond the scope of this chapter and will only be described briefly here. All of these uses rely on the fact that radionuclides are used at tracer concentrations. In order to be used as tracers, the radionuclides and the compounds to which they are attached must obey the tracer principles, which state that:

(1) The tracer behaves or interacts with the system to be probed in a known and reproducible fashion.
(2) The tracer does not alter or perturb the system in any measurable fashion.
(3) The tracer concentration can be measured.

In internal radiotherapy for treating cancer and other diseases, the second principle is, in a strict sense, broken since the purpose of delivering the radiotoxic substance is to have the emitted radiation cause damage to the tumour tissues. However, in order for the radiotoxic substance to be localized, it must follow the known chemical behaviour without perturbing that pathway. The following are some typical radionuclides used in each of the broad categories:

(a) Carbon-11 is a positron emitting radionuclide with a half-life of 20.3 min used for PET imaging. It is generally produced as $^{11}CO_2$, which can be converted into a wide variety of labelling agents, such as $^{11}CH_3I$ or $H^{11}CN$. Since almost all biological compounds contain carbon, ^{11}C finds widespread use as a tracer in PET. In fact, more than 200 compounds have been labelled with ^{11}C [2.1].

(b) Nitrogen-13, with a half-life of 10 min, is also a positron emitting radionuclide. However, in addition to its use as a cardiac blood flow agent (as $^{13}NH_4^+$), it is used in applications other than PET imaging. For example, it is widely used in botany studies to determine the kinetics of nitrogen uptake in a variety of plant systems under a variety of conditions [2.2, 2.3].

(c) Iodine-123, with a half-life of 13.1 h, emits gamma rays with an energy of 159 keV, which is ideally suited to imaging in SPECT cameras that have been optimized for use with ^{99m}Tc (with a gamma ray energy of 140 keV). In addition, the ease with which an iodine atom can be inserted into a compound makes ^{123}I extremely versatile as a radiotracer in SPECT [2.4–2.6].

(d) Rhenium-186 is a β^- emitter with a low abundance 140 keV gamma ray. The 1 MeV β^- ray and its 90 h half-life make it a promising radiotoxic nuclide for therapy. As a chemical analogue of technetium, rhenium possesses similar chemical properties as ^{99m}Tc and can be used with some of the same compounds that have been developed for imaging tumours [2.7, 2.8].

Most of the radiotracers used in vivo should have relatively short half-lives (less than a few hours to at most a few days). There are definite advantages in using short lived radionuclides; for example, there is a low radiation dose associated with each study, serial studies are possible (sometimes on the same day for tracers such as ^{11}C) and radioactive waste disposal problems are minimized if not eliminated. The disadvantages are the need for an accelerator nearby or within easy shipping distance for the longer lived species (a few hours), and for rapid chemical procedures, especially for formation of more complex compounds.

2.2. RADIOISOTOPE/RADIONUCLIDE PRODUCTION

Radionuclide production is indeed true alchemy, which is converting the atoms of one element into those of another. This conversion involves altering the number of protons and/or neutrons in the nucleus (target). If a neutron is added without the emission of particles, then the resulting nuclide will have the same chemical properties as those of the target nuclide. If, however, the target nucleus is bombarded by a charged particle, for example a proton, the resulting nucleus will usually be that of a different element. The exact type of nuclear reactions a target undergoes depends on a number of parameters, including the type and energy of the bombarding particle. A more complete description of the process of radionuclide production is given in Chapter 4.

The binding energy of nucleons in the nucleus is of the order of 8 MeV on average. Therefore, if the incoming projectile has more than this amount of energy, the resulting reaction will cause other particles to be ejected from the target nucleus. By carefully selecting the target nucleus, the bombarding particle and its energy, it is possible to produce a specific radionuclide (see Chapter 4).

2.2.1. Specific activity

Specific activity is a measure of the number of radioactive atoms or molecules as compared with the total number of those atoms or molecules present in the sample. The specific activity is usually expressed in terms of radiation units per mass unit. The traditional units have been Ci/mol (or Ci/g) or a fraction thereof (now expressed as GBq/mol). If the only atoms present in the sample are those of the radionuclide, then the sample is referred to as carrier free. For example, a compound labelled with ^{211}At will be carrier free since there are no stable isotopes of astatine.

However, in most cases, there are small quantities of non-radioactive atoms or molecules that have a similar chemical behaviour and can act as pseudo-carriers. The SA of an isotope or radiopharmaceutical is important in determining the chemical and/or biological effect the substance may have on the system under investigation.

The number N of radioactive atoms in a sample can be calculated from the relationship of radioactivity to quantity expressed as:

$$\mathrm{d}N/\mathrm{d}t = -\lambda N$$

where $\mathrm{d}N/\mathrm{d}t$ is the disintegration rate in seconds and λ is the decay constant in reciprocal seconds ($\lambda = \ln(2)/t_{½}$).

As an example of SA, assume that glucose has been labelled with 10 mCi of ^{11}C with a half-life of 20.3 min (1 mCi is 3.7×10^7 disintegrations per second or dis/s). The carrier free SA can be calculated from the number of atoms contained in the 10 mCi of ^{11}C. The number of atoms will be:

$$^{11}\mathrm{C} = N = \frac{1}{\lambda}\frac{\mathrm{d}N}{\mathrm{d}t} = \frac{(10\ \mathrm{mCi})(3.7\times 10^{7}\ \mathrm{dis/(s{\cdot}mCi\ )})}{\dfrac{\ln(2)}{(20.3\,\mathrm{min})(60\ \mathrm{s/min})}} = 6.5\times 10^{11}\ \text{atoms}$$

using Avogadro's number, the number of moles is then 1.08×10^{-12} and $\mathrm{SA} = 9.3 \times 10^9$ Ci/mol (3.44×10^{20} Bq/mol).

If the radionuclide had been ^{14}C with its 5715 year half-life and following the same process but using the decay constant ($\lambda = 3.82 \times 10^{-12}\ \mathrm{s}^{-1}$) for ^{14}C, then the SA would be 62 Ci/mol (2.294×10^3 TBq/mol). If the radiolabelled glucose had been prepared in a plant, the naturally occurring glucose would have lowered the SA due to the non-radioactive glucose molecules. Therefore, it is easy to see that short lived radioisotopes potentially have a much higher SA.

The use of nuclear reactors for the production of radioisotopes relies on the fact that during the fission process in a reactor, there are large numbers of neutrons produced and thermalized by the surrounding media. These thermalized neutrons are ideal for initiating (n, γ) reactions. In some reactors, the higher energy neutrons are used to produce radioisotopes via other reactions involving the ejection of a charged particle, for example, (n, p) or (n, α) reactions. The fission process is a source of a number of widely used radioisotopes. For example, ^{90}Sr, ^{99}Mo, ^{131}I and ^{133}Xe are all produced in reactors by fission, and can be separated from the uranium fuel cells or from targets of enriched ^{235}U placed in the reactor for radioisotope production directly. The major drawbacks from using fission produced materials are the large quantities of radioactive waste material generated, and the large amounts of radionuclides produced, including other radioisotopes of the desired species. In producing ^{131}I from fission, the isotopes ^{127}I and ^{129}I are also formed, thus reducing the SA. A more detailed discussion is beyond the scope of this chapter, and the reader is referred to Ref. [2.9].

It is ironic that the first artificially produced radionuclides were created on E. Lawrence's cyclotrons in the 1930s [2.10, 2.11] but that it took another 30 years before accelerator produced radionuclides began to play a major role in the production of medically important radiopharmaceuticals. The principal advantage of accelerator produced radioisotopes is the high SAs that can be obtained through the (p, xn) and (p, α) reactions, as well as the other reactions involving charged particles, which result in the product being a different element than the target. Another significant advantage is that a smaller amount of radioactive waste is generated from charged particle reactions.

Cyclotrons designed for producing medical radioisotopes were initially capable of accelerating protons, deuterons, $^3He^{2+}$ and alpha particles (the nucleus of ^4He). However, the principal radioisotopes currently used in medical applications can all be produced by protons. The simplicity of design of proton only cyclotrons has resulted in cyclotrons that are capable of generating two or more simultaneous beams of varying energies and intensities. The modern cyclotron is completely controlled by a computer and can be in continuous operation for many days with only minimal attention.

As shown in Table 2.1, the PET radionuclides are produced from either proton or deuteron reactions. Since most PET research was performed at major research laboratories having accelerators capable of proton or deuteron production, these reactions were the standard. However, in the early 1980s, small compact proton only cyclotrons became available, and cyclotrons specifically designed for producing PET radionuclides were installed in many hospitals.

The major drawback with these proton only cyclotrons lies in the fact that in some cases an enriched target material must be used for a sufficient amount of radionuclide to be generated.

2.3. RADIOACTIVE TRACERS

The term radiotracer refers to a radioactive species that is used to follow (trace) the uptake into, or function of, an organ system in a living plant or

TABLE 2.1. THE MOST COMMONLY USED POSITRON EMITTERS AND TYPICAL REACTIONS FOR THEIR PRODUCTION

Radionuclide	$t_{½}$ (min)	Decay mode	Reaction	Energy (MeV)
C-11	20.3	β^+	$^{14}N(p, \alpha)$	11–17
N-13	9.97	β^+	$^{16}O(p, \alpha)$ $^{13}C(p, n)$	19 11
O-15	2.03	β^+	$^{15}N(p, n)$ $^{14}N(d, 2n)$ $^{16}O(p, pn)$	11 6 >26
F-18	110	β^+	$^{18}O(p, n)$ $^{nat}Ne(d, \alpha)$	11–17 8–14

animal or of a physical and chemical process. Initially, the radiotracers used were radioactive isotopes of naturally occurring elements or chemical congeners of these elements. Other early examples of simple elements as radiotracers were the use of radioiodine to monitor iodine uptake in the thyroid and the use of radioactive phosphorus to monitor metabolism.

Radioactive isotopes of the elements sodium and potassium (^{24}Na, ^{42}K) have been used to measure the sodium and potassium contents of the body, employing the isotope dilution technique. Analysis by isotope dilution involves adding a known mass and SA of a substance to a mixture containing an unknown quantity of the substance, and taking an aliquot of the mixture and determining the new SA of the substance under investigation. It can be shown that the mass of the substance of interest in the unknown mixture can be expressed as:

$$M = M_1(\mathrm{SA}_1/\mathrm{SA}_2 - 1)$$

where M is the mass of the substance in the system under investigation, and SA_1 and SA_2 are the SAs of the tracer added before and after addition to the system, respectively, while M_1 is the mass of the spike added to the system.

As an example, suppose we need to know the amount of copper in a system. A spike of copper containing 10 mg with 1 kBq of ^{64}Cu is added to 20 mL of the unknown sample. After addition and mixing, a portion of the mixture is isolated, and the total amount (mass) of copper and the radioactivity determined. In this example, the analysis yields 10.5 mg and 0.5 kBq, respectively, yielding an SA_2 value of 0.048 kBq·mg^{-1}. Using the above equation, the amount of copper in the unknown sample is:

$$M = 10\ \mathrm{mg} \times [(0.1\ \mathrm{kBq{\cdot}mg^{-1}}/0.048\ \mathrm{kBq{\cdot}mg^{-1}}) - 1] = 21\ \mathrm{mg\ of\ copper}$$

This method has a number of applications, especially in tracer elemental analyses in living systems.

Another example of the tracer principle is radioimmunoassay (RIA). All RIA procedures are based on the original observation by Yalow and Berson [2.12, 2.13] that low concentrations of antibodies to the antigenic hormone, insulin, could be detected by their ability to bind radiolabelled (^{131}I) insulin. The general principles of RIA are readily summarized in the set of competing reactions. Hormone, labelled with a radioactive atom, binds to a specific antibody to form a labelled antigen–antibody complex. Radioimmunoassay exploits the ability of unlabelled hormones in plasma or other solutions to compete with labelled hormones for antibodies and thereby to inhibit the binding of labelled hormones. As a result of the competitive inhibition, the amount of labelled hormone that is bound to the antibody decreases as the concentration of unlabelled hormone is increased. A calibration or standard curve is set up with increasing amounts of hormone, and from this curve the amount of hormone in the unknown samples can be calculated. This same principle can be applied to a wide variety of hormones, antigens and other biological compounds. Thus, the four basic necessities for an RIA system are:

(1) An antiserum to the compound to be measured;
(2) Availability of a radioactively labelled form of the compound;
(3) A method whereby antibody-bound tracer can be separated from unbound tracer;
(4) A standard unlabelled material.

After an incubation of the three essential components, the antigen antibody complexes or bound antigens are separated from the free antigens, and the radioactivity of either or both phases is measured.

2.4. MEDICAL APPLICATIONS

Nuclear medicine makes use of the fact that certain radioisotopes emit gamma rays with sufficient energy that they can be detected outside of the body.

If these radioisotopes are attached to biologically active molecules, the resulting compounds are called radiopharmaceuticals. They can either localize in certain body tissues or follow a particular biochemical pathway. The following discussion will concentrate on the uses of radioactive substances for the diagnosis or therapeutic treatment of human pathology.

2.4.1. Historical background

Nuclear medicine has its origins in the pioneering work of the Hungarian physician de Hevesy, who, in 1924, used radioactive isotopes of lead as tracers in bone studies. Shortly thereafter, Stevens made intravenous injections of radium chloride to study malignant lymphomas.

However, it was not until the discovery of artificially produced radioactive isotopes that the number of available species suitable for use as tracers began to increase. The invention of the cyclotron by E. Lawrence in 1932 made it possible to produce radioactive isotopes of a number of biologically important elements. The use of these artificially produced radiotracers continued, with Hamilton and Stone using radioactive sodium clinically in 1937. Hertz, Roberts and Evans in

1938 used radioactive iodine in the study of thyroid physiology, followed in 1939 by J.H. Lawrence, Scott and Tuttle studying leukaemia with radioactive phosphorus. By 1940, Hamilton and Soley were performing studies in iodine metabolism by the thyroid gland in situ by using radioiodine in normal subjects and in patients with various types of goiter.

The first medical cyclotron was installed in 1941 at Washington University, St Louis, where radioactive isotopes of phosphorus, iron, arsenic and sulphur were produced. With the development of the fission process during World War II, most radioisotopes of medical interest began to be produced in nuclear reactors. After the war, the widespead use of radioactive materials in medicine established the new field of what was then called atomic medicine, and only later became known as nuclear medicine. Radioactive carbon, tritium, iodine, iron and chromium began to be used more widely in the study of disease processes.

Cassen et al., in 1951, developed the concept of the rectilinear scanner, which opened the way to obtaining in a short amount of time the distribution of radioactivity in a subject [2.14]. This was followed by production of the first gamma camera by Anger in 1958 [2.15]. The original design was modified in the late 1950s to what is now known as the Anger scintillation camera, thus heralding the modern era of gamma cameras whose principles are still in use today.

The ^{99}Mo/^{99m}Tc generator system was developed by the Brookhaven National Laboratory (BNL) in 1957 [2.16]. Technetium-99m produced via this generator system has become the most widely used radionuclide in nuclear medicine at the present time, accounting for as much as 85% of all diagnostic procedures.

The modern era of nuclear medicine has become known as molecular medicine, since it is now possible to translate advances in molecular biology and biochemistry into an understanding of human physiology, and from there into clinical treatment as well as diagnosis of pathology and anatomical abnormalities. The advent of clinical PET for cancer diagnosis makes use of sophisticated tracers to unravel cancer biology.

2.4.2. Radionuclides for imaging

Nuclear medicine imaging differs from other radiological imaging in that the radiotracers used in nuclear medicine map out the function of an organ system or metabolic pathway and, thus, imaging the concentration of these agents in the body can reveal the integrity of these systems or pathways. This is the basis for the unique information that the nuclear medicine scans described in Table 2.2 provide for various scanning procedures for the various organ/functional systems of the body.

TABLE 2.2. TYPICAL RADIOISOTOPES AND THEIR USES FOR IMAGING

Radioisotope	Half-life	Uses
Technetium-99m	6 h, derived from Mo-99 parent (66 h)	Used to image the skeleton and heart muscle, in particular; but also used for brain, thyroid, lungs (perfusion and ventilation), liver, spleen, kidneys (structure and filtration rate), gall bladder, bone marrow, salivary and lachrymal glands, heart blood pool, infections and numerous specialized medical studies.
Cobalt-57	272 d	Used as a marker to estimate organ size and for in vitro diagnostic kits.
Gallium-67	78 h	Used for tumour imaging and localization of inflammatory lesions (infections).
Indium-111	67 h	Used for specialist diagnostic studies; e.g. for the brain, infections and colon transit.
Iodine-123	13 h	Increasingly used for diagnosis of thyroid function, it is a gamma emitter without the beta radiation of I-131.
Krypton-81m	13 s from Rb-81 (4.6 h)	Kr-81m gas can yield functional images of pulmonary ventilation, e.g. in asthmatic patients, and for the early diagnosis of lung diseases and function.
Rubidium-82	65 h	Convenient PET agent for myocardial perfusion imaging.
Strontium-92	25 d	Used as the ‘parent’ in a generator to produce Rb-82.
Thallium-201	73 h	Used for diagnosis of coronary artery disease and other heart conditions, such as heart muscle death and for location of low grade lymphomas.
Carbon-11 Nitrogen-13 Oxygen-15 Fluorine-18	20.4 min 9.97 min 2 min 110 min	These are the positron emitters used in PET for studying brain physiology and pathology, in particular for localizing epileptic focus, and in dementia, psychiatry and neuropharmacology studies. They also have a significant role in cardiology. Fluorine-18 in FDG has become very important in detecting cancers and in monitoring progress in their treatment, using PET.

TABLE 2.3. THE MOST COMMONLY USED RADIOISOTOPES FOR IMAGING

SPECT	PET
Tc-99m	C-11
I-123	F-18
Tl-201	Rb-82
Ga-67	N-13

While there is a wide range of other radioisotopes that are used in imaging, a relatively small number make up the vast majority of all studies in SPECT and PET imaging. Table 2.3 lists the most widely used radioisotopes for imaging.

Table 2.4 provides the various low energy production routes along with the half-life of the radioisotopes. Technetium-99m is included since this isotope alone accounts for nearly 85% of all nuclear medicine imaging studies. There have been a number of proposals suggesting that ^{99m}Tc could be produced in an accelerator. The economics of producing ^{99m}Tc in an accelerator can never compete with the extremely low costs of producing it in a reactor. While there is concern about the ability to build new reactors and thus jeopardizing the availability of this important isotope, the recent construction of reactors in Canada dedicated to ^{99}Mo production removes this concern for the present.

Iodine-123 has been of interest for nearly three decades because of its unique chemistry, which makes it possible to attach this isotope to a wide variety of molecules, and its gamma ray energy of 159 keV, which is well matched to SPECT cameras. The ability to produce this isotope in high purity from enriched ^{124}Xe targets made it possible to ship ^{123}I over long distances and still have high SA ^{123}I available for labelling. However, the production costs are still very high in comparison with those of other radioisotopes, which will limit its use for the foreseeable future. While ^{123}I can be produced for local use via the ^{123}Te(p, n) or ^{124}Te(p, 2n) reactions, the co-production of ^{124,125}I limits the product's shelf-life.

TABLE 2.4. NUCLEAR REACTIONS EMPLOYED TO PRODUCE SOME COMMONLY USED IMAGING RADIOISOTOPES

Radionuclide	Half-life	Reaction	Energy (MeV)
Tc-99m	6.0 h	^{100}Mo(p, 2n)	30
I-123	13.1 h	^{124}Xe(p, 2n)^{123}Cs	27
		^{124}Xe(p, pn)^{123}Xe	
		^{124}Xe(p, 2pn)^{123}I	
		^{123}Te(p, n)^{123}I	15
		^{124}Te(p, 2n)^{123}I	25
Tl-201	73.1 h	^{203}Tl(p, 3n)^{201}Pb → ^{201}Tl	29
C-11	20.3 min	^{14}N(p, α)	11–19
		^{11}B(p, n)	10
F-18	110 min	^{18}O(p, n)	15
		^{20}Ne(d, α)	14
		^{nat}Ne(p, X)	40
Cu-64	12.7 h	^{64}Ni(p, n)	15
		^{68}Zn(p, αn)	30
		^{nat}Zn(d, αxn)	19
		^{nat}Zn(d, 2pxn)	19
I-124	4.14 d	^{124}Te(p, n)	13
		^{125}Te(p, 2n)	25

Thallium-201 was developed at BNL, where it was shown that ^{201}Tl could be used as an ideal tracer for detecting myocardial perfusion [2.17]. Thallous chloride labelled with ^{201}Tl has been used extensively for more than 25 years and remains the gold standard for measuring blood flow. Over this period, there have been numerous reports of its demise due to the availability of ^{99m}Tc labelled alternatives; however, the demand for this isotope is still growing.

The remaining isotopes listed are used in PET imaging. Carbon-11 is extremely attractive because, in principle, an existing carbon atom in the molecule of interest can be replaced by the radioactive isotope. However, because of the short half-life, its availability will be limited to those sites possessing an accelerator or which are in the vicinity of one. The demand for ^{18}F exceeds its availability. To overcome this shortage, a number of central distribution centres have been placed in large metropolitan areas in Asia, Europe and North America. Although several nuclear reactions are possible, the (p, n) reaction is chosen for producing large quantities of ^{18}F. If the availability of ^{18}F continues to grow, ^{18}F labelled compounds may begin to compete with other SPECT agents such as ^{123}I.

Two other isotopes (^{124}I and ^{64}Cu) are candidates for both PET imaging and radiotherapy. The interest in these two is primarily related to their relatively long half-lives. Such properties would enable studies to be performed where the kinetics are slow and exceed the ability for imaging with ^{18}F.

The disadvantages include low production rate (^{124}I) and the need for expensive enriched target material (^{64}Ni and ^{124}Te). Results from Washington University in St Louis have shown that high resolution PET images are possible even with the high energy β^+ particles associated with ^{124}I decay, and other photons in coincidence with the β^+ decay present in ^{64}Cu [2.18, 2.19].

2.4.3. Radionuclides for therapy

The idea of a radioisotope used in therapy is based on the desire to link a radionuclide that has a high linear energy transfer (LET) associated with its decay products, such as Auger electrons, beta particles or alpha particles, to a biologically active molecule that can be directed to a tumour site. Since the beta emitting radionuclides are neutron rich, they have, in general, been produced in reactors. Table 2.5 lists some of the radionuclides that have been proposed as possible radiotoxic tracers.

Most of these radionuclides are produced in a reactor, although a few are best produced via charged particle reactions. Table 2.6 provides the charged particle nuclear reactions that can be used for selected radiotoxic nuclides.

The attractive feature of ^{77}Br is its chemical versatility in addition to its half-life. Production rates are relatively low, and purity may be an issue since ^{76}Br is often co-produced. The demand for ^{103}Pd, which is used in treating prostate cancer, is continuing to grow. A large number of low energy (18 MeV) cyclotrons are dedicated solely to the production of this isotope.

TABLE 2.5. RADIONUCLIDES THAT HAVE BEEN PROPOSED FOR USE AS POSSIBLE RADIOTOXIC ISOTOPES FOR TREATMENT OF CANCER

Sc-47	Cu-64	Cu-67	Br-77	Y-90
Rh-105	Pd-103	Ag-111	I-124	Pr-142
Pm-149	Sm-153	Gd-159	Ho-166	Lu-177
Re-186/188	Ir-194	Pt-199	At-211	Bi-213

TABLE 2.6. CHARGED PARTICLE PRODUCTION ROUTES AND DECAY MODES FOR SELECTED THERAPY ISOTOPES

Radionuclide	Half-life	Decay mode	Reaction	Energy (MeV)
Br-77	2.4 d	Auger electrons	^{75}As(α, 2n)	27
			^{77}Se(p, n)	13
			^{78}Se(p, 2n)	24
			^{79,81}Br(p, xn)^{77}Kr	45
			^{nat}Mo(p, spall.)	>200
Pd-103	17.5 d	Auger electrons	^{103}Rh(p, n)	19
			^{nat}Ag(p, xn)	>70
Re-186	90.6 h	β^-	^{186}W(p, n)	18
			^{186}W(d, 2n)	20
			^{197}Au(p, spall.)	>200
			^{nat}Au(p, spall.)	>200
			^{nat}Ir(p, spall.)	>200
At-211	7.2 h	α	^{209}Bi(α, 2n)	28
			^{209}Bi(^{7}Li, 5n)^{211}Rn	60
			^{232}Th(p, spall.)^{211}Rn	>200

Rhenium-186 is attractive for a number of reasons. Besides the decay characteristics, rhenium is in the same chemical family as technetium; thus, much of the chemistry developed for technetium can be applied to rhenium.

The production rates from all of the reactions for this radioisotope listed in Table 2.6 are very low. Thus, the only practical route to this potentially important isotope is via neutron capture in a reactor. This route results in a very low SA product, which severely limits its utility.

Finally, the alpha emitting isotopes have been of interest for use in therapy because of the high LET associated with alpha decay. Astatine is of interest because it possesses many of the properties of halogens and each decay of ^{211}At has an alpha particle associated with it. Because of its short half-life, multiple production sites would be required for practical applications. Thus, production of its parent radionuclide (^{211}Rn, $t_{1/2}$ = 14.6 h) has been suggested as a way of producing and shipping ^{211}At to remote sites.

2.5. RADIOPHARMACEUTICALS

Radiopharmaceuticals differ in one major aspect from regular pharmaceuticals in that they are given in such small concentrations that they do not elicit any pharmacological response. Therefore, there have been a number of attempts to change the name used to describe these substances, for example radiotracers. Present day radiopharmaceuticals are used for diagnostic purposes in about 95% of cases and for therapy in the remainder [2.20–2.22].

In order for a radiotracer (radiopharmaceutical) to be used safely in humans, it must meet high quality standards that include chemical and radiochemical purity, sterility and freedom from pyrogenic material.

The ideal diagnostic radiopharmaceutical should:

(a) Be readily available at a low cost.
(b) Be a pure gamma emitter, i.e. have no particle emission such as alphas and betas. These particles contribute radiation dose to the patient while not providing any diagnostic information.
(c) Have a short effective biological half-life so that it is eliminated from the body as quickly as possible.
(d) Have a high target to non-target ratio so that the resulting image has a high contrast (the object has much more activity than the background).
(e) Follow or be trapped by the metabolic process of interest.

As in all matters concerning life, there are no ‘ideal’ radiopharmaceuticals [2.23]. Thus, in designing a realistic candidate for a radiopharmaceutical, the following three factors must be considered:

(1) Develop a radiotracer that binds preferentially to a specific site;
(2) Determine the sensitivity of the radiotracer to a change in biochemistry;
(3) Find a specific biochemical change as a function of a specific disease that matches that sensitivity.

2.6. INDUSTRIAL APPLICATIONS

Applications of the radiotracer technique in industry have taken the form of embedding the tracer into a system, or actually inducing radioactivity in the system directly by charged particles or neutron activation. The references for this section provide examples of how this technique can be applied to a variety of problems. The IAEA has published a guidebook on radiotracer applications in industry [2.24], which provides an excellent overview of recent research in the use of radiotracers in a variety of applications. A few examples are given in Sections 2.6.1–2.6.3.

2.6.1. Material processing and quality control

Radioisotopes are used to improve the quality of materials in many different ways. All forms of radioactive emissions (alpha, beta and gamma rays) lose intensity as they travel through matter, and this loss of intensity can be used to determine the properties of the material. The thickness and density of a material can be determined easily by the attenuation of the radiation, and flaws or cracks may be easily identified by anomalies in the attenuation. As an example, beta particles with an average energy of 250 keV from ^{85}Kr can be used to measure the thickness of thin layers of plastics very accurately.

Small amounts of a radioactive isotope can be used in a tracer to track down problems in the processing of materials. They make it possible to track leakage from piping systems, monitor the rate of engine wear and corrosion of processing equipment, observe the velocity of materials through pipes and gauge the efficiency of filtration systems. As an example, ^{192}Ir is used to test the integrity of pipeline welds and aircraft parts.

2.6.2. Instruments using radioisotopes

Instruments containing radioisotopes are widely used because they make it possible to take measurements without direct physical contact with the substance being measured. For example, level gauges containing radioactive sources are used where heat, pressure or corrosive substances, such as molten glass or metal, make it difficult or impossible to use direct contact gauges. Strong gamma sources such as ^{192}Ir and ^{60}Co are often used in this way. A series of collimated sources with detectors on the opposite side of a conveyor belt can easily detect the level of substance on the belt.

2.6.3. Consumer products and services

Radioactive materials are essential for the provision of some necessities and conveniences that virtually everyone depends on, for example:

(a) Many smoke detectors rely on a tiny radioactive source (usually ^{241}Am) to sound an alarm when smoke is present.
(b) Computer disks ‘remember’ data better when they are treated with radiation.
(c) Non-stick pans are treated with radiation to ensure that the coating will stick to the surface.
(d) Photocopiers use small amounts of radioactive materials to eliminate static and prevent paper from sticking together and jamming the machine.

(e) Cosmetics, hair products and contact lens solutions are sterilized with radiation to remove irritants and allergens.

(f) Medical bandages and a variety of personal health and hygiene products are sterilized by radioactive materials.

2.7. ENVIRONMENTAL/BIOLOGICAL APPLICATIONS

Radioisotopes can be used to help understand chemical and biological processes in the environment and in plants. There are two reasons for this usefulness:

(1) Radioisotopes are chemically identical with other isotopes of the same element and will react in the same way in chemical reactions.

(2) For many elements some radioactive isotopes of the element have appropriate half-lives and can easily be detected.

2.7.1. Agricultural applications

There are many applications of radioisotopes in agriculture. Radiation has been used to breed new seed varieties with higher yields, such as the ‘miracle’ rice that has greatly expanded rice production in Asia.

The ionizing radiation from radioisotopes increases the number of variations in plants and, with careful selection, can produce crops that are more resistant to drought and disease, as well as crops with increased yields or shorter growing times. This has been the practice for several decades, and has helped to increase food output.

Radioisotopes are ideally suited as tools for the investigation of fertilizers. Important plant nutrients, such as calcium, phosphorus, iron, potassium, copper, sodium, sulphur and zinc, have radioisotopes with the appropriate half-lives and decay characteristics to be used as tracers. These elements can be incorporated in fertilizers and applied to the soil to determine the effect on plant utilization of fertilizer composition or the method of application. Plant uptake of the activated fertilizer can be readily measured and can be distinguished from uptake of the same compound already present in the soil. Phosphorus-32 as a tracer has a wide application in the field of plant physiology and soil chemistry. Research has also been carried out on the mechanism of nutrient uptake by use of this radioisotope of phosphorus. Using rice as a test crop, studies are being done on the absorption, translocation and distribution of phosphate, carbon and nitrogen with the help of superphosphate, urea and ammonium sulphate labelled with ^{32}P, ^{14}C and ^{15}N, which were applied both in soils and on leaves by spraying.

2.7.2. Insect control

Insects destroy about 10% of the world's crops. Releasing sterile insects raised in the laboratory into the wild can sometimes control these pests. The male insects are made sterile using ionizing radiation (usually ^{60}Co). Female insects that mate with sterile male insects do not reproduce, and the population can be quickly curbed as a consequence. The technique is considered to be safer and better than conventional chemical insecticides, since insects can develop resistance against insecticides and there can be health concerns about chemically treated crops.

2.7.3. Plant physiology

Probably the most widely used tracer for studies in tracer kinetics in plants is ^{13}N. In spite of its relatively short half-life (<10 min), a wide variety of studies has been undertaken to understand the incorporation of nitrogen into plant systems. The use of ^{11}C provides the opportunity for producing more complex molecules, as is seen in medical applications.

2.7.4. Water resources

Adequate water is essential for life. However, in many parts of the world water is scarce and in others it is becoming scarcer. Isotope hydrology using tritium (or other readily soluble radioisotopes) makes accurate tracing of underground water resources possible. These techniques are important analytical tools in the management and conservation of existing water supplies, and in the identification of new and/or renewable sources of water. The results permit planning and sustainable management of these water resources. Neutron probes can measure soil moisture very accurately, enabling better management of land affected by salinity, particularly with respect to irrigation.

For surface waters, radiotracers can provide information about leakage through dams and irrigation channels, the dynamics of lakes and reservoirs, flow rates and river discharge rate measurements, and silt sedimentation rates. Many countries have used isotope techniques to investigate their water resources in collaboration with the IAEA.

2.8. BASIC CHEMICAL AND PHYSICAL SCIENCE BACKGROUND

Tracers have long been used to probe the kinetics of chemical reactions. With the high sensitivity associated with radioactive decay, very short lifetimes could be monitored accurately.

One of the major uses of kinetic isotope effects (KIEs) is to help chemists model the transition states of organic reactions so that they can understand how and why reactions occur. Kinetic isotope effects are the major tool used in these investigations because they give both qualitative and semi-quantitative information about the structure of the transition state. For instance, a leaving group KIE is used to determine the length of the alpha carbon, leaving group bond in an SN_2 transition state:

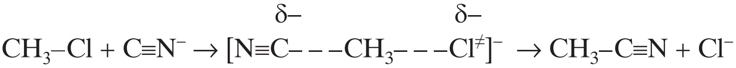

$$CH_3\text{–}Cl + C{\equiv}N^- \rightarrow [N{\equiv}\overset{\delta-}{C}\text{– – –}CH_3\text{– – –}\overset{\delta-}{Cl^{\neq}}]^- \rightarrow CH_3\text{–}C{\equiv}N + Cl^-$$

The theoretical equation relating transition state structure to the magnitude of the KIE is given by:

$$\frac{k_L}{k_H} = \frac{\nu_L^{\mp}}{\nu_H^{\mp}}\left(1 + \sum_i^{3n-6} Gu_i\Delta u_i - \sum_i^{3n-7} Gu_i\Delta u_i^{\mp}\right)$$

where

$\sum_i^{3n-6} Gu_i\Delta u_i$ represents the vibrational energy in the reactant;

$\sum_i^{3n-7} Gu_i\Delta u_i^{\mp}$ represents the vibrational energy in the transition state.

As the per cent C_α–Cl bond rupture in the transition state increases, the vibrational energy of the C_α–Cl bond (the $\Sigma Gu_i\Delta u_i^{\neq}$ term) decreases and the chlorine KIE increases. Therefore, the magnitude of the leaving group KIE can be used to estimate the amount of C_α–Cl bond rupture in the transition state.

It has been shown that, by using artificially manufactured isotopes, it is possible to increase the magnitude of the KIE for a particular element by increasing the mass difference between the isotopes used in the experiment [2.25]. For example, increasing the mass difference between the carbon isotopes used in measuring a carbon KIE to 3 by using ^{11}C and ^{14}C increased the magnitude of the KIE by a factor of 4.

2.9. SUMMARY

Radioisotopes have very useful properties: radioactive emissions are easily detected and can be tracked until they disappear, leaving no trace. These properties lead to many applications for radioisotopes in the scientific, medical, forensic and industrial fields. Table 2.7 provides a list of radioisotopes and their varied uses.

TABLE 2.7. COMMON RADIOISOTOPES AND THEIR USES
(material derived from http://www.nei.org and other sources)

Radioisotope	Use
Americium-241	Used in many smoke detectors for homes and businesses: to measure levels of toxic lead in dried paint samples, to ensure uniform thicknesses in rolling processes such as in steel and paper production, and to help determine where oil wells should be drilled.
Cadmium-109	Used to analyse metal alloys for checking stock and sorting out scrap.
Caesium-137	Used to treat cancers; to calibrate the equipment used to measure correct patient dosages of radioactive pharmaceuticals; to measure and control the liquid flow in oil pipelines; to indicate to researchers whether oil wells are plugged by sand; and to ensure the correct filling level for packages of food, drugs and other products. (The products in these packages do not become radioactive.)
Calcium-47	Used as an aid to biomedical researchers studying the cell function and bone formation of mammals.
Californium-252	Used to measure the mineral content of coal ash and to measure the moisture of materials stored in silos.
Carbon-11, -14	Used in research to ensure that potential new drugs are metabolized without forming harmful by-products.
Chromium-51	Used in research in red blood cell survival studies.
Cobalt-57	Used in nuclear medicine to help physicians interpret diagnostic scans of patients' organs, and to diagnose pernicious anaemia.
Cobalt-60	Used to sterilize surgical instruments; to improve the safety and reliability of industrial fuel oil burners; and to preserve poultry, fruits and spices.

TABLE 2.7. COMMON RADIOISOTOPES AND THEIR USES
(material derived from http://www.nei.org and other sources) (cont.)

Radioisotope	Use
Copper-64	Tracer for blood flow, hypoxia and cell binding studies as PTSM[a].
Copper-67	When attached to monoclonal antibodies and injected into a cancer patient, helps the antibodies bind to and destroy the tumour.
Curium-244	Used in mining to analyse material excavated from pits and slurries from drilling operations.
Fluorine-18	Used in biological tracer molecules such as FDG and FLT[b] for detection of cancer.
Gallium-67	Gallium citrate may be useful in demonstrating the presence of several types of malignancies.
Iodine-123	Widely used to diagnose thyroid disorders.
Iodine-124	PET tracer used in the same way as iodine is used for SPECT.
Iodine-129	Used in diagnostic testing laboratories to check some radioactivity counters in vitro.
Iodine-131	Used to diagnose and treat thyroid disorders.
Iridium-192	Used to test the integrity of pipeline welds, boilers and aircraft parts.
Krypton-85	Used in indicator lights in appliances like washing machines and dryers, stereos and coffee makers; to gauge the thickness of thin plastics, sheet metal, rubber, textiles and paper; and to measure dust and pollutant levels.
Nickel-63	Used to detect explosives, and as voltage regulators and current surge protectors in electronic devices.
Nitrogen-13	Used as ammonia for cardiac imaging.
Phosphorus-32	Used in molecular biology and genetics research.
Plutonium-238	Has safely powered at least 20 NASA[c] spacecraft since 1972.
Promethium-147	Used in electric blanket thermostats and to gauge the thickness of thin plastics, thin sheet metal, rubber, textiles and paper.
Rubidium-82	Used as a blood flow tracer.
Selenium-75	Used in protein studies in life science research.
Sodium-24	Used to locate leaks in industrial pipelines and in oil well studies.

TABLE 2.7. COMMON RADIOISOTOPES AND THEIR USES
(material derived from http://www.nei.org and other sources) (cont.)

Radioisotope	Use
Strontium-85	Used to study bone formation and metabolism.
Strontium-90	Used in survey meters by schools, the military and emergency management authorities.
Technetium-99m	The most widely used radioactive isotope for diagnostic studies in nuclear medicine. Different chemical forms are used for brain, bone, liver, spleen and kidney imaging, as well as for blood flow studies.
Thallium-201	Used in cardiac stress tests.
Thallium-204	Measures the dust and pollutant levels on filter paper, as well as gauging the thickness of plastics, sheet metal, rubber, textiles and paper.
Thoriated tungsten	Used in electric arc welding rods in the construction, aircraft, petrochemical and food processing equipment industries. It produces easier starting, greater arc stability and less metal contamination.
Thorium-229	Prolongs the life of fluorescent lights.
Thorium-230	Provides colouring and fluorescence in coloured ceramic glazes and glassware.
Tritium	Used for life science and drug metabolism studies to ensure the safety of potential new drugs; for self-luminous aircraft and commercial exit signs; for luminous dials, gauges and wristwatches; and to produce luminous paint.
Uranium-235	Used in fuel for nuclear power plants and naval nuclear propulsion.
Uranium-238	Used in dental fixtures such as crowns and dentures to provide natural colour and brightness.
Xenon-133	Used in nuclear medicine for lung ventilation and blood flow studies.

[a] PTSM: pyruvaldehyde-bis(N_4-methylthiosemicarbazone).
[b] FLT: 3′-deoxy-3′-^{18}F-fluorothymidine.
[c] NASA: National Aeronautics and Space Administration.

REFERENCES TO CHAPTER 2

[2.1] IWATA, R., Reference Book for PET Radiopharmaceuticals, http://kakuyaku.cyric.tohoku.ac.jp/public/preface2002.html

[2.2] GLASS, A.D.M., et al., The regulation of nitrate and ammonium transport systems in plants, J. Exp. Bot. **53** (2002) 855–864.

[2.3] BINGHAM, I.J., GLASS, A.D.M., KRONZUCKER, H.J., ROBINSON, D., SCRIMGEOUR, C.M., "Isotope techniques", Root Methods: A Handbook (SMIT, A.L., et al., Eds), Springer-Verlag, Berlin (2000) 365–402.

[2.4] LAMBRECHT, R.M., MANTESCU, C., REDVANLY, C., WOLF, A.P., Preparation of high purity carrier-free ^{123}I-iodine monochloride as iodination reagent for synthesis of radiopharmaceuticals: IV, J. Nucl. Med. **13** (1972) 266–273.

[2.5] KULKARNI, P.V., Recent developments in ^{99m}Tc- and ^{123}I-radiopharmaceuticals for SPECT imaging, Int. J. Radiat. Appl. Instrum. B **18** (1991) 647–654.

[2.6] KUNG, H.F., KUNG, M.P., CHOI, S.R., Radiopharmaceuticals for single-photon emission computed tomography brain imaging, Semin. Nucl. Med. **33** (2003) 2–13.

[2.7] KOLESNIKOV-GAUTHIER, H., et al., Evaluation of toxicity and efficacy of ^{186}Re-hydroxyethylidene diphosphonate in patients with painful bone metastases of prostate or breast cancer, J. Nucl. Med. **41** (2000) 1689–1694.

[2.8] MAXON, H.R., et al., Re-186(Sn) HEDP for treatment of painful osseous metastases: Initial clinical experience in 20 patients with hormone-resistant prostate cancer, Radiology **176** (1990) 155–159.

[2.9] INTERNATIONAL ATOMIC ENERGY AGENCY, Manual for Reactor Produced Radioisotopes, IAEA-TECDOC-1340, IAEA, Vienna (2003).

[2.10] LAWRENCE, E.O., LIVINGSTON, M.S., The production of high speed light ions without the use of high voltages, Phys. Rev. **40** (1932) 19.

[2.11] LAWRENCE, J.H., Nuclear physics and therapy: Preliminary report on a new method for the treatment of leukemia and polycythemia, Radiology **35** (1940) 51.

[2.12] YALOW, R.S., Radioimmunoassay: A probe for the fine structure of biologic system, Science **200** (1978) 1236–1245.

[2.13] YALOW, R.S., BERSON, S.A., Assay of plasma insulin in human subjects by immunological methods, Nature **184** (1959) 1648.

[2.14] CASSEN, B., et al., Instrumentation for ^{131}I use in medical studies, Nucleonics **9** (1951) 46.

[2.15] ANGER, H.O., Scintillation camera, Rev. Sci. Instrum. **29** (1958) 27.

[2.16] TUCKER, W.D., GREENE, M.W., WEISS, A.J., MURRENHOFF, A.P., Trans. Am. Nucl. Soc. **1** (1958) 160.

[2.17] LEBOWITZ, E., et al., Thallium-201 for medical use, J. Nucl. Med. **16** (1975) 151–155.

[2.18] McCARTHY, D.W., et al., Efficient production of high specific activity ^{64}Cu using a biomedical cyclotron, J. Nucl. Med. Biol. **24** (1997) 35–43.

[2.19] LEWIS, M.R., et al., In vivo evaluation of pretargeted ^{64}Cu for tumor imaging and therapy, J. Nucl. Med. **44** (2003) 1284–1292.

[2.20] HARBERT, J., DA ROCHE, A.F.G., Textbook of Nuclear Medicine, Vol. 1: Basic Science, 2nd edn, Lea and Febiger, Philadelphia, PA (1984).
[2.21] SAHA, G.B., Fundamentals of Nuclear Pharmacy, Springer-Verlag, Berlin (1979).
[2.22] SORENSON, J.A., PHELPS, M.E., Physics in Nuclear Medicine, 2nd edn, Grune and Stratton, New York (1987).
[2.23] ECKELMAN, W.C., The status of radiopharmaceutical research, Int. J. Radiat. Appl. Instrum. B **18** (1991) iii–vi.
[2.24] INTERNATIONAL ATOMIC ENERGY AGENCY, Radiotracer Applications in Industry — A Guidebook, Technical Reports Series No. 423, IAEA, Vienna (2004).
[2.25] AXELSSON, S., LANGSTROM, B., MATSSON, O., $^{11}C/^{14}C$ kinetic isotope effects, J. Am. Chem. Soc. **109** (1987) 7233.

Chapter 3

ACCELERATORS

3.1. INTRODUCTION

The production of radionuclides with an accelerator demands that particle beams be delivered with two specific characteristics. The beam must have sufficient energy to bring about the required nuclear reactions, and there must be sufficient beam current to give practical yields. This chapter describes the various types of accelerators, their characteristics and their basic operation in relation to isotope production.

The transformation of one element into another was first demonstrated by Rutherford in 1919 [3.1] when he directed alpha particles emanating from a sample of polonium onto nitrogen gas and detected the protons that were emitted. The future of accelerator production of radioisotopes reached a turning point with the construction of the first cyclotron by E. Lawrence, Edlefsen and Livingston in 1930 [3.2, 3.3]. With the cyclotron, it became possible to produce a wide variety of radioactive isotopes for the first time. Researchers from around the world came to Berkeley in California to use the artificially produced radiotracers such as radioactive sodium and iodine in the late 1930s. Cyclotron produced radionuclides were used in the late 1930s for biomedical research, some clinical research and basic research in biochemistry. In 1936, the University of California officially established the Radiation Laboratory as an independent entity within their Physics Department. The reorganized laboratory was dedicated to nuclear science rather than, as in its first incarnation, to accelerator physics. A centre for nuclear medicine already existed at the University of California Hospital in San Francisco, where Hamilton and Stone operated the X ray tube built by Sloan. They were joined by Lawrence's brother John, who had been interested in the biological effects of neutrons during a visit to Berkeley in the summer of 1935. Finance for the machine promised by Lawrence in 1936 was raised on the ground of its utility in medicine [3.4].

Even with this background, in the early years, cyclotrons were mainly used in physics research. Radionuclides for medical applications were a sideline. The first cyclotron dedicated to medical applications was installed at Washington University, St Louis, in 1941, where radioactive isotopes of phosphorus, iron, arsenic and sulphur were produced. During World War II, a cyclotron in Boston also provided a steady supply of radionuclides for medical purposes. In the mid-1950s, a group at Hammersmith Hospital in London put into operation a cyclotron wholly dedicated to radionuclide production. The major change occurred in the early and mid-1960s when the work in hot atom chemistry (e.g. the in situ chemistry of nucleogenic atoms occurring in a target being bombarded) laid the foundations for the synthesis of organic compounds labelled with positron emitters. An article by Ter-Pogossian and Wagner in 1966 focused on the use of ^{11}C [3.5]. As the field of nuclear medicine has progressed, the number of available types of particle accelerators with varying characteristics dedicated to radionuclide production for nuclear medicine has also expanded. The major classes of accelerators are the positive and negative ion cyclotrons. More recent innovations include superconducting magnet cyclotrons, small low energy linacs, tandem cascade accelerators and helium-particle-only linacs. These types of accelerators have not gained wide acceptance, mainly as a result of lack of experience in radionuclide production applications. While traditional van de Graaff accelerators have been used for radionuclide production, they probably should not be considered for new installations.

Wolf and Jones [3.6–3.8] have reviewed the application of cyclotrons for the production of radionuclides and suggested that accelerators can be classified into four categories, reflecting the particle type and the energy of these particles. These categories are listed in Table 3.1 (adapted from Wolf and Jones [3.7, 3.8]).

Each class of machine is described in Sections 3.2 and 3.3, while Section 3.5 focuses on the considerations pertinent to the choice of an accelerator and the placement of the accelerator in a typical operating environment.

TABLE 3.1. CLASSIFICATION OF ACCELERATORS

Classification	Characteristics	Proton energy (MeV)	Comments
Level I	Single particle, p or d (some dual particle)	10	
Level II	Single or multiple particle, p, d	20	He-3, He-4: not usually available
Level III	Single or multiple particle, p, d	50	He-3, He-4: may be available
Level IV	Usually p only	70–500	

Note: Here, p denotes proton and d denotes deuteron.

3.2. DEVELOPMENT OF LINEAR ENERGY ACCELERATORS (LINACS)

The concept of the linac arose because there is a practical limit to the energy that can be supplied to a particle between two single electrodes. No matter how well the electrodes are insulated, there will be a discharge of the potential to ground. To overcome this limitation, Wideroe devised a system in Germany in the 1930s that would allow particles to be accelerated in many small steps, which add up to a much greater potential than one giant push.

3.2.1. Principle of operation

The principle of acceleration used in all accelerators is the fact that a charged particle has its energy changed when it is acted on by an electric field. In the linac, this change in energy is applied by an alternating potential, which must be applied in exactly the proper sequence to keep accelerating the particle. In practice, this is achieved with the use of hollow electrodes called drift tubes, which allow the particle to drift at constant velocity within the tube and then be accelerated between the tubes. The particle is accelerated into the tube by an electric field that is opposite in sign to the charge on the particle. As the particle passes through the hollow tube, the phase of the electric field is changed and, at the exit of the tube, the particle is accelerated with a push from the field which now has the same sign as the particle. This is shown in Fig. 3.1.

One fact that helps to maintain the timing of the acceleration is what is referred to as phase stability. The potential at each stage of the accelerator can be set so that the maximum potential is applied just after the particles have passed a given point.

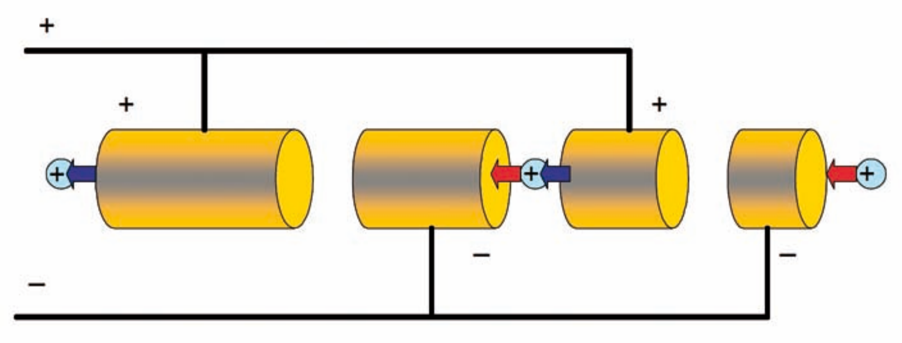

FIG. 3.1. Positively charged particles are pulled into the hollow electrode and then pushed out as the phase of the accelerating field is changed.

This allows for some margin of error in the timing. If the particle arrives too early, the potential applied will be slightly less than optimum and the particle will traverse the next section more slowly and will be in phase for the next accelerating potential. If the particle is moving too slowly and arrives a little late, the phase of the accelerator can give it a little extra push and again the particle will move to be in phase at the next section of the accelerator. This effect will result in the particles emerging from the end of the linac in bunches. The magnitude of this effect can sometimes be a problem in the design of targetry for a linac, since the instantaneous power delivered to a target can be quite high.

3.2.1.1. Radiofrequency acceleration

The radiofrequency power for current designs of medical linacs is supplied at high frequency (200–500 MHz), which allows the overall length of the linac to be much shorter. The power for the RF system is usually supplied with a bank of power tubes contained within a coaxial cavity. The employment of very high frequencies allows the use of shorter sections for the drift tubes and allows a linac to be shorter. This is an extremely important factor, since the particles must traverse the length of one drift tube in one cycle of the radiofrequency. This implies that the length of the drift tube must be

$$l = \beta\lambda$$

where

l is the length of the tube;
β is the fraction of the speed of light for the particle; and
λ is the free space wavelength of the radiofrequency.

In order to build a linac supplying reasonable energies and of reasonable size, a high frequency is essential. Power supplies that can provide high power at high frequency have only recently become available.

3.2.1.2. Structure of the linac

A linac design that is typical of new developments incorporates four sections, as shown in Fig. 3.2. The first section is an ion source that produces a pulsed proton beam of 30 keV with a single electrode system. In the second section, this beam is bunched and then injected into a radiofrequency quadrupole (RFQ), which is the third section. The energy at the end of this

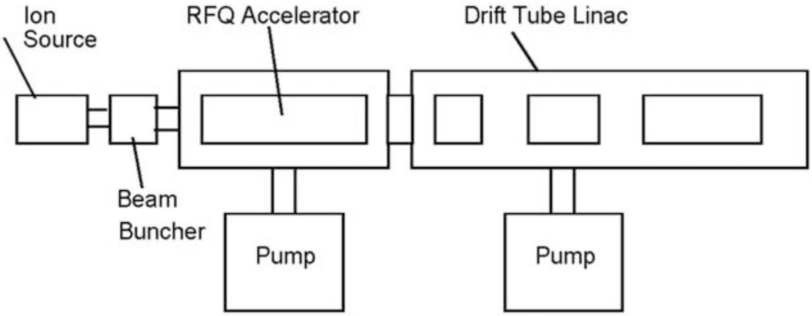

FIG. 3.2. Structure of a modern (RFQ) drift tube linac for production of radionuclides.

section is of the order of 2 MeV. The beam is then transported to the fourth section, where the phase space of the beam is matched to the phase space acceptance of the drift tube linac, and where the protons are accelerated to the final energy of 11 MeV.

3.2.1.3. High vacuum

In any linac, a fairly good vacuum must be maintained in order that the charged particles have a mean free path long enough to pass from one drift tube to the next without being scattered. In most cases, this is done either with a turbomolecular pump, a cryopump or a diffusion pump. The turbopump and diffusion pumps must be backed up by a mechanical pump, as is the case with cyclotrons. In linacs, this vacuum must be maintained at a level of better than 1×10^{-6} mm of Hg.

3.2.1.4. Radiofrequency quadrupole

This concept was developed in the Russian Federation but was first applied in the United States of America (USA). The concept is that instead of a hollow electrode drift tube, the sections of the acceleration structure are made of vanes that are set at 90° to each other and to the path of the beam. These vanes are charged by the radiofrequency field and serve the same function as the drift tubes of the traditional linac design. The components of a typical linac are shown in Fig. 3.3.

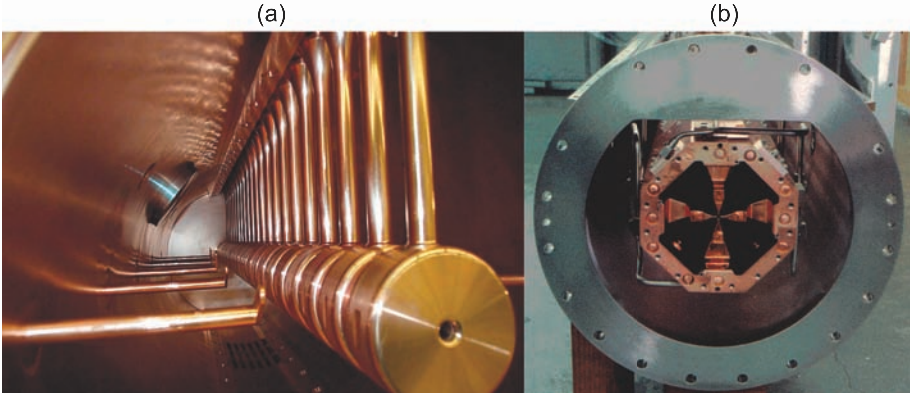

FIG. 3.3. A typical drift tube linac and an RFQ: (a) the interior of a drift tube linac; (b) a section of an RFQ.

3.2.2. Current linacs

In the late 1980s, the United States Department of Defense supported research and development of new accelerators based on the ‘Star Wars’ technology. There were three funded projects, all of which were of a linear design [3.9]. The aim was to make use of technology that could produce a very high density of particle beams of low energy. These new accelerators were to compensate for the low production cross-sections at low energy (<10 MeV) with the increased beam current (100–1000 μA).

While the accelerator technology had advanced to achieve these beam currents, the target technology had not been tested under these severe conditions. Science Applications International Corporation, San Diego, California, planned to build an 8 MeV $^{3}He^{2+}$ RFQ accelerator. Its unique features included simplicity in design and operation with a low neutron field from the accelerator (with no inherent neutrons from the accelerating particles or the nuclear reactions to be utilized — (^{3}He, ^{4}He) and (^{3}He, p)). The machine had a particle energy of 10 MeV. AccSys Technology Inc., Pleasanton, California, proposed a linac, also powered by an RFQ, but accelerating protons. A variety of energies could be achieved by varying the length of the accelerator (adding on accelerating cavities). Science Research Laboratory Inc., Somerville, Massachusetts, proposed a 3–4 MeV tandem cascade accelerator (TCA), which would accelerate deuterons for ^{15}O and ^{13}N production, as well as protons for ^{18}F production.

The TCA is an electrostatic accelerator that starts with negative ions which pass through a charge stripper to convert them to positive ions, and doubles the energy for the same potential difference. At the same time, Ion Beam Applications, Louvain-la-Neuve, Belgium, built a 3 MeV D^+ cyclotron dedicated to the production of ^{15}O. Several of these small cyclotrons have been situated in Europe. Of the Star Wars machines, only the TCA was built, installed and operated on a routine basis to produce radioisotopes for PET.

3.3. DEVELOPMENT OF CYCLOTRONS

Cyclotrons are the most commonly used devices for acceleration of particles to energies sufficient for bringing about the required nuclear reactions. It was the remarkable idea of E. Lawrence to bend the path of the particles in a linac into a circle and therefore to use the same electrode system over and over again to accelerate the particles. This idea is the basis of all modern cyclotrons, and has made the cyclotron the most widely used type of particle accelerator. The first model was built in 1930, with proof of particle acceleration being provided by Livingston in 1931.

Unfortunately, the literature on cyclotrons for medical purposes is somewhat sparse. The book by Livingood published in 1961 [3.10] and a more recent review by Scharf [3.11] are general texts on cyclotrons and other particle accelerators. Detailed information on advances in cyclotrons and other accelerators is available as a series of symposia papers [3.12]. Cyclotrons for biomedical radionuclide production have been reviewed in Ref. [3.8].

3.3.1. Principles of operation

According to the theory of electrodynamics, the rotational frequency of a charged particle travelling in a magnetic field is independent of the radius of its orbit. The energy of the particle increases as the velocity of the particle increases. The cyclotron utilizes this fact to produce particles of reasonably high energy in a relatively confined space. The acceleration chamber of the cyclotron is placed between the poles of a homogeneous magnetic field, as shown in Fig. 3.4.

The cyclotron magnetic field causes particles to travel in circular orbits. Ions are produced in an ion source at the centre of the machine and are accelerated out from the centre. The ions are accelerated by a high frequency electric field through two or more hollow electrodes called ‘dees’. The ions are accelerated as they pass from one dee to the next through a gap between the

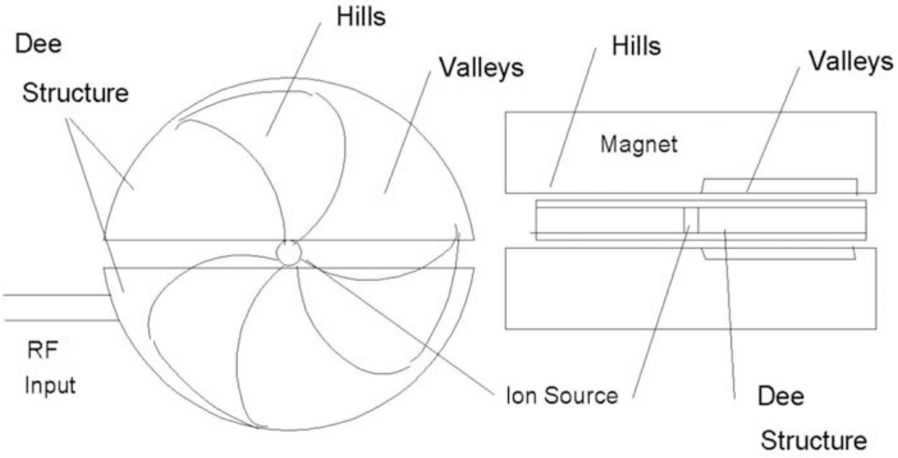

FIG. 3.4. Structure of a cyclotron showing the magnet, 'dee' structure and ion source.

dees. Since the rotational frequency of the particles remains constant as the energy of the particles increases, the diameter of the orbit increases until the particle can be extracted from the outer edge of the machine. The limit on the energy of a particle is determined on a practical basis by the diameter of the magnet pole face. Some very large, high energy cyclotrons have been built, but, for the most part, the proton energies are less than about 70 MeV.

3.3.1.1. Radiofrequency acceleration

Both the fundamental frequency and higher order harmonics of RF fields may be used for acceleration of charged particles in a cyclotron. The energy of the particle and the harmonic used will determine the exact structure of the hollow electrodes (dees), as shown in Fig. 3.5. When the RF field is coupled to the dees, electric field gradients are produced. In each pair, one of the dees is at ground potential and the other is at a higher voltage. Since the particle will feel an electric field when entering and leaving a dee, the number of gap crossings per revolution equals twice the number of dees. An accelerating structure may have one, two, three or even more dees. The energy gain of a particle crossing an accelerating gap depends on the charge, the amplitude of the potential difference, the phase relationship of the particle to the electric field and the path length between the electrodes.

The particle must cross the gap between two dees at a given time or it will not be accelerated. For a two dee system operating at the fundamental frequency, the time interval is given by the following relation:

$$1/\omega = r/v$$

where

ω is the orbital frequency;
r is the radius in the median plane; and
v is the orbital velocity.

3.3.1.2. Magnetic field for a circular path

The radius of the orbit of a particle in a magnetic field is given by the following relation:

$$r = p/[qB_z(r)]$$

where

r is the radius of the particle in the median plane;
p is the momentum of the particle;
q is the charge of the particle; and
$B_z(r)$ is the magnetic induction in the median plane at the radius r.

This is the stable equilibrium orbit, and particles usually oscillate around this orbit. This equation and the equation for the radius of the particle in the magnetic field are the fundamental equations for cyclotrons. Although in theory the frequency of the orbit is constant, in practice the frequency of the orbit decreases with the radius as a result of relativistic mass increases and the decreasing magnetic field strength with radius. A particle in phase with the accelerating voltage at the centre of the cyclotron will gradually become out of phase, limiting the highest energy achievable with this type of cyclotron to about 20 MeV.

This problem can be solved by azimuthally varying field (AVF) cyclotrons that apply the principle of alternating gradient focusing to allow an increase in the magnetic field as the radius increases. The alternating gradient is produced by making the gaps between the poles of the magnets alternately smaller and larger.

The areas where there is a smaller gap (stronger field) are called ‘hills’ and those with a larger gap (weaker field) are called ‘valleys’ (Fig. 3.5). The use of spiral, instead of radial, hills and valleys enhances the effect so that cyclotrons of up to 500 MeV may be built. Strong magnetic fields will have an

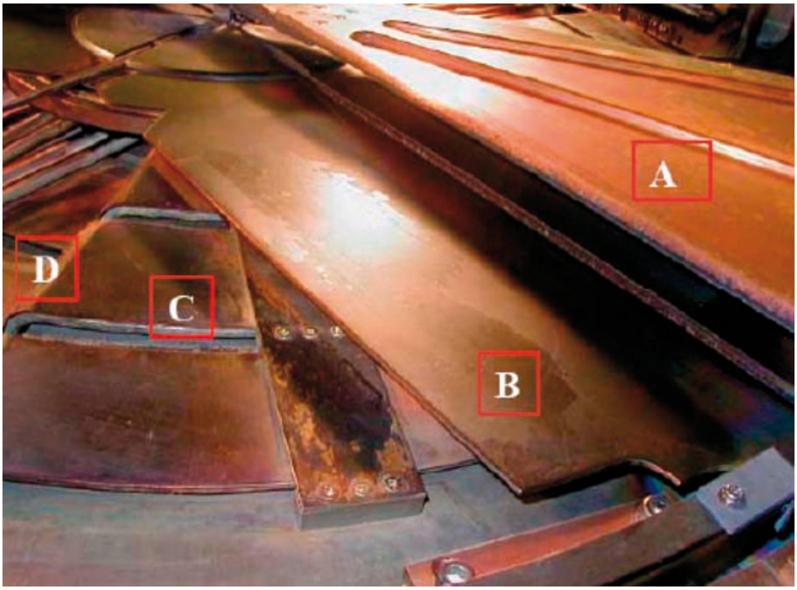

FIG. 3.5. Inside a cyclotron vacuum tank, showing the dees (A), the lower dee cover (B), the circular coils (C), and the transition between the hill and the valley (D).

effect on the focusing of the beam, and this fringing field must be considered in the design of a cyclotron.

3.3.1.3. Ion sources

There are several types of ion sources with different operating characteristics. The extraction of positive and negative ions from the ion source and the path in the central region of the cyclotron are determined in part by the ion source characteristics. Cyclotrons may have either an internal or an external source of ions for acceleration. On most commercial cyclotrons, the source is internal. Charged ions are usually produced by the arc discharge in a gas yielding plasma. The two main types used in cyclotrons are the hot cathode and the cold cathode. In the hot cathode type, a heated filament is used to maintain the arc.

In the cold cathode type, once the discharge has been initiated, no hot filament is used to maintain the plasma during normal operation of the ion source. The spatial distribution and output of an internal source are not well defined. In addition, the ions usually have a broad distribution of energies. These problems are usually overcome by using slits on the ion source that reduce the beam intensity but produce a well defined beam profile. Once the ions are out of the ion source, the path of the beam is further defined by a ‘puller’. This is a small slit in a metal plate that accepts only those ions with the proper energy and position to continue past the first orbit (Fig. 3.6). The whole assembly is referred to as the central region. Misalignment of the central region results in a beam that is off-centre. This can usually be detected and corrected by the use of internal probes (to measure beam current) and by ion source positioning and intensity adjustments.

3.3.1.4. Vacuum systems

The vacuum inside the cyclotron must be maintained at a fairly high level in order that the particles have a mean free path long enough to be accelerated effectively. In the case of cyclotrons, this translates into a pressure inside the tank between 1×10^{-5} and 1×10^{-7} mm of Hg, depending on the charge of particle being accelerated, whether the ion source is internal or external, and the type of cyclotron. A higher vacuum (10^{-6}–10^{-7} mm of Hg) is required for negative ion machines than is required for positive ion machines, since gas collisions may cause charge stripping.

There are three major types of vacuum pumps commonly used for cyclotrons. The first is the oil diffusion pump, the second is the turbomolecular pump and the third is the cryopump. Oil diffusion pumps are very reliable and easy to maintain, but have the disadvantage that oil vapour can get into the cyclotron and cause carbon deposits to build up on some surfaces in spite of in-line trapping systems. The usual cause of failure of diffusion pumps is heater burnout. The heaters are easily replaced, and the cyclotron can be back on-line in a short time.

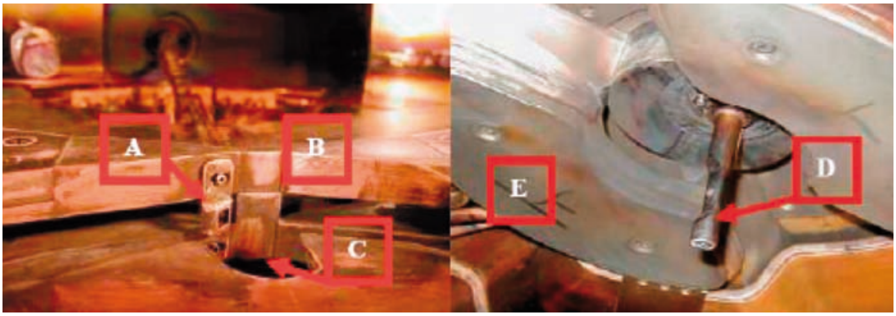

FIG. 3.6. Axial ion source configuration showing the puller (A), dee (B), central region where the ion source is lowered into place (C), ion source cone (D) and magnetic central region (E).

Turbomolecular pumps are much cleaner and have much higher pumping speeds but suffer from the disadvantage of being susceptible to damage to the vanes by a sudden burst of air, as would occur in the case of a foil failure on a target. There are now turbomolecular pumps on the market that are nominally capable of withstanding a sudden burst of gas with no damage. Turbomolecular pumps are also very sensitive to alignment. They must be protected from small pieces of metal that may be in the cyclotron from ruptured foils or flakes. When these pumps fail it is usually necessary to replace the vane assembly, which is an expensive and time consuming proposition.

Cryopumps are gas entrapment vacuum pumps. The principle of their operation is that gaseous substances are bound to the cold surfaces within the pump by means of cryocondensation, cryosorption or cryotrapping. In order to be able to produce a high or an ultrahigh vacuum, the cold surfaces (cryopanels) must be cooled to a sufficiently low temperature. Typical temperatures on the cryopanels are 10–20 K. An important aspect in the operation of cryopumps is that of regeneration. Since a cryopump is a gas entrapment pump, the gases that have accumulated in the pump during the ‘pumping’ mode must, from time to time, be removed from the pump. This is done by switching the compressor unit off and by warming up the cryopanels to room temperature or slightly higher so that the released substances can be pumped out by a conventional fore-pump. It is often advantageous to have a valve between the cryopump and the vacuum chamber.

3.3.1.5. Extraction systems

Extraction of the beam depends on whether the charge on the particles is positive or negative. If the particles are positively charged, extraction is carried out electrostatically, as shown in Fig. 3.7(a). If the particles are negatively charged, extraction is carried out by stripping electrons off the negatively charged ions and allowing the magnetic field to reverse the curvature of the resulting positively charged particle paths and to transport the particles out of the cyclotron, as shown in Fig. 3.7(b).

A photograph of the positive ion extraction system showing the septum and deflector is presented in Fig. 3.8. The septum in this case is a split septum. The purpose of the septum is to separate the extracted beam from the circulating beam.

A photograph of a negative ion extraction system is shown in Fig. 3.9. A thin carbon foil is used to remove electrons from the negatively charged ions. This type of foil positioning system can allow extraction of beams at variable energies.

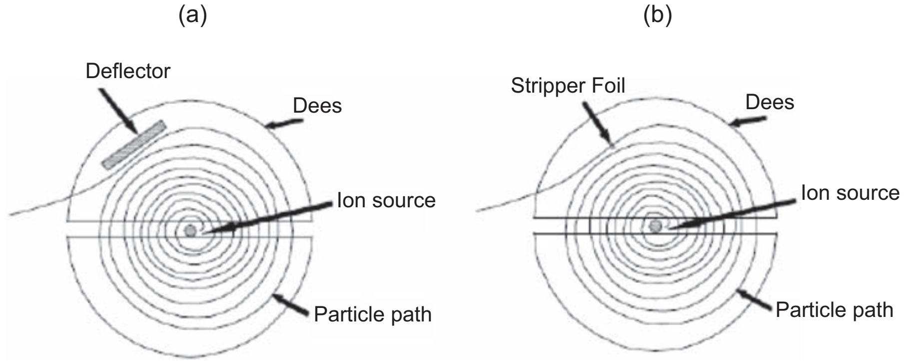

FIG. 3.7. Extraction process in modern cyclotrons using either (a) a deflector for positive ions or (b) a stripper foil for a negative ion source.

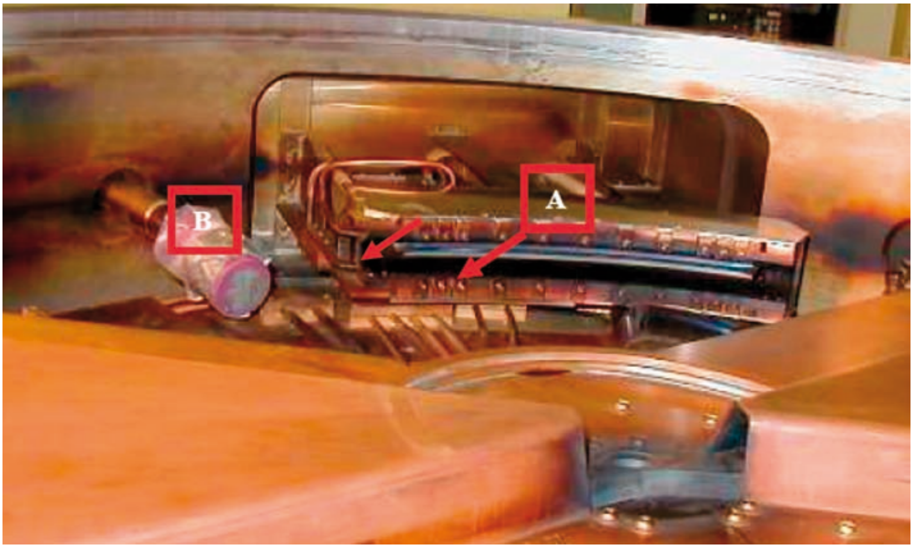

FIG. 3.8. Deflector showing the split septum (A), with the deflector bar being immediately behind the septum. Also shown is a beam probe that has been shielded with lead for maintenance operations (B).

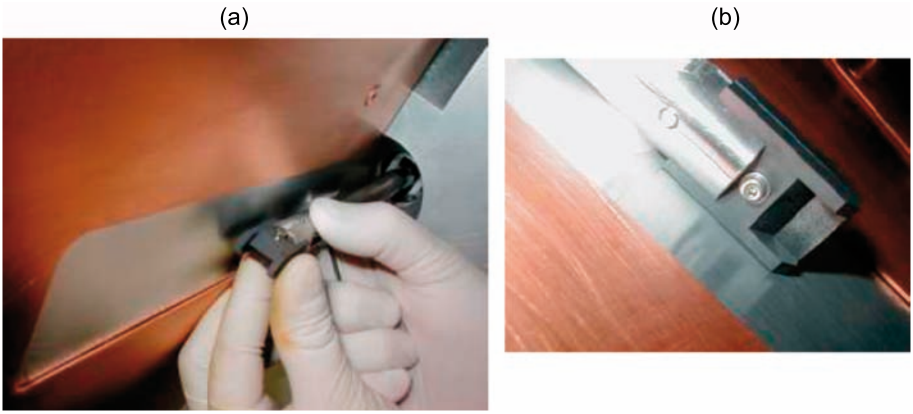

FIG. 3.9. (a) Thin carbon foil and (b) positioning arm in a modern negative ion cyclotron.

3.3.2. Current cyclotrons

The technology of cyclotrons has improved significantly over the last decade. Cyclotrons are now stable machines, controlled by computers, which can produce a wide variety of radioisotopes. The technology underlying these machines has become more complex, but a basic understanding of the principles and practical limitations of these machines is very helpful in understanding the problems that can arise with them.

3.3.2.1. Negative and positive ion machines

Nearly all modern cyclotrons use a negative ion source. Ions are generated by passing the source gas through a plasma maintained in an electric field that generates negative and positive ions (e.g., in the case of H_2, the resulting primary ions will be H^+ or protons, and H^{2-} ions (a proton with two electrons)). The advantage of negative ions resides in the ability to easily have a variable energy cyclotron, to have nearly 100% extraction and to be able to extract multiple beams simultaneously. Modern ion source technology allows the ion source to reside either inside the cyclotron, where the ions are generated directly in the central region of the cyclotron (internal ion sources), or outside the cyclotron (external ion sources), where the ions are injected into the central region for acceleration.

There are obviously advantages and disadvantages to each approach. With an external ion source, the vacuum can be operated at very low pressures with very little beam loss due to stripping of the negative ion by the residual gas. However, the vacuum system must be very efficient and clean (no oil contamination) to maintain this high vacuum. With an external ion source, maintenance can be performed without opening the cyclotron or breaking the vacuum. In addition, the centre region is not disturbed as in the case of an internal ion source that is part of the central region.

3.3.2.2. Extraction of beams

Some early cyclotron designs did not extract particle beams, and target irradiations were performed by bombarding internal targets. In order to extract a beam, an electrostatic device was inserted at the requisite radius to obtain the desired energy and the beam was deflected out of its normal circular path. The beam was directed by this electrostatic field to a position where there was an exit window in the vacuum tank and then impinged on a target attached to the vacuum tank, or was directed to a target station through an evacuated beamline. The relatively poor efficiency of the deflection system meant that as much as 30–40% of the beam was lost through collisions with the deflector or surrounding materials. This loss of beam has two effects:

(1) A low efficiency in beam production;
(2) Activation of cyclotron components due to particle interaction inside the cyclotron tank.

With negative ion machines, the beam is extracted by passing the negative ions through an ultra-thin foil (usually graphite) that strips the loosely bound electrons from the atom, resulting in a change in the electrical charge of the beam. Thus, the original negatively charged particle (H^-) will now be positively charged (H^+), and the beam will rotate in the opposite direction. By placing exit ports on the cyclotron tank wall, the beam can be directed out to the appropriate target systems. The variable energy feature is accomplished by moving the extraction foil to different radii. The extraction of multiple beams is accomplished by inserting the extraction foil(s) so that they only intercept part of the beam, allowing the remainder to continue its acceleration to the next extraction foil. Thus, not only are two simultaneous beams possible, but also beams of different energies and intensities. In general, the extraction arm is calibrated according to position and energy.

3.3.2.3. Energies and particles

The energy of the accelerator needed again depends on the demands of the programme. As can be seen from Table 3.2, the range of nuclides produced

TABLE 3.2. POPULAR RADIONUCLIDES VERSUS THE PROTON ENERGIES REQUIRED FOR THEIR PRODUCTION

Proton energy (MeV)	Radionuclides easily produced
0–10	F-18, O-15
11–16	C-11, F-18, N-13, O-15, Na-22, V-48
17–30	I-124, I-123, Ga-67, In-111, C-11, F-18, N-13, O-15, Na-22, V-48, Tl-201
30+	I-124, I-123, Ga-67, In-111, C-11, F-18, N-13, O-15, Sr-82, Ge-68, Na-22, V-48

and the quantities increase with particle energy. This table shows only proton reactions and only a few of the radionuclides that can be produced at these energies.

However, this increase in the number of radionuclides that can be produced comes at a cost both in equipment and in infrastructure. In addition, the number of side channel reactions increases as the energy increases, and unwanted radionuclides can be produced. This is especially true at energies greater than 30 MeV.

The production of the traditional radioisotopes used in nuclear medicine (^{201}Tl, ^{67}Ga, ^{123}I and ^{111}In) has been via proton reactions for more than 25 years. However, many of the most useful radionuclides can be produced with proton energies of below 30–40 MeV. Higher energy cyclotrons (energies greater than 40 MeV) are usually installed only at large laboratories, government facilities or large commercial facilities where radionuclides are produced for sale. The particular choice of particle(s) and energy will depend on the envisioned programme. The selection of a cyclotron will also depend on which radionuclides are needed to prepare the radiopharmaceuticals used in the clinical and research programmes, and on whether these radioisotopes will be distributed to other locations.

3.4. OTHER TYPES OF ACCELERATOR

3.4.1. Tandem cascade accelerators

Tandem cascade accelerators use a single large potential to accelerate charged particles. This type of accelerator was first developed by van de Graaff in 1931. The physical principle underlying these machines is that an electric charge placed within a hollow metal conductor must move to the outside surface of the conductor. The accelerator based on the van de Graaff principle in use today for PET isotope production is the tandem cascade accelerator [3.13]. This type of accelerator is composed of four sections:

(1) The first is an ion source.
(2) The second is an acceleration chamber.
(3) The third is a high voltage terminal with a stripper foil.
(4) The fourth is a second acceleration chamber.

A positive charge is accumulated on the high voltage terminal at the centre of the acceleration tube assembly. Negatively charged ions are inserted at ground potential from the ion source at one end of the tube. Ions are accelerated from ground potential to a high voltage at the central high voltage terminal. At this point, the charge is stripped off the ions by a thin stripper foil and the repulsive forces accelerate the ions to twice the energy of the high voltage terminal. The acceleration assembly is usually insulated from the outside by sulphur hexafluoride gas, which is capable of maintaining a high electric field gradient without ionizing. At the end of the second acceleration tube is the target for the production of the radioisotopes.

3.4.2. Van de Graaff accelerators

The most common van de Graaff accelerator is the self-excited type. A self-excited generator refers to what happens when two different materials come together and are then pulled apart. The generator consists of a well rounded high voltage terminal isolated from ground potential on an insulating column and a charge conveying system consisting of one or more flat endless belts of insulating material running between this terminal and ground. Electric charge is transported by the belt into the hollow terminal, where it is removed. The maximum voltage that can be maintained on the terminal depends only on its geometry and the dielectric of the surrounding insulating medium. The original van de Graaff generator was patented by van de Graaff [3.14]. A diagrammatic represention of a van de Graaff generator is shown in Fig. 3.10.

The Pelletron® charging chain used in most modern van de Graaff accelerators was developed in the mid-1960s as an improvement over the older charging belts. These belts suffered from a number of operational difficulties, including terminal voltage instability and susceptibility to spark damage. In addition, they generated belt dust that necessitated frequent cleaning inside the accelerator tank. Chains rapidly proved to be more durable than belts, while

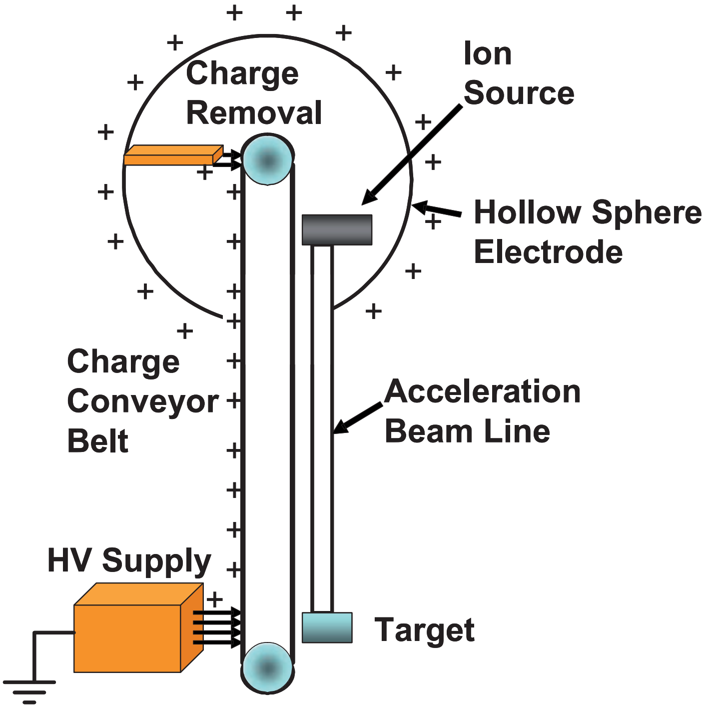

FIG. 3.10. Schematic diagram of a van de Graaff accelerator.

producing a greater terminal stability than had been possible before. Chains also eliminated the belt dust problem.

The chain does not limit the ultimate terminal potential, and it is in use in electrostatic accelerators up to and above 25 MV. Current van de Graaff accelerators are used mainly for physics research and are rarely used for radionuclide production.

3.4.3. Superconducting cyclotrons

The basic principles of operation of these machines are the same as those of conventional cyclotrons. Using a superconducting magnet, these cyclotrons can be made very compact but they must be maintained at liquid helium temperatures. The weight of the magnet is about a fifth of the weight of the magnet for a conventional cyclotron. Since the magnet is superconducting, the power requirements are much less. The higher magnetic field causes the orbits to be spaced closer together. The accelerated particle is H^-, so the extraction system utilizes a stripper foil.

3.5. CHOICE OF AN ACCELERATOR

The question we are left with is ‘Which type of accelerator is best for my situation?’ There are some practical considerations when making this decision. The main factors are initial cost, reliability, radiological hazards, installation costs, operating costs and the support available from the manufacturer. Some of these aspects are outlined in the following sections.

3.5.1. Comparison of cyclotrons with other accelerators

There are several aspects to consider when choosing an accelerator. Some of the characteristics that may be considered are given in Table 3.3.

The first consideration with any accelerator is whether or not it is capable of producing sufficient quantities of radionuclides for the particular needs of the facility. Regardless of what type of accelerator is installed, it must be kept in mind that the accelerator delivers protons, deuterons or, less commonly, ^{3}He and ^{4}He ions. The cross-sections of nuclear reactions for production of most

TABLE 3.3. GENERAL CHARACTERISTICS OF ACCELERATORS FOR RADIONUCLIDE PRODUCTION

Accelerator type	Advantages	Disadvantages
Positive ion cyclotron	Proven record Versatility Ease of maintenance	High cost High activation
Negative ion cyclotron	Extraction efficiency Low activation Beam uniformity	High cost High vacuum requirements Maintenance of stripper foil
Superconducting cyclotron	Compact size Low power	Liquid helium maintenance
Linac	Stable operation Low power	Targetry Size
Tandem cascade	Low power Low cost	Targetry
Helium-3 linac	Low power Stable operation	Low SA Targetry

radioisotopes are well characterized, and the practical yields as a function of particle energy are also well known. Selection of an accelerator is determined in practice by the energy of the particle beam required (Table 3.1) or the desired nuclear reaction. For example, for a facility wishing to produce only the conventional PET isotopes (^{11}C, ^{11}N, ^{15}O and ^{18}F), a Level I cyclotron that delivers a 10 MeV proton beam may be sufficient.

On the other hand, a centre wishing to manufacture the SPECT isotopes (e.g. ^{201}Tl, ^{67}Ga, ^{123}I and ^{111}In) must consider a cyclotron capable of delivering a higher energy particle beam (Level II or Level III).

Of all the various types of accelerators, cyclotrons are by far the most extensively used for the production of PET and SPECT radioisotopes. It is, therefore, to be expected that there is a great deal more information concerning the application and reliability of cyclotrons in comparison with the other types of accelerators. In general, cyclotrons have proven to be reliable accelerators and to provide optimum conditions for consistent isotope production. Linacs and van de Graaff accelerators have also been used for production of isotopes, but not commonly. Although linacs are also stable machines, they have been used in centres where there are accelerator physicists to address any problems, and they do not have a history in radioisotope production facilities. As more linacs are placed in radioisotope production centres, however, a better idea can be obtained as to how reliable they will be. The tandem cascade accelerator and the ^{3}He-RFQ are accelerators that have been built and tested but have proven to have very limited application to radionuclide production.

3.5.2. Radioisotope yield considerations

For routine production of radioisotopes, the practical yield can be quite different from the saturation yield of a radionuclide usually stated in the literature. Saturation occurs when the production rate of the radionuclide equals the decay rate. For any radionuclide $R = N\lambda/(1 - e^{-\lambda t})$, where R is the saturation value, N is the number of atoms and λ is the decay constant. In a practical sense, this limit is reached at about five half-lives. For example, the irradiation time for ^{18}F production to reach saturation is about 9 hours, which is much longer than one would normally irradiate this type of target. Oxygen-15 production, on the other hand, reaches saturation at about 10–12 min, which is a more practical irradiation time. Currently, each manufacturer will offer buyers a ‘guaranteed’ yield of radionuclides under defined conditions. This is a primary consideration, especially if clinical applications are contemplated.

The chemical form of the radionuclide is also of major interest in considering the attributes of any machine. The target material must withstand the intensely ionizing particle beam and must be able to withstand the intense radiation field accompanying particle bombardment. The questions of the chemical form of the radioisotope coming from the target, which target material to use and the specific bombardment conditions have been the subjects of research since the early 1950s. Target conditions can be manipulated to some extent to provide the desired precursors for syntheses of labelled compounds directly from the target.

Another aspect relating to chemistry is the choice between proton-only machines and two particle, proton and deuteron, machines. If a proton-only machine is chosen (Table 3.1), enriched isotopes are needed to produce some of the four PET radionuclides. If a dual particle machine is chosen, ^{15}O and ^{13}N can be produced from natural abundance target materials. Other radioisotopes may require enriched isotope targets with either protons or deuterons.

3.5.3. Characteristics of commercial cyclotrons

A table with the characteristics of commercial cyclotrons designed for PET radionuclide production (Annex I) and a table with the characteristics of commercially available cyclotrons with energies of 30 MeV or more (Annex II) are presented. These tables are not complete and are based on the data available in 2005. The entries are the understanding of the authors of these annexes and should always be verified with commercial suppliers. The purpose of these tables is to give the basic characteristics of cyclotrons and to show how one cyclotron would be preferable to another for a particular application. With these characteristics in mind, it should be possible to discuss options with the manufacturers and obtain the best match between a cyclotron and a particular situation.

There are models and types that have proven to be free from problems, while others need constant attention. Sometimes these two extremes are seen in cyclotrons from the same manufacturer and depend entirely on the design of the cyclotron. With the advent of crystal oscillators, computer mapping of magnetic fields, and computer control of source position, arc voltage and so forth, the amount of time spent tuning a cyclotron has been greatly reduced. The best indicator of how a machine will perform is how that machine has performed in the past and the experience of other centres which have that particular machine.

3.5.4. Operating costs

Table 3.4 presents typical operating expenses for a cyclotron. These include routine operations and consumable supplies. The exact cost of all these

TABLE 3.4. ESTIMATED OPERATING COSTS OF A CYCLOTRON

Description	Quantity per annum	Estimated cost (US $/a)
Electric power (cyclotron operations)	250 MW·h	25 000[a]
Electric power (building and air handling)	100 MW·h	10 000[a]
Parts and supplies	n.a.[b]	10 000
Annual service	1	50 000–80 000

[a] On the basis of a cost of US $0.10/kW·h.
[b] n.a.: not applicable.

items will depend on the location of the facility and the infrastructure available to it. Some very general estimates are given from experience in the USA.

3.5.5. Maintenance

Routine maintenance is extremely important for all accelerators. Since accelerators are often in constant use, some parts tend to wear quickly. Because the power involved in a typical cyclotron is often more than 30 kW, the power delivery chain is an especially vulnerable link in the operation of the cyclotron and requires special attention. O-rings and other seals, especially on moving parts, have a relatively short life and need to be replaced frequently. Vacuum pump maintenance is another key factor.

3.5.5.1. Maintenance schedule

The following is a routine maintenance schedule based on a modern cyclotron. The maintenance schedule should be supplied for each cyclotron by the manufacturer. This list is only to give an idea of the tasks involved in maintaining a cyclotron. The routine maintenance tasks have been broken down into three categories related to the difficulty of performing the procedure.

(a) Level I: Routine maintenance

The cyclotron does not have to be shut down to perform Level I maintenance operations. These tasks are performed by trained cyclotron operators.

(b) Level II: Preventive routine maintenance

These maintenance tasks are to be performed during regularly scheduled maintenance shutdowns of the cyclotron. They should be performed only by on-site service crew. Spare parts required for this maintenance level should be kept on-site.

(c) Level III: Major repairs and replacements

This level includes major repairs and replacements that cannot be performed during a regularly scheduled maintenance shutdown of the cyclotron.

A cyclotron specialist from the manufacturer must be contacted prior to the work and possibly be present when the maintenance and repair tasks at this level are performed. The spare parts required to complete these tasks will be delivered from the manufacturer as required.

The frequency of each maintenance task is summarized in Tables 3.5–3.7. The frequency times may vary depending on the intensity of machine operation. The times shown in brackets are those for a typical installation.

TABLE 3.5. LEVEL I MAINTENANCE TASKS

Procedure	Frequency
Inspect dry nitrogen gas supply	Before use, as required
Inspect helium gas supply	Before use, as required
Inspect hydraulic system	Before use
Reset fuses and breakers	As required
Replace bolus transfer lines	As required
Inspect chilled water system	Daily
Inspect compressed air system (+ check for water)	Daily
Monitor water system	Daily
Inspect hydrogen gas supply	Weekly
Check and record water resistivity	Every two weeks
Replace ion exchange column	As required
Check hydrogen gas circuit for leaks	Monthly

TABLE 3.5. LEVEL I MAINTENANCE TASKS (cont.)

Procedure	Frequency
Check and record cryo-compressor helium pressure	Monthly
Inspect the rough vacuum pump oil level and condition	Monthly
Check for water in compressed-air–water separator	Daily
Change water filters	As required (expect every two to four weeks until system is clean)
Clean compressed air dust collectors and breathers	Monthly
Inspect air hoses	Annually

TABLE 3.6. LEVEL II MAINTENANCE TASKS

Procedure	Frequency
Replace O-rings	As required
Replace ion source gas bottles (H_2)	As required
Remove water from cooling circuit	As required
Regenerate the ion source and injection system (ISIS) cryopump	Monthly
Vacuum leak testing	As required
Purge cryopump coldheads	As required
Change the ion source filament	As required
Clean the roughing network	Every six months
Regenerate the main tank cryopump	On every tank access
Add helium to the cryopump system	As required
Clean/replace radiofrequency amplifier filter	Every three weeks
Clean dust from equipment and filters	Monthly
Replace the oil in rough vacuum pump BP	Every three months
Clean the turbopump backing line	Every BP oil change
Change the adsorber in the cryopump compressor	Every three years

TABLE 3.6. LEVEL II MAINTENANCE TASKS (cont.)

Procedure	Frequency
Replace the PLC battery	Annually
Replace the helium system 7 m filter	Annually
Replace SMC quick release fittings	Every two years
Replace BNC bulkhead connectors	Every two years

TABLE 3.7. LEVEL III MAINTENANCE TASKS

Procedure	Frequency
Clean or change inflector insulators	As required
Realign inflector	As required
Replace inflector	As required (about every five years)
Change extraction foil	As required (every 20–50 mA·h)
Clean or change Einsel lens insulators	As required
Set water flow in a cooling circuit	As required
Repair probe cooling line	As required
Repair extraction probe	As required
Replace hydraulic cylinder/line	As required
Replace He compressor adsorber	Every three years
Replace an ion source lens or insulator	As required
Replace target windows	Every six months
Repair target selector	As required
Repair radiofrequency cooling line	As required
Replace radiofrequency amplifier tube	As required
Calibrate Convectron gauges	Annually
Calibrate cryopump temperature sensors	Annually

Routine maintenance of the services involves only the small number of simple tasks described in (a)–(c) below.

(a) Checks made of hydrogen, nitrogen and helium supplies

Checks of the following should be made:

(i) The pressure in the nitrogen bottle in advance of any venting;
(ii) The pressure in the hydrogen and deuterium bottles on a regular basis as established by site usage.
(iii) The pressure in the helium bottle prior to starting the beam.

(b) Replacement of ion source gas bottles

Ion source gas bottles should be replaced when the bottle pressure is less than 300 lbf/in^2 (2.07×10^4 Pa).

(c) Obtaining a list of recommended spare parts

A typical list of recommended spare parts, which should be obtained from the manufacturer while the cyclotron is being commissioned, is given below. The parts list will vary, but a few items will be common to all cyclotrons. These items are listed in Table 3.8.

TABLE 3.8. TYPICAL SPARE PARTS INVENTORY

Item	Quantity
Ion source filaments	10
Final amplifier tube	1
Driver amplifier (tube or transistors)	1 each
Cryopump	1
Power supply boards	One of each type
Diodes	One of each type
Transistors	General assortment
Filters	Assortment
Target foils	Assortment
Stripper foils	A supply for six months

3.6. CONCLUSIONS

This chapter has attempted to provide the reader with a brief introduction to the various types of accelerators, their characteristics and their practical utility for production of radioisotopes for clinical applications. Comparison of the advantages and disadvantages of each type of accelerator indicates that cyclotrons are by far the preferred type of accelerators for practical production of radioisotopes. Choice of an accelerator depends on the intended radioisotope production objectives of the facility, as well as the location and environment of the accelerator.

There are, however, some key questions to be asked when choosing an accelerator for production of PET radioisotopes. A short list of such questions is provided below:

(a) Will this machine produce the amount of radioisotopes necessary for our operations?
(b) Is this machine reliable?
(c) What are the initial costs and how do they compare with the operational costs?
(d) What personnel will be needed to operate and maintain the machine and its associated hardware?
(e) What will be required to shield this accelerator in our environment?
(f) What are the power and water requirements, and are adequate supplies of both available?
(g) Is assistance from the manufacturer readily available and, if so, at what cost?
(h) How will the radiation safety aspects be implemented and documented?
(i) How will radioisotope emissions to the environment be monitored and controlled?
(j) Are the target materials (enriched isotopes) required readily available?

This list of questions is a starting point; answers should have been found for all the accelerators under consideration before a final decision is taken. The best course of action is always to obtain as much information as is possible.

REFERENCES TO CHAPTER 3

[3.1] RUTHERFORD, E., Collisions of alpha particles with light atoms, IV. An anomalous effect in nitrogen, London, Edinburgh and Dublin Phil. Mag. and J. Sci. **37** (1919) 581.

[3.2] LAWRENCE, E.O., EDLEFSEN, N.E., On the production of high speed protons, Science **72** (1930) 376–377.

[3.3] LAWRENCE, E.O., LIVINGSTON, M.S., The production of high speed protons without the use of high voltages, Phys. Rev. **38** (1931) 834.

[3.4] HEILBRON, J.L., SEIDEL, R.W., WHEATON, B.R., Lawrence and His Laboratory, A Historian's View of the Lawrence Years, LBL Newsmagazine, Lawrence Berkeley Natl Lab., Berkeley, CA (1981), http://www.lbl.gov/Science-Articles/Research-Review/Magazine/1981/

[3.5] TER-POGOSSIAN, M.M., WAGNER, H.N., Jr., A new look at the cyclotron for making short-lived isotopes, Nucleonics **24** (1966) 50.

[3.6] WOLF, A.P., "Cyclotrons for biomedical radioisotope production", Medical Radionuclide Imaging (Proc. IAEA Symp. Los Angeles, 1977), Vol. 1, IAEA, Vienna (1978) 343–353.

[3.7] WOLF, A.P., Cyclotrons, radionuclides, precursors, and demands for routine versus research compounds, Ann. Neurol. **15** (Suppl.) (1984) S19–S24.

[3.8] WOLF, A.P., JONES, W.B., Cyclotrons for biomedical radioisotope production, Radiochim. Acta **34** (1983) 1–7.

[3.9] RUTH, T.J., PATE, B.D., ROBERTSON, R., PORTER, J.K., Radionuclide production for the biosciences, Nucl. Med. Biol. **16** (1989) 323–336.

[3.10] LIVINGOOD, J.J., Principles of Cyclic Particle Accelerators, Van Nostrand, Princeton, NJ, and New York (1961).

[3.11] SCHARF, W., Biomedical Particle Accelerators, American Institute of Physics Press, New York (1994).

[3.12] DUGGAN, J.L., MORGAN, I.L., Applications of accelerators in research and industry, Nucl. Instrum. Methods Phys. Res. B **56** (1990) 57.

[3.13] SHEFER, R.E., KLINKOWSTEIN, R.E., HUGHEY, B.J., WELCH, M.J., "Production of PET radionuclides with a high current electrostatic accelerator", Targetry and Target Chemistry (Proc. 4th Int. Workshop Villigen, 1992), TRIUMF, Vancouver (1992) 4–10, http://trshare.triumf.ca/~buckley/wttc/proceedings.html

[3.14] VAN DE GRAAFF, R.J., Electrostatic Generator, US Patent 1991236, 1935, filed Dec. 1931; copies available from United States Patent and Trademark Office, Washington, DC.

Chapter 4

THEORY OF RADIOISOTOPE PRODUCTION

4.1. INTRODUCTION

The production of radioisotopes for use in biomedical procedures, such as diagnostic imaging and/or therapeutic treatments, is achieved through nuclear reactions in reactors or from charged particle bombardment in accelerators. In reactors, the nuclear reactions are initiated with neutrons, while in accelerators the typical charged particle reactions utilize protons, although deuterons and helium nuclei ($^{3}He^{2+}$ and alpha particles) play a role. While ^{99}Mo for the $^{99}Mo/^{99m}Tc$ generator is produced in reactors and the procedures using this generator account for nearly 90% of all nuclear medicine procedures, this chapter will focus on utilization of low energy (<50 MeV protons/20 MeV deuterons) accelerators for the production of radioisotopes.

One clear advantage that accelerators possess is the fact that, in general, the target and product are different chemical elements. This makes it possible to:

(a) Find suitable chemical or physical means for separation;
(b) Obtain high SA preparations, owing to the target and product being different elements;
(c) Produce fewer radioisotopic impurities by selecting the energy window for irradiation.

The available accelerators fit into three categories (see Chapter 3):

(1) Firstly, there are university based cyclotrons, which are typically multiparticle machines with energies around 30–50 MeV.
(2) Secondly, there are hospital based machines, which are generally dedicated to the production of the standard PET radioisotopes (^{11}C, ^{13}N, ^{15}O and ^{18}F). These cyclotrons accelerate protons in the 10–19 MeV range, and some also produce deuterons with an energy of about half that of the protons (5–9 MeV).
(3) Thirdly, there are the cyclotrons used by industry for large scale production. These are typically 30 MeV proton-only machines, although some use lower energies for dedicated production of ^{103}Pd.

Several national laboratories are involved in the production of radioisotopes that are not produced by commercial radioisotope producers. Examples of these are ^{82}Sr for ^{82}Sr/^{82}Rb generators, ^{68}Ge for ^{68}Ge/^{68}Ga generators and PET calibration sources. These machines are typically operated above 100 MeV and accelerate protons with beam currents exceeding 150–200 μA. The limitations of these high energy facilities include the difficulty associated with scheduling, since most of these facilities have machines that have been built around nuclear physics programmes with medical applications using the accelerator in parasitic mode or have no operational medical physics programme. Another problem is the range of products produced. Because of the high energy of the proton beam, the dominant reaction mechanism is spallation, which produces not only many different atomic species but also many isotopes of the same element. This produces not only possible radioactive contaminants but also stable species that can affect the SAs of the desired product.

There are three major reasons that accelerator produced radioisotopes are used widely and that they are becoming ever more popular. These are:

(1) Accelerator produced radioisotopes have more favourable decay characteristics (particle emission, half-life, gamma rays, etc.) in comparison with reactor produced radioisotopes.
(2) Radioisotopes cannot usually be produced in reactors with high SAs.
(3) Access to reactors is often very limited (perhaps the most important reason). The number of reactors available to the scientific community has become significantly less than the number of cyclotrons available. This reduction in the number of available reactors is a problem that was already predicted in 1983 to become more severe [4.1]. This prediction has been borne out over the last 20 years.

4.2. NUCLEAR REACTION MODELS

In the classic sense, a reaction between a charged particle and a nucleus cannot take place if the centre-of-mass energy of the two bodies is less than the Coulomb barrier. In the case that applies to the production of radionuclides with a cyclotron, this implies that the charged particle must have an energy greater than:

$$B = Zze^2/R$$

where Z and z are the atomic numbers of the two species involved, e^2 is the electric charge, squared, and R is the separation of the two species in centimetres.

In fact, these reactions take place at energies well below this barrier due to the effects of quantum tunnelling.

4.2.1. Compound nuclei

The exact mechanism of nuclear reactions is not yet completely understood, but a simple approximation may be used to visualize the process. The first, and one of the most useful models, was proposed by Bohr in 1936, in which a nuclear reaction occurs as two distinct processes.

The first process is the formation of a 'compound' nucleus, which then decomposes into decay products. An important corollary of this model is that the compound nucleus 'forgets' how it was formed, except for all the fundamental conservation laws remaining in effect [4.2]. As the incident nuclear particle combines with the nucleus, it looses its identity, and the total energy of the compound nucleus is shared among all the nuclear particles. In essence, the nucleus comes to some form of equilibrium before decomposing by emission of particles.

The next process in a nuclear reaction is the decomposition of the compound nucleus. This decomposition can take place by numerous paths, usually called exit channels. These channels are independent of the way in which the nucleus was formed and are only constrained by the conservation of mass–energy, charge, angular momentum, spin and total momentum. These two steps are considered to be independent of one another. The total amount of excitation energy contained in the nucleus is given by the following equation:

$$U = [M_A/(M_A + M_a)]T_a + S_a$$

where

U	is the excitation energy;
M_A	is the mass of the target nucleus;
M_a	is the mass of the incident particle;
T_a	is the kinetic energy of the incident particle; and
S_a	is the binding energy of the incident particle in the compound nucleus.

The nucleus can decompose along several channels as shown in Fig. 4.1.

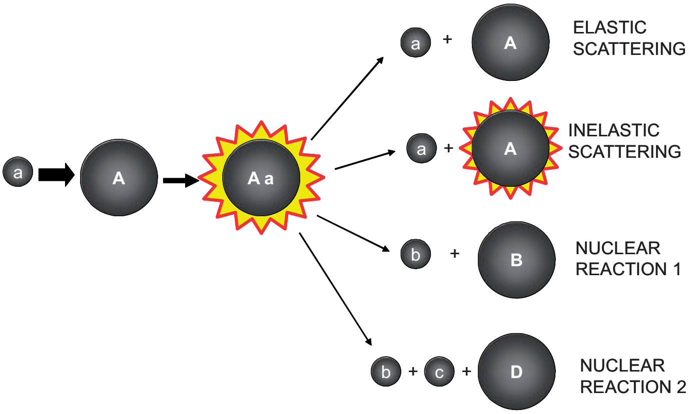

FIG. 4.1. Compound nucleus formation with possible exit channels; the symbol a represents the bombarding particle, and b and c are the emitted particles, while A, B and D are the nuclei.

4.3. KINEMATICS

When a compound nucleus decomposes, the kinetic energy of all the products may be either greater than or less than the total kinetic energy of all the reactants. If the energy of the products is greater, then the reaction is said to be exoergic. If the kinetic energy of the products is less than that of the reactants, then the reaction is said to be endoergic.

4.3.1. *Q* values

If the reaction is endoergic, then energy of an amount greater than Q must be supplied in order for the reaction to proceed. The magnitude of this difference is called the Q value. If the reaction is exoergic, Q values are positive. An example of possible reaction pathways is shown in Fig. 4.2, along with their corresponding Q values. The energy changes in a nuclear reaction are large enough that changes in the masses of the reactants and products are observable.

The nuclear reaction cross-section represents the total probability that a compound nucleus will be formed and will then decompose along a particular channel. This is often called the excitation function. This function determines the amount of a radionuclide that can be produced in a given cyclotron and the levels of contamination of other radioisotopes that may be present in the target

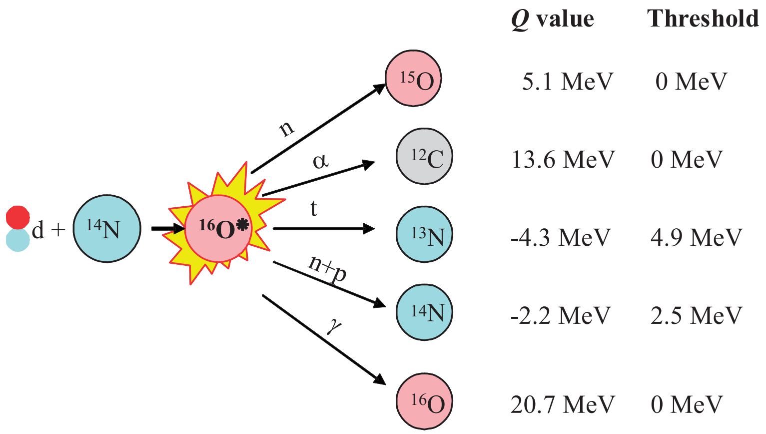

FIG. 4.2. Q values and thresholds of nuclear decomposition for the reaction of a deuteron with a ^{14}N nucleus after forming the compound nucleus ^{16}O.

material. A detailed examination of the various theories of how a charged particle interacts with a nucleus to produce a nuclear transformation are beyond the scope of this chapter; but a general description of how this interaction occurs may provide an insight into the parameters that are important in the production of radioisotopes and, therefore, a better feel for which reactions are possible at a given energy. Such a description can also provide an insight into how important competing reactions might be under various irradiation conditions.

4.3.2. Nomenclature

The nomenclature for nuclear reactions as it is usually used throughout this book needs to be defined. If a ^{13}C nucleus is irradiated with a proton beam to produce a nucleus of ^{13}N with a neutron emitted from the compound nucleus, then this reaction will be written as $^{13}C(p, n)^{13}N$. In a similar manner, if a ^{20}Ne nucleus is bombarded with a deuteron beam to produce a nucleus of ^{18}F with concomitant emission of an alpha particle, then this reaction sequence will be abbreviated as $^{20}Ne(d, \alpha)^{18}F$.

4.3.3. Model estimates

Using this model, it is possible to make some observations and predictions about the behaviour of the cross-sections of nuclear reactions. The cross-section is the probability of a nuclear reaction occurring and is expressed in geometric terms as an area (cm^2). For any nuclear reaction, the cross-section may be represented by the following relation:

$$\sigma_i = \sigma_{com}(P_i/\Sigma P_j)$$

where

σ_i is the cross-section for a particular product i;
σ_{com} is the cross-section for formation of the compound nucleus;
P_i is the probability of process i; and
ΣP_j is the sum of the probabilities of all such processes.

The theoretical representation of σ_{com} is complicated, but several qualitative generalizations should be noted [4.3]:

(a) σ_{com} is small but finite for bombarding energies that are far below the Coulomb barrier height.
(b) σ_{com} increases very rapidly with incident particle kinetic energy when the kinetic energy is less than the barrier height, behaving in a similar manner to a Gamow type barrier function.
(c) σ_{com} does not reach its maximum at a point where the kinetic energy is equal to the barrier height.
(d) σ_{com} approaches asymptotically a maximum value that is simply the geometrical area of the target nucleus, πR^2, where R is the nuclear radius, when the kinetic energy is much greater than the barrier height.

From these facts, it is possible to gain some insight into reaction cross-sections. The Coulomb barrier for protons on the heavier elements is of the order of 10 MeV. It is, therefore, unlikely that reactions between protons and the heavier nuclei will have a very significant cross-section below this energy. If the particle is an alpha particle, the barrier height increases to 25 MeV, so that this energy is usually required before the cross-section becomes significant. From the Q value of the various reactions, it is possible to estimate where the threshold of a reaction will occur. These rules of thumb can often provide an insight into the probabilities of the desired and interfering nuclear reactions in a given situation. In a similar vein, it is possible to estimate the energies required to release one or two neutrons. At lower energies on light nuclei, the emission of one neutron usually occurs at energies between 2 and 8 MeV, and the probability decreases or remains the same at energies higher than this. The second neutron will require an energy of between 6 and 12 MeV, and higher energies will be needed for more neutrons. There is, of course, some overlap between the emission profiles, but, by carefully choosing the energy range of the particles in the target material, it is often possible to minimize one reaction in favour of another.

4.4. PRODUCTION RATES AND CROSS-SECTIONS

The rate of radionuclide production is dependent on a number of factors, including the magnitude of the reaction cross-section as a function of energy, the incident particle energy, the thickness of the target in nuclei per cm^2, which will determine the exit particle energy, and the flux (related to beam current) of incoming particles. The rate of production is given by:

$$-\frac{\mathrm{d}n}{\mathrm{d}t} = R = nI(1-\mathrm{e}^{-\lambda t})\int_{E_\mathrm{s}}^{E_0} \frac{\sigma(E)}{\mathrm{d}E/\mathrm{d}x}\mathrm{d}E$$

where

R	is the number of nuclei formed per second;
n	is the target thickness in nuclei per cm^2;
I	is the incident particle flux per second and is related to the beam current;
λ	is the decay constant and is equal to $(\ln 2)/T_{1/2}$;
t	is the irradiation time in seconds;
σ	is the reaction cross-section, or probability of interaction, expressed in cm^2, and is a function of energy (Fig. 4.3);
E	is the energy of the incident particles;
x	is the distance travelled by the particle; and
$\int_{E_\mathrm{s}}^{E_0}$	is the integral from the initial to final energy of the incident particle along its path.

It is of historical interest to note that the unit for cross-section is the barn, which is equivalent to 10^{-24} cm^2. The expression barn comes from the fact that the probability for a neutron to interact with a target is proportional to the area of the nucleus, which compared with the size of the neutron is as large as a barn.

In all cases, the cross-section for a particular reaction should either be taken from the literature or be measured, since the theoretical estimate of these parameters is not as accurate as is desirable, especially for light nuclei.

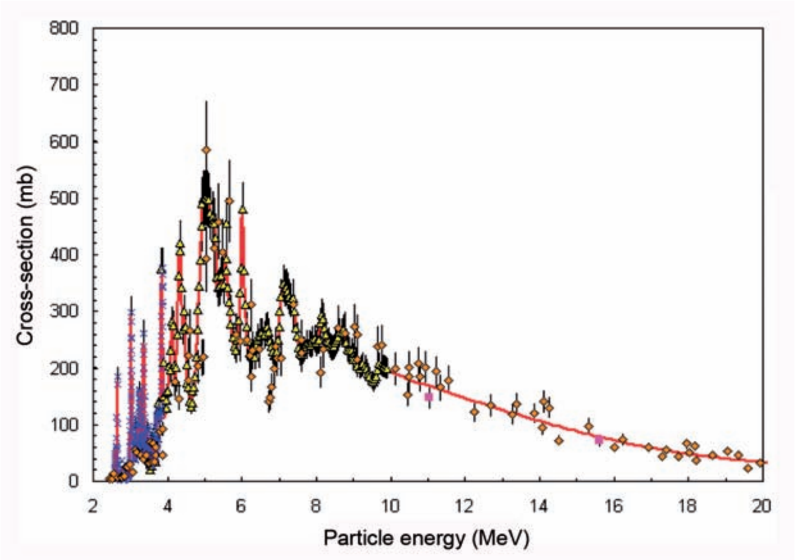

FIG. 4.3. Excitation function for the $^{18}O(p, n)^{18}F$ reaction, illustrating the energy dependence of the cross-section σ.

Experimentally, the cross-section of a particular reaction [4.4] can be reduced to:

$$R_i = Inx\sigma_i$$

where

R_i is the number of processes of type i in the target per unit time;
I is the number of incident particles per unit time;
n is the number of target nuclei per cubic centimetre of target;
σ_i is the cross-section for the specified process in cm^2; and
x is the the target thickness in centimetres.

This relationship is a simplification of the previous equation arrived at by making a few assumptions:

(1) The first is that the beam current is constant over the course of the irradiation.
(2) The second is that the target nuclei are uniformly distributed in the target material.
(3) The third is that the cross-section is independent of energy over the energy range used.

The cross-section can then be reduced to:

$$\sigma_i = 2.678 \times 10^{-10}\, AN_i/It\rho x$$

where

σ_i is the cross-section for a process in millibarns for the interval in question;
A is the atomic mass of the target material in atomic mass units;
N_i is the number of nuclei created during the irradiation;
t is the time of irradiation in seconds;
ρ is the density of the target in g/cm^3;
x is the thickness of the target in centimetres; and
I is the beam current in microamperes.

It should be noted that the yields quoted in the literature assume 100% enrichment unless otherwise noted, and the calculation of yields for practical purposes must use the actual enrichment of the target material under consideration. For determining the target thickness, a number of approaches can be used. The easiest method is to use the SRIM computer program, which calculates stopping powers for a variety of materials, including compounds. The SRIM program was developed at the IBM laboratories and is available at no cost on the web [4.5].

4.5. SATURATION FACTORS AND PRACTICAL YIELDS

The rate of production is, of course, affected by the fact that the resulting nuclide is radioactive and is thus undergoing radioactive decay. For short lived nuclides, the competition between formation and decay will come to equilibrium at sufficiently long bombardment times. This point is called saturation, which means that no matter how much longer the irradiation is carried out, the production rate is equal to the rate of decay and the amount of radioactivity remains constant.

4.5.1. Radionuclide production rates

The rate of formation in this case is given by:

$$R = N\lambda/(1 - e^{-\lambda t})$$

where

R is the rate of formation of nuclei;
N is the number of target nuclei present at the end of the process; and
λ is the decay constant.

The term in the denominator is often referred to as the SF, and accounts for the competition between the production of nuclei due to the particle reaction and the radioactive decay of the nuclei that have been produced.

It is clear why the assumption has had to be made that the beam current was nearly constant, since a variation in beam current would affect the relative number of the nuclei being created versus the number being destroyed by decay. If this relation is substituted back into the cross-section equation, then the result is:

$$\sigma_{\mathrm{i}} = 2.678 \times 10^{-10}\{A\lambda N_{\mathrm{i}}/[I\rho x(1 - \mathrm{e}^{-\lambda t})]\}$$

where

σ_{i} is the cross-section for the process (mb);
A is the atomic mass of the target (amu);
λ is the decay constant for species i (s^{-1});
ρ is the density of the target material ($\mathrm{g/cm}^3$);
t is the time of irradiation (s);
x is the thickness of the target (cm); and
I is the beam current (μA).

It should be noted that the time of irradiation and the decay constant are both given in seconds. This is due to the fact that the beam current is defined in microamperes (μA), which is 6.2×10^{12} electronic charges/s.

4.5.2. Saturation factors

At shorter irradiation times, the fraction of product produced is related to the SF, given by $1 - \mathrm{e}^{-\lambda t}$, where λ is the decay constant of the decaying nuclide and t is the bombardment time. It is evident that an irradiation equivalent to one half-life would result in a saturation of 50%. For practical reasons, irradiations rarely exceed three half-lives (a saturation of 90%), except for the shortest lived radioisotopes. The practical production limits of a given radionuclide are determined by the half-life of the isotope. It is relatively easy to come near saturation for the production of ^{15}O with a 2 min half-life; but it is not reasonable to irradiate a target for the production of ^{18}F to the point of saturation because of the excessively long times involved. When the SF is plotted as a function of the ratio of the irradiation time to the half-life of the radionuclide produced, it can be clearly seen (Fig. 4.4) that with increasing half-life, a compromise must be made with respect to expected yield versus the length of the irradiation.

For an irradiation of one half-life, one obtains 50% of the saturation yield. For a two half-life irradiation one obtains 75%, and so on.

For long lived species, the production rates are usually expressed in terms of integrated dose or total beam flux (μA·h). For example, with a long lived radionuclide such as ^{82}Sr (t = 25 d), the amount of radionuclide at the end of bombardment will be essentially the same whether it is produced from 100 μA in 1 h or 2 μA in 50 h (both represent 100 μA·h of beam). For a shorter lived radionuclide such as ^{18}F, the two irradiation conditions will produce very different amounts.

In order to optimize the production of a particular radionuclide, the following production considerations must be taken into account:

- The threshold energy for the desired reaction;
- The energy where the maximum yield occurs;
- The chemical form of the target nucleus;
- The physical form of the target nucleus;
- The chemical form of the desired product;
- The physical form of the desired product;
- The ease of separation of product from the target.

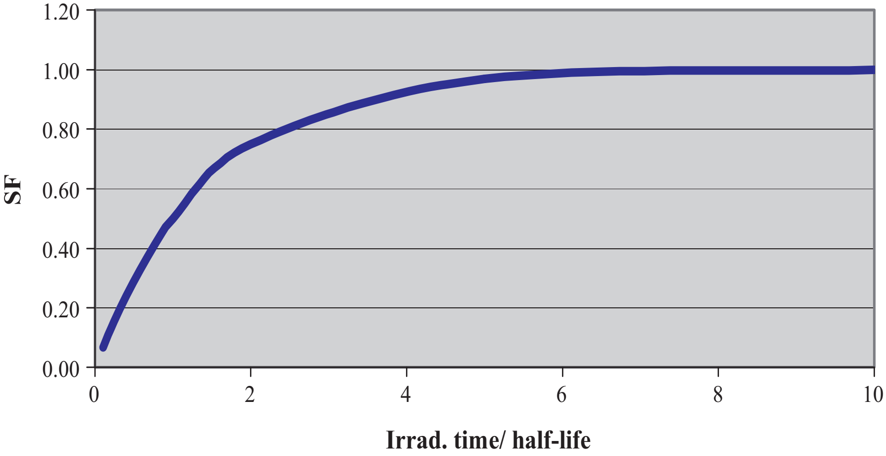

FIG. 4.4. Saturation factor (1 – $e^{-\lambda t}$) as a function of the ratio of irradiation time to the half-life of the radionuclide produced.

4.5.2.1. The example of ^{18}F

To illustrate the application of these estimates, the case where ^{18}F is needed as fluoride is considered. The two nuclear reactions most widely used for producing ^{18}F are ^{20}Ne(d, α)^{18}F and ^{18}O(p, n)^{18}F. Both reactions have relatively low threshold energies (0–2 MeV), and the maximum yield occurs at less than 10 MeV for each particle (Figs 4.3 and 4.5).

However, the (p, n) reaction has a much higher cross-section, so that the quantity of ^{18}F that can be produced is more than double that for a thick target reaction using protons of about 12 MeV in comparison with deuterons of comparable energy. A thick target refers to the situation in which the number of target nuclei present is sufficient to lower the beam energy to below the threshold energy for the reaction under consideration. Since both reactions produce the same radionuclide, the SF will be the same, assuming that the same beam current can be reached with both particles. Having selected the mode of production and energy, the next issue is to examine the chemical and physical forms of the target and product. The most convenient target material for

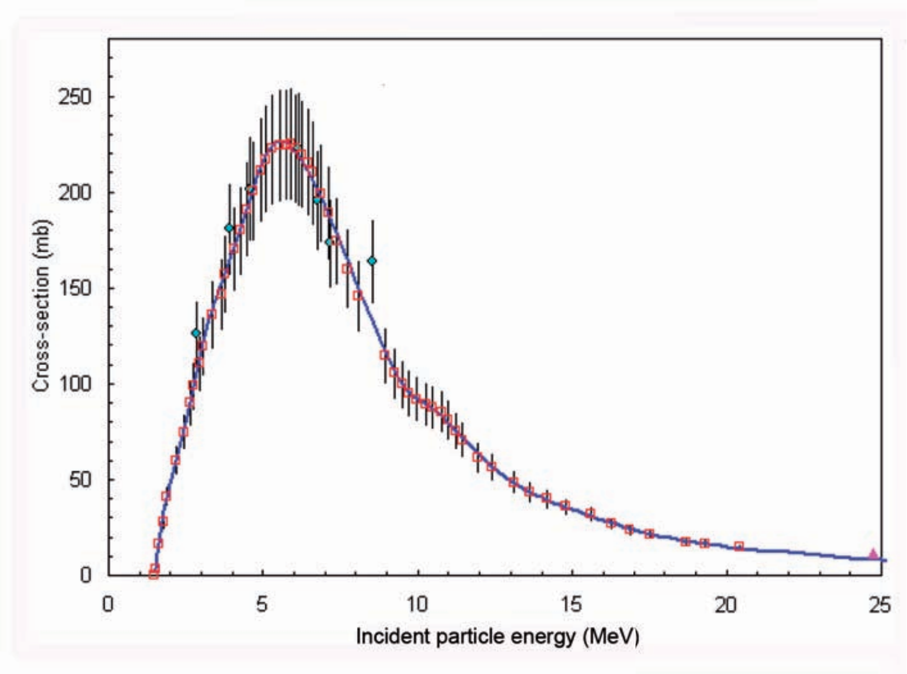

FIG. 4.5. Excitation function for the ^{nat}Ne(d, α)^{18}F reaction; the ^{nat}Ne symbol refers to the fact that the target gas, neon, is of natural isotopic composition (^{20}Ne, 90.5%; ^{21}Ne, 0.3%; ^{22}Ne, 9.2%).

producing ^{18}F as fluoride is a water target enriched in ^{18}O. The resulting ^{18}F is produced directly as the fluoride ion, which can be extracted from the target water by simple ion exchange columns. Obviously, if the chemical form of ^{18}F desired is elemental fluorine (F_2), then a different approach is needed. Elemental ^{18}F requires the use of a non-radioactive fluorine carrier through some exchange reaction that is beyond the scope of this section.

Annex II in the CD attached to this publication gives the detailed calculation of the yield of ^{67}Ga by the ^{68}Zn(p, 2n)^{67}Ga reaction in a 30 MeV cyclotron. Annex II also provides details about the hot cell shielding needed for the above production. Annex III in the CD is an Excel worksheet for the calculation of production yields of ^{67}Ga, ^{111}In, ^{201}Pb(^{201}Tl) and ^{18}F by (p, xn) reactions. The dose rates and the lead shielding of hot cells required are also included.

4.6. CONCLUSIONS

Production of radioisotopes in an accelerator is a complicated process, but understanding a few of the fundamental processes involved in these reactions can make the choice of an appropriate reaction easier. The kinematics of the reaction can determine which radioisotope will predominate in a reaction in which several are possible, which in turn affects the usefulness of the radioisotope produced. The irradiation time will depend on the half-life of the desired product and on the half-lives of potential contaminants. All of these factors must be taken into account when designing a production process [4.6].

REFERENCES TO CHAPTER 4

[4.1] HELUS, F., COLOMBETTI, L.G. (Eds), Radionuclide Production, CRC Press, Boca Raton, FL (1983).

[4.2] DECONNINCK, G., Introduction to Radioanalytical Physics, Nuclear Methods Monographs No. 1, Elsevier, Amsterdam and New York (1978).

[4.3] EVANS, R.D., The Atomic Nucleus, McGraw-Hill, New York (1955).

[4.4] FRIEDLANDER, G., KENNEDY, J.W., MACIAS, E.S., MILLER, J.M., Nuclear and Radiochemistry, 3rd edn, Wiley, New York (1981).

[4.5] ZIEGLER, J.F., SRIM — The Stopping and Range of Ions in Matter, http://www.srim.org/

[4.6] GANDARIAS-CRUZ, D., OKAMOTO, K., Status on the Compilation of Nuclear Data for Medical Radioisotopes Produced by Accelerators, Rep. INDC (NDS)-209/GZ, IAEA, Vienna (1988).

Chapter 5

TARGETRY

5.1. INTRODUCTION

There are literally hundreds of radioisotopes that can be produced with charged particle accelerators. The cyclotron is the most frequent choice of accelerator, but the linac and other accelerators may become more common with the development of smaller, more reliable, machines. This chapter will deal only with targetry for a small subset of the radionuclides produced with charged particle accelerators.

The goal of cyclotron targetry is to place the target material into the beam, keep it there during irradiation, and remove the product radionuclide from the target material quickly and efficiently. The specific design of the target is what allows this goal to be achieved. Unless care is taken in the design and fabrication of the target, the production of the radioisotope can be far from optimal and may even be impossible. Over time, many facilities will need to increase the number of radioisotopes being produced or to optimize the yields of their currently produced radioisotopes. If an increase in production with commercial targets is being sought, modifications of existing targets and procedures or development of new targets may be ways of accomplishing this objective.

The purpose of this chapter will be to explore some of the problems in the design and construction of cyclotron targets, and to demonstrate with practical examples how to evaluate some of the solutions to the numerous problems encountered in achieving the optimal design of a cyclotron target. An attempt has been made to present some useful formulas and 'rules of thumb' that may be used in the design of cyclotron targetry. Even if the reader is not concerned with the design of cyclotron targets, these equations may provide an insight into the processes occurring in targets. The formulas are taken from a number of textbooks on nuclear physics, nuclear chemistry and engineering, and compiled here merely for easy access.

One of the challenges to those involved with the design of targets is that not all cyclotrons are the same. The design of targetry associated with one cyclotron may not be optimal for a different cyclotron. In addition to the characteristics of mechanical design, beam energy and beam current, the major variables are the beam size and profile. An uncontrolled or unstable beam profile may result in an unreliable radioisotope yield. If the beam profile cannot be controlled, then allowances must be made in the targetry in order to obtain predictable yields. There are often significant differences in the characteristics of the beam profile between a positive ion cyclotron and a negative ion cyclotron. Negative ion cyclotrons usually have a more uniform beam profile incident on the target. This is a result of the extraction process through a stripping foil that will scatter and, therefore, tend to eliminate hot spots in the beam [5.1–5.3]. Focusing magnets and steering them along the transport line, if there is one, can alter the beam shape to a more homogeneous one. Positive ion cyclotrons may have a uniform beam profile, or the profile may be quite 'hot' in spots and not uniform at all, depending on the extraction characteristics and focusing magnets used to transport the beam. In general, the extraction process for positive ions tends to create areas of high intensity in the beam. Most of the newer, commercially available cyclotrons for PET are negative ion cyclotrons and have targets mounted directly on the cyclotron without any focusing or steering magnets to alter the beam shape.

Other factors that are important for effective radioisotope production are whether or not an internal beam is available, and whether or not multiple targets can be irradiated simultaneously. Internal targets were first developed because the extraction efficiency of older cyclotrons was quite low.

The extraction efficiency of a cyclotron is defined as the beam current extracted from the machine divided by the beam current circulating before extraction. In older positive ion cyclotrons, most of the beam was lost inside the machine (an extraction efficiency of 10% being thought quite acceptable, although more modern positive ion machines are capable of extracting more than 60% of the beam). The use of negative ion cyclotrons and the greatly improved extraction efficiency of newer positive ion cyclotrons have reduced the need for internal targets, but they are still quite common since they work well. Internal targets are usually set as grazing incidence targets, because this allows the heat generated from the target to be dispersed over a wider area. Negative ion cyclotrons allow for irradiation of multiple targets simultaneously. This is not usually possible with positive ion cyclotrons, unless the targets are 'piggyback' or tandem targets with one target following another along the same beamline.

A great deal of useful information about targets and target chemistry can be found in a book by Clark and Buckingham [5.4] and in the proceedings of the International Workshops on Targets and Target Chemistry [5.5]. These proceedings are very valuable resources for all those who are concerned with the production of radioisotopes.

5.2. TARGET TYPES

For production of radioisotopes, the target material may be either gas, liquid or solid. Targets are, consequently, designed to accommodate the material being irradiated. The design of the target will also depend upon whether the target is placed inside (internal) or outside (external) the cyclotron.

5.2.1. Internal targets

Internal targets were the first targets to be used in cyclotrons. The real advantage of these targets at present is that the target may be built to exactly match the beam curvature and, therefore, spread the power of the beam over the maximum area and increase the amount of beam current that may be applied to the target. A schematic diagram of an internal target is shown in Fig. 5.1.

These targets are very widely used at present for the production of non-volatile solid radioisotopes such as ^{123}I, ^{124}I, ^{201}Tl, ^{67}Ga and ^{111}In. The target material is typically a solid, usually in the form of a thin metal layer, although internal targets using powders and liquids have been designed and used.

Figure 5.2 shows a typical internal target used for the production of radioisotopes in nuclear medicine. This particular target was used for production of ^{201}Tl. The thallium is electroplated onto the copper surface and then dissolved after irradiation [5.6].

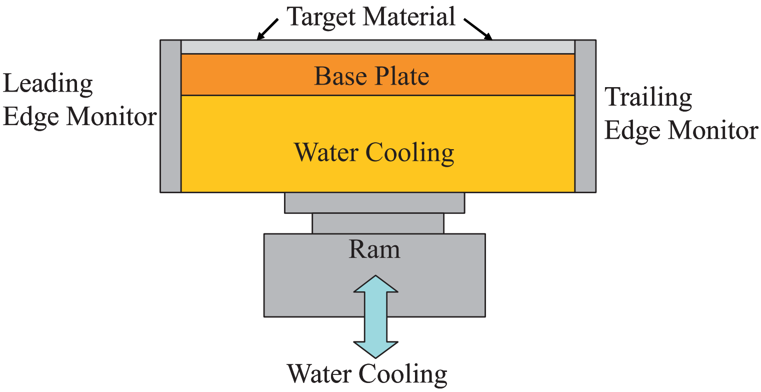

FIG. 5.1. Schematic diagram of an internal target, showing a plated surface on a base plate for cooling.

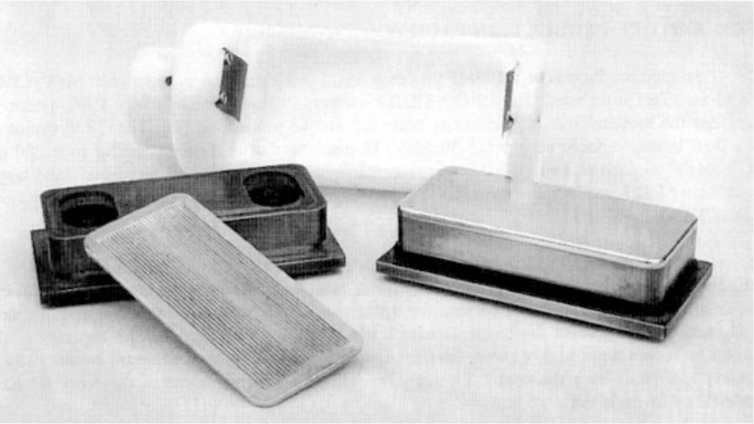

FIG. 5.2. An internal target used for production of ^{201}Tl.

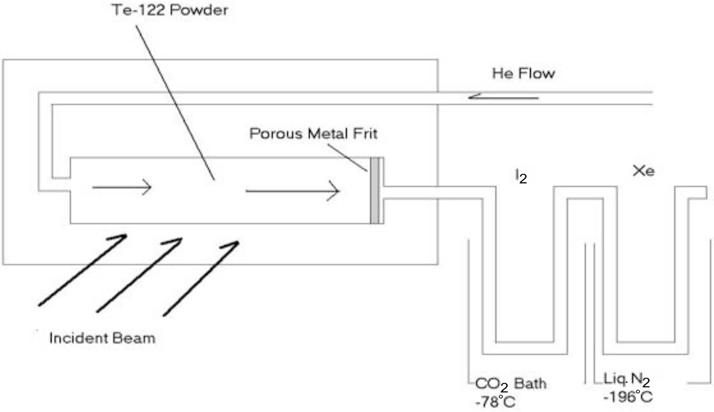

FIG. 5.3. An example of an internal target using ^{122}Te powder to produce ^{123}I.

An example of an internal powder target is shown in Fig. 5.3 [5.7]. This particular target was used to produce ^{123}I from ^{122}Te, using deuterons as the bombarding particle. The ^{123}I is swept out of the target by the helium gas flow, and the target never has to be removed from the cyclotron except for maintenance.

5.2.2. External targets

There is a very wide variety of external targets that can be used for irradiation of solids, liquids and gases. It is impossible to give a complete description of all the designs in use. What follows is a general description of each of these target types.

5.2.2.1. Solid targets

Because the density of solids is typically higher than that of liquids or gases, the path length of the beam is shorter, and the target somewhat smaller. The solid can be in the form of a foil or a powder. If the solid is a good heat conductor, then the beam can be aligned to be perpendicular to the solid. A typical solid target for conductive powders is shown in Fig. 5.4.

A photograph of a typical external solid target is shown in Fig. 5.5. The powder is held in the small cavity in the target. The cover foil is shown next to the cavity.

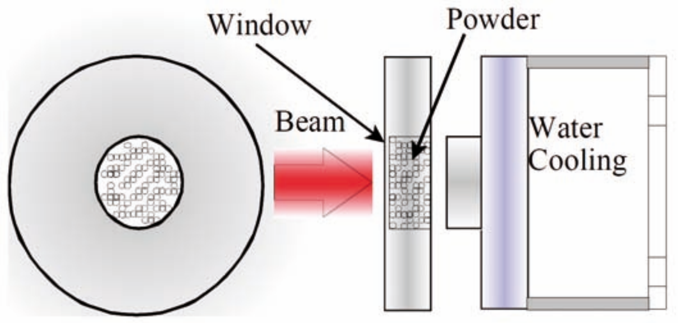

FIG. 5.4. A typical solid powder target for use with low beam current or with thermally conductive solids.

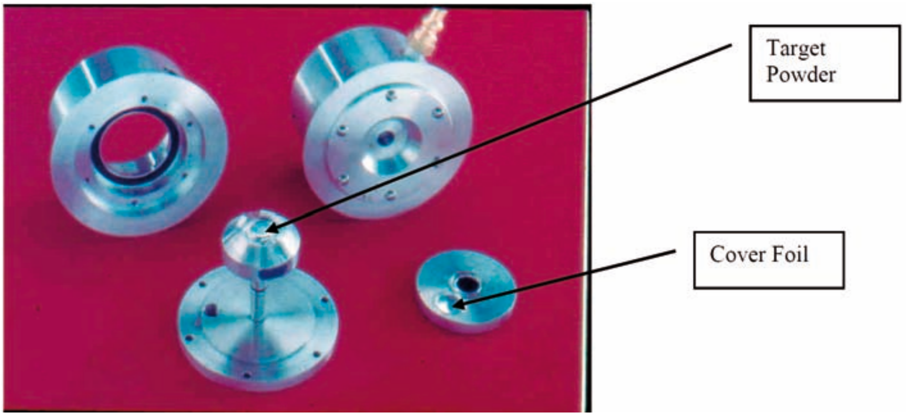

FIG. 5.5. Photograph of the solid powder target used at BNL.

If the solid is not a good thermal conductor, or when very high beam currents are used, it is typical to form the solid on an inclined plane (Section 5.5.4).

5.2.2.2. *Liquid targets*

In the case of liquids, targets have similar dimensions to those of solid targets, since the target material occupies a specific volume unless the liquid volatilizes. The difference is that the liquid is typically added and removed from the target while it is in place on the cyclotron. A typical liquid target for the production of ^{18}F from ^{18}O in water is shown in Figs 5.6 and 5.7.

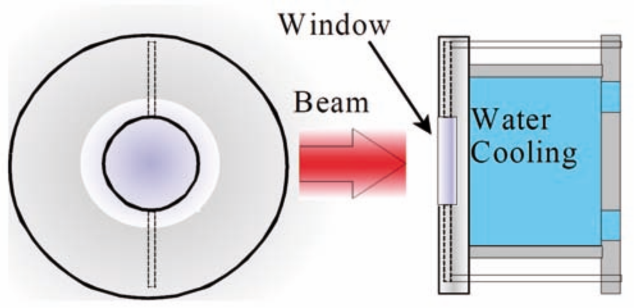

FIG. 5.6. Schematic diagram of a typical external target used for irradiating liquids. This particular target is constructed of silver and is used to produce ^{18}F from ^{18}O enriched water.

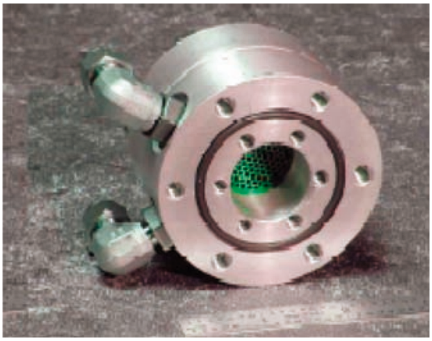

FIG. 5.7. Photograph of ^{18}O water target at the PULSAR linac from AccSys Technology, Inc. Note the grid covering the front foil to enable the latter to withstand higher pressures and beam currents.

5.2.2.3. Gas targets

Gas targets are widely used and are usually some type of cylinder to hold the gas under pressure, with a thin beam entry foil usually referred to as a window. The principal constraint on gas targets is removal of heat from the gas, since gases are not very good heat conductors and the targets must be quite large in comparison with solid or liquid targets in order to hold the necessary amount of material. A schematic diagram of a typical gas target is shown in Fig. 5.8, and a photograph is shown in Fig. 5.9.

The cold finger (Fig. 5.9) on the bottom of the target allows the gas to be transferred into the target more efficiently. The large volume at the front of the target was used to capture the xenon if the front foil ruptured.

The design and construction of cyclotron targets is a multidisplinary field. Engineering, physics and chemistry each play an important part in the way cyclotron targets are constructed. In almost all cases, it is necessary to make some compromises in the design, since very often the best solution of a problem from one aspect of the target will introduce an unacceptable constraint on another aspect of the target.

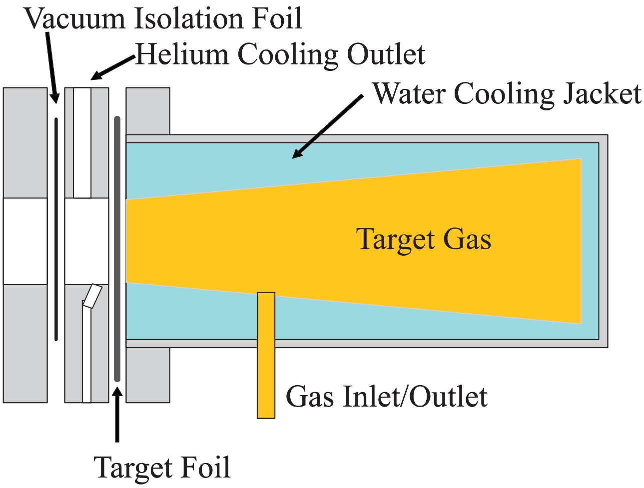

FIG. 5.8. Schematic diagram of a typical gas target, showing the chamber for the gas cut at an angle to account for multiple scattering.

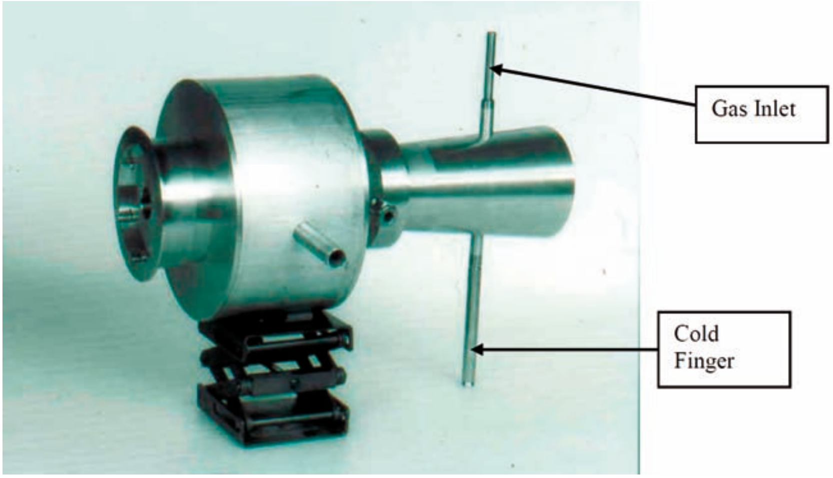

FIG. 5.9. Photograph of a gas target used for production of ^{123}I *from* ^{124}Xe*.*

5.3. APPLICATION OF PHYSICS TO TARGETRY

A major concern in target design is the generation and dissipation of heat during irradiation. Efficient cooling not only ensures that the target material will remain in the target but also allows the target to be irradiated at higher beam currents, which in turn allows production of more radioisotopes in a given time. Factors to be considered in relation to thermodynamics include:

- Interactions of charged particles with matter;
- Stopping power and ranges;
- Energy straggling;
- Small angle multiple scattering.

Each of these factors will be described in some detail in Sections 5.3.1–5.3.4.

5.3.1. Interactions of charged particles with matter

As a charged particle moves through a surrounding medium, it interacts through ionization, scattering and various types of radiative losses. There are four main modes of interaction involved.

In the first mode of interaction, the particles undergo inelastic collisions with the atomic electrons of the surrounding medium. In this case, the electrons are promoted to a higher energy level (excitation), or an unbound state (ionization) [5.1]. If ionization occurs, then the ions and electrons recombine to form an excited neutral atom or molecule. In either case, the excited atom or molecule must transfer the excess energy to the surrounding molecules. The transfer of energy from the charged particle to the surrounding medium in this fashion is the primary energy loss mechanism for the charged particle beam and the major source of heat in the target material.

In the second mode of interaction, the particles undergo inelastic collisions with nuclei of the target material. In this case, the charged particle is deflected by an amount depending on the proximity of the encounter and the charges involved. In some of these deflections, a quantum of energy is lost from radiation (bremsstrahlung) and a corresponding amount of kinetic energy is lost from the colliding pair. The total bremsstrahlung intensity varies inversely with the square of the mass of the charged particle, so that it is not usually important for protons or more massive particles.

In the third mode of interaction, the particles undergo elastic collisions with the nuclei of the target material. In an elastic collision, the incident particle is deflected but neither radiates nor results in any excitation of the target nucleus. The only kinetic energy lost is due to conservation of momentum by the deflection of the particle. This process is common for electrons, but is much less probable for charged particles.

In the last mode of interaction, the particles undergo elastic collisions with atomic electrons. This process usually occurs only at low energy when the charged particle does not transfer enough energy to the atomic electron to promote it to the lowest excited state energy level.

The charged particle loses energy as a result of all four of these processes as it moves through the target material. At energies typical for radioisotope production, a particle will undergo more than a million collisions before it comes to rest. Of course, the type of collisions and the exact path of an individual particle cannot be predicted. However, since the probabilities can be calculated and the number of particles is large, the overall behaviour of the beam can be predicted with high accuracy and reliability.

5.3.2. Stopping power and ranges

The slowing (loss of kinetic energy) of a charged particle by any and all means is called the stopping power and is defined as:

$$S(E) = -\mathrm{d}E/\mathrm{d}x$$

where E is the particle energy (MeV) and x is the distance travelled (cm).

Exact calculation of this quantity is complex, but a reasonable approximation may be obtained rather easily [5.1]. The result is:

$$\frac{-\mathrm{d}E}{\mathrm{d}x} = \frac{4\pi z^2 e^4 NZ}{m_0 V^2 A} \ln\left(\frac{2m_0 V^2}{I}\right)$$

where

z is the particle atomic number (amu);
Z is the absorber atomic number (amu);
e is the electronic charge (esu);
m_0 is the rest mass of the electron (MeV);
A is the atomic mass number of the absorber (amu);
V is the particle velocity (cm/s);
N is Avogadro’s number; and
I is the ionization potential of the absorber (eV).

The assumption is made in the above approximation that the particle is massive in comparison with the electron. This assumption leads to a maximum energy transfer of $2m_0V^2$. Therefore, the above expression can be reduced to the following formula:

$$\frac{-\mathrm{d}E}{\mathrm{d}x} = \frac{144Zz^2}{AE} \ln\left(\frac{2195E}{I}\right)$$

where

z is the particle atomic number (amu);
Z is the absorber atomic number (amu);
A is the atomic mass of the absorber (amu);
E is the energy (MeV); and
I is the absorber effective ionization potential (eV).

If the effective ionization potential is known, then it may be used. Tables of the effective ionization potentials of atoms can be found in the report by Janni [5.8] or on the SRIM web site [5.9]. If an ionization potential is not known, it may be approximated by the following relations [5.7]:

$$I = 13Z \qquad \text{for } Z \leq 13, \text{ and}$$

$$I = 9.76Z + 58.8Z^{-0.019} \qquad \text{for } Z > 13$$

The range of a charged particle through the absorber medium is simply the integral of the energy loss equation. This gives the range as:

$$\text{Range} = R = \int_{0}^{E_{\max}} \frac{1}{S(E)}\,\mathrm{d}E$$

where $S(E)$ is the stopping power at energy E.

If the simplified energy loss equation is used with all the same assumptions, then the range relationship can be numerically integrated to energies of 0.1 MeV as:

$$R = \sum_{0}^{E_{\max}} \frac{1}{S(E)} \Delta E$$

which becomes

$$R = \sum_{0}^{E_{\max}} \frac{AE}{144z^2 Z \ln\left(\frac{2195E}{I}\right)} \Delta E$$

This relation can be easily programmed on a personal computer, or even on some pocket calculators, to give a reasonable approximation of the range in a particular target material. Using this formula and an integration interval of 0.1 MeV, the range of 20 MeV protons in aluminium was determined to be 0.5808 g/cm^2. The value from the tables of Williamson, Boujot and Picard (WBP) [5.10] is 0.5740 g/cm^2. Thus, it can be seen that the values agree to within about 1–2%. The agreement is better at lower energies and somewhat worse at higher energies, although the agreement is nearly always better than about 2% at energies typical of a radioisotope production cyclotron [5.11]. Table 5.1 gives values for ranges of protons in aluminium.

There are two other considerations in the calculation of the range of a particle for cyclotron targetry:

TABLE 5.1. RANGES (g/cm^2) OF PROTONS ON ALUMINIUM, CALCULATED BY DIFFERENT METHODS

Energy (MeV)	Range (simple)	Range (SRIM)	Range (Janni)	Range (WBP) [5.10]
15	0.3477	0.3431	0.3430	0.3448
14	0.3077	0.3026	0.3038	0.3053
13	0.2699	0.2662	0.2668	0.2679
12	0.2344	0.2313	0.2319	0.2327
11	0.2011	0.1987	0.1992	0.1998
10	0.1702	0.1681	0.1687	0.1691
9	0.1416	0.1401	0.1405	0.1407
8	0.1155	0.1142	0.1146	0.1147
7	0.0917	0.0907	0.0910	0.0910
6	0.0705	0.0696	0.0699	0.0698
5	0.0517	0.0511	0.0513	0.0511
4	0.0357	0.0350	0.0352	0.0351
3	0.0223	0.0217	0.0219	0.0218
2	0.0118	0.0112	0.0114	0.0113
1	0.0044	0.0039	0.0040	0.0039

(1) The ranges of particles other than protons;
(2) The range in a compound made up of several elements so that the ionization potential, atomic number and atomic mass are composites of the constituent elements.

In the case of the stopping power, the fact that is usually used to calculate the range of particles other than the proton is that the stopping power for these particles can be related to the stopping power of the proton in the following fashion [5.8]:

(a) Deuterons, $S_d(E) = S_p(E/2)$;
(b) Tritons, $S_t(E) = S_p(E/3)$;
(c) Helium-3, $S_{He\text{-}3}(E) = 4S_p(E/3)$;
(d) Helium-4, $S_{He\text{-}4}(E) = 4S_p(E/4)$.

These relationships are valid above the energy where the ion charge has reached its maximum (for ^{4}He this is about 1.7 MeV). In a similar fashion, the stopping power of a particle in a chemical compound, alloy or composite material is the stopping power of the particle in each element of the compound multiplied by the atomic fraction of that element in the compound. The stopping power and ranges may also be obtained from the SRIM computer code [5.9].

5.3.3. Energy straggling

Charged particles having the same initial velocity do not travel the same distance through the absorbing medium. The ranges of an initially monoenergetic source will have a distribution of ranges centred about the mean range of the particles, owing to the statistical nature of the atomic collision processes described earlier. This phenomenon is referred to as energy straggling and has a significant application to cyclotron targetry in determining the expected yield from a target that does not stop all the incident charged particles. In this situation, a foil used to degrade the energy of the beam can have a significant effect on the yield from a target, even if the calculated energy of the beam is the same as that of a beam that enters the target without passing through a degrader foil. As an example, Fig. 5.10 shows the distribution of energies resulting from degradation of the beam energy from 200 to 15 MeV, from 70 to 15 MeV, and from 30 to 15 MeV, all with the same number of particles.

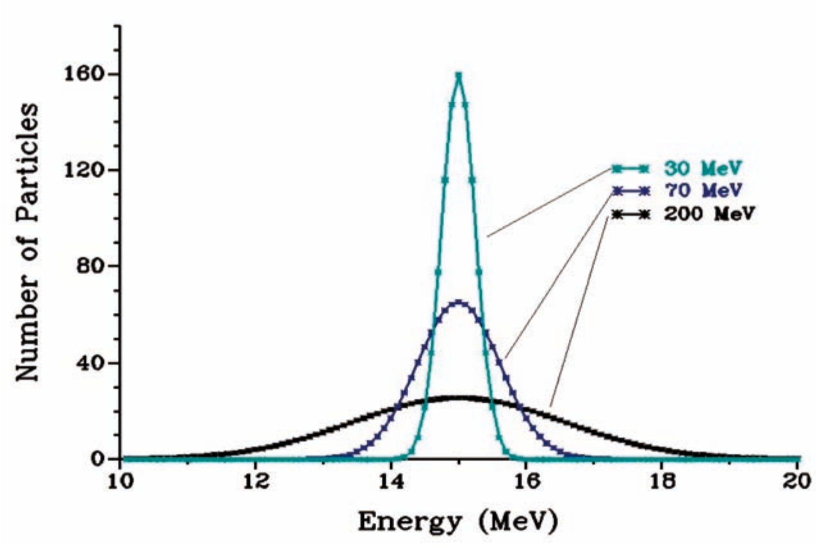

FIG. 5.10. Distribution of beam energy when protons are degraded from an initial energy of 200, 70 or 30 MeV to a final energy of 15 MeV.

It is clear that if an initial energy of 30 MeV has an energy spread of about 2 MeV, then an initial energy of 200 MeV will have an energy spread of about 10 MeV. A beam with an initial energy of E_0 travelling through an absorber will lose energy according to the stopping power equation. The average distance the particles will have travelled when they reach the energy E_1 is given by the following relation [5.2]:

$$\bar{x} = \int_{E_1}^{E_0} \frac{1}{S(E)} \mathrm{d}E$$

The distribution of distances travelled by the individual particles is approximately Gaussian. Another way to view this is that, at a given point in the absorber, the particles will have a distribution of energies. The standard deviation of this straggling function can be approximated quite accurately by the following relation:

$$\sigma = 0.395z\left(\frac{Z}{A}x\right)^{1/2} \text{ (MeV)}$$

where

z is the projectile atomic number (amu);
Z is the absorber atomic number (amu);
A is the absorber atomic mass number (amu); and
x is the particle path length (g/cm^2).

The straggling function is assumed to be Gaussian and σ is in units of MeV. This expression is not valid at very short ranges (for energy losses of less than 1%) or at very long ranges, where the particle energy is near thermal energies (beam stopped completely).

5.3.4. Small angle multiple scattering

As the particles travel through the absorber, they also undergo small angle multiple scattering. This type of scattering has an important implication for the design of cyclotron targets, because any foils or target material in the beam path will spread the beam. The shape of the target must account for this increase in beam diameter if the yield is to be maximized. This is especially important in the design of gas targets, since the target medium is usually at a lower density than a liquid or solid target and, therefore, must be longer, and the effects of the small angle multiple scattering will be greater. In the normal analysis of the scattering angle, large angle scattering is ignored, since the fraction of particles that are scattered by this mechanism is rather small and, therefore, not of great importance to the yield from the target. The sigma of the scattering angle may be approximated by the following relation [5.3]:

$$\sigma^2 = QG$$

where σ is the standard deviation of a Gaussian distribution.

The term Q is given by:

$$Q = \frac{4\pi\phi I e^4 Z^2 z^2}{p^2 v^2}$$

where

z is the atomic number of the particle (amu);
Z is the atomic number of the absorber (amu);
e is the electronic charge (esu);
p is the particle momentum (g·cm/s);
v is the particle velocity (cm/s);
ϕ is the number density (atoms/cm^3);
I is the thickness of the absorber (cm);

and the term G is given by:

$$G = 0.5 \ln\left(\frac{E a_0}{z Z^{4/3} e^2}\right)$$

These two relations can be combined and simplified to the following relation:

$$\sigma^2 = 0.0536\left[\frac{x Z^2 z^2 \ln\left(\frac{3.67\times 10^4 E}{z Z^{4/3}}\right)}{A E^2}\right]$$

where

x is the density of the absorber (g/cm^2);
E is the projectile energy (MeV);
A is the absorber atomic mass (amu);
z is the atomic number of the particle (amu); and
Z is the atomic number of the absorber (amu).

This approximation is correct to within a few per cent if the energy used is the average energy of the beam in the absorber. The angular distribution can also be obtained by using the SRIM program [5.9].

The initial distribution of the beam can be approximated with any degree of resolution from a simple step function to a more accurate and complex function determined by a beam profile monitor. In practice, the shape of the beam may be approximated by dividing the beam into smaller segments (as many as are felt to be necessary for accuracy) and then multiplying each segment by a Gaussian function with a standard deviation (σ) derived from the equation. Each of these segments is overlaid with each other in space, and summed. The function after scattering is then normalized to the known beam current. This gives a good approximation to the beam profile. The relation is less accurate when the path length is very long and the energy at the exit of the absorber is close to zero. In this situation, a more accurate approximation may be achieved by dividing the total range of the particle into smaller segments. The beam distribution in the first segment is then calculated, and the output of that segment used as the input to the next segment.

5.4. APPLICATION OF CHEMISTRY TO TARGETRY

The chemistry occurring inside a cyclotron target is the source of the chemical products that are produced during irradiation. The reactions of the highly excited nucleogenic atom with its surroundings during the de-excitation are the determining factor for radiolabelled molecules to be formed. Many of the chemical reactions occurring were first studied using hot atom chemistry. A ‘hot atom’ is an atom formed nucleogenically with a great deal of excess energy. However, the conditions inside production targets are quite different from those in a typical hot atom experiment. In the case of a hot atom experiment, the beam current is usually less than 1 mA and the gas is at a pressure of much less than 1 atm (1.01×10^5 Pa). In a normal production gas target, the beam current may be 20 or 30 mA (or higher with the newer targets) and pressure up to 70 atm (7.09×10^6 Pa). However, in many cases, the results from hot atom experiments have been very successful in explaining the product distributions from production gas targets.

5.4.1. Chemical interactions in the target

The state of the matter inside a cyclotron target depends on the state of the matter being bombarded. In a gas target, the gas is highly ionized, and ion–molecule and highly endothermic reactions are occurring. A view inside the target during irradiation is shown in Fig. 5.11.

Nearly any chemical species can be formed in this gaseous plasma or 'ionic soup'. When other gases are present, either as contaminants or as additives, the situation becomes very complex. In most cases, the final product distribution will be determined by the thermodynamics of the situation, since there is more than enough energy to overcome the kinetic activation barriers that would place constraints on the product distribution at lower temperatures. In a liquid target, the material may be in the form of a liquid or a vapour, depending on the beam density and temperature. The target material may boil intermittently, as has been seen in water targets for the production of ^{18}F [5.12, 5.13]. An example of water boiling and excited water molecules emitting light during irradiation is shown in Fig. 5.12.

In a solid target, the solid may liquefy or sublime and change the physical state of the target. The final chemical form of the radionuclide from a gas target depends on the gases that are present in the mixture. An example is the production of $^{11}CO_2$ from the $^{14}N(p, \alpha)^{11}C$ reaction in pure nitrogen gas. Nitrogen gas obtained from any commercial source contains at least 0.5 ppm of oxygen as an impurity.

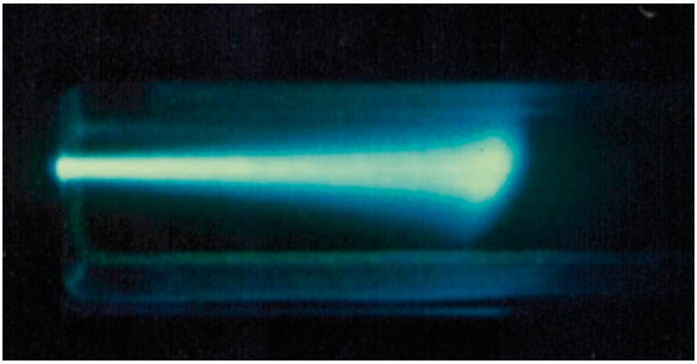

FIG. 5.11. View inside a gas target during irradiation in which highly excited and ionized gas molecules emit light and heat (courtesy of S.J. Heselius).

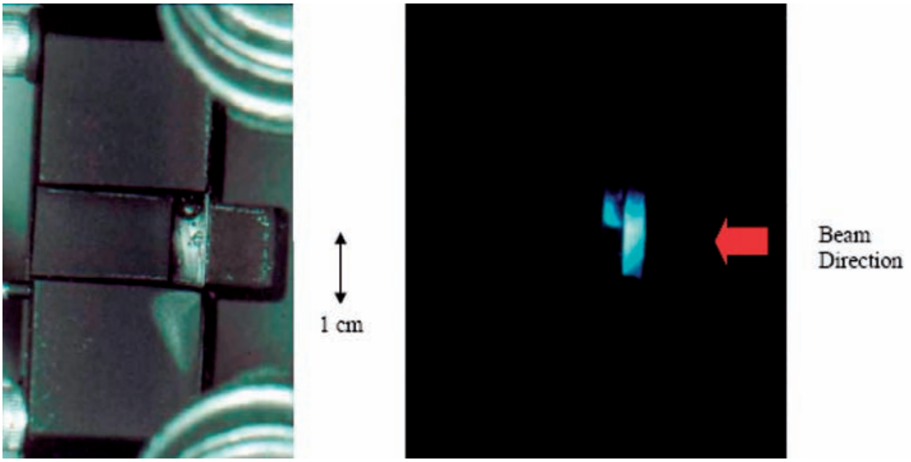

FIG. 5.12. Water boiling and emitting light during irradiation.

This quantity is usually sufficient to convert all hydrocarbon impurities to CO_2, with enough O_2 left over to convert all the ^{11}C produced in the target to carbon dioxide if the carbon does not reach the walls of the target before it is thermalized. If other chemical forms of carbon are desired, then another gas must be added in great excess, since the reaction with oxygen is such a thermodynamically favourable one. If the desired product is methane, then about 5% H_2 must be added to the gas in order to ensure that methane will be the final product [5.14, 5.15]. It is thought the reason carbon dioxide is not the final product is that the hydrogen reacts with the oxygen to produce water and, therefore, is not available to form carbon dioxide. There is almost certainly hydrogen cyanide produced in this same target, but the thermal energy is high enough that this product is quickly converted to the more thermodynamically stable methane and ammonia. Another processing step must take place outside the target to convert the methane and ammonia back to hydrogen cyanide, which is often the desired product. The thermodynamic stability of the molecules is often the determining factor in the final product distribution. The large amounts of energy present in the target during irradiation make the kinetics of the reactions less important than the thermodynamics, since most activation barriers are easily overcome.

One development in targetry has been the use of mixed phase targets to alter the chemical form of the radionuclide. One example of this is the ^{13}C powder water slurry target developed by CTI, Inc. (Knoxville, TN) [5.16]. In this target, the slurry of ^{13}C powder in water is irradiated in the cyclotron beam to produce $^{13}NH_3$. A schematic diagram of the target is shown in Fig. 5.13.

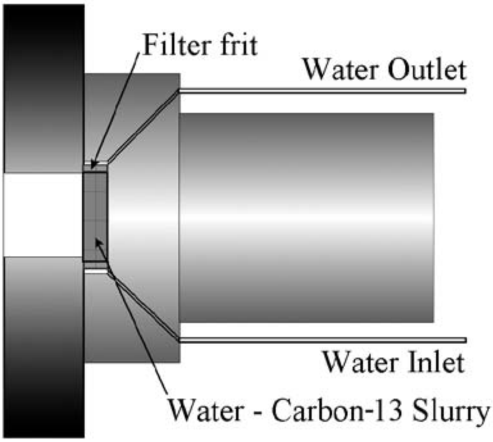

FIG. 5.13. Carbon-13 slurry target developed by CTI, Inc. for the production of [^{13}N]ammonia.

This development is interesting since water targets have been used for many years to produce ^{13}N, but the chemical forms were nitrates and nitrites, which were then converted to ammonia by reduction with Devarda's alloy in base or with $TiCl_3$. The ^{13}C carbon powder produces ^{13}N from the $^{13}C(p, n)^{13}N$ nuclear reaction, as well as the $^{16}O(p, \alpha)^{13}N$ nuclear reaction on the oxygen in water. There is some doubt about whether much ^{13}N is coming from ^{13}C or if it is locked tightly into the matrix. The fact that the product is [^{13}N]ammonia suggests that the carbon powder is removing or at least binding the oxygen dissolved in the water so that it cannot react with the atomic nitrogen produced. Another example of the additives used to make ammonia directly in the target is that involving addition of ethanol to a water target. A few parts per thousand of ethanol will change the chemical form of the ^{13}N from nitrate and nitrites to ammonia. The exact nature of the effects of these additives is still under study. This type of 'in-target' chemistry offers opportunities for altering the chemical form of the radioisotope in many ways, depending on the properties of the target material and the additives [5.17].

5.4.2. Specific activity and contaminants in the target material

The SA of a radionuclide is defined as the quantity of radionuclide divided by the total mass of the compound. As an example, if a sample of [^{11}C]carbon dioxide is measured to have 200 mCi and the amount of mass is determined to be 0.1 μmol, then the SA is 2 Ci/μmol. There is, of course, an ultimate limit, which occurs only when radioactive atoms or radiolabelled molecules are present. A list of some common PET radionuclides and some relevant information is given in Table 5.2 [5.18].

The SA is a critical factor for some types of clinical agents and radiotracers for biological work. The radiotracers used to probe brain chemistry and receptor occupancy are examples of this need for high SA or, more correctly, low injected mass. Mass in excess of a few nanomoles can have an effect on the receptor occupancy and, therefore, alter the apparent receptor characteristics with respect to those observed with high SA (low mass) radiotracers. The SA of the radiotracer should be monitored and, if the amount of mass is too great or starts to increase, then steps should be taken to remedy the situation. The sources of carrier in the final product may be, for example, the chemicals used in the synthesis of the radiotracer, target material, target walls or foils.

The only way to determine the source of the carrier is to measure the SA at each step in the processing of the target material to the final radiotracer preparation. The methods for measuring the SA of the target material after irradiation will depend on the physical state of the target material. Gaseous target material can often be analysed with the use of radiogas chromatography, using flame ionization detectors, nitrogen phosphorus detectors or electron capture detectors. Liquids can often be analysed with high pressure liquid chromatography or ion chromatography, using ultraviolet and conductivity detectors, respectively. Solid target materials pose the most difficult problems.

TABLE 5.2. COMMON PET RADIONUCLIDES AND THEIR DECAY CHARACTERISTICS

Nuclide	Half-life (min)	Decay mode	Maximum energy (MeV)	Mean energy (MeV)	Max. range (mm)	Max. SA (theoretical) (Ci/μmol)[a]
C-11	20.4	100% β^+	0.96	0.386	4.1	9 220
N-13	9.98	100% β^+	1.19	0.492	5.4	18 900
O-15	2.03	100% β^+	1.7	0.735	8.0	91 730
F-18	109.8	97% β^+	0.69	0.250	2.4	1 710
Cu-62	9.74	99.7% β^+	2.93	1.314	14.3	19 310
Ga-68	68.0	89% β^+	1.9	0.829	9.0	2 766
Br-75	96.0	75.5% β^+	1.74	0.750	8.2	1 960
Rb-82	1.25	95.5% β^+	3.36	1.5	16.5	150 400
I-122	3.62	75.8% β^+	3.12	1.4	15.3	51 950
I-124	6019.2	23.3% β^+	2.13	0.8	10.2	31

[a] 1 Ci = 37 GBq.

These materials can sometimes be analysed by X ray fluorescence or mass spectrometry.

A major concern in PET is the SA of ^{11}C. This carbon can come from the walls of the target during irradiation. The amount of carbon can be reduced by irradiating an inert gas mixture with oxygen in the target. If the target is kept leaktight and pressurized, the amount of carrier carbon should remain low. The quantity of activity recovered from the target is often reduced as the SA is increased. The yields can be increased by adding additional oxygen to the nitrogen gas. Further examples of target care are provided in Chapter 6.

The carrier fluoride in the water target used for the production of [^{18}F] fluoride is another example. Here the SA is often limited by the amount of carrier fluoride in the ^{18}O-enriched water used.

It has been shown that the amount of fluoride does not increase on prolonged irradiation as was the case with ^{11}C. This suggests that the target material is not a source of fluoride. Carrier fluoride can be added through the water handling system, since the valves used in most of these systems contain polymeric O-rings or gaskets, which are manufactured with fluorine in some form or other. This makes it very difficult to obtain very high SA [^{18}F]fluoride without taking extreme care in the choice of materials used in the handling system. Some common materials and the amount of covalently bound fluorine contained in each are given in Table 5.3.

5.4.3. Target temperatures

The temperature inside the target will have an effect on the product distribution. The effect of temperature on the density reduction has already been mentioned [5.13]. The temperatures inside an argon gas target are shown in Figs 5.14 and 5.15. In both cases, the beam was formed of protons at 14.7 MeV, a current of 15 μA was incident on the gas, and the beam has a range longer than the target thickness.

TABLE 5.3. FLUORINE IN COMMON MATERIALS

Material	Fluorine (wt%)
Teflon (PTFE)	76
Kel-F	49
Needle valve packing material	50
Viton	0.002
Polyethylene	n.d.[a] (<0.0004%)

[a] n.d.: not detectable.

Temperatures are shown at two different pressures of gas in the target: Fig. 5.14 shows the temperatures recorded at a pressure of 675 kPa and Fig. 5.15 shows the temperatures at a pressure of 550 kPa.

As can be seen from Figs 5.14 and 5.15, these temperatures can be quite high, and most kinetic barriers can be easily overcome. The thermodynamics of the particular components of the system are, therefore, likely to determine the final chemical form of the radioisotope.

The values of the temperature inside a water target during bombardment have been published [5.12, 5.19]. Under the conditions of normal production, the temperature of the water attained the boiling point and remained at this point during the irradiation. When pressure was applied to the target, the temperature of the target water increased to the boiling point of water at that pressure. When the target is boiling, the production of the radioisotope is lower than if the target had remained in liquid form. This result is based on the assumption that the range of the particles in the target is similar to the dimensions of the target. To increase the yield while boiling, the target can be made much longer than the dimensions of the particle path. This technique has been used with several commercial targets. These observations show that density reduction is at work in nearly all gaseous and liquid targets to some extent, and yields can be increased by compensating for this phenomenon.

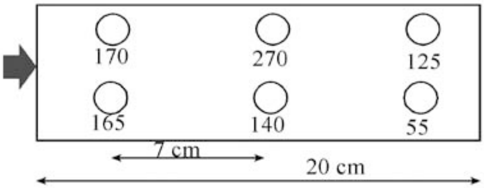

FIG. 5.14. Temperatures (in °C) in six regions of an argon target at a gas pressure of 675 kPa.

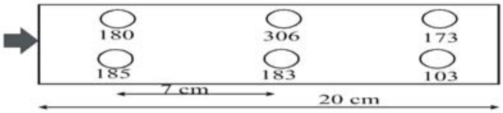

FIG. 5.15. Temperatures (in °C) in six regions of an argon gas target at a gas pressure of 550 kPa.

TABLE 5.4. SUSCEPTIBILITY OF MATERIALS TO RADIATION DAMAGE

Material	Radiation resistance	Tolerance level (kGy)
Teflon	Poor (becomes powdery)	5
Polyethelyene	Good	1 000
Polypropylene	Fair	50
PEEK (polyethyletherketone)	Excellent	10 000
Nylon (aliphatic or amorphous)	Fair	50
Polycarbonate	Good	1 000
Polystyrene	Excellent	10 000

5.4.4. Radiation damage

Another problem in cyclotron targetry is the degradation of certain materials with radiation exposure. Gamma and beta radiation have little effect on metals, but they break chemical bonds and prevent bond recombination of organic compounds. This is particularly true of plastics, some of which are quite radiation resistant while others degrade under prolonged exposure. For a given gamma or neutron flux, the degree of degradation observed depends on the type of chemical bonding present. The chemical bond with the least resistance to decomposition is the covalent bond. There is considerable variation in the strength of the covalent bonds present in different plastics and a wide variation in their stability under radiation. Common chemical reactions that take place in organic compounds during irradiation are polymerization, oxidation, halogenation and changes in isomerism. A short list of some common plastic materials used in cyclotron targets and their radiation resistances is presented in Table 5.4.

5.5. APPLICATION OF ENGINEERING TO TARGETRY

5.5.1. Heat transfer

As was mentioned earlier, the energy lost when charged particles pass through the target medium is dissipated in the form of heat. One of the most challenging problems in the design of cyclotron targets is finding methods to remove this heat from the target during irradiation. The heat generated in the target often has several detrimental effects. A few of these, such as reduction of target density, chemical reactions occurring in the target material or products, as well as possible damage to the target foil or body, have been discussed already.

The choice of materials for the target body and entrance foil will depend not only on their strength and chemical stability but also on their thermal properties. In the following sections, we will explore some basic principles in heat transfer as they relate to accelerator targets.

From the first law of thermodynamics we can write:

$$E = Q - W$$

where

E is internal energy;
Q is heat; and
W is work done.

Any mode of heat transfer involves a temperature differential as the driving force, and, as one might expect, the greater the temperature gradient, the faster the heat transfer will be. There are three modes of heat transfer that are involved to some extent in accelerator targetry. These modes are: radiation, conduction and convection.

5.5.1.1. Heat transfer by radiation

The heat loss by radiation is usually minor, except for target foils or solid targets with low thermal conductivity when high beam currents are used. It is usually assumed in these cases that the heat emitted by the surface is all absorbed in the beamline or target, and very little is radiated back to the target. The radiative heat loss is the easiest term to estimate. If the thermal radiation emitted from a body is thought of as a photon gas, then it is possible to show from thermodynamics that the energy density of the radiation is given by:

$$Q_{\mathrm{rad}} = A\sigma T^4$$

where

Q_{rad} is the heat emitted as radiation (W);
A is the area of the surface (cm^2);
σ is the Stefan–Boltzmann constant; and
T is the absolute temperature (K).

The Stefan–Boltzmann constant has a value of 9.66×10^{-14} $\mathrm{W \cdot cm^{-2} \cdot K^{-4}}$. This is the amount of heat radiated from a black body into an infinite heat sink. A black body is one in which the absorptivity and emissivity are both 1. This is not the case for real objects, but the emissivity and absorptivity are usually equal to one another:

$$\beta\,(\text{emissivity}) = \alpha\,(\text{absorbtivity})$$

This implies that the heat given off by a body at temperature T_1 to surroundings at temperature T_2 is:

$$Q_{\mathrm{rad}} = A\beta\sigma(T_1 - T_2)^4$$

A very important aspect of radiative heat transfer is the system geometry. When an object is heated as it is with an accelerator beam, radiation is emitted in all directions, and only a fraction of this will actually strike a surface where it can be absorbed and removed. This fraction is called the shape factor, F. The shape factor is defined as the fraction of thermal energy leaving the surface of object 1 that reaches the surface of object 2, and is determined entirely from geometrical considerations. Stated in other words, it is the fraction of object 2 visible from the surface of object 1, and ranges from 0 to 1. The shape factor is dimensionless. Shape factors can be calculated using formulas, but the usual method is to consult one of the tables of shape factors that have been compiled [5.20]. The values of the heat lost by radiation for a metal with a heated surface area of 3 $\mathrm{cm^2}$ (a typical value for the area of a beam spot on the front foil of a cyclotron target) and an emissivity of 0.5 (also typical of metal foils at high temperature) is given in Table 5.5.

It can be seen from Table 5.5 that the amount of heat eliminated by this process is not significant below about 500°C. Since the amount of heat deposited in a foil can be of the order of 2–40 W (1 MeV × 20 μA to 0.2 MeV × 200 μA), it is usually necessary to apply some other method of heat transfer such as convective cooling to the target foil.

5.5.1.2. Heat transfer by conduction

The second mode of heat transfer is conduction. Conductive heat transfer is extremely important in the design of cyclotron targets, especially in the construction of the target body, since this is where most of the heat from the beam will be deposited.

TABLE 5.5. HEAT LOSS BY RADIATION

Temperature (°C)	Temperature (°K)	Q_{rad} (W)
100	373	0.0001
200	473	0.0023
300	573	0.0117
400	673	0.0371
500	773	0.0906
600	873	0.1878
700	973	0.3479
800	1073	0.5935
900	1173	0.9507
1000	1273	1.449
1100	1373	2.122
1200	1473	3.000
1300	1573	4.138
1400	1673	7.336
1500	1773	9.496

The heat will be conducted from the hotter region of a material to the cooler region according to Fourier's law, which in one dimension is given by:

$$Q_{\text{cond}} = -kA\,\mathrm{d}T/\mathrm{d}x$$

where

Q_{cond}	is the heat transferred by conduction (W);
A	is the cross-sectional area (cm^2);
k	is the thermal conductivity (W·cm^{-1}·°C^{-1});
$\mathrm{d}T$	is the temperature differential (°C); and
$\mathrm{d}x$	is the distance differential (cm).

If this equation is integrated holding k, A and Q constant, then the result is the heat transfer equation in one dimension given by:

$$Q_{\text{cond}} = \frac{-kA(T_1 - T_2)}{x}$$

where

k is the coefficient of thermal conductivity (W·cm^{-1}·°C^{-1});
A is the cross-sectional area (cm^2);
x is the distance (cm);
T_1 is the temperature of the hotter part (°C); and
T_2 is the temperature of the cooler part (°C).

In the case of a foil where the beam radius is r_i and the foil radius is r_o, the steady state heat transfer from the inner hot area to the outer cooled area is given by:

$$Q_{\text{cond}} = -\frac{2\pi kL(T_i - T_o)}{\ln\left(\frac{r_o}{r_i}\right)}$$

where

L is the thickness of the foil (cm);
T_i is the temperature of the beam strike area (°C);
T_o is the temperature of the outer radius of the foil (°C);
r_o is the foil radius (cm);
r_i is the beam radius (cm); and
k is the thermal conductivity (W·cm^{-1}·°C^{-1}).

Two assumptions have been made in this equation:

(1) The thermal conductivity does not change as a function of temperature.
(2) The inner beam strike area is at a uniform temperature.

These assumptions are rarely valid, but they do give a place to start in the estimate of the heat dissipated by the different processes. They are also fairly valid in a few specific cases. It is usual, in this situation, to know the power being deposited into the window (which is the beam current multiplied by the beam energy lost in the window). The parameter we need to calculate is the temperature of the foil in the beam strike area, in order to determine if the foil will withstand the heat load. In the case of a 0.0254 cm (0.010 in) thick aluminium foil, the energy deposition of an 18 MeV proton beam in the foil will be 1.35 MeV. At a beam current of 20 μA, the heat load will be 27 W. The thermal conductivity of aluminium at 300 K is 2.37 W·cm^{-1}·K^{-1}. If the beam spot radius is 0.75 cm and the foil radius is 1.5 cm, then the temperature at the centre of the foil is:

$$T_\mathrm{i} = \frac{\left[Q_\mathrm{cond} \ln\left(\frac{r_\mathrm{o}}{r_\mathrm{i}}\right)\right]}{2\pi kL} + T_0$$

which yields

$T_\mathrm{i} = (27)(0.693)/[2\pi(2.37)(0.0254)] + 300\ \mathrm{K} = 350\ \mathrm{K}$

Therefore, this amount of power only raises the temperature of the foil by 50 K, well within the boundaries of any significant change in the yield strength of the foil. However, if the foil is 0.051 cm (0.002 in) thick Havar, the energy loss will be 0.8 MeV (16 W at 20 μA) and the temperature of the foil will be:

$T_\mathrm{i} = (16)(0.693)/[2\pi(0.17)(0.0051)] + 300\ \mathrm{K} = 2335\ \mathrm{K}$

This foil temperature is well above the melting point of Havar. The conclusion is that conductive cooling will not be sufficient for low thermal conductivity materials.

5.5.1.3. Heat transfer by convection

The final mode of heat transfer is convection, which is the most difficult to estimate accurately. The equation for heat transfer is given by:

$Q_\mathrm{conv} = hA(T_1 - T_2)$

where

Q_conv is the heat transferred by convection (W);
A is the surface area (cm^2);
h is the film coefficient (W·cm^{-2}·K^{-1}); and
T is the temperature (K).

There are two modes of convective heat transfer, free and forced. In free convection, the flow patterns are determined mainly by the buoyant effects of the fluid, whereas in forced convection, the flow pattern is determined by other forces, such as fans or jets. In most cases, the film coefficient for a particular system must be experimentally determined in order to obtain an accurate value.

Some empirical relationships may be used to estimate this quantity for a wide range of situations, which have been tabulated in reference books on heat transfer. The problem in estimating this quantity comes from the boundary layer that exists between a flowing fluid and a stationary solid surface. For example, if a fluid is flowing in a laminar fashion parallel to a sharp edged plate, as is shown in Fig. 5.16, a boundary layer is created along the flat plate.

The velocity of the fluid in this boundary layer in close proximity to the surface of the plate is nearly zero as a result of the viscosity of the fluid. As the fluid flows along the plate, the thickness of the boundary layer will increase. Each lamination in the fluid 'drags' on the layer adjacent to it and causes an increase in the thickness as one proceeds along the plate. The thickness of the boundary layer decreases as the velocity increases. If the fluid and the plate are at different temperatures, then there will also be a thermal boundary layer created. As a consequence of the increasing thickness of this boundary layer, heat transfer will decrease as the fluid flows over the plate. In the layer nearest to the surface of the plate, the heat is transferred nearly entirely by conduction through the fluid. In the next layer, some of the heat is carried away by the flowing fluid and some is transferred by conduction to the next layer, and so on, throughout the boundary layer. It should be pointed out that this boundary layer is, in fact, a continuous change in the velocity of the fluid from nearly zero at the plate to the velocity of the bulk fluid at some distance from the plate. If

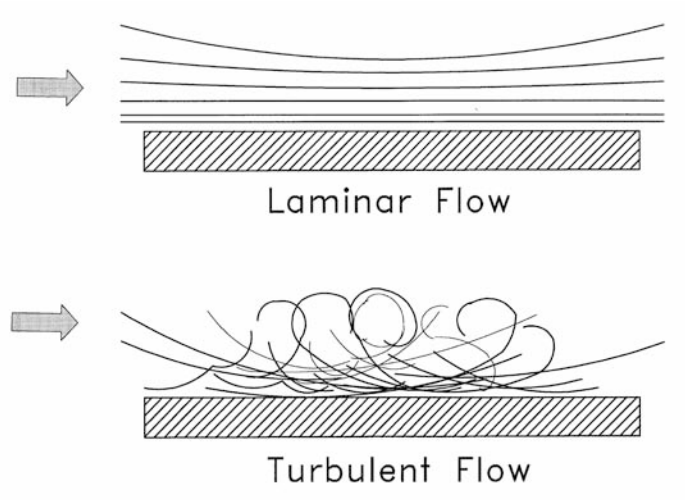

FIG. 5.16. Laminar and turbulent flow across a flat plate.

there is turbulence in the system, then heat will be transferred much more efficiently by the eddy currents that are created by the turbulent flow.

The characteristics of fluid flow across a surface are often described in terms of several dimensionless parameters. The first of these is the Reynolds modulus, which is given by the following relation:

$$\mathrm{Re} = \frac{xV\rho}{\mu}$$

where

Re	is the Reynolds number (dimensionless);
V	is the velocity of the bulk fluid (cm/s);
ρ	is the fluid density (g/cm^3);
μ	is the fluid viscosity (poise (g·cm^{-1}·s^{-1}), hereafter denoted by P); and
x	is the significant dimension (cm).

The Reynolds number represents the ratio of the inertial forces of the fluid to the viscous forces of the fluid. The definition of x needs some explanation.

In certain situations, it is clear what this dimension should be. For example, for a fluid flowing inside a tube, the significant dimension would be the diameter of the tube. In a fluid flowing over a flat plate, it is not so easily defined; but if there is a restriction on the thickness of the boundary layer, then this is usually chosen as the significant dimension. The transition from laminar flow to turbulent flow is determined by the Reynolds number. At low Reynolds numbers, the flow is laminar, and at high Reynolds numbers, the flow is turbulent. The transition from one type to the other will depend on a number of factors including the surface roughness and the exact geometry. A good rule of thumb is that Reynolds numbers below 1000 represent laminar flow and Reynolds numbers above 5000 represent turbulent flow. In the transition region between 1000 and 5000, the flow may be either laminar or turbulent, depending on the fluid and the surface. The second dimensionless parameter that is used in convective heat transfer is the Prandtl number, which is given by the following relation:

$$\mathrm{Pr} = C_\rho \mu / k$$

where

Pr	is the Prandtl number (dimensionless);
C_ρ	is the heat capacity of the fluid ($\mathrm{J\cdot g^{-1}\cdot K^{-1}}$);
μ	is the viscosity of the fluid (P ($\mathrm{g\cdot cm^{-1}\cdot s^{-1}}$)); and
k	is the thermal conductivity ($\mathrm{W\cdot cm^{-1}\cdot K^{-1}}$).

The Prandtl number represents the ratio of the viscous properties of the fluid to the heat transfer properties. It serves to compare the hydrodynamic boundary layer with the thermal boundary layer. In free convective flow, there is a dimensionless parameter called the Grashof number, which is given by the following relation:

$$\mathrm{Gr} = \frac{L^3 \rho^2 g \beta (T_\mathrm{w} - T_\mathrm{b})}{\mu^2}$$

where

Gr	is the Grashof number (dimensionless);
L	is the characteristic length (cm);
ρ	is the density of the fluid ($\mathrm{g/cm^3}$);
β	is the coefficient of volume expansion ($\mathrm{K^{-1}}$);
g	is the gravitational constant ($\mathrm{cm/s^2}$);
μ	is the fluid viscosity (P);
T_w	is the wall temperature (K); and
T_b	is the bulk fluid temperature (K).

This number expresses the ratio between the forces that cause the fluid to have buoyancy and those forces that tend to retard fluid flow.

The final parameter to be dealt with in convective heat transfer is the Nusselt number, which is defined in the case of forced convection by the following relation:

$$\mathrm{Nu} = \frac{hx}{k}$$

where

Nu	is the Nusselt number (dimensionless);
h	is the film coefficient ($\mathrm{W\cdot cm^{-2}\cdot K^{-1}}$);
x	is the significant distance (cm); and
k	is the thermal conductivity ($\mathrm{W\cdot cm^{-1}\cdot K^{-1}}$).

The Nusselt number has the form of a thermal conductance, and may be thought of as the ratio between the heat transported by convection and the heat transported by conduction through the fluid. This expression contains the term *h*, which is the coefficient required to determine the heat transfer according to the initial equation. The design equations for the various types of convective heat transfer are based, mostly, on empirical relationships between the Nusselt number and the other dimensionless parameters. For example, the expression for laminar flow in tubes is:

$$\frac{hx}{k} = 1.86(\mathrm{Re})^{1/3}(\mathrm{Pr})^{1/3}\left(\frac{x}{L}\right)^{1/3}\left(\frac{\mu_\mathrm{b}}{\mu_\mathrm{w}}\right)^{0.14}$$

where

x is the tube diameter (cm);
L is the tube length (cm);
μ_b is the bulk fluid viscosity (P); and
μ_w is the fluid viscosity at the wall (P).

In this case, the viscosity at the wall (μ_w) will be approximated by using the viscosity at a temperature that is the average of the wall temperature and the fluid temperature. If the flow in the tube is turbulent (as defined by the Reynolds number), then the relationship is:

$$\frac{hx}{k} = 0.023(\mathrm{Re})^{0.8}(\mathrm{Pr})^{1/3}\left(\frac{\mu_\mathrm{b}}{\mu_\mathrm{w}}\right)^{0.14}$$

If the convective heat transfer is free (e.g. no forced movement of the fluid past the object), then the Nusselt number is given by the following relations:

$\mathrm{Nu} = 0.61(\mathrm{Gr})^{1/4}(\mathrm{Pr})^{1/4}$ for $10^3 < \mathrm{Gr} < 10^7$

$\mathrm{Nu} = 0.73(\mathrm{Gr})^{1/4}(\mathrm{Pr})^{1/4}$ for $10^8 < \mathrm{Gr} < 10^{10}$

These particular relations are for flow past a vertical wall, which is a common situation in cyclotron targetry, especially the case of water flowing

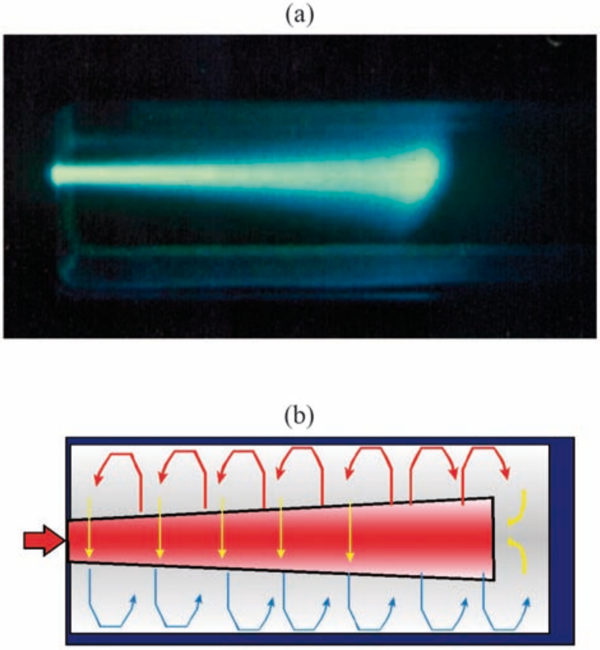

FIG. 5.17. An example of a heat flow pattern set up in a gas target during irradiation: (a) gas during irradiation; (b) the corresponding flow pattern (courtesy of S.J. Heselius).

over a plate. A possible flow pattern for the gas inside a target is shown in Fig. 5.17.

The pattern in Fig. 5.17 shows how convection currents might be set up in a static target during irradiation [5.19]. If the gas is flowing through the target, the situation is changed to one of forced convection, and the appropriate equations for this type of heat transfer have to be used.

In cyclotron targetry, it is usual to have both free convection and forced convection. In a gas or liquid target during irradiation, the heating of the fluid inside the target body will set up free convection currents. This flow will aid in removing some heat from the fluid and reduce the effects of density reduction. It is also usual to have some forced convective flow of gas over the front entrance window and forced flow of water through the target body. For many reasons, the gas used to cool the windows is often helium. Since this gas has a very low viscosity, it is very efficient in cooling the front window (and it does not become activated). Some typical values for the fluids used in the cooling of windows and target bodies are given in Tables 5.6(a) and (b).

TABLE 5.6(a). HEAT TRANSFER PARAMETERS FOR WATER AND NITROGEN

Fluid	Temperature (K)	Heat capacity, C_p ($J \cdot g^{-1} \cdot K^{-1}$)	Thermal conductivity, k ($mW \cdot cm^{-1} \cdot K^{-1}$)[a]	Viscosity, μ (cP)[b]
Water	273	4.2177	5.65	1.787
	280	4.197	5.74	1.472
	290	4.184	5.9	1.081
	300	4.179	6.04	0.8513
	320	4.1799	6.37	0.5755
	340	4.1879	6.59	0.4213
	360	4.2023	6.75	0.3259
	373	4.216	6.83	0.2818
Nitrogen	250	0.05833	0.19	0.01563
	284	—	—	0.01707
	300	0.05886	0.2598	0.01781
	350	0.05939	0.2939	0.01986
	400	0.05993	0.3252	0.02191
	450	0.06046	0.3564	—
	500	0.06099	0.3864	0.02554
	572	—	—	0.02791
	600	0.06206	0.441	—
	763	—	—	0.03374

[a] Milliwatts multiplied by 10^{-3} gives units of J/s.
[b] Centipoise multiplied by 0.01 gives units of $g \cdot cm^{-1} \cdot s^{-1}$.

TABLE 5.6(b). HEAT TRANSFER PARAMETERS FOR HELIUM[a]

Temperature[b] (K)	Thermal conductivity, k ($mW \cdot cm^{-1} \cdot K^{-1}$)[c]	Temperature (K)[d]	Viscosity, μ (cP)[e]
200	1.151	273	0.01861
300	1.499	293	0.01941
350	1.646	373	0.02281
400	1.795	473	0.02672
450	1.947	523	0.02853

TABLE 5.6(b). HEAT TRANSFER PARAMETERS FOR HELIUM[a] (cont.)

Temperature[b] (K)	Thermal conductivity, k (mW·cm^{-1}·K^{-1})[c]	Temperature (K)[d]	Viscosity, μ (cP)[e]
500	2.114	680	0.03436
600	2.47	879	0.04087

[a] The heat capacity for helium is constant at 0.2967 J·g^{-1}·K^{-1}.
[b] This temperature is the reference for the thermal conductivity.
[c] Milliwatts multiplied by 10^{-3} gives units of J/s.
[d] This temperature is the reference for the viscosity.
[e] Centipoise multiplied by 0.01 gives units of g·cm^{-1}·s^{-1}.

Linear interpolation between temperatures, although not completely accurate, gives reasonably good values for the parameters needed in most cases. If more accurate values are required, they can be obtained from tables and equations in standard engineering handbooks.

5.5.2. Target window foil materials

One of the most important components of any target system is the foil through which the beam enters the target material. This component is sometimes absent in solid targets, but is usually required in both liquid and gaseous targets. There are several important parameters in the choice of a foil. Often, the best choice with regard to one parameter will not be the best choice with regard to another parameter, so compromises are often necessary. The important parameters in the choice of a foil are:

- Its thermal conductivity;
- Its tensile strength;
- Its chemical reactivity (inertness);
- The energy degradation properties to which it is subject;
- Radioactive activation;
- Its melting point.

Each of these parameters interacts with the others in subtle ways. For example, the stopping power will determine the amount of power deposited in the foil, which in combination with the thermal conductivity will set the temperature. The temperature will have an effect on the yield strength of the foil and may affect the chemical reactivity of the foil.

5.5.2.1. Thermal conductivity

The thermal conductivity of the foil will determine the rate at which heat will be removed from the foil. If the foil is also cooled by either forced or free convection on the front surface (not in a vacuum), the heat deposited by the beam will be removed by a combination of these two processes. Foil materials such as aluminium are very good thermal conductors. The thickness of the foil will also determine the amount of heat that can be removed by this process, as is evident from examining the equation for heat transfer by conduction. A list of some common foil materials and the thermal conductivity for each is given in Table 5.7.

As can be seen from Table 5.7, the thermal conductivity of foil materials varies over a wide range. If the thermal conductivity of a foil material is not sufficient to remove the heat deposited in the foil from the beam, then the convective cooling must be increased to make up the difference.

The rear of the foil is usually only cooled with free convection from the circulating target gas or liquid. In some flow-through target designs, however, the target gas is injected through a jet onto the rear of the foil to increase heat removal. This can be an effective cooling method in gas targets.

TABLE 5.7. PHYSICAL AND THERMAL PROPERTIES OF SOME FOIL MATERIALS

Material	Density (g/cm^3)	Melting point (°C)	Tensile strength ($klbf/in^2$)[a]	Thermal conductivity ($W\cdot cm^{-1}\cdot K^{-1}$)	dE/dx ($MeV\cdot g^{-1}\cdot cm^{-2}$)
Carbon	2.2	>3000	—	2.51	41.08
Aluminium	2.71	660	30	2.37	33.96
Titanium	4.5	1668	120	0.31	29.77
Stainless steel	8.02	1427	120	0.29	28.91
Havar	8.3	1493	250	0.17	28.6
Nickel	8.9	1453	120	0.91	28.53
Tantalum	16.6	2996	70	0.53	18.57
Tungsten	19.3	3387	500	1.8	18.42
Platinum	21.4	1769	20	0.72	18.3
Niobium	8.57	2477	40	0.54	—

[a] 1 lbf/in^2 = 6.895 kPa.

As an illustration of the effects that convective cooling can have on the temperature of a foil, a simulation has been carried out, the results of which are presented in Table 5.8. Increasing the film coefficient h reduces the temperature of the foil so that it can withstand higher beam currents. Havar was chosen as an example because the thermal conductivity is low, which means that convective cooling must be the primary means of heat removal. The dashes in the table mean that the temperature was above the melting point of Havar at 1493°C.

Another important parameter of the foil is its tensile strength. The stress placed on a circular membrane is given by the following relation:

$$\varphi = 0.25\left(\frac{P^2 E a^2}{h^2}\right)^{1/3}$$

where

φ is the stress placed on the membrane;
P is the pressure (lbf/in^2);

TABLE 5.8. FOIL TEMPERATURE AS A FUNCTION OF THE CONVECTIVE FILM COEFFICIENT

Beam current (μA)	Power density (W/cm^2)	Foil temperature (°C)			
		$h = 0$	$h = 0.01$	$h = 0.03$	$h = 0.06$
20	15.3	—	1114	484	240
40	30.6	—	—	936	491
60	45.8	—	—	1331	735
80	61.1	—	—	—	973
100	76.4	—	—	—	1199

Note: The parameters in this example were:
$Q_{\text{conv}} = hA(T_2 - T_1)$;
Material, Havar;
Ambient temperature, 300 K;
Cooling gas (helium) temperature, 260 K;
Beam diameter, 0.5 cm;
Foil diameter, 2.0 cm;
Emissivity, –0.13;
Thermal conductivity, –0.12 W·cm^{-1}·K^{-1};
Energy of proton incident beam, 16 MeV.

E is Young's modulus (lbf/in^2);
a is the radius of the foil (cm); and
h is the thickness of the foil (cm).

If the stress on the foil exceeds the tensile strength of the foil, then the foil will burst. Rupture will usually occur in the centre of the foil, since this is where maximum stress occurs on a well clamped foil (i.e. a clamping flange where edges have been radiused). Some values for the tensile strength of some common foil materials are given in Table 5.7. The deflection of the foil from the plane of the foil [5.21] is given by the following relation:

$$w = a\left(\frac{Pa}{Eh}\right)^{1/3}$$

where w is the deflection in centimetres. The other symbols in this expression have the same meanings as in the equation for the stress on the foil.

In addition to these equations, which are valid for all circular membranes, there is an empirical relationship for aluminium 5052-0, which is an alloy often used for targets and target foils. The empirical relationship is:

$$P_{\mathrm{max}} = 13.8t - [75 + 63(1 - \mathrm{e}^{-0.2(x-2)})](0.057t + 0.0042t^2) \quad \text{for } x > 2$$

$$P_{\mathrm{max}} = 13.8t - 75(x - 1)(0.0575t + 0.00425t^2) \quad \text{for } 1 < x < 2$$

$$P_{\mathrm{max}} = 55.2(t/D) \quad \text{for } 0 < x < 1$$

where

P_{max} is the bursting pressure (lbf/in^2);
D is the diameter (in);
t is the thickness (0.001 in); and
x is $D/4$.

For stainless steel, the empirical relationship is:

$$P_{\mathrm{ss}} = 5.6P_{\mathrm{max}}$$

where P_{ss} is the maximum pressure for 316 stainless steel and P_{max} is the maximum pressure for aluminium 5052-0.

In all the above estimates, the calculated values are for room temperature, and the maximum stress the foil will withstand decreases with increasing temperature. The temperature dependence of yield strength can vary considerably with material. Yield strength versus temperature curves for several materials are shown in Fig. 5.18. It can be clearly seen that, for most materials, the yield strength decreases rapidly with increasing temperature. This is not the case, however, with certain types of stainless steels, where the yield strength increases slightly before decreasing with increasing temperature. Thus, the pressure in the target and the temperature during irradiation will determine the thickness of the foil that will be necessary to withstand a given stress.

5.5.2.2. Chemical reactivity

The next important characteristic of a foil is its chemical reactivity. This depends on the target material. In nitrogen targets, the foil is often aluminium, since this material is chemically inert to nitrogen gas and to the ^{11}C products produced.

Aluminium cannot be used in a target for production of ^{18}F from ^{18}O in water, since fluorine interacts with aluminium and it is very difficult to remove ^{18}F from the target. An aluminium target can be used for gaseous ^{18}F production, since the surface can be made non-reactive by exposure to fluorine

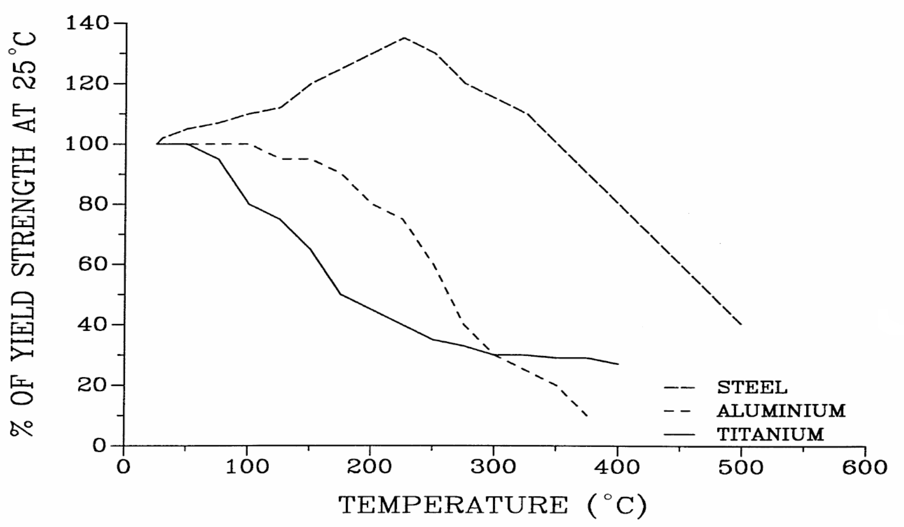

FIG. 5.18. Yield strength as a function of temperature for some common foil materials. Yield strength is given as a percentage of yield strength at 25°C.

gas at low concentrations. It is necessary to consider the chemical combination of the foil material with the target material not only at room temperature but also at elevated temperatures, since this is often the situation inside the target. Each target must be considered on a case by case basis, and there are no rules other than those of chemistry.

5.5.2.3. Energy degradation

Energy loss in the foil is another consideration, since this will have an impact on the beam energy incident on the target material and also on the heat that is deposited in the foil. The energy degradation relates to the stopping power of the material, as was calculated in the previous section. The ideal situation is to have a foil no thicker than is necessary to withstand the pressure in the target, so that the minimum amount of energy is deposited in the foil. An exception to this rule is when it is necessary to reduce beam energy in order to have the energy incident on the target material at an optimum value with respect to the cross-section of the desired nuclear reaction.

5.5.2.4. Activation of foils

Another consideration is the radioactivation of target foils, since this will often determine how radioactive the target will be. All target foils need to be replaced at fairly frequent intervals, which can result in a radiation dose to the person working on the target. Aluminium is often the material of choice in this regard, because there are very few long lived isotopes formed in the foil. Nickel alloys and steels, which must be used for chemical inertness in certain situations, are perhaps the worst commonly used materials with respect to activation, since these metals often have several long lived activities associated with them.

5.5.2.5. Melting point

The final item in the list of important foil parameters is the melting point. The ideal foil material would have a very high melting point so that heating of the foil by the beam would not be a problem. The most widely used foil is aluminium, which has a low melting point. In this case, the other attractive properties of aluminium outweigh the disadvantage of a low melting point.

5.5.3. Target body materials

There are five important characteristics for target body materials. These are:

(1) Thermal conductivity;
(2) Chemical reactivity;
(3) Activation;
(4) Ease of machining/manufacture;
(5) Mechanical strength.

These characteristics share nearly equal importance in the choice of a material for the target body. Samples of common materials used in target body construction, along with some values for the five characteristics mentioned, are given in Table 5.9.

The most common material for construction of target bodies is aluminium. It has a high thermal conductivity, activation products that have short half-lives or are not made in great abundance, is chemically inert to most gases under irradiation conditions and is easily machined. The disadvantage is that it is difficult to weld to other materials.

The thermal conductivity of the target body is important since the heat, which is generated inside the target, must be transferred through the target body material to a heat sink. The normal method of heat dissipation is water cooling. The number of cooling channels, the distance between the inner wall and the water cooling channel, and the way in which the water cooling channels are cut, determine the heat transfer from the metal target body to the water. Increasing the surface area between the water and the metal body (assuming similar Reynolds numbers) increases the heat transfer, as was shown in Section 5.5.1.3 on convective heat transfer. Fins to increase surface area, as well as parallel water channels, have been used in targets with high heat loads. In some cases, it is not possible to use water for cooling. In some situations, other liquids or gases must be used.

The chemical reactivity of the target body material is significant, particularly if the material retains the radioisotope chemically [5.22]. This can be used to advantage if the radioisotope can be easily removed by washing or some other form of chemical dissolution. Chemical compatibility is more important with solid and liquid targets, since for these the reactive material is more concentrated. Activation of the target body is an obvious consideration when the time comes for target repair or maintenance. This may be the deciding factor in determining whether to build a duplicate target that can be put into service while the radioactivity in the other target is allowed to decay.

TABLE 5.9. PHYSICAL AND THERMAL PROPERTIES OF SOME TARGET BODY MATERIALS

Material	Thermal conductivity ($W\cdot m^{-1}\cdot °C^{-1}$)	Chemical reactivity	Nuclear activation	Ease of machining	Tensile strength ($klbf/in^2$)[a]
Aluminium	2.37	Good	p negligible d–^{24}Na	Good	110
Aluminium 3003	2.63	Good			130
Aluminium 6061	1.80	Good			115
Copper	4.03	Fair	p–^{65}Zn, ^{62}Zn, ^{64}Cu d–^{65}Zn	Excellent	344
Nickel	0.91	Excellent	p–^{57}Ni, ^{55}Co d–^{64}Cu	Good	175
Monel	0.32	Excellent	As for nickel	Good	112
Silver	4.27	Good	p, d–^{107}Cd, ^{109}Cd	Good	170
Titanium	0.31	Excellent	p–^{48}V d–^{49}V	Good	300
Stainless steel	0.29	Good	p–^{56}Co, ^{55}Co d–^{57}Co, ^{56}Co	Good	860
Brass	2.01	Fair	As for copper		250
Niobium	0.54	Excellent		Good	300

[a] 1 lbf/in^2 = 6.895 kPa.

Machining is a consideration even when a high quality machine shop is available for fabrication. The cost of a target will depend, to a great extent, on the time required to machine it. The compatibility of different materials will also enter into this question. If welding, brazing or soldering must be employed, the materials (solders and fluxes) used must be compatible with the target material. Some target designers have begun using electric discharge machining (EDM) to form target bodies. This method uses no organic solvents or cutting oils. This, in turn, can significantly reduce contamination with target materials, such as for ^{11}C targets, where SA is so important.

In general, any use of cutting lubricants should be avoided, unless well established cleaning procedures are available. Ultrasound baths may be used to remove solvents. The use of all-metal O-rings or C-rings is recommended.

5.5.4. Power density with inclined planes

As has been discussed in previous sections, one of the more difficult problems in accelerator targetry is dissipation of the heat generated as the beam passes through the absorber. One approach, often taken with solid targets, is to use an inclined plane to spread the beam out over a larger area and thereby reduce the power density in the beam strike area. This can be accomplished relatively easily on internal targets by inclining the target to the beam and bending the target plate to the curvature of the beam in the outer orbits of the cyclotron. An example of this is shown in Fig. 5.19.

In Fig. 5.19, the difference in beam profile can be seen easily in the beam profiles shown. The first is obtained by using a flat plate at a grazing incidence of a few degrees. The second profile is for a plate that has been shaped by hand to approximate the curvature of the beam in the outer orbits. The third is the beam strike profile when the target plate has been optimized to match the exact curvature of the beam.

Inclined planes may also be used on external targets. A simple example of this type of target is shown in Fig. 5.20.

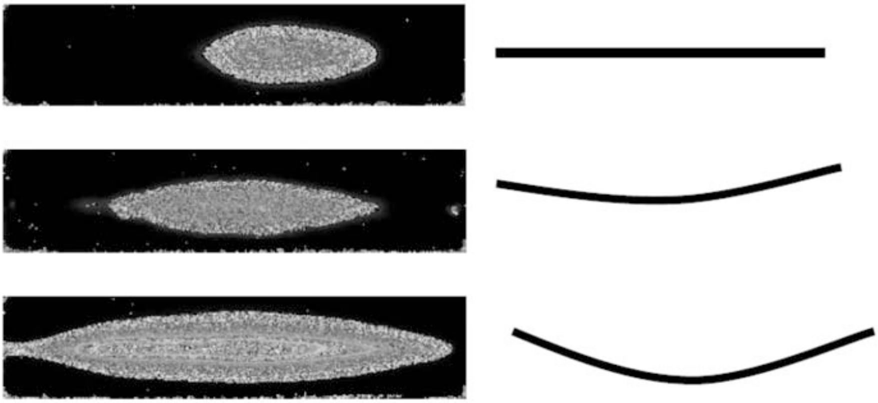

FIG. 5.19. Beam profiles of internal target beams incident on plates of various shapes. The closer the plate matches the beam curvature, the better the distribution of the beam along the plate.

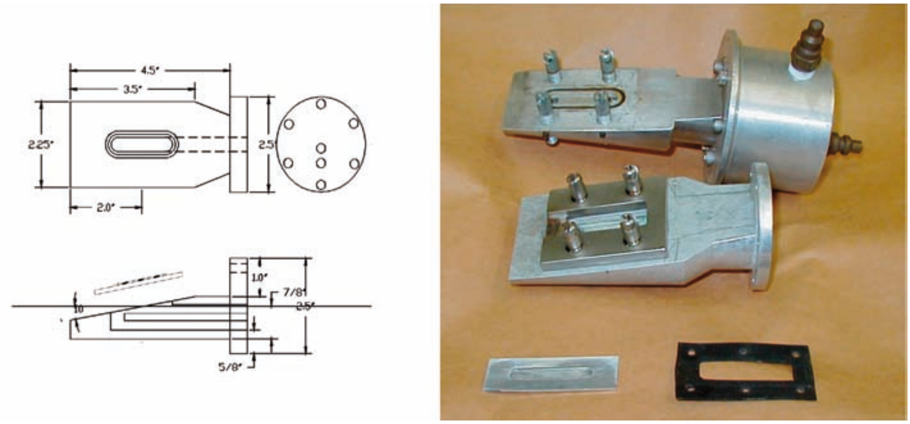

FIG. 5.20. Example of an inclined plane external target used for solid materials either pressed or melted into the depression in the target plate.

5.6. BEAM TRANSPORT

Extracted beams are often transported from the accelerator to the target by the beam transport system. This can consist of a series of dipole and quadrupole magnets, magnetic lenses, collimators and beam monitors, or, as in the case of many small cyclotrons where the targets are attached directly to the machine, it is just a beam collimator. The arrangement of magnets, vacuum chambers and diagnostic instrumentation is called a beamline. The beam transport system modifies and monitors the beam to achieve the optimum beam distribution inside the target volume. The ease of adjusting the beam through the beamline (tuning the beamline) and the reproducibility of the state of beamline tune are critical for efficient and reliable radioisotope production. Beam tuning means adjusting the beam optics to transport the beam to the desired location with the desired shape and intensity at that location.

5.6.1. Collimators

Collimators are usually designed to be slightly smaller than the target opening or window. This is important for two reasons:

(1) Firstly, the size of the beam is limited to the size of the target opening and, therefore, the beam current that is read on the target is an accurate indication of the beam hitting the target.
(2) Secondly, it prevents the front flange of the target from becoming activated and therefore lowers the radiation dose to the operator when maintenance is required.

The ideal collimator is divided into several sectors that may be monitored independently. This allows the beam to be steered so as to obtain the maximum beam current incident on the target more efficiently.

5.6.2. Beam focusing

Beams leaving an accelerator can have unusual shapes depending on the dynamics of the acceleration and extraction, as well as on the fringing field in cyclotrons. It is sometimes desirable to focus the beam with quadrupole magnets. This also allows some smoothing of the beam in those accelerators where the beam may have some ‘hot spots’, or spikes in the intensity profile.

5.6.3. Wobbling and rastering

The purpose of ‘wobbling’ or rastering the beam is to lower the power density on the target. This in turn allows the target to be operated at higher beam currents with the resulting higher yields of radioisotope production. It is necessary to have a beamline of some kind in order to take advantage of this method of power dissipation. These dynamic beam delivery systems (wobblers or scanners) are developed to overcome the undesirable necessity of scattering materials in the beam and, therefore, of lowering the energy.

5.6.4. Beam profile monitoring

Beamlines are often equipped with beam profile monitors. These devices monitor the shape of the beam, usually in two dimensions. They allow the operator to adjust the beam shape with steering and focusing magnets in order to obtain the ideal beam shape on the target. There are many different designs of beam scanners, from simple wires, which can be inserted into the beam, to more sophisticated scanners with a rotating wire attached to an oscilloscope, which provide high resolution images of the beam shape.

5.7. ENRICHED MATERIALS IN TARGETS

For many years, enriched stable isotopes have been the foundation for the production of isotopically pure radionuclides. In the past decade, there has been a significant increase in the acquisition and use of ‘small’ cyclotrons devoted principally to production of the radiolabelled compounds or radiopharmaceutical drugs required for biomedical research. The availability and application of stable enriched target materials for production of biologically equivalent radionuclides is of paramount concern, given the energy constraints typical of the various accelerators chosen for installation into imaging facilities.

5.7.1. Natural abundance or isotopic enrichment

There are two major reasons to use targets that have been enriched in a particular isotope:

(1) Firstly, the target may use isotopically enriched material in order to produce more of the isotopes of interest.
(2) Secondly, the use of the natural abundance target element often results in the production of unwanted by-products.

A simple example involves using ^{18}O labelled water for ^{18}F production. The abundance of ^{18}O in natural oxygen is about 0.2%. This means that using natural abundance water for production of ^{18}F not only would produce very little ^{18}F but also would produce much larger quantities of ^{13}N. It is necessary to use water isotopically enriched in ^{18}O for the production of ^{18}F.

5.7.2. Availability of enriched isotopes

The major difficulties with using enriched materials are that they can be very expensive and that they may be unavailable at times. This is due to the extensive separations that are often necessary to produce highly enriched isotopes from a low abundance starting material. For this reason, the isotopically enriched materials need to be recovered after each use and reused. This can require involved chemistry and great care in separation and purification to ensure the chemical and isotopic purity of the target material.

5.8. TWO SIMPLE EXAMPLES: SOLID TARGETS FOR ^{201}Tl AND GAS TARGETS FOR ^{11}C PRODUCTION

The purpose of this section is to give some very simple examples of the application of the formulas and suggestions contained in this chapter. The examples are:

(1) The production of ^{201}Tl using a solid ^{203}Tl target;
(2) The design of a gas target for production of ^{11}C from nitrogen gas.

5.8.1. Solid target for ^{201}Tl production

The first step in the design of a target is to decide the optimum energy interval for a particular nuclear reaction. The nuclear reaction used for production of ^{201}Tl is the ^{203}Tl(p, 3n)^{201}Pb reaction. The ^{201}Pb ($T_{1/2}$ = 9.33 h) produced in the reaction is then allowed to decay to ^{201}Tl ($T_{1/2}$ = 76.03 h) in a separate column. In this case, there are two competing nuclear reactions, which is typical of reactions that evaporate more than one neutron from the nucleus. The data for the nuclear reaction cross-sections can be found in the literature, and many nuclear reaction cross-sections can be found on-line at the US National Nuclear Data Center (http://www.nndc.bnl.gov/index.jsp). A graph of the competing cross-sections is shown in Fig. 5.21.

From Fig. 5.21, it is seen that at energies greater than 30 MeV, production of ^{200}Pb starts to become significant. At energies less than 20 MeV, production

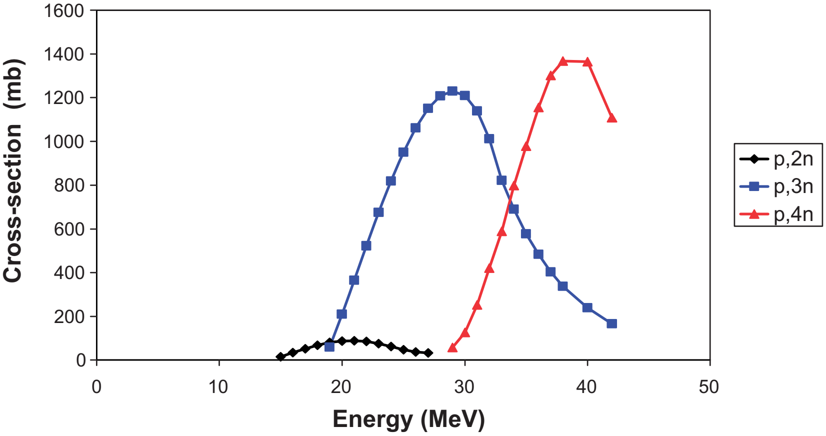

FIG. 5.21. Cross-section versus energy plot for the ^{203}Tl(p, 2n)^{202}Pb, ^{203}Tl(p, 3n)^{201}Pb and ^{203}Tl(p, 4n)^{200}Pb nuclear reactions.

TABLE 5.10. SOME IMPORTANT PROPERTIES OF COPPER AND THALLIUM

Element	Density (g/cm^3)	Melting point (°C)	Thermal conductivity (W·cm^{-1}·K^{-1})
Copper	8.96	1083	4.03
Thallium	11.85	303	0.46

of ^{201}Tl drops to very low levels. Therefore, the best energy interval to maximize yields and minimize impurities is 20–30 MeV.

The target itself will be a thin layer of thallium electroplated onto a copper plate. Copper is chosen because it is relatively easy to electroplate thallium onto copper; and copper has an excellent thermal conductivity, which is important for removal of heat from the thallium. At the rear of the copper plate is a water cooling stream to transfer heat convectively. There are several important parameters for these materials, which are listed in Table 5.10.

The next step is to calculate the thickness of the thallium layer. The range of protons can be determined from the SRIM code referenced earlier in this chapter. The range of a 30 MeV proton in ^{203}Tl is 1.75 mm. The range of a 20 MeV proton is 0.89 mm. Thus, the depth of thallium needed to degrade 30 MeV protons to 20 MeV is 0.86 mm (1.75–0.89). In a similar fashion, to degrade 20 MeV protons to 0 MeV, 0.8 mm of copper is required. In order to make the copper plate mechanically stable, the thickness will be set at 2 mm.

In order to make sufficient ^{201}Tl in a reasonable amount of time (on the basis of cross-section, time and SF), a beam current of about 50 μA is needed. This means that the total power deposited in the target is 1500 W (30 MeV × 50 μA). In order to explore the efficiency of cooling the copper plate, a proposed design needs to be set up to test if it will work. A preliminary design is shown in Fig. 5.22.

The cyclotron beam profile is assumed to be uniform (which is not usually true) and to have a diameter of 1 cm. The first step is to determine if it is possible to remove the heat in this configuration. The convective heat transfer equation can be used to determine the required film coefficient. The area of the cooling will be slightly larger than the beam profile. The beam area is 0.78 cm^2, so it will be assumed that the cooling area is 1 cm^2. It is desirable to keep the temperature of the plate well below the melting point of thallium, so that T_2 can be set at a value of 200°C. The temperature of the water is assumed to be 20°C:

$$Q_{\text{conv}} = hA(T_1 - T_2) \quad \text{or} \quad h = Q/[A(T_1 - T_2)]$$

$$h = 1500\ \text{W}/(1\ \text{cm}^2)(200 - 20°\text{C}) = 8.3\ \text{W·cm}^{-2}\text{·°C}^{-1}$$

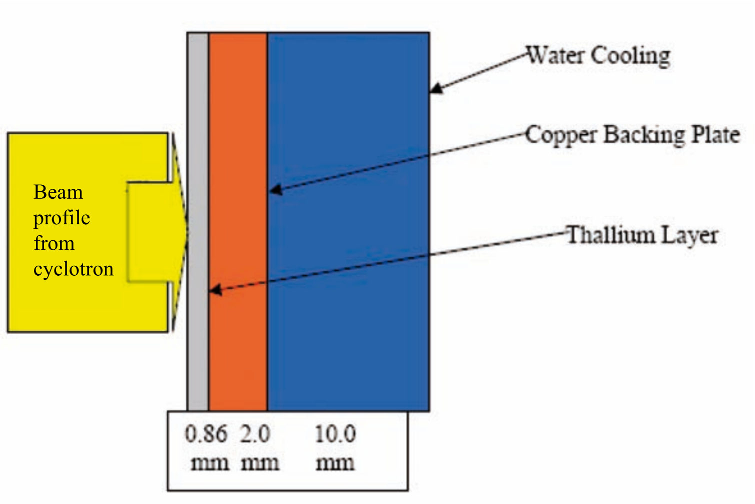

FIG. 5.22. Preliminary design of a solid thallium target.

It is possible to set the Nusselt number based on this value,

$$\mathrm{Nu} = \frac{hx}{k} \quad \text{or Nu} = (8.3\ \mathrm{W{\cdot}cm^{-2}{\cdot}{}^{\circ}C^{-1}}) \times (1\ \mathrm{cm})/(0.00593\ \mathrm{W{\cdot}cm^{-1}{\cdot}{}^{\circ}C^{-1}})$$

$$\mathrm{Nu} = 1400$$

If it is assumed that the flow is over a flat plate, the formula for the Nusselt parameter can be used, which is:

$$\mathrm{Nu} = 0.332\ \mathrm{Re}^{1/2}\ \mathrm{Pr}^{1/2}$$

The Prandlt number is given by:

$$\mathrm{Pr} = \frac{C_p \mu}{k}$$

For water at 290 K, this becomes:

$$\mathrm{Pr} = (4.179\ \mathrm{J{\cdot}g^{-1}{\cdot}K^{-1}}) \times (0.008513\ \mathrm{g{\cdot}cm^{-1}{\cdot}s^{-1}})/(0.00604\ \mathrm{W{\cdot}cm^{-1}{\cdot}K^{-1}})$$

or

$$\mathrm{Pr} = 5.89$$

Therefore, the Reynolds number must be:

$$\mathrm{Re}^{1/2} = \mathrm{Nu}/[(0.332) \times (\mathrm{Pr}^{1/2})] = 1400/[(0.332) \times (2.43)] = 1737$$

$$\mathrm{Re} = 3.02 \times 10^6$$

This flow is turbulent. The Reynolds number is given by the following relation:

$$\mathrm{Re} = \frac{xV\rho}{\mu}$$

If the critical dimension x is assumed to be 1 cm, then the velocity of water necessary to cool the target can be calculated:

$$V = \mathrm{Re}\,\mu/x\rho = (3.02 \times 10^6)(0.008513\ \mathrm{g{\cdot}cm^{-1}{\cdot}s^{-1}})/(1\ \mathrm{cm})(1.0\ \mathrm{g/cm^3})$$

$$V = 2.6 \times 10^4\ \mathrm{cm/s}$$

If the inside of the target cooling volume is assumed to be 0.5 cm by 2 cm, then the volume of water that must be pumped through the target has to be:

$$\mathrm{Volume} = (2.6 \times 10^4\ \mathrm{cm/s})\ (1\ \mathrm{cm^2}) = 2.6 \times 10^4\ \mathrm{cm^3/s} = 26\ \mathrm{L/s}$$

This is an unreasonable amount of water flow. Heat transfer can be improved in several ways, such as reducing the volume of the cooling water chamber to increase the flow velocity or increasing the surface area being cooled by inclining the target to the beam.

There is another parameter that has not yet been considered: the heat transfer from the thallium layer through the copper plate to the water. Determination of this is a conductive heat transfer problem, and the equation for the transfer is given by the following relation:

$$Q_{\mathrm{cond}} = \frac{-kA(T_1 - T_2)}{x}$$

The heat transfer can also be thought of as:

$$Q = \frac{T_\mathrm{i} - T_\mathrm{f}}{R_\mathrm{total}}$$

In analogy to the electrical resistance to flow, the total resistance is the sum of the individual resistances. In this case, there are two metals. As a first approximation, it can be assumed that all the heat has to travel through the copper plate, in which case:

$$T_1 - T_2 = Qx/kA = (1500\ \mathrm{W})(0.2\ \mathrm{cm})/(4.03\ \mathrm{W{\cdot}cm^{-1}{\cdot}K^{-1}})(1\ \mathrm{cm}^2)$$

which gives

$$T_1 - T_2 = 74\ \mathrm{K}$$

So there is no problem with the heat transfer through a copper plate. It will easily accommodate the power density.

For the thallium layer, it is necessary to pass 500 W through the layer, but it will be deposited throughout the layer. As an approximation for this, it can be assumed that 500 W is being deposited halfway through the layer. The same analysis will be applied:

$$T_1 - T_2 = Qx/kA = (500\ \mathrm{W})(0.043\ \mathrm{cm})/(0.46\ \mathrm{W{\cdot}cm^{-1}{\cdot}K^{-1}})(1\ \mathrm{cm}^2)$$

which gives

$$T_1 - T_2 = 47\ \mathrm{K}$$

Even if it is assumed that the power has to be transferred through the whole layer, then the temperature differential will only be 94 K. It can be seen that the limiting factor in this target is the water cooling at the rear of the target. If the cooling surface area is increased by a factor of 5 and the flow velocity increased by a factor of 5, then the flow can be reduced from 26 L/s to about 1 L/s. A much more rigorous evaluation of these parameters is provided in Chapter 6.

5.8.2. Gaseous target for ^{11}C production

The first step is to determine the energy interval for the production of ^{11}C from the ^{14}N(p, α)^{11}C nuclear reaction. Here there are no real competing reactions, so that the whole energy interval for radioisotope production can be explored. The cross-section for the production of ^{11}C from the reaction on nitrogen is shown in Fig. 5.23.

It can be seen that the optimum energy for this reaction is between 4 and 20 MeV. The cross-section falls beyond about 15 MeV.

Since many of the cyclotrons that are used for PET have energies of about 17 MeV, it will be assumed that the entrance energy will be 17 MeV, and we require the energy incident on the gas to be at least 15 MeV. The range of a 15 MeV proton in nitrogen gas at atmospheric pressure is 2.31 m. The pressure inside the target needs to be increased in order to have a reasonable length. We need to calculate the maximum pressure that can be withstood by the front foil of the target. If an aluminium front foil is used and we can afford to lose 2.0 MeV of energy in the foil, then:

(a) The range of 17.0 MeV protons in the foil is 1.58 mm.
(b) The range of 15.0 MeV protons in the foil is 1.27 mm.
(c) The thickness of the aluminium foil is 0.31 mm.

For this foil thickness, the empirical relationship for aluminium can be used. It will be assumed that the diameter of the foil is 2.54 cm (1 in). Thus,

$$P_{\max} = 55.2(t/D) \quad \text{for } 0 < x < 1$$

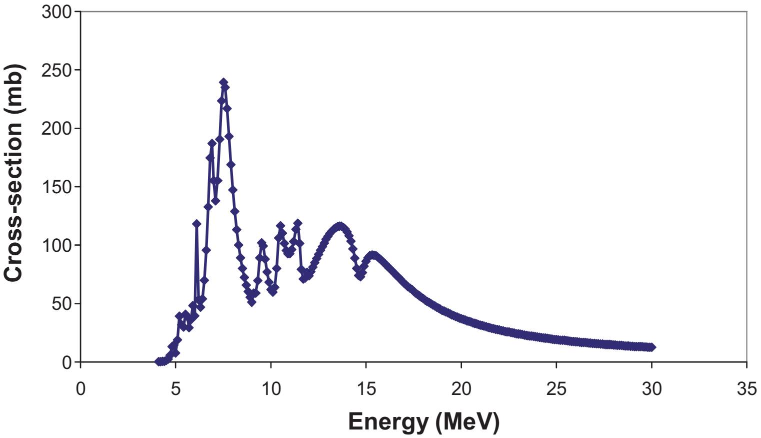

FIG. 5.23. Cross-section for the ^{14}N(p, α)^{11}C nuclear reaction.

Here, the thickness in thousands of an inch is:

$$(0.31 \text{ mm}/25.4 \text{ mm/in}) \times 1000 = 12.2 \text{ mil, or}$$

$$P_{\text{max}} = 55.2(12.2/1) = 671 \text{ lbf/in}^2 = 45 \text{ atm} = 4.626 \text{ MPa}$$

This is the pressure with the beam on. It is also obvious that the yield strength of aluminium decreases with increasing temperature, so we need to estimate the temperature of the foil, and the pressure inside the target during irradiation. Since the major heat transfer mode will be conduction, the temperature in the centre of the foil will be directly related to the beam current on the target. The assumption will be made that the beam current is 30 μA, giving a power of 60 W (2 MeV and 30 μA) in the front of the foil. A first order estimate of the foil temperature can be obtained by carrying out a simple calculation, using the diagram shown in Fig. 5.24.

We can assume that the thermal conductivity of aluminium is 2.37 $\text{W}\cdot\text{cm}^{-1}\cdot{}^{\circ}\text{C}^{-1}$. The surface area for heat transfer can be assumed as the cross-sectional area of the foil at the edge of the beam spot. The distance the heat has to travel to the heat sink is the distance from the edge of the foil to the outer flange. This is given by:

$$A = \pi D \times \text{thickness} = (3.14159)(1 \text{ cm})(0.031 \text{ cm}) = 0.097 \text{ cm}^2$$

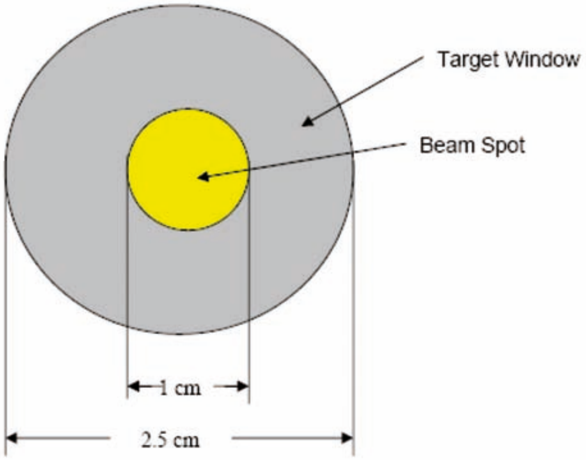

FIG. 5.24. Diagram of beam spot on the front entrance window of a gas target.

The distance the heat has to travel is 1.25 cm – 0.5 cm = 0.75 cm, providing the final relationship:

$$T_1 - T_2 = Qx/kA = (60\ \mathrm{W})(0.75\ \mathrm{cm})/(2.37\ \mathrm{W{\cdot}cm^{-1}{\cdot}{}^{\circ}C^{-1}})(0.097\ \mathrm{cm^2})$$

which gives:

$$\Delta T = 183^{\circ}\mathrm{C}$$

If it is assumed that the ambient temperature is 20°C and that the outer flange is an infinite heat sink, then the temperature at the centre of the foil will be about 200°C. Assuming the worst case scenario, i.e. the distance the heat has to travel is from the exact centre of the foil to the flange, the temperature differential will be 305°C, with a maximum temperature of about 325°C. From Fig. 5.18, it can be seen that the yield strength is about one third of the strength at room temperature. This means that the target cannot be used above about 15 atm (1.52 MPa). A more exact analysis of the foil temperature gives a temperature in the centre of the foil of 201°C, which means that the crude estimate was very reasonable. The yield strength at 200°C is close to that at room temperature. In a conservative way, the pressure in the target will be limited to 15 atm (1.52 MPa). Since the proton beam will travel through 2.31 m of nitrogen gas at standard temperature and pressure, at 15 atm, 15 cm of gas is needed to stop the beam. Because the beam will be thinned by heating during the irradiation, the estimated length is 20 cm for the target.

It is necessary to calculate the other dimensions of the target. The usual method is to construct a conical target, since this shape minimizes the volume of gas used. It is assumed that an aluminium target body will be used, as most carbon targets are now constructed out of aluminium. It is necessary to avoid hitting the side of the target with the beam, since this can reduce the SA of the final product. The angle at which the beam comes out of the foil into the target needs to be calculated. There is also scattering in the gas, but this can be ignored for the moment. The scattering in the front foil is given by the relation (Section 5.3.4):

$$\sigma^2 = 0.0536\left(\frac{xZ^2z^2\ln\left(\dfrac{3.67\times10^4 E}{zZ^{4/3}}\right)}{AE^2}\right)$$

$$\sigma^2 = 0.0536\{0.084\times13^2\times1^2\times\ln[(3.67\times10^4\times16/1\times13^{4/3})]\}/27\times16^2$$

which gives

$$\sigma = 0.0329 \text{ rad} = 1.67°$$

Since the target is 20 cm long, the distribution of the beam at 20 cm from the front foil can be calculated to determine the geometry of the target. The value of σ of the distribution at 20 cm corresponds to a distance of 0.58 cm. A flat distribution beam shape of the proper dimensions (1 cm diameter) can be used to estimate the distribution at the rear of the target. The rear of the target will be made 3 cm in diameter. The beam distribution at the rear of the target is shown in Fig. 5.25.

It can be seen that a target with a diameter of 3 cm at the rear of the target will accommodate the beam. With this, a basic volume for the target can be designed. Uncertainty in the beam diameter and beam position may dictate that the diameter be increased slightly.

5.9. CONCLUSIONS

Simple rules and formulas can be used to design new targets for cyclotrons and to help individuals unfamiliar with cyclotron targetry to

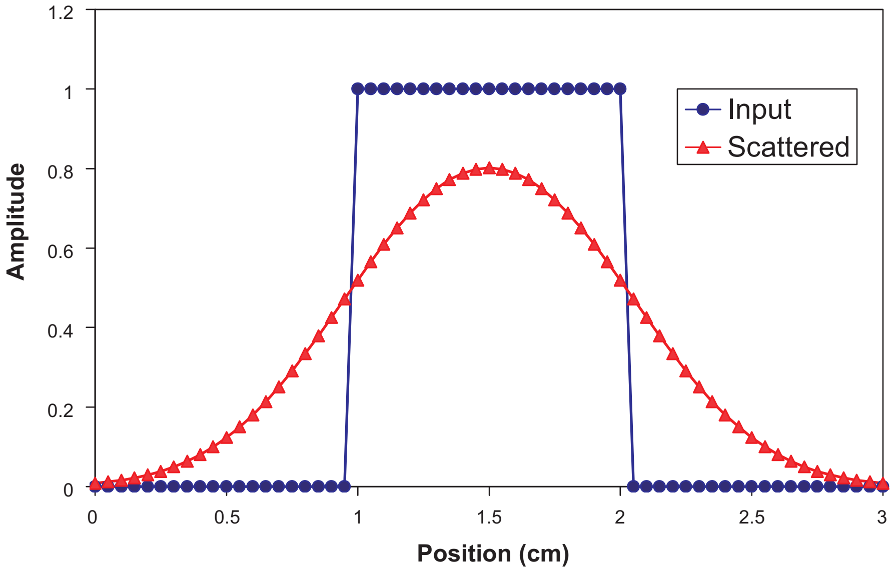

FIG. 5.25. Distribution of the beam before and after being scattered by a 0.031 cm aluminium foil at a distance of 20 cm from the foil.

appreciate the interplay of forces [5.23]. More sophisticated descriptions or computer simulations can be used to advantage, but these simple calculations that can be done quickly can be used to compare results with, in order to ensure that a problem is well described and that the results obtained are reasonable.

REFERENCES TO CHAPTER 5

[5.1] EVANS, R.D., The Atomic Nucleus, McGraw-Hill, New York (1955).

[5.2] DECONNINCK, G., Introduction to Radioanalytical Physics, Nuclear Methods Monographs No. 1, Elsevier, Amsterdam and New York (1978).

[5.3] SCHLYER, D.J., PLASCJAK, P.S., Small angle multiple scattering of charged particles in cyclotron target foils: A comparison of experiment with simple theory, Nucl. Instrum. Methods Phys. Res. B **56/57** (1991) 464–468.

[5.4] CLARK, J.C., BUCKINGHAM, P.D., Short-Lived Radioactive Gases for Clinical Use, Butterworths, London (1975).

[5.5] Targetry and Target Chemistry, Proceedings Publications, TRIUMF, Vancouver, http://trshare.triumf.ca/~buckley/wttc/proceedings.html

[5.6] STEVENSON, N.R., et al., "Pushing beam currents to the limit", Targetry and Target Chemistry (Proc. 5th Workshop New York, 1993), TRIUMF, Vancouver (1993) 5–11, http://trshare.triumf.ca/~buckley/wttc/proceedings.html

[5.7] ZAIDI, J.H., QAIM, S.M., STOCKLIN, G., Excitation functions of deuteron induced nuclear reactions on natural tellurium and enriched ^{122}Te: Production of ^{123}I via the ^{122}Te(d, n)^{123}I-process, Int. J. Appl. Radiat. Isot. **34** (1983) 1425–1430.

[5.8] JANNI, J., Stopping Power and Ranges, Rep. AFWL-TR-65-150, Air Force Weapons Lab., Kirtland AFB, NM (1965).

[5.9] ZIEGLER, J.F., SRIM — The Stopping and Range of Ions in Matter, http://www.srim.org/

[5.10] WILLIAMSON, C.F., BOUJOT, J.P., PICARD, J., Tables of Range and Stopping Power of Chemical Elements for Charged Particles of Energy 0.5–500 MeV, Rep. CAE-R 3042, Centre d'études nucléaires de Saclay, Gif-sur-Yvette (1966).

[5.11] BERGER, M.J., et al., Stopping Powers and Ranges for Protons and Alpha Particles, ICRU Rep. 49, International Commission on Radiation Units and Measurements, Bethesda, MD (1993).

[5.12] HESELIUS, S.J., SCHLYER, D.J., WOLF, A.P., A diagnostic study of proton-beam irradiated water targets, Appl. Radiat. Isot., Int. J. Radiat. Appl. Instrum. A **40** (1989) 663–669.

[5.13] WIELAND, B.W., SCHLYER, D.J., WOLF, A.P., Charged particle penetration in gas targets designed for accelerator production of radionuclides used in nuclear medicine, Int. J. Appl. Radiat. Isot. **35** (1984) 387–396.

[5.14] CHRISTMAN, D.R., FINN, R.D., KARLSTROM, K.I., WOLF, A.P., Production of carrier-free H^{11}CN for medical use and radiopharmaceutical synthesis IX, J. Nucl. Med. **14** (1973) 864.

[5.15] FINN, R.D., CHRISTMAN, D.R., ACHE, H.J., WOLF, A.P., The preparation of cyanide-^{11}C for use in synthesis of radiopharmaceuticals, Int. J. Appl. Radiat. Isot. **22** (1971) 435.

[5.16] BIDA, G., et al., An economical target for nitrogen-13 production by proton bombardment of a slurry of ^{13}C powder in ^{16}O water, J. Labelled Compd. Radiopharm. **23** (1986) 1217.

[5.17] FERRIERI, R.A., SCHLYER, D.J., WIELAND, B.W., WOLF, A.P., On-line production of ^{13}N-nitrogen gas from a solid enriched ^{13}C-target, and its application to ^{13}N-ammonia synthesis using microwave radiation, Int. J. Appl. Radiat. Isot. **34** (1983) 897–900.

[5.18] FOWLER, J.S., WOLF, A.P., The Synthesis of Carbon-11, Fluorine-18, and Nitrogen-13 Labeled Radiotracers for Biomedical Applications, Nuclear Science Series Rep. NAS-NS-3201, National Technical Information Service, Springfield, VA (1982).

[5.19] HESELIUS, S.-J., LINDBLOM, P., SOLIN, O., Optical studies of the influence of an intense ion beam on high pressure gas targets, Int. J. Appl. Radiat. Isot. **33** (1982) 653–659.

[5.20] HOLMAN, J.P., Heat Transfer, 9th edn, McGraw-Hill, New York (2002).

[5.21] WESTIN, J.L., Mechanical Safety Subcommittee Guideline for Design of Thin Windows for Vacuum Vessels, Rep. TM-1380, FermiLab, Batavia, IL (1991).

[5.22] BISHOP, A., SATYAMURTHY, N., BIDA, G., PHELPS, M., BARRIO, J.R., Metals suitable for fluorine gas target bodies: First use of aluminum for the production of [^{18}F]F_2, Nucl. Med. Biol. **23** (1996) 181–188.

[5.23] SCHLYER, D.J., Production of short-lived radiopharmaceuticals for PET, Nucl. Instrum. Methods Phys. Res. B **24/25** (1987) 925–927.

Chapter 6

TARGET PREPARATION AND IRRADIATION

6.1. INTRODUCTION

The care of targets is one of the prime considerations in maintaining good production yields and ensuring the longest useful lifetime. It is also important in attaining high SA radioisotopes. Section 6.2 examines the preparation, routine maintenance, and care of gas and liquid targets. The remainder of the chapter focuses on the preparation and analysis of solid targets, since these are much more complex matters.

6.2. PREPARATION OF GAS AND LIQUID TARGETS

The preparation of gas and liquid targets is generally less labour intensive than the preparation of solid targets. There are, however, a few examples where some significant preparation of gas targets is required [6.1, 6.2]. One of these is the cleaning of the target. Certainly before first use and at regular intervals afterwards, the target needs to be cleaned. For liquid targets, a routine maintenance procedure is also recommended, especially for targets made from certain metals such as silver. In the following sections (6.2.1–6.2.5), some guidelines for the initial fabrication and maintenance of both gas and liquid targets are discussed.

6.2.1. Initial fabrication of gas targets

If SA is a concern with gas targets, there are some fabrication techniques and cleaning procedures that may be used to reduce the amount of carrier present in the target. One prime example is the target for production of ^{11}C. In this target, it is essential that carbon be kept out of the target. For this reason, the technique of EDM is recommended. This process can be carried out in aqueous solution and eliminates the necessity for cutting oils in fabricating the target. Once the machining has been done, the surface is rather rough but can be polished using aluminium oxide grit. Silicon carbide should never be used, as carbon may thus be introduced into the surface of the metal. If EDM is not available, extensive cleaning after the machining will be necessary using organic solvents or detergents to remove the oil and then washing with water repeatedly to remove the solvents. Cutting oils should be avoided if at all possible.

6.2.2. Cleaning of gas targets

The use of organic solvents should be kept to a minimum when cleaning targets, and they should be employed only with extensive washing with water after their use. Ethanol and acetone are preferred, as they are soluble in water and can be washed out more easily. If immiscible organic solvents such as hexane are used, rinsing is necessary with a solvent, such as acetone, miscible with both hexane and water. It has been our experience that carbon targets essentially never need to be cleaned, unless there is accidental introduction of some foreign material into the target. Carbon-11 production targets can also be rejuvenated by irradiating a mixture of 10% oxygen in neon for a short time and then removing this mixture completely from the target before filling the target with normal nitrogen gas for irradiation. This step is often referred to as a 'burnout'. Fluorine gas targets can be passivated using a similar procedure with 1% fluorine in neon or argon [6.3].

6.2.3. Initial fabrication of water targets

Water targets for the preparation of ^{18}F should, if possible, be fabricated without soldering or brazing of connections. The flux commonly used in soldering usually contains boric oxide, which is high in fluoride. This fluoride can leach into the water during irradiation and reduce the SA of the ^{18}F. There are many designs of water targets that are in current use [6.4–6.7], and new designs are constantly being put into routine production. The proceedings of the Workshops on Targetry and Target Chemistry [6.8] are the best source for new concepts and designs.

6.2.4. Maintenance of water targets

Suggested procedures for the cleaning of water targets are given in Table 6.1, together with the frequencies with which they should be carried out. A general outline is given, and the procedures used should be discussed with the manufacturer of the target to agree on the final procedure. The procedures listed here have been used by several laboratories with good results. Further information on target care and maintenance can be found in Ref. [6.8].

The procedure used and the frequency of cleaning depend on the material of construction and the total number of microamp-hours applied to the target. There is no doubt that silver targets require the highest maintenance.

TABLE 6.1. RECOMMENDED CLEANING PROCEDURES FOR WATER TARGETS USED FOR PRODUCTION OF FLUORINE-18

Material	Frequency	Recommended procedure
Silver	3 to 6 months	Open the target and remove the front foil. Discard this in a shielded container for decay. Remove all O-rings or C-rings depending on the design. Scrub the exposed surfaces with an abrasive pad or with very fine abrasive paper. In extreme cases, it may be necessary to remove the pits from the surface with a high speed mechanical wire brush (Dremel tool). Care should be taken that no fine particles are lodged in the entrance and exit channels. Finally, the target should be copiously rinsed with water, remembering that the water and all other wastes will contain Cd-109 radioactivity and should be disposed of properly as radiological waste.
Titanium	6 months to 1 year	The procedure is very similar to that for silver targets, except that the metal is harder and a harder abrasive is usually required. The radioactive isotope present in the wash water will be V-48.
Niobium	1 to 2 years	The procedure is the same as that for titanium targets.

6.2.5. Cleaning and polishing of metal surfaces

It is often difficult to get inside a target body to polish the surface after cleaning with an abrasive tool. There are a few procedures for the chemical polishing of metal surfaces that have been used to prepare cyclotron targets. After these procedures have been carried out, the target body should be thoroughly cleaned with water to remove any traces of the chemicals used in the procedures. These procedures must be followed exactly in order to obtain a polished surface. Any deviation from the reagent concentrations, temperatures or times may result in an undesirable finish, which could affect target performance. Testing of the procedures on scrap metals is highly encouraged until reliable results are obtained. The procedures for polishing are presented in Table 6.2.

Obviously, the procedure for titanium should not be used if high SA ^{18}F is desired from this target. In this case, mechanical cleaning is recommended using only non-fluorine-containing abrasives and other materials.

TABLE 6.2. CHEMICAL POLISHING PROCEDURES FOR SOME METALS

Metal	Reagent	Volume (mL)	Time	Temperature (°C)
Copper–zinc alloys	Fuming nitric acid	80	5 s	40
	Water	20		
	Use periods of immersion of 5 s followed immediately by washing in a rapid stream of water. Slight variations in composition are needed for some alloys to prevent differential attack. With some alloys, a dull film can form that can be removed by immersion in a saturated solution of chromic acid in fuming nitric acid for a few seconds.			
Irons and steels	Distilled water	80	15 s	35
	Oxalic acid (100 g/L)	28		
	Hydrogen peroxide (30%)	4		
	The solution must be prepared freshly before use. Careful washing is necessary before treatment. A microsurface is obtained similar to that produced by mechanical polishing, followed by etching with Nital.			
Nickel	Nitric acid (conc.)	30	1 min	85–95
	Sulphuric acid (conc.)	10		
	Orthophosphoric acid	10		
	Glacial acetic acid	30		
	This solution gives a very good polish. Temperature is critical.			
Tantalum	Sulphuric acid	50	5–10 s	20
	Nitric acid	20		
	Hydrofluoric acid	20		
	This solution is useful for preparing surfaces prior to anodizing. Extreme care must be taken in handling hydrofluoric acid.			
Titanium	Hydrofluoric acid (100 vol.)	8–10	30–60 s	20
	Hydrogen peroxide	60		
	Water	30		

6.3. PREPARATION OF SOLID TARGETS BY ELECTRODEPOSITION

Many useful radionuclides can be produced with the cyclotrons available using solid target technology. In order to be reliable, plated targets must meet a series of requirements. In this chapter, ^{201}Tl is used as an example of target preparation and processing. Further information on other radionuclides can be found in Ref. [6.9].

For most solid targets, the best method for producing targets that will withstand high beam currents and that can still be easily processed is electroplating. Good thermal contact between the target material and the cooling plate allows beam currents to be higher; and by using electrochemical processing and recovery of the material, the processing is greatly simplified [6.10–6.14].

6.3.1. Physiochemical requirements on metal layers

There are several prerequisites for successful preparation of a solid target. The requirements for a solid target are as follows:

(a) The layer must be homogeneous to ±5% over the entire surface area.
(b) The layer must adhere strongly to the carrier, up to the irradiation temperatures.
(c) The layer must be smooth (not spongy), dense (no occlusions or vacuoles) and free of stress.
(d) The layer must be free of any organic plating additives (complexing agents or surfactants).

Given these requirements for a good quality target, a ‘poor quality’ ^{203}Tl target layer means that one or more of these conditions are not satisfied. The main causes of poor quality layers are:

(a) Gas (hydrogen) evolution at the cathode during plating resulting in spongy and irregular deposits;
(b) Concentration polarization of the electro-active species (i.e. the hydrated or complex target metal ion), giving rise to tree-like structures called dendrites, requiring post-plating mechanical fashioning such as rolling with an enhanced risk of plating solution occlusions;
(c) Ill-considered choice of additives such as organic complexing agents and tensides, bringing about peeling off of the target layer and/or target damage on irradiation;
(d) Unidirectional stirring and maladjusted plating temperature causing inhomogeneous layers and dendrites;
(e) Non-homogeneous electric field and badly adjusted plating voltage waveform causing inhomogeneous layers and dendrites.

There are additional chemical requirements for an industrial process concerning the solutions, set-ups and other conditions. These are:

(a) The plating solution must be free of toxic ions (e.g. CN^-).
(b) The process must be well suited for repetitive plating (up to ten batches) at room temperature.
(c) It must be possible to prepare several targets, with a minimum of four, at the same time.
(d) It should be possible to complete processing in one shift (7 h).
(e) The layer thickness should be time controlled (100% plating current efficiency).
(f) Post-plating mechanical preparation, such as pressing and rolling, must be excluded.

6.3.2. Simultaneous multitarget preparation

The goal of the plating methodology used here is to produce a homogeneous electric field over the entire cathode surface area, a homogeneous layer thickness, and to plate several targets at the same time to increase consistency and production efficiency. Simultaneous multitarget plating resulting in homogeneous target metal layers requires an appropriate plating vessel design to ensure a homogeneous electric field. It also requires a well designed stirring system that avoids local concentration gradients and hence local concentration polarization of the electro-active species.

As far as the plating vessel is concerned, a cylindrical geometry is recommended. The requirements can be met by using a hollow Perspex cylinder having an appropriate diameter/height ratio (typically 1/3) and, for an even number of targets ($n = 4, 8$), a diameter/nw ratio of 1.25, where w is the width of the plating area of a single target and n is the number of targets. The vessel should be fitted with a single axial and grounded platinum anode wire (1 mm) mounted at the bottom, and properly shielded at both ends. Four (or eight) vertical slots in the outside wall of the cylinder allow the introduction of four target carriers. The geometry results in a quasi-homogeneous electric field at the surface of the cathodes.

The stirring system should allow fast and efficient homogenization of the plating solution. This is feasible by introducing a hollow perforated Perspex or POM cylinder surrounding the platinum anode and mounted on the axis of a DC motor–tachometer combination with variable rotation speed (up to 1200 rev./min), while the direction of rotation should be reversed periodically (typically every 8 s). The vigorous bidirectional stirring reduces the thickness of the hydrodynamic layer and hence the concentration polarization. The geometry of the stirrer (the length of the cylinder, and the number and diameter of the circular holes) needs some optimization for narrow ($d < 4.5$ cm) plating vessels.

Plating temperature is an important quality parameter for some noble metals such as rhodium. At higher temperature, the viscosity of the solution decreases and the mobility of the ions increases, while in well stirred conditions the thickness of the hydrodynamic layer is substantially reduced. Higher temperature, therefore, reduces concentration polarization. On the other hand, overvoltages are lowered at higher temperatures, even for heavy metals such as thallium, with an increased risk of hydrogen gas evolution. Furthermore, the required electromechanical plating set-up should be much more sophisticated (with a heating element and associated feedback electronics for temperature control, and solution level monitoring and feedback electronics to add water to compensate for evaporation).

The optimum temperature for a given metal electrolysis can only be determined experimentally. Whenever possible, plating at room temperature is preferred. An example of a multitarget plating apparatus is shown in Fig. 6.1.

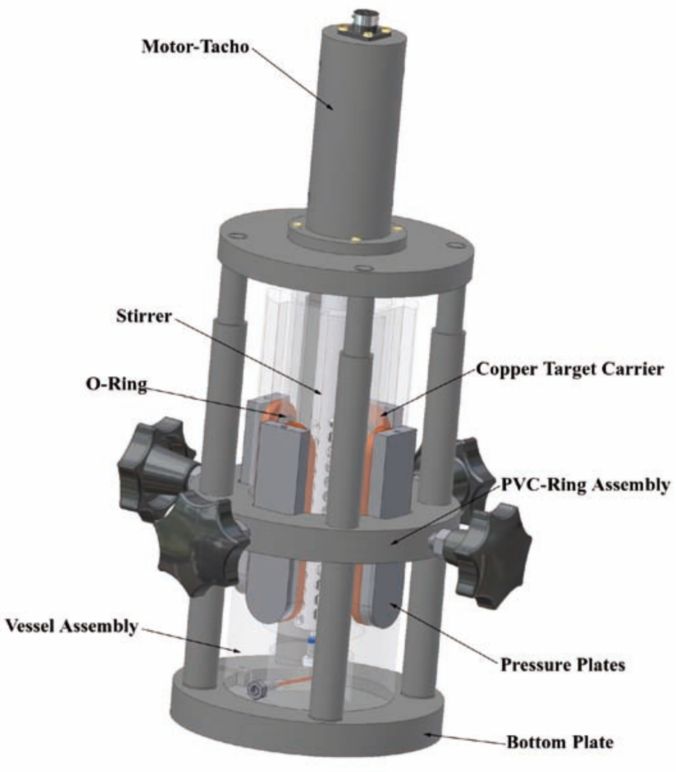

FIG. 6.1. A four target plating chamber.

A photograph of the four target plating chamber is presented in Fig. 6.2, showing the Perspex cylinder, the perforated stirrer and the slots in which the target plates can be mounted.

An eight target set-up is shown in Fig. 6.3. The electrodeposition vessel is fitted with an axial platinum wire anode mounted in the bottom by means of a tube-end fitting with a perforated septum. Eight vertical slots in the outside wall allow introduction and positioning of eight copper target carriers.

The target carriers are copper backing plates onto which the target material is deposited. The plates are water cooled to prevent damage or volatilization of the target material during irradiation. Typical target plates are shown in Fig. 6.4.

A schematic diagram of an electronic circuit for plating control in a four plate bath is presented in Fig. 6.5.

In Fig. 6.5, an astable multivibrator (AMV-1) generates a sawtooth (ST) signal of appropriate frequency and duty cycle. The ST signal is amplified by a non-inverting amplifier (NIA) and summed with a positive DC offset voltage (P-DC-O) by an inverting summing amplifier (ISA-1). The output forms the base for the positive alternation of the compound signal. The ST signal is amplified by an inverting amplifier (IA) and summed with a negative DC offset voltage (N-DC-O) by an inverting sum amplifier (ISA-2). This output forms

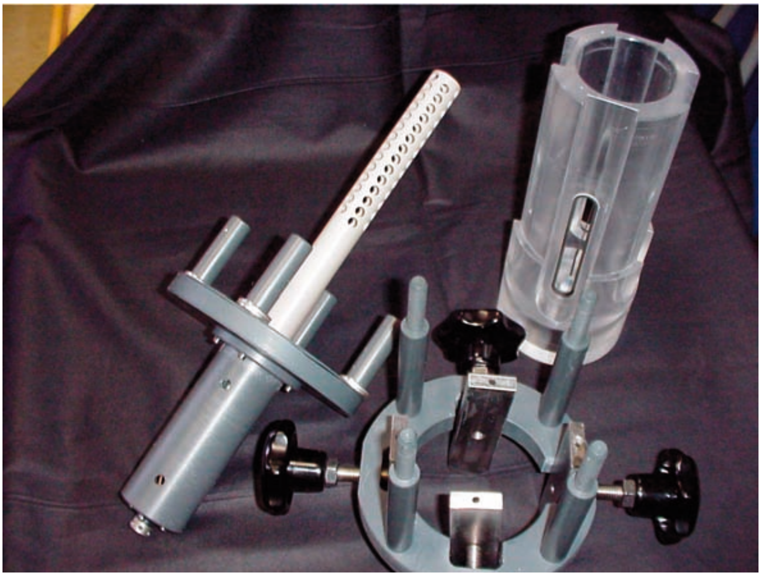

FIG. 6.2. Plating chamber for plating four targets simultaneously. The materials of construction are Lucite for the bath and various plastics for the other elements.

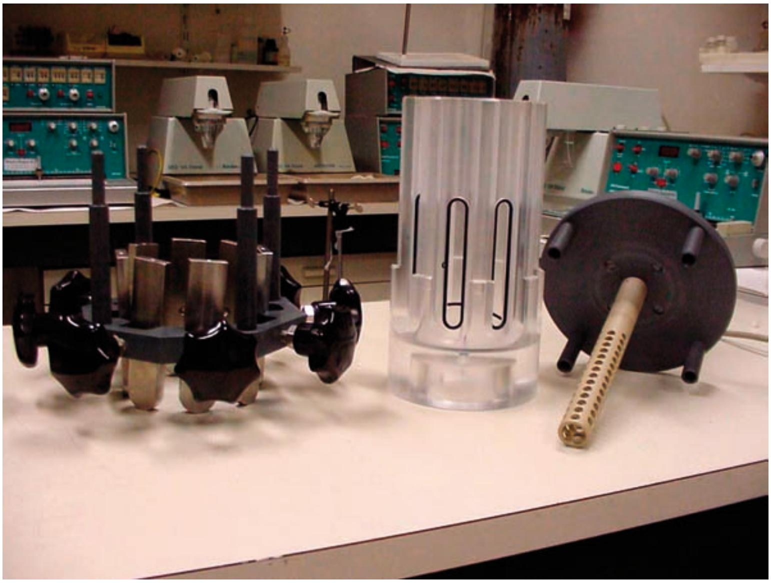

FIG. 6.3. Plating chamber for production of eight targets simultaneously.

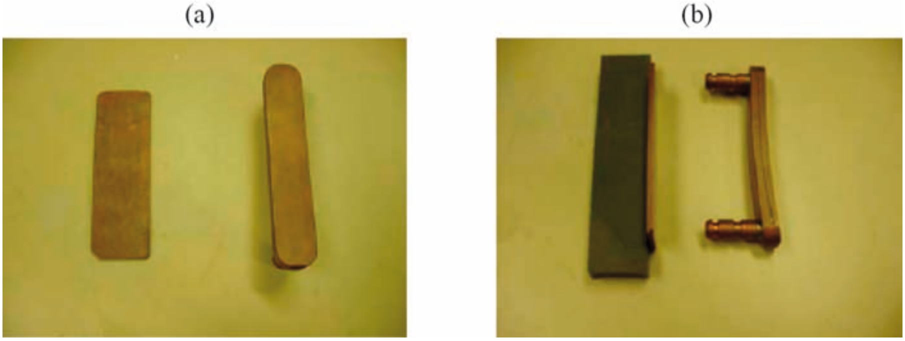

FIG. 6.4. (a) View from front of the target carriers; (b) view from the side showing the water cooling connections.

the base for the negative alternation of the compound signal. An astable multivibrator (AMV-2) generates a square wave (SW), with appropriate frequency and duty cycle, which chops the outputs of ISA-1 and ISA-2 in such a way that only one alternation is active at the same time.

The outputs of the negative alternation chopper (NAC) and the positive alternation chopper (PAC) are summed in an inverting amplifier (ISA-3), the output of which delivers the compound signal. This signal is fed into four

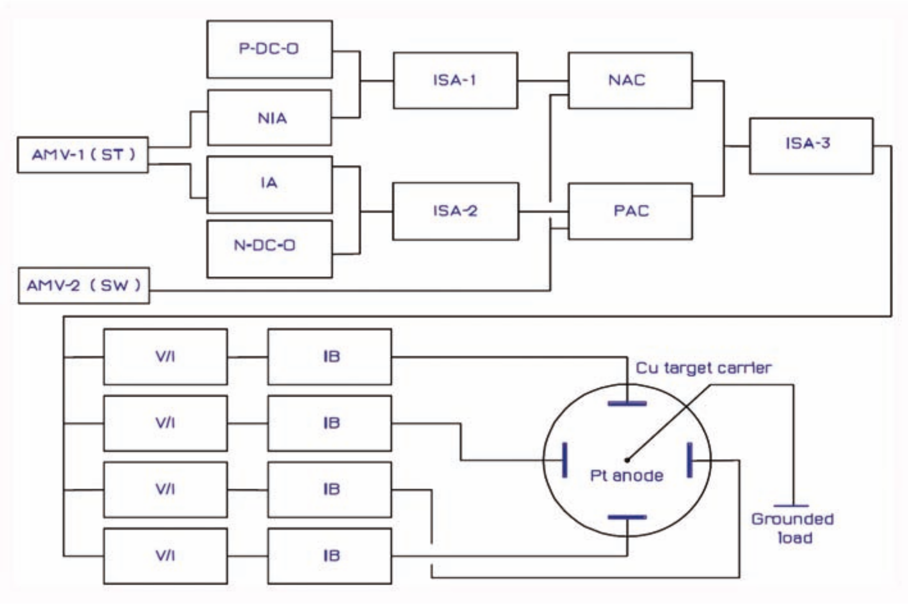

FIG. 6.5. Electronics diagram of a control circuit for a four plate bath. The various abbreviations are explained in the text.

independent voltage-to-current (V/I) converters with associated push-pull current boosters (IBs) and a grounded load. This circuitry allows simultaneous deposition of four thallium targets at four different current densities using a single and grounded platinum anode.

The electrodeposition electronics consists of a rack with:

- — Eight eurocards;
- — Two power supplies;
- — One stirrer controller;
- — One signal generator;
- — Eight V/I converters with associated push-pull current boosters.

A photograph of the complete electronics for an eight target system is shown in Fig. 6.6.

FIG. 6.6. The complete electronics for an eight target system.

6.3.3. Optimization of plating technology

There are four fundamental plating methods that can be used. Each of these has some advantages and disadvantages, which are described in this section.

In constant voltage electrolysis, a fixed voltage is applied between the anode and the target carrier cathode immersed in the plating bath. During electrolysis, the current is decreasing as a result of depletion of the electro-active species (hydrated or complex metal ions), and the cathode potential shifts towards more negative values. This carries with it an enhanced risk of hydrogen evolution. This can be prevented by the addition of a suitable cathodic depolarizer (NO_3^-) that fixes the cathode potential at a constant value and that is reduced to a non-volatile species (NH_4^+) in an acidic medium. Although this technique is frequently used in industrial coating and in analytical electrogravimetry, the current efficiency (and hence the plating current density) varies during the plating process and is generally much less than 100%, making the method less attractive for time-controlled layer thickness plating.

In constant current electrolysis (CCE), a fixed current is forced through an electrochemical cell and the applied plating voltage automatically adjusted (i.e. increased) such that the current set is maintained. Using concentrated solutions of appropriate composition that show a limited depletion ratio for the electro-active species (with a maximum of 50%) at the end of the plating, and applying an optimized plating current density, a 100% current efficiency can easily be obtained.

For time-controlled layer thickness plating, the controlled cathode potential electrolysis (CCPE) technique is preferred, which involves introduction of a reference electrode into the system. The potential of the cathode is set at a fixed value versus the potential of the reference electrode. This value corresponds to 99.99% depletion of the electro-active species, i.e. to the lower limit of its discharge interval. The current decreases exponentially as the process progresses, and the current reading may be used to monitor the depletion of the bath. The CCPE technique is well suited for quantitative separation of metals and is a very attractive tool in the framework of the recovery of enriched target material.

Internal electrolysis (IE) does not involve the application of an external voltage or current source to the electrochemical cell built up from two different electrodes. External short-circuiting of both electrodes results in a spontaneous current that decreases exponentially as a function of time. The anode dissolves and the electro-active species required is quantitatively plated out onto the cathode. This method has a limited number of applications and was frequently used in destructive neutron activation analysis in the 1960s. It is not suited for thick target preparations. Given these characteristics, CCE should be preferred for preparation of high current beam cyclotron targets, and CCPE should be used for purification and recovery of enriched material.

In spite of the optimized conditions discussed above, a slight tendency towards dendrite formation is found when DC constant current electroplating is performed. This phenomenon can be suppressed completely by application of AC voltages and currents. During the cathodic part of applied signal deposition, microdendrite formation takes place, but during the anodic part the metal is redissolved. This redissolution rate is higher for fine tree-like structures (showing a high surface area per unit of mass) than for real massive crystals. Appropriate choice of the waveform of the AC signal and of the amplitudes of the cathodic (I_c) and anodic (I_a) currents ($I_c > I_a$) results in a net cathodic deposition with suppressed dendrite formation. Of four different waveforms tried, a bipolar chopped sawtooth gives the optimum results in the case of thallium. The signal frequency is 100 Hz, the chopper frequency is 1000 Hz and the chopper duty cycle is 60%. The waveform is schematically represented in Fig. 6.7.

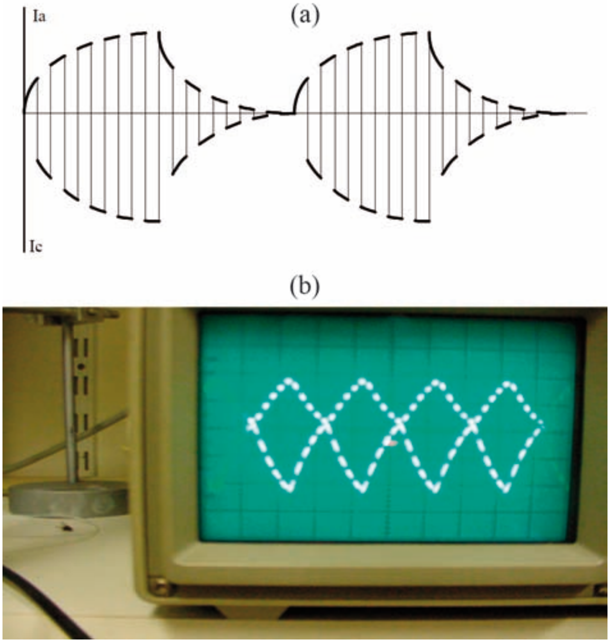

FIG. 6.7. (a) A bipolar chopped sawtooth plating voltage, showing the ideal situation; (b) an oscilloscope trace of the voltages applied for the plating of ^{203}Tl.

6.4. EXAMPLE OF ^{201}Tl PRODUCTION

Thallium-201 has been chosen as an example of typical production conditions and procedures. Similar procedures can be used for other target materials.

6.4.1. Cleaning of target carriers (copper backings)

The following steps should be carried out to clean the surface prior to electrodeposition:

(a) Rub the deposition area of the copper backing successively with abrasive wool of types 1 and 2 for 1 min, respectively;
(b) Rinse with water;
(c) Rinse with acetone;
(d) Dry the carrier with adsorbing paper and weigh the carriers.

Introduce the backings in the four slots of the deposition vessel and turn the knobs of the mechanical pestles in pairs, clockwise to ensure liquid tightness.

6.4.2. Electroplating bath

A thallium metal layer, which meets all metal layer quality requirements and all industrial stipulations, can be obtained by CCE of ^{203}Tl from alkaline (pH > 12) solutions that contain concentrated monovalent thallium (holding an amount of thallium that is equal to twice the amount plated out), 0.5M in EDTA (ethylene diamine tetra-acetic acid), a non-incorporated surfactant (BRIJ-35) and a strong reducing anodic depolarizer (hydrazine hydrate). By applying a bipolar chopped sawtooth (f_{ST} = 100 Hz; f_{CH} = 1000 Hz; CDC = 60%) to the cylindrical plating vessel as described in Section 6.3.3, the following results are obtained:

(a) A relatively high maximum allowable current density (2–3 mA/cm^2), allowing simultaneous time controlled (with a plating current efficiency of 100%) production of four targets carrying more than 100 mg ^{203}Tl/cm^2 within less than six hours and requiring no post-plating mechanical fashioning;

(b) Plating performed from cyanide-free solutions that are well suited to repetitive plating cycles (up to ten batches) by simple adjustment of the metal contents of the plating bath and from which the remaining enriched material can be readily recovered by CCPE;

(c) Target layers that are homogeneous (±5%), smooth (dendrite-free), dense (have no occlusions or vacuoles) and free of traces of organic bath additives (EDTA and BRIJ-35). The layer remains intact and sticks strongly to the copper target carrier up to 270°C, a temperature about 30°C below the melting point of the metal.

Specific procedures for these plating techniques can be found in Ref. [6.9].

Thallium-203 layers (surface area: 11.6 cm^2; total amount of thallium: 1.1 g) plated on copper carriers in this way can withstand a 9 h irradiation with a circularly ‘wobbled’ 270 μA proton beam without loss of material.

Figure 6.8 shows a typical ^{203}Tl target after a plating procedure.

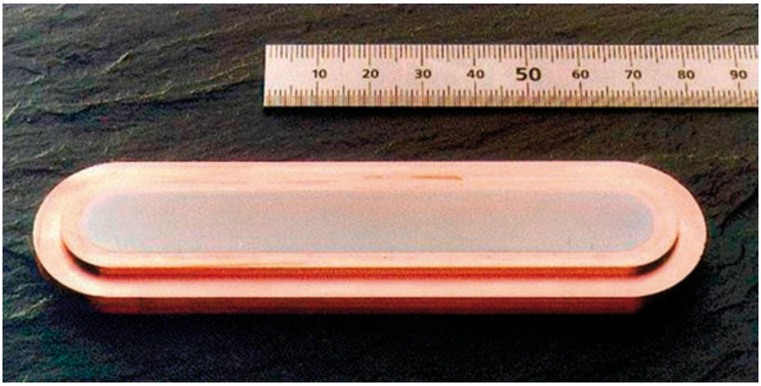

FIG. 6.8. Thallium-203 plated on a copper target plate.

6.5. PLATING SOFTWARE: EXCEL PLATING WORKBOOK

An Excel workbook is contained in the CD accompanying this book, which can calculate the conditions for electroplating (Annex III).

6.6. THALLIUM TARGET QUALITY CONTROL

There are two important aspects of QC for this procedure. The first is in the plates that are being used for irradiation. These plates must meet certain quality assurance guidelines or they are likely to be damaged in the beam and produce low yields of ^{201}Tl. The other aspect is the QC of the final product. These tests are critical for the release of ^{201}Tl for use.

6.6.1. Quality control of ^{203}Tl plates

The new electroplating technology from alkaline EDTA solutions allows production of high quality ^{203}Tl targets that do not require any post-plating mechanical smoothing. The homogeneity of the thallium layer, determined by micrometry (12 measurements spread over the surface area) is acceptable: a standard deviation of the mean thickness of less than 5% is observed. The surface area granulometry (visual microscopic inspection, ×250 scanning electron microscope shots) results are excellent as compared with those of targets plated in acid plating baths. The granulometry results obtained may be used as a reference for future thallium plating techniques. Because the melting point of thallium metal is low (303°C), a thermal shock test should be performed at 270°C. Heating up to this temperature in air, followed by submersion in cold water (15°C) and multiple bending does not give rise to crater formation or to peeling. This proves that no plating additives (EDTA or BRIJ) are present in the thallium metal lattice or at the thallium–copper carrier interface. Application of the plating technology used industrially resulted in an increase of the ^{201}Tl yield of up to 20%, as compared with that obtained with targets plated from acid solutions.

6.6.2. Quality control of the ^{201}Tl produced

The ^{201}Tl produced by using the new plating technology meets all chemical, radiochemical and radionuclidic quality criteria required by the pharmacopoeia.

6.7. IRRADIATION OF ELECTROPLATED SOLID TARGETS

There are several factors which contribute to the maximum beam currents that may be run with a solid target. The beam density is the primary factor. If there are ‘hot’ spots in the beam, the highest current at which the target may be run will be much lower than if the beam has a uniform profile. Target cooling is another factor, and some examples of calculations for optimizing the cooling based on the geometry of the target and backing plates are given in Section 6.7.1.

6.7.1. Heat transfer model

Thallium targets can be considered as a three layer system, facing the accelerator vacuum on one side and the coolant fluid on the other (Fig. 6.9).

Layer 1, the ^{203}Tl deposit, has a physical thickness of 80×10^{-4} cm, denoted by ‘a’ in Fig. 6.9. In this layer, ^{201}Pb is produced by the ^{203}Tl(p, 3n)^{201}Pb threshold reaction caused by 30 MeV protons impinging under a beam–target angle of $\theta°$. Owing to excitation, ionization and bremsstrahlung, protons do lose kinetic energy in this layer, which is converted into heat. Assuming homogeneous irradiation, i.e. that the current density (μA/mm^2) is constant over the whole surface area S (= 11.69 cm^2), the total heat production rate q_{Tl} (J/s) and the heat production rate per unit of volume q'''_{Tl} (J·cm^{-3}·s^{-1}) in this layer are related as:

$$q_{\mathrm{Tl}} = q'''_{\mathrm{Tl}}\, aS$$

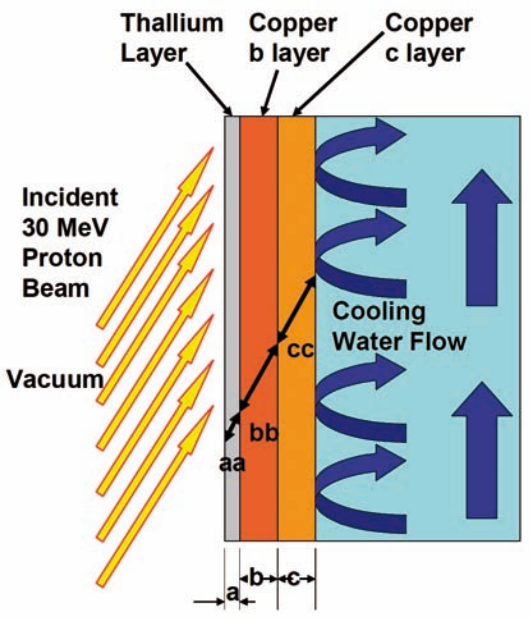

FIG. 6.9. The three layers of a thallium target.

Layer 2, the Cu-*b* layer, has a physical thickness of *b* cm. In this layer, protons emerging from the thallium layer are stopped completely. The heat production rate q_{Cu}, and the heat production rate per unit of volume q'''_{Cu} in this layer, are linked by:

$$q_{\mathrm{Cu}} = q'''_{\mathrm{Cu}}\, bS$$

Layer 3, the Cu-*c* layer, has a physical dimension of *c* cm and merely serves as a mechanical support for the thallium layer. The total heat (q_{T}) produced in the layers q_{Tl} and q_{Cu} is transferred to the coolant fluid through this layer by conduction:

$$q_{\mathrm{T}} = q_{\mathrm{Tl}} + q_{\mathrm{Cu}}$$

At the Cu-*c*/coolant interface, the heat is transferred to the coolant solely by convection, i.e. no subcooled nucleate boiling occurs, and the bulk temperature of the coolant is a constant (T_{w}).

In steady state conditions, the heat and heat transfers result in the temperature profile shown in Fig. 6.10.

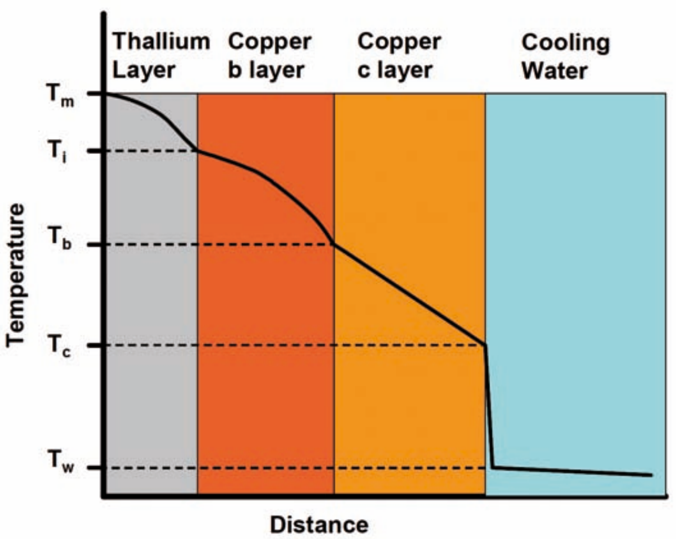

FIG. 6.10. Temperature profile through the thallium target. Here, T_m is the maximum temperature at the vacuum/Tl interface, T_i is the temperature at the Tl/Cu-b interface, T_b is the temperature at the Cu-b/Cu-c interface, T_c is the temperature at the Cu-c/coolant interface and T_w is the temperature of the coolant.

A detailed analysis of the heat transfer and temperature profile of the solid targets is given in Appendix I.

6.8. ACCELERATOR BEAM PROFILES

Beam current density is often a critical parameter in determining how much radionuclide can be produced in a target. If the current density is too high, the solid target may be burned and the fluid target (gas or liquid) may have a very large density reduction.

If the beam has hot spots (spikes in the beam intensity), there may be areas where the solid target material is burned away or, in the case of fluids, areas where the target material is pushed aside. All the above conditions will result in a loss of yield, and therefore the beam current density should be as uniform as possible. Negative ion machines have an advantage over positive ion machines in this respect. Since negative ion machines use a foil for beam extraction, this tends to make the beam more homogeneous. It is possible to calculate this effect by using the equations for small angle multiple scattering found in Section 5.3.4 or with the SRIM Monte Carlo simulations [6.15].

A Gaussian current density distribution is assumed at the exit of a cylindrical collimator as described by the following equation:

$$i = i_{\mathrm{m}} \mathrm{e}^{-a^2 r^2}$$

where

i_{m} is the maximum current density (μA/mm^2);
a^2 is the Gaussian exponent ($a^2 = 1/2\sigma^2$ (mm^{-2}));
σ is the standard deviation of the Gaussian distribution; and
r is the radial distance from the collimator circle.

The total beam current I_{B} is given by:

$$I_{\mathrm{B}} = \int_0^{\infty} i_{\mathrm{m}} \mathrm{e}^{-a^2 r^2} 2\pi r \mathrm{d}r = -\frac{\pi i_{\mathrm{m}}}{a^2} \int_0^{\infty} \mathrm{d}(\mathrm{e}^{-a^2 r^2}) = \frac{\pi i_{\mathrm{m}}}{a^2}$$

and the target current I_{T} is given by the following equation:

$$I_{\mathrm{T}} = \int_0^{R} i_{\mathrm{m}} \mathrm{e}^{-a^2 r^2} 2\pi r \mathrm{d}r = -\frac{\pi i_{\mathrm{m}}}{a^2} \int_0^{R} \mathrm{d}(\mathrm{e}^{-a^2 r^2})$$

$$I_{\mathrm{T}} = \frac{\pi i_{\mathrm{m}}}{a^2} (1 - \mathrm{e}^{-a^2 R^2})$$

The beam current efficiency ε_{B} can be defined as:

$$\varepsilon_{\mathrm{B}} = \frac{I_{\mathrm{T}}}{I_{\mathrm{B}}} = 100(1 - \mathrm{e}^{-a^2 R^2})$$

which is the percentage of the total beam current striking the target.

In Table 6.3, the beam current efficiency is represented as a function of the full width at half-maximum (FWHM) and σ.

Figure 6.11 demonstrates graphically the beam profiles for beams of different FWHM. This figure also shows the amount of beam lost on a 20 cm diameter collimator. The total beam current on the target is the same for all the distributions.

TABLE 6.3. BEAM CURRENT EFFICIENCY ε_B FOR DIFFERENT BEAM SHAPES PASSING THROUGH A 20 cm COLLIMATOR

FWHM (mm)	σ (mm)	ε_B(%)	Loss on collimator (%)
5	2.1	100	0
10	4.3	98	2
15	6.4	88	12
20	8.5	76	24

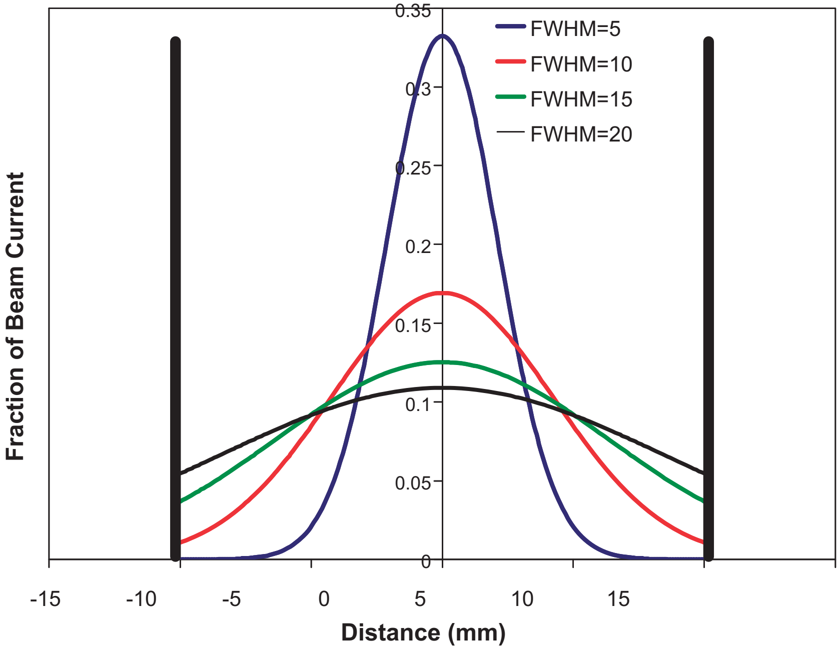

FIG. 6.11. Beam profile of beams passing through a 20 cm diameter collimator with differing Gaussian distributions.

It can be seen from Fig. 6.11 that the current density is much higher for the narrower beam than it is for the beam with the wider distribution. Since the amount of beam that may be applied to a target is a function of current density, the more uniform distribution is usually the preferred distribution. In the above case, for the narrowest distribution, about 77% of the beam will be in the central 5.0 mm diameter spot, whereas only about 31% of the widest beam will be in this same area. If we assume a 50 mA beam current and a 15 MeV beam energy, the target will have a power density of nearly 3000 W/cm^2 with the narrow beam and a power density of about 1200 W/cm^2 with the widest distribution. For a detailed calculation of the effect this will have on the heat transfer and the maximum current that may be applied to a solid target, see Annex I in the CD attached to this publication.

6.8.1. Beam wobbling during irradiation

One of the best ways to reduce the current density on a particular target is to ‘wobble’ the beam over the entire surface of the target. This smoothes out beam irregularities (hot spots) and allows the target to be run at higher beam currents. Further increases of beam current can be obtained by circular wobbling of the beam. Therefore, the Gaussian distribution is shifted over a distance RW, the wobbling circle radius, from the collimator axis, after which the proton beam is forced to rotate around the axis, as shown in Fig. 6.12.

Although a part of the beam is collected on the collimator body, a further increase of target current can be expected by optimizing the radius of the wobbling circle. The calculations of the mean current density distribution and of the total beam and target currents cannot be done analytically: numerical integrations are required. An example of a typical beam current distribution in two dimensions is shown in Fig. 6.13.

This density distribution can then be applied to the heat transfer model in order to determine the temperature profile across the target. This will in turn give an indication of the maximum beam current that may be applied to the target without incurring any damage. A caveat here is to note that sparks in the cyclotron vacuum tank may cause severe distortions in the beam shape and, therefore, give rise to transient spikes in the beam current distribution. For this reason, a common practice is to limit the beam current to 50% of that calculated as being the maximum allowable beam current using these approximations.

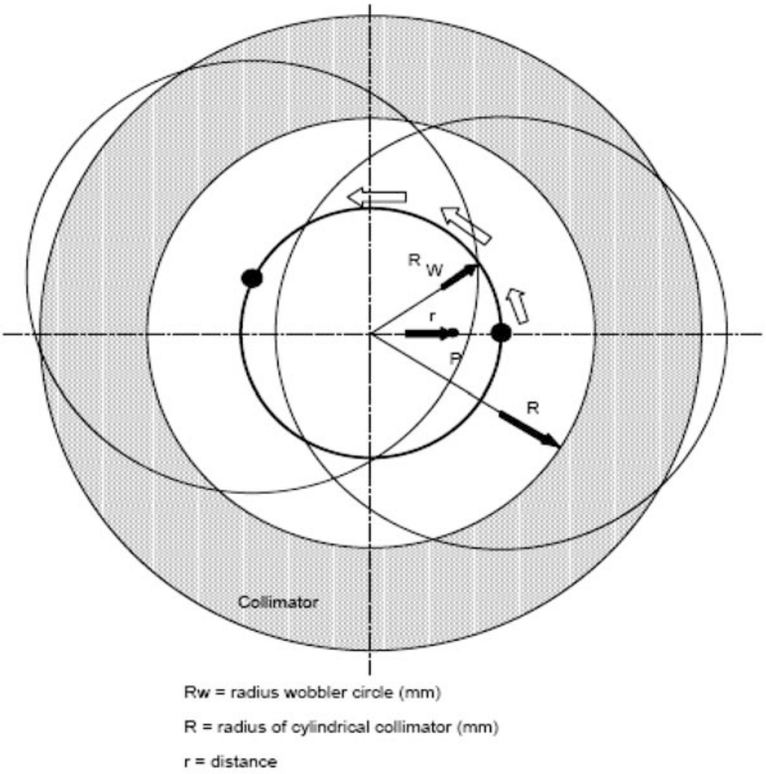

FIG. 6.12. Circular wobbling of a beam during irradiation.

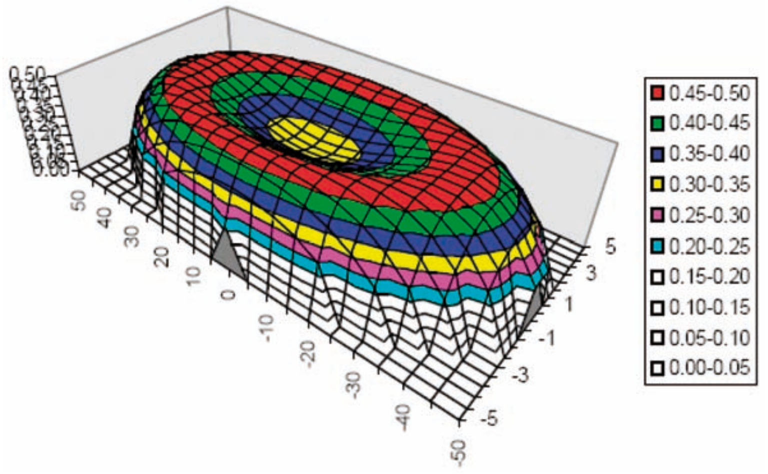

FIG. 6.13. Current density distribution for a 'wobbled' beam.

REFERENCES TO CHAPTER 6

[6.1] RUTH, T.J., et al., A proof of principle for targetry to produce ultrahigh quantities of ^{18}F-fluoride, Appl. Radiat. Isot. **55** (2001) 457–461.

[6.2] ROBERTS, A.D., OAKES, T.R., NICKLES, R.J., Development of an improved target for [^{18}F]F_2 production, Appl. Radiat. Isot. **46** (1995) 87.

[6.3] BISHOP, A., SATYAMURTHY, N., BIDA, G., PHELPS, M., BARRIO, J.R., Metals suitable for fluorine gas target bodies: First use of aluminum for the production of [^{18}F]F_2, Nucl. Med. Biol. **23** (1996) 181–188.

[6.4] NICKLES, R.J., HICHWA, R.D., DAUBE, M.E., HUTCHINS, G.D., CONGDON, D.D., An ^{18}O-target for the high yield production of ^{18}F-fluoride, Int. J. Appl. Radiat. Isot. **34** (1983) 625–629.

[6.5] SCHMITZ, F., et al., "Production of multi Curie [^{18}F]fluoride using a niobium target chamber at small PET cyclotrons", in Targetry and Target Chemistry (Proc. 9th Int. Workshop Turku, 2002), TRIUMF, Vancouver, http://trshare.triumf.ca/~buckley/wttc/proceedings.html

[6.6] SALVADORI, P.A., et al., Preliminary results from an enriched water target for the production of [^{18}F]fluoride, Acta Radiol. Suppl. **376** (1991) 60.

[6.7] STEEL, C.J., DOWSETT, K., PIKE, V.W., CLARK, J.C., "Ten years experience with a heavily used target for the production of [^{18}F] fluoride by proton bombardment of [^{18}O]", Targetry and Target Chemistry (Proc. 7th Int. Workshop Heidelberg, 1997), TRIUMF, Vancouver, http://trshare.triumf.ca/~buckley/wttc/proceedings.html

[6.8] Targetry and Target Chemistry, Proceedings Publications, TRIUMF, Vancouver, http://trshare.triumf.ca/~buckley/wttc/proceedings.html

[6.9] INTERNATIONAL ATOMIC ENERGY AGENCY, Standardized High Current Solid Targets for Cyclotron Production of Diagnostic and Therapeutic Radionuclides, Technical Reports Series No. 432, IAEA, Vienna (2004) CD-ROM.

[6.10] LOWENHEIM, F.A. (Ed.), Modern Electroplating, 3rd edn, Wiley, New York (1973).

[6.11] CANNING, W., The Canning Handbook on Electroplating, E.&F.N. Spon Ltd, London (1977).

[6.12] CHARLOT, G., Les réactions chimiques en solution aqueuse, 7th edn, Masson, Paris (1983).

[6.13] DURNEY, L.J., Electroplating Engineering Handbook, 4th edn, Chapman & Hall, London (1996).

[6.14] LAITINEN, H.A., Chemical Analysis, MacGraw-Hill, New York (1960).

[6.15] ZIEGLER, J.F., SRIM — The Stopping and Range of Ions in Matter, http://www.srim/org

Chapter 7

TARGET PROCESSING AND MATERIAL RECOVERY

7.1. INTRODUCTION

The processing of the target after irradiation is one of the most critical steps in the production of radioisotopes. Each of the three states of matter poses specific problems in the recovery of a radioisotope.

In the case of gaseous targets, the transfer out of the target is relatively simple, using pressure gradients or ‘sweep’ gases, but the lines must be kept free from leaks in order to maintain the purity of the gases and to prevent any contamination of the surrounding area. The radioisotope must be trapped or separated from the target gas or, in the case of some gaseous targets where the radioisotope is deposited on the walls of the target during irradiation, it must then be brought into solution and removed.

In the case of liquid targets, it is often possible to transfer the liquids over short distances using ‘push’ gases, although there may be a problem in transferring all of the material since droplets may stick to the walls of the transfer line. A special problem with liquid targets is the tendency of the liquid to dissolve some material from either the vacuum isolation foil or from the target body. These impurities may be radioactive, a metal salt or a colloid. In all cases, they must be removed from the liquid before synthesis.

In the case of solid targets, the problem is usually to remove the radioisotope from the target matrix efficiently. The techniques used may be thermal diffusion, dissolution with solvent extraction, separation with ion exchange resins or electrochemical separation. Examples of some of these techniques are included in this chapter, but the particular conditions and reagents will need to be gathered from the literature.

Another important aspect of target processing is recovery of the enriched isotopes used to make the target. Such recovery can have substantial economic implications, since the enriched isotopes can be very expensive and few centres can afford to waste these isotopes. For liquids and gases, this often means a simple extraction using resins or a cryogenic recovery of the target gas. In the case of solid targets, a more elaborate electrochemical recovery may be required.

7.2. SPECIFIC ACTIVITY

Specific activity is the number of radiolabelled molecules compared with the total number of molecules and is usually expressed as a unit of radioactivity per mole of compound. It is further defined in Chapter 2. Specific activity is a critically important property in the preparation of radiotracers. It is particularly important in PET, where the radionuclide is incorporated into a radiotracer that is used to probe some physiological process, in which very small amounts of the native biomolecule are used. When carrying out these studies, such as probing the number of receptors or the concentration of an enzyme, considerations of the total mass of compound injected become even more important [7.1, 7.2]. There is, of course, an ultimate limit to SA when only the radioactive atoms or radiolabelled molecules are present. The characteristics of some radioisotopes are given in Table 7.1.

TABLE 7.1. DECAY CHARACTERISTICS AND MAXIMUM SPECIFIC ACTIVITY OF SOME IMPORTANT RADIONUCLIDES

Nuclide	Half-life (min)	Decay mode	Maximum SA (theoretical)
C-11	20.4	100% β^+	9220 Ci/μmol (341 TBq/μmol)
N-13	9.98	100% β^+	18 900 Ci/μmol (700 TBq/μmol)
O-15	2.03	100% β^+	91 730 Ci/μmol (3394 TBq/μmol)
F-18	109.8	97% β^+	1710 Ci/μmol (63.4 TBq/μmol)
Cu-62	9.74	99.7% β^+	19 310 Ci/μmol (714 TBq/μmol)
Ga-67	4696.8	100% EC	40 Ci/μmol (1.5 TBq/μmol)
Ga-68	68.0	89% β^+	2766 Ci/μmol (102 TBq/μmol)
Br-75	96.0	75.5% β^+	1960 Ci/μmol (73 TBq/μmol)
Rb-82	1.25	95.5% β^+	150 400 Ci/μmol (5565 TBq/μmol)
In-111	4048.8	100% EC	46 Ci/μmol (1.7 TBq/μmol)
I-122	3.62	75.8% β^+	51 950 Ci/μmol (1922 TBq/μmol)
I-123	793.4	100% EC	237 Ci/μmol (8.8 TBq/μmol)
I-124	6019.2	23.3% β^+	31 Ci/μmol (1.15 TBq/μmol)
Tl-201	4374.7	100% EC	42.6 Ci/μmol (1.58 TBq/μmol)

As an example, the typical SAs for ^{11}C labelled molecules are of the order of 10 Ci/μmol (370 GBq/μmol). Hence, it can be seen that only 1 in 1000 tracer molecules is actually labelled with ^{11}C. The remainder contain ^{12}C. There is a clear need to achieve reliable production of high SA radiopharmaceuticals.

Present-day tracers, and certainly future ones, include receptor/transporter ligands that are very potent and, therefore, require very little mass to activate the receptor. In order for PET to be a true tracer technique, receptor occupancy with the radiolabelled tracer should be kept below 5% in order to avoid pharmacological or pharmacodynamic effects.

7.3. GAS TARGET PROCESSING

When a gaseous target is irradiated, the irradiation is very often carried out with a high pressure of gas in the target. Pressures can be anywhere from 2 atm (0.202 MPa) to 50 atm (5.06 MPa). The gas may be retained in the target during bombardment or it may be processed in a flow mode, where the target gas flows through the target during irradiation.

7.3.1. Gaseous transfer

In a flow-through target, a gas flow is established based on the pressure in the target during bombardment. This pressure is usually set with a regulator and is at equilibrium. In a closed target, when a valve is opened that connects the target to a processing module or other trapping station, the gas will flow along the pressure gradient to the desired location. If the pressure is low or the volume of the line is high, then a ‘push’ stream of gas is often used to increase the efficiency of the transfer. In either case, the flow rate through the tubing is usually given by the Poiseuille equation. This following equation holds if the flow is laminar:

$$F = \frac{\pi g r^4}{8 \mu L} \Delta P$$

where

F is the flow (cm^3/s);
g is the gravitational acceleration (980.6 cm/s^2);
r is the radius of the tubing (cm);

L is the length of the tubing (cm);
μ is the viscosity in poise ($g{\cdot}cm^{-1}{\cdot}s^{-1}$); and
ΔP is the pressure differential (g/cm^2).

The Reynolds number can be calculated to determine whether the flow is really laminar or not. This relation is:

$$\mathrm{Re} = \rho VD/\mu$$

where

Re is the Reynolds number (dimensionless);
V is the flow velocity (cm/s);
ρ is the density (g/cm^3);
μ is the viscosity in poise ($g{\cdot}cm^{-1}{\cdot}s^{-1}$); and
D is the tube diameter (cm).

If the Reynolds number is greater than about 2000, then the Poiseuille equation is not valid and the flow will be slower than that calculated. However, laminar flow is usual for low viscosity gas flows through long lines of small diameter connecting the target to the chemistry laboratory. Some useful parameters for common fluids at 25°C are given in Table 7.2. These can be used in the flow equations to obtain approximate flow rates for gases or for water.

Bends or fittings in a line will also slow the flow of gas. There are tables, which can be found in most mass transfer texts, that provide corrections for these flow reductions.

TABLE 7.2. PARAMETERS FOR FLUIDS COMMONLY USED TO TRANSFER RADIOACTIVITY

Compound	Viscosity (cP)*	Density (g/cm^3)
Air	0.0182	0.001185
Nitrogen	0.0176	0.00016
Helium	0.0196	0.001138
Water	0.890	1.0

* 1 P = 0.1 Pa·s.

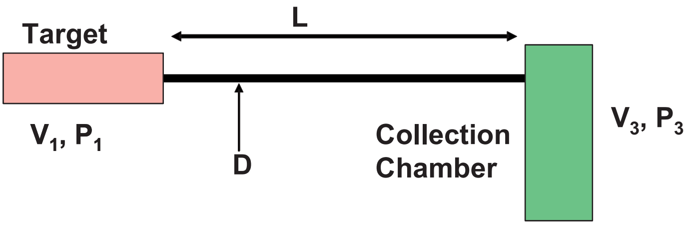

FIG. 7.1. Schematic diagram of a 'tuned' gas transport line.

Another analysis was carried out to determine the optimum parameters to be used to transfer a gas through a tube at a specified flow rate without the use of metering valves [7.3] in a constant flow target. A schematic diagram of the situation is shown in Fig. 7.1.

In this analysis, the equation used is:

$$A = \frac{R}{1+\frac{t_1}{\tau}} e^{-\frac{t_2}{\tau}} (1 - e^{\frac{-t_3}{\tau}})$$

where

A	is the optimum activity delivery rate;
R	is the radioactivity production rate;
t_1	is the target chamber dwell time ($t_1 = V_1P_1/Q$);
t_2	is the tube transit time ($t_2 = \int_0^L \mathrm{d}z/v(z)$);
t_3	is the collection chamber dwell time ($t_3 = V_3P_3/Q$);
τ	is the decay constant for the radionuclide ($\ln(2)/T_{1/2}$)

in which

L	is the length of the tubing;
D	is the diameter of the tubing;
Q	is the mass flow rate;
V_1	is the target volume;
P_1	is the target pressure;
$v(z)$	is velocity as a function of distance;
z	is the distance;
V_3	is the collection chamber volume; and
P_3	is the collection chamber pressure.

In these calculations, the goals are to:

(a) Minimize t_1 by reducing V_1 as much as possible;
(b) Attempt to match $t_2 = t_3$ to τ;
(c) Minimize L;
(d) Use a trap at the outlet to increase the effective value of V_3.

7.3.2. In-line separation and processing

Whether gaseous radioisotopes are produced in a static target or in a continuous flow target, they must be processed before they are ready to be used directly or before they can be used as a precursor in a more complex chemical reaction. The processing may include trapping the desired radioisotope, converting it into some other chemical form or removing other gaseous impurities in an on-line process. One of the most widely used and simplest processing schemes is that for the production of $C^{15}O_2$ from ^{15}O. This on-line processing system is shown in Fig. 7.2 [7.4]. The oxygen from the target is converted into a mixture of carbon monoxide and carbon dioxide over a charcoal furnace at 525°C. The conversion from CO to CO_2 is completed in a cupric oxide furnace at 500°C, and any residual oxygen or ozone is scrubbed out by the elemental copper furnace operating at 300°C.

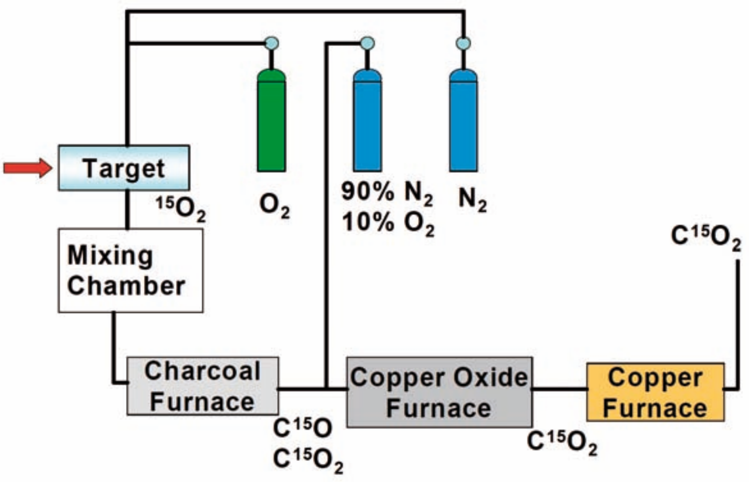

FIG. 7.2. Schematic diagram of a processing system for the production of [^{15}O]CO_2.

7.3.2.1. Trapping of gases

One of the most common in-line traps in use is the NO_x trap described by Tewson et al. [7.5]. This trap is used to scrub oxides of nitrogen from the carbon dioxide coming out of the gas target. The oxides of nitrogen are known to interfere with some reactions. They can also be converted to ammonia under some of the same conditions that convert carbon dioxide to methane. Another common in-line trap is a CO_2 scrubber used on the inlet to the ^{11}C production target. The removal of carbon dioxide from the nitrogen target gas prior to irradiation helps to increase the SA. An example of gas processing for ^{81m}Kr is shown in Fig. 7.3.

This system was chosen as an example, since it uses almost all of the processes common for gas targets. The system to recycle the target gas, steam the target and transport the solution to a hot cell for loading onto the generator columns is illustrated in Fig. 7.3 [7.6]. All of the critical areas use stainless steel piping and 'Swagelok' fittings. A sequence of the steps used in operating this target is given as an example of the steps that usually have to be taken to prepare, use and clean a gas target. The operating sequence is outlined in Sections 7.3.2.2–7.3.2.4.

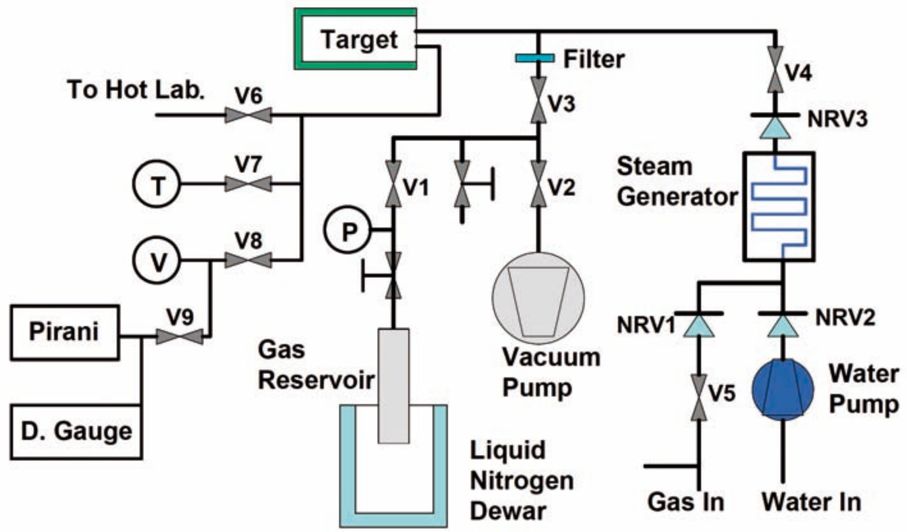

FIG. 7.3. Example of a gas handling system for production of ^{81m}Kr. Here, the Vs and Ps are mechanical pressure gauges and the NRVs are one way valves to prevent backflow.

7.3.2.2. System checks

It is checked that:

- The krypton pressure in the gas reservoir is adequate.
- There is sufficient water for steaming.
- There is sufficient pressure in the gas cylinder for target emptying.
- The cryogenic Dewar vessel is filled with liquid nitrogen.
- All valves are closed.

7.3.2.3. Target load sequence

The sequence for target loading is as follows:

(1) The target is pumped down by turning on the rotary pump and opening valves V2 and V3. After a delay, valve V8 opens to allow measurement of the pressure in the target.
(2) To allow a more sensitive measurement of pressure, valve V9 opens after the mechanical gauge has been below the low detection limit (25 inHg (84.66 kPa)) for 2 s.
(3) Once the indicated pressure on the Pirani gauge is less than 2×10^{-1} mbar (20 Pa), valves V9 and V2 are closed to isolate the target from the vacuum pump and the low pressure sensors.
(4) Valve V1 is opened and then closed after the pressure, as read on the mechanical gauge, has reached 550 kPa.
(5) Valve V3 is closed to isolate the target, and a ‘ready’ signal is sent to the cyclotron control system; valve V8 remains open to measure the pressure during irradiation.

7.3.2.4. Target unload sequence

The sequence for target unloading is as follows:

(1) The heaters for the steam generator and target body are turned on to increase the temperature of the target walls.
(2) The cryogenic Dewar vessel is slowly raised to cool the ‘pump’ gas reservoir.
(3) Cooling of the reservoir is indicated by the reservoir pressure falling to 0 Pa. After a short delay, valves V1 and V3 open to pump out any residual gas from the target.

(4) Valve V9 opens after the mechanical gauge has been below the low detection limit for 2 s.

(5) Wait for the absolute pressure diaphragm gauge to reach 19 mbar (1900 Pa). This indicates that the target gas has been recovered in the reservoir.

(6) After a delay, *all* valves are closed, and a ‘blowout’ signal is sent to the target cooling system. This closes off the target gas reservoir, sends a gas stream and clears the water from the target cooling lines.

(7) Valves V4 and V5 are opened for a short time to relieve the target vacuum.

(8) Wait for the steam generator to reach its temperature and for blowout to be completed.

(9) Valve V6 to the hot laboratory is opened, valve V4 to the steam generator is opened and a ‘ready’ signal is sent to the hot cell that delivery of radioactivity is imminent.

(10) Start the water pump to inject steam into the target for a preset time. Steam is used to remove the radionuclide.

(11) The water pump is stopped and valve V5 is opened to empty the target to the cell, using helium at 50 lbf/in^2 (0.345 MPa). The helium gas pushes the water through the lines and into the hot cell.

(12) After 9 min, close all valves and turn off the steam generator heater.

(13) Valves V2 and V3 are opened and the rotary pump and target heater run for 1 h. This dries the target and prepares it for the next irradiation.

(14) Heat is turned off and the target remains under active vacuum until the next load cycle.

7.3.3. Quality control of target gases

The purity of the gases used as target gases can have a profound effect on the chemical form of the radioisotope, and on the SA of the radioisotope. The SA is especially important for ^{11}C-containing compounds.

For these reasons, the gases used should be of the highest purity possible and they should have a certificate of analysis. This is an extra cost, but maintaining production of radioisotopes of the highest quality is well worth the expense.

7.3.4. Maintenance schedule for gas targets

The maintenance schedule for gas targets is relatively simple (Table 7.3). The front foil is usually the first item to fail, and so it should be inspected often for signs of damage. If there are small bulges in the foil, it should be replaced.

The two different kinds of foil commonly used on gas targets are aluminium and Havar foils, and they have very different characteristics. Aluminium foils often deteriorate slowly, with a small leak developing first, which becomes larger until the foil fails. Havar foils, on the other hand, often fail with no warning. To minimize radiation dose, the best time for inspection is after an extended period of no beam on the target when the activity of the foil has had a chance to decay. In those facilities that operate five days a week, this would be after the weekend on the first workday.

7.4. LIQUID TARGET PROCESSING

There are only a few liquid targets in routine use for radionuclide production. By far the most common liquid target is the ^{18}O water target for the production of ^{18}F using the $^{18}O(p, n)^{18}F$ nuclear reaction. In water targets, the activity is removed in the aqueous phase. There are two general methods of utilization:

(1) The first is to use the ^{18}O water containing the [^{18}F]fluoride ion directly in the synthesis. This method is used by several groups who have small volume water targets, and the cost of losing the ^{18}O water is minor compared with the cost of the cyclotron run.
(2) The second method is to separate the fluoride from the ^{18}O water, either by distillation or by using a resin column [7.7–7.9]. Use of resin can also remove the metal ion impurities from the enriched fluoride solution, which, in general, increases the reactivity of the fluoride. The fluoride is usually made more reactive by combination with a metal ion complexing agent, such as crown ether or tetrabutylammonium salts [7.10].

TABLE 7.3. A SUGGESTED MAINTENANCE SCHEDULE FOR GAS TARGETS

Weekly	Visually check for damaged tubing or fittings Leak check the system Check the front foil for signs of damage
Monthly	Test plastics for radiation damage Track target yields to establish trends

7.4.1. Contaminants in water targets

Water targets can be made of a variety of metals. The most common are silver, titanium and niobium. Some of the advantages and disadvantages of these materials are given in Table 7.4.

In silver targets, especially, there are colloids formed that can clog transfer lines. An example of the silver colloid deposited on the inside of a target foil is shown in Fig. 7.4.

TABLE 7.4. MATERIALS COMMONLY USED FOR THE CONSTRUCTION OF WATER TARGETS
(adapted from Schmitz et al. [7.11])

Material properties	Ag	Ti	Nb
Chemical resistance	Poor	Good	Good
Thermal conductivity ($W \cdot cm^{-1} \cdot K^{-1}$)	4.29	0.219	0.537
Radioisotopes from the target body	Cd-109	V-48	None
Reactivity of F-18 produced	Average	Good	Good
Maintenance frequency	High	Medium	Low
Target pressure	Low	Medium	High
Maximum beam current (limit by target design and thermal conductivity)	70	55	100

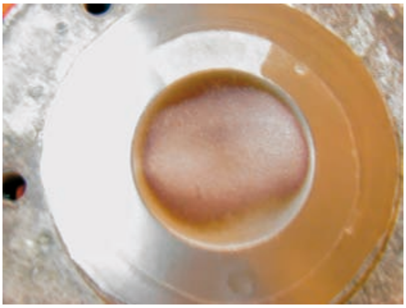

FIG. 7.4. An example of silver colloid being deposited from solution inside the front foil of a water target.

7.4.2. Water transfer

The transfer of ^{18}O enriched water through long lengths of small diameter (1/16 in (1.59 mm)) tubing has been studied [7.12]. A single bolus of water was easily able to pass through the tubing. In this case, the transfer gas pressure only has to overcome two components due to surface tension acting at the two liquid–air interfaces at the beginning and end of the bolus, i.e.:

$$P > F_1 + F_2$$

where P is the force required to move the water through the tubing, and F_1 and F_2 are the two components due to surface tension.

It is found that with less controlled target emptying, the bolus of water is broken into two or three segments. The more segments there are, the slower the transfer through the tubing and the higher the gas pressure required. As the single bolus breaks up into many pieces, there are a larger number of components (due to surface tension) that the transfer gas pressure has to overcome. For example, for n components:

$$P > F_1 + F_2 + F_3 + F_4 + \cdots F_{2n}$$

At higher pressures, the rear end of the bolus tends to break up, leaving a small number of small droplets in the tubing. This effect is also seen when contaminated ^{18}O enriched water is used or when cleaning solvents are not completely removed from the tubing. Once the small droplets are present in the tubing, a bolus of water has a tendency to break up into segments, even when slow controlled transfer conditions are used. When the number of segments in the tubing becomes too great, the transfer gas pressure cannot overcome the surface tension of the combined segments. Increasing the transfer gas pressure only squeezes the segments closer together rather than continuing to push the water through the tubing.

If extreme pressure is used to force the water through the tubing, a fine coating of small droplets forms inside the tube. If another bolus is put into the tubing, it will not pass through without severe segmentation. Further drying of the line does not remove these droplets effectively. The only solution to removing the small droplets is to wash the lines with a suitable solvent miscible with water and then dry the lines thoroughly with air.

Another effect is seen when the previous emptying process is incomplete (i.e. water is left behind in the tubing). A bolus of water from the current transfer can displace a bolus of water from the previous transfer. At the end of the transfer, the bolus of water from the previous transfer will arrive at the cell with the bolus from the current transfer remaining in the tube. It will appear that the target has emptied, but, in reality, the radioactivity will be stuck in the lines, implying that there has been a target failure rather than a transfer problem. Only by thoroughly cleaning the lines can the transfer be returned to its normal operation.

There are a few solutions to this problem of water transfer. One is to extract the ^{18}F from the water near the target and avoid long distance transfer of the enriched water. The other, less robust, solution is to filter the water near the target with a fine polyethylene filter before passage through the tubing. This method also requires careful control of the pressure used to unload the target as well as frequent cleaning of the transfer lines.

7.4.3. Extraction

The most common method for the extraction of ^{18}F from an aqueous solution of $[^{18}O]H_2O$ is with the use of an anion exchange resin. The resins commonly in use are the Dowex1X8 resin in carbonate form and the quaternary methyl amine (QMA) resin cartridges supplied by Alltec [7.7–7.9]. Once the ^{18}F has been extracted from the resin, it can be mixed with acetonitrile and transferred through fine bore tubing. The presence of acetonitrile reduces the surface tension of the water and allows a smoother transfer without the problems mentioned above. However, the bolus may still break up into pieces, and some of the liquid and activity will be left on the inside of the tubing. One solution to this problem is to use a second rinse of pure acetonitrile to help remove the remaining activity. A schematic diagram of a water recovery system incorporating these features is shown in Fig. 7.5 [7.13].

In the system shown in Fig. 7.5, which consists of four six-way valves, the water from the target is passed through the resin column and the ^{18}O water recovered in the ^{18}O recovery reservoir. The column is then switched and the carbonate reservoir empties through the resin column into the mixing reservoir. Acetonitrile is added to this reservoir, and the resulting mixture is transferred through a long line to the chemistry laboratory, which is 50 m away. A second rinse of pure acetonitrile is passed through the line and is used to rinse any residual fluoride from the tubing. This second rinse typically recovers about 20% of the activity.

7.4.4. Distillation

If the water is to be reused, it must be distilled before being irradiated a second time. Fractional distillation is the common method and will remove

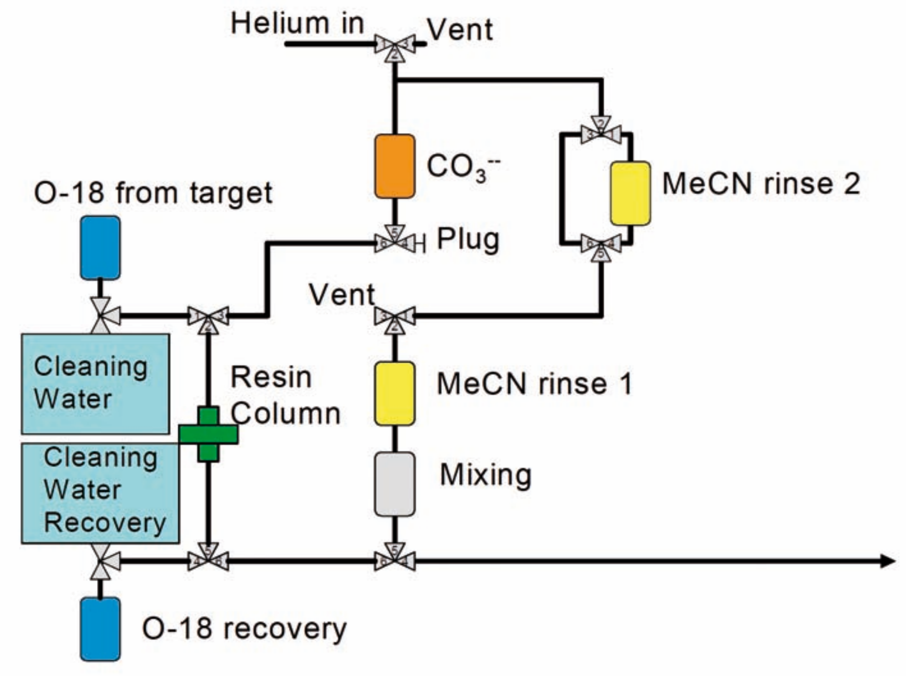

FIG. 7.5. Schematic diagram of a resin system for recovery and elution of ^{18}F.

many impurities and any metal radioisotopes that may have been introduced during irradiation. It is also important to maintain the pH of the water near 7.0. If the water becomes acidic, ^{19}F ions can distil over with the water. One method to keep the pH high is to add a very small piece of sodium metal (carefully cleaned of all oil) to the water before distillation. This will raise the pH and not introduce any isotopic dilution to the enriched water.

7.4.5. Quality control of ^{18}O water

Oxygen-18 enriched water, after passing through an AG-1-X8 column in carbonate form, can become contaminated with amine residues from the resin. If acetonitrile is used in the extraction process, the water can be contaminated with organic residue [7.12]. Fractional distillation of the recovered ^{18}O enriched water will not effectively separate these impurities. Distillation from potassium permanganate and potassium hydroxide, or other treatments to remove organic molecules, may improve the purity of the water. After two or three distillations, the buildup of impurities in the enriched water can become significant and may cause breakup of the ^{18}O enriched water in empty target lines. The organics can be removed from the water by ultraviolet irradiation and filtering or treatment with potassium permanganate. The water can also be cleaned by passage through an activated charcoal filter, but significant amounts of enriched water will be lost in this purification process.

The best solution to this problem is never to expose the resin to any organic solvents. If acetonitrile is added to aid in the transfer of water over long distances, it should be added downstream of the resin column. Alcohol or acetone should never be used to clean the resin system, unless the entire apparatus can be taken apart and completely dried.

Organic impurities in the enriched water can be identified by passing the water through a gas chromatograph with a flame ionization detector. For the most common impurities, a 4.3 m 80–100 mesh Porapak Q column at 135ºC can be used [7.14].

One method to remove fluoride from the water is distillation from a basic solution, as was described in Section 7.4.4. Fluoride ions will remain in the reservoir and will not be distilled into the receiver vessel. This should also improve the SA of the ^{18}F.

7.4.6. Maintenance schedule for water targets

A routine maintenance procedure should be established and followed for the target processing and QC. Table 7.5 gives a suggested schedule for maintenance [7.12].

TABLE 7.5. SUGGESTED MAINTENANCE SCHEDULE FOR O-18 WATER TARGETS

Frequency	Maintenance
Weekly	Visually check for damaged tubing Leak test the system Prepare fresh O-18 water for use Blow the transfer lines clean and dry with nitrogen gas Replace any rubber seals on the system (e.g. Burrell seals)
Monthly	Test plastics for radiation damage Back-flush valves and check operation Track target yields to establish trends
Six monthly	Clean target Replace all foils Replace plastic parts if there is any degradation in them
Generally	Refrigerate O-18 water Use sterile needles

7.5. SOLID TARGET RECOVERY

It is often difficult to separate the product radioisotope from the target material in the solid phase. There are several techniques that may be applied. Three separate techniques are described here in some detail as examples:

1. The first is the solvent extraction method for ^{201}Tl, which is described in Section 7.5.1.
2. The second is the thermal diffusion technique for ^{211}At, which is described in Section 7.5.2.
3. The third is the electrochemical recovery of thallium, which is described in Section 7.6.

7.5.1. Solvent extraction

One of the classical methods for extraction of radioisotopes from targets is solvent extraction [7.15–7.17]. In this technique, the entire target is dissolved in a solvent (usually an aqueous solution of either an acid or a base), and the radioisotope is extracted by using an organic solvent. Certain compounds of some elements, under the proper conditions, will preferentially transfer from the aqueous phase into immiscible organic solvents. Some solvent extraction processes are highly specific. Another technique is chelation of metal ions. It is usually possible to alter the conditions of the solvent extraction system so that the desired element passes back into the aqueous phase. This 'back-extraction' may act further to increase the specificity of the solvent extraction operation, as well as to return the substance under investigation to a more convenient medium for further purification. An example of solvent extraction for the production of ^{201}Tl is given below. The ^{201}Pb is made from the ^{203}Tl(p, 3n)^{201}Pb nuclear reaction [7.18]. The target is usually a copper plate with the ^{203}Tl target material electroplated. After irradiation, the ^{201}Pb must be extracted from the target plate. There are two steps in this procedure. The first is the separation of ^{201}Pb from the target plate, and the second is the separation of the ^{201}Tl that has grown in from the ^{201}Pb.

7.5.1.1. Step 1: Separation of ^{201}Pb from the ^{203}Tl target plate

This separation step involves the following stages:

(a) A thallium-203 target is dissolved in 2–4 mL of 4M sulphuric acid. This will dissolve the thallium without dissolving much of the copper plate. A barrier or hold is used to protect the copper plate from the sulphuric acid.

(b) The dissolved target material is transferred into a flask and the target plate is rinsed with dilute sulphuric acid; this solution is also added to the flask.

(c) Aqua regia (20 mL conc. HCl + 3 mL conc. nitric acid) is added to the flask to convert all the thallium into the thallic (+3) oxidation state.

(d) The solution is transferred to a separatory funnel and mixed thoroughly by bubbling with a stream of filtered air. This ensures that all the thallium will be in the higher (+3) oxidation state.

(e) Fifty millilitres of n-butyl acetate, equilibrated with 6M HCl, is added to the separatory funnel, and the two phases are mixed well by bubbling with the airstream.

(f) After separation of phases, the aqueous layer containing the ^{201}Pb is collected into a clean quartz beaker.

(g) The organic phase is extracted again with two 5 mL portions of 6M HCl, collecting the aqueous phase in the same beaker. The same procedure, using an airstream to mix and equilibrate the phases, is carried out.

(h) The aqueous layer containing all the ^{201}Pb is transferred to another separatory funnel.

(i) Any residual chemical ^{203}Tl is now removed by repeated extractions with n-butyl acetate. This ^{203}Tl will later be recovered from the organic phase for reuse.

(j) The aqueous phase is collected in a flask containing 3 mL of concentrated nitric acid.

(k) The aqueous phase should be tested for ^{203}Tl in the ^{201}Pb solution at this stage to ensure compliance with the required chemical purity of the ^{201}Tl bulk; if no ^{203}Tl is detected in the solution, it should be set aside for ^{201}Tl to grow for about 32 hours.

(l) The n-butyl acetate phase containing enriched ^{203}Tl is set aside for recovery at a later stage.

7.5.1.2. *Step 2: Separation of ^{201}Tl from ^{201}Pb*

This separation step involves the following stages:

(a) After a sufficient period of ^{201}Tl growth, the solution is transferred to a separatory funnel.

(b) The 50 mL of DIPE (diisopropyl ether) equilibrated with 6M HCl is transferred to the extractor and phases are mixed well with a stream of filtered air.

(c) The aqueous phase containing ^{201}Pb is removed, and the organic phase is washed twice with 20 mL of 6.0M HCl to remove residual ^{201}Pb.

(d) The ^{201}Tl is back-extracted into the aqueous phase in two portions of 10 mL each of sterile water saturated with SO_2 gas (the mild reducing agent will convert the oxidation state from thallic ions (+3) into thallous ions (+1)).
(e) The combined aqueous phase containing ^{201}Tl is carefully evaporated to dryness.
(f) The ^{201}Tl activity is dissolved in 0.9% NaCl solution, the solution is then filtered and the quality testing is carried out.

Some difficulties, such as emulsion formation or slow attainment of equilibrium, may arise in solvent extraction. The organic phase may extract enough of the reagents from the aqueous phase to alter the original conditions of extraction. There may be a tendency for radiocolloidal impurities, not in themselves extractable, to collect on the interface between the phases. Substances that are extracted in macro-sized amounts may not be extracted as readily in trace amounts.

7.5.2. Thermal diffusion

One of the more common methods for the separation of radioisotopes from solid targets is thermal diffusion, which is also known as dry distillation. In this technique, a solid target is heated to a temperature at which the radioisotope can be volatilized but where the target material does not diffuse away from the target. This technique is common for radiohalogens because of the relative volatility of the halogen when compared with the target material. A dry distillation system for isolation of ^{211}At from a bismuth cyclotron target is shown in Fig. 7.6 [7.19].

The efficiency of the recovery for this type of thermal diffusion varies depending on a number of factors, which include the relative vapour pressures of the target and product. For ^{211}At, extraction has been reported anywhere from 45% up to 75%. A typical procedure for the thermal diffusion method is given below.

Prior to each distillation, the quartz and glassware components of the distillation apparatus were cleaned as follows:

(1) Soaked in concentrated HNO_3 for at least 5 h;
(2) Rinsed in cold water;
(3) Soaked in hot soapy water (Alconox, New York) for 30 min, followed by ‘brush-washing’;

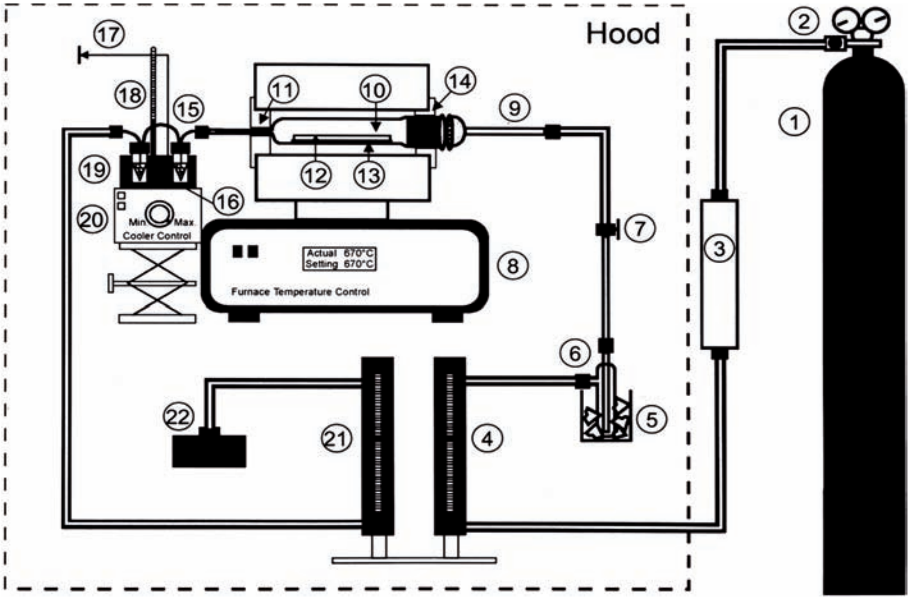

FIG. 7.6. A distillation system used for isolation of ^{211}At from a bismuth cyclotron target: (1) argon cylinder, (2) argon gas regulator, (3) gas filter, (4) inlet flow meter and valve, (5) Dewar containing dry ice, (6) ether trap, (7) Teflon valve, (8) tube furnace, (9) quartz inlet tube, (10) quartz still, (11) insulation ring, (12) aluminium-backed bismuth cyclotron target, (13) quartz support plate, (14) insulation ring, (15) glass still outlet tube, (16) radioactivity detector, (17) detector output to amplifier, counter and strip chart recorder, (18) thermometer, (19) aluminium cooling block, (20) thermoelectric cooler, (21) outlet flow meter, (22) charcoal filter trap.

(4) Rinsed with cold tap water and, finally, with distilled water;
(5) Baked in an oven for at least 12 h at 120°C.

Before each distillation, the still and condensing unit were assembled and inserted into the furnace, and heated to 150–200°C under a flow of argon [7.20]. The target is removed from the cyclotron and transferred to the hot cell containing the distillation apparatus. A flow of argon is started in the apparatus through the dry ice trap to remove any traces of water and the furnace turned on. After insertion of the target in the apparatus, the temperature of the plate is brought up to the desired distillation temperature of 670°C.

The distillation is terminated when a plateau in activity, determined by the scintillation detector, has been reached (usually after about 20–30 min). In this operation, the ^{211}At is trapped by condensation in two gas-washing bubbler traps of approximately 2 mL volume (near the radioactivity detector, item (16) in Fig. 7.6) in series, to which is added 300 μL of the desired solvent for collection of the distilled ^{211}At. The bubbler traps are cooled with ice [7.19] during distillations.

7.6. DISSOLUTION OF ^{201}Tl TARGETS

Irradiated thallium targets can be dissolved in diluted nitric acid, sulphuric acid or concentrated hydrogen peroxide.

7.6.1. Classical methods

There are several classical methods for dissolution of ^{203}Tl targets. An automated device for this dissolution is shown in Fig. 7.7.

7.6.2. Flow-through strippers

Using a flow-through stripper that allows heating (70–80°C) on the coolant side, the fast (10–15 min) solubilization in 20–30 mL of 0.7N HNO_3

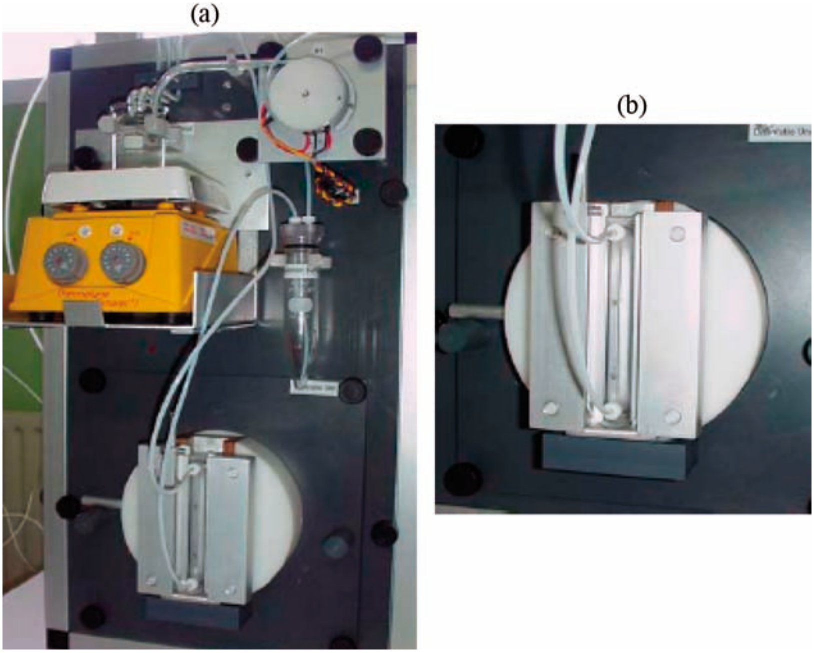

FIG. 7.7. (a) Manifold for dissolution and precipitation of target material. (b) A close-up of the dissolution plate holder.

results in co-dissolution of milligram amounts of copper. Consequently, apart from the ^{203}Tl and the lead and thallium radionuclides formed during the irradiation, the stripping solution will be contaminated with copper and some carrier-free ^{65}Zn.

When time-consuming (1 h) dissolution in 4–5M sulphuric acid at room temperature is performed, only microgram amounts of copper are dissolved. Although attractive from the analytical point of view, sulphuric acid dissolution will give rise to a loss of about 10% of the ^{201}Tl during the solubilization step. Heating up to 60–70°C and vigorous stirring will increase the dissolution rate but will also result in a higher copper and ^{65}Zn contamination. Appropriate chemical processing is then essential. The dissolution in H_2O_2 is carried out by means of drop by drop moistening of thallium. This step gives rise to a violent autocatalytic oxidation reaction, resulting in the formation of a dark brown to black slurry consisting of a mixture of thallium hydroxides. The latter are readily dissolved and the thallium reduced to the monovalent oxidation state in 1N hot perchloric acid.

Chemical processing involves two steps: fast separation of ^{201}Pb from irradiated and dissolved ^{203}Tl target material (Chemistry-1) at the end of the bombardment, and separation of non-carrier added ^{201}Tl from the remaining ^{201}Pb (Chemistry-2) after an appropriate grow-in period (25–35 h). It should be noted that only about 90% of the ^{201}Pb has decayed into ^{201}Tl at this point. Re-extraction of ^{201}Tl from the resulting lead solution after a second decay period may increase the ^{201}Tl yield by more than 5%.

Many radiochemical procedures for preparation of good quality ^{201}Tl raw material are available in the literature [7.21, 7.22]. For Chemistry-1 precipitation ($PbSO_4$ after addition of lead carrier), co-precipitation (with $Fe(OH)_3$ and $SrSO_4$), anion and cation exchange chromatography, and adsorption chromatography are frequently applied. Chemistry-2 often involves a two step separation: chromatography for separation of monovalent ^{201}Tl after reduction (with SO_2) from the ^{201}Pb bulk (upon decay of lead into thallium, a mixture of monovalent and trivalent thallium is obtained), and chromatography and solvent/solvent extraction of trivalent ^{201}Tl (oxidation with $KbrO_3$ and O_3 gas). Upon reduction (with SO_2 and $NaHSO_3$), back-extraction is performed followed by ^{201}Tl bulk conditioning (pH and isotonicity adjustment, and sterilization). Some examples are summarized in Table 7.6 (procedures for ^{201}Tl production) and Table 7.7 (typical ^{201}Tl yields).

TABLE 7.6. PROCEDURES FOR Tl-201 PRODUCTION IN DIFFERENT INSTITUTIONS

Institute	Dissolution Tl-203	Chemistry-1
NRCAM VUB[a]	0.7N HNO_3 Flow-through stripper at 60–70°C	Precipitation of $PbSO_4$ Redissolution in EDTA (pH5) Cation exchange to remove co-precipitated Tl-203 Pb-201/EDTA bulk solution decay
CNEA[b]	0.7N HNO_3 Bulk dissolution at room temperature	Cationic exchange 0.1M HNO_3 Pb-201 decays on-column
INP[c]	5M H_2SO_4 Bulk dissolution at 80ºC	Co-precipitation with $SrSO_4$ Pb-201 decays adsorbed at precipitation

[a] VUB: Vrige Universiteit Brussel.

[b] CNEA: Comisión Nacional de Energía Atomica, Buenos Aires.

[c] INP: Institute of Nuclear Physics, Kraków.

TABLE 7.7. TYPICAL Tl-201 YIELDS

Institute	Chemistry-2	Tl-201 yield (GBq)
NRCAM VUB	Reduction with SO_2, cation exchange (0.1M EDTA) Elution of Tl-201 (6N HCl), Oxidation (O_3), extraction with DIPE Reduction (SO_2), back-extraction 0.01M HCl	37–55.5
CNEA	Elution of Tl-201 (0.1M HCl)	44.4–59.2
INP	Redissolution (6M HCl) Oxidation ($KBrO_3$) Solvent extraction (butyl acetate) Reduction (H_2SO_3), back-extraction (0.01M HCl)	11.1

Precipitation of ^{201}Pb can be carried out using the apparatus shown in Fig. 7.8.

It is possible to use electrochemical techniques to perform all the tasks associated with the preparation, recovery and separation of targets for producing radioisotopes. As has been mentioned before, this is a separation of metals by CCPE.

In principle, separation of metals by CCPE can be performed if their discharge intervals do not overlap. The interval for a given metal and hydrogen can be shifted by the addition of appropriate complexing agents and adjustment of pH. The upper limit of the discharge interval can be determined

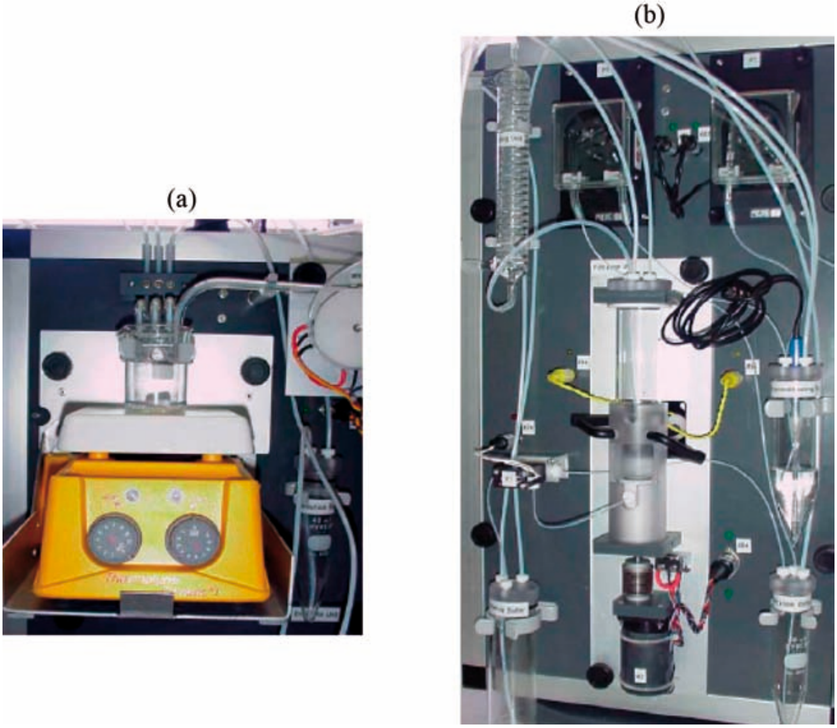

FIG. 7.8. Manifolds used for: (a) precipitation of ^{201}Pb and (b) filtration of the final solution.

from current–voltage curves, and the lower limit can be easily detected by current monitoring (for an exponential decrease).

As an example, the following conditions can be used for thallium solutions:

(a) Electrodes: Reference electrode Hg/Hg_2SO_4/sat. K_2SO_4 (+412 mV);
(b) Anode: A platinum wire;
(c) Cathodes: Copper deposition — a home-made cylindrical copper gauze;
(d) Thallium deposition: A platinum gauze (Johnson–Matthey);
(e) Zinc deposition: A home-made cylindrical copper gauze;
(f) The values of cathodic potential versus the reference for selective deposition.

These are the solution requirements for deposition of:

(a) Copper: Acid solution (HNO_3/H_2SO_4) at $1.5 < pH < 3$ with a N_2H_4 depolarizer;

(b) Thallium: An alkaline (pH > 12) $Tl(EDTA)_3^-$ solution with a N_2H_4 depolarizer;
(c) Zinc: A strong alkaline solution (pH ≫ 12).

The current–voltage curves for these reactions are given in Fig. 7.9.

7.6.3. Centrifugal electrochemistry

There is a more recent technique that has been developed to dissolve target material, which is especially useful for the dissolution of rhodium targets. This is the centrifugal electrodissolution technique. It has several advantages:

(a) Limited final volume (±40 mL);
(b) Quantitative dissolution (>99%);
(c) High current density (>2 A/cm^2);
(d) Time controlled dissolution (rate);
(e) Suitable for rhodium fragments, powder, cut wires and foils.

An assembly for basic centrifugal electrodissolution is shown in Fig. 7.10. It shows how the liquid level is raised and the solids are drawn away from the central electrode by centrifugal forces.

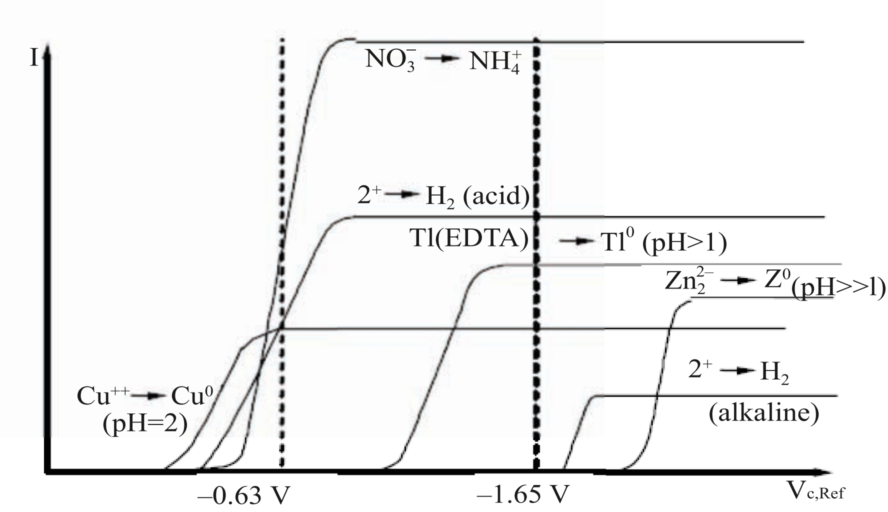

FIG. 7.9. Current–voltage curves and possible reactions.

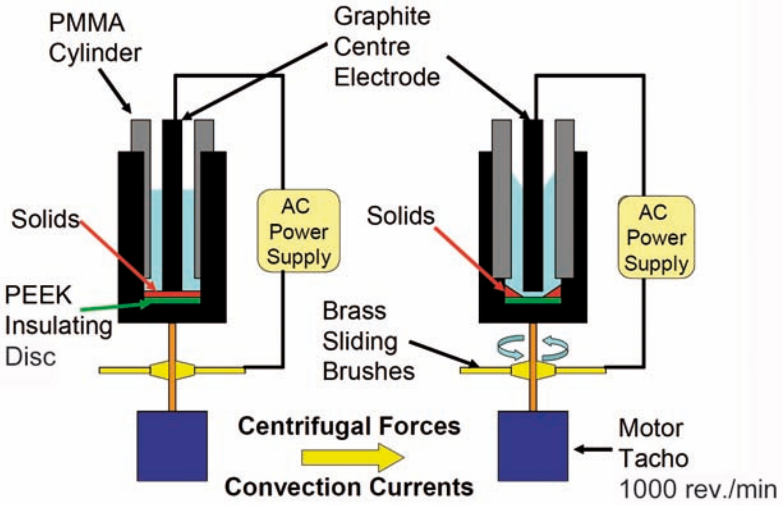

FIG. 7.10. Schematic diagram of a centrifugal electrodissolution assembly.

7.7. RECOVERY OF MATERIAL FROM PLATING SOLUTIONS

One of the aspects of solid targets is to recover the enriched isotope used for the target. The following section describes the recovery of ^{203}Tl used to produce ^{201}Tl as an example for solid target recovery. Further examples can be found in Ref. [7.23]. Quantitative and rapid recovery of enriched ^{203}Tl from partially depleted plating baths or from recovery solutions can be achieved using these methods [7.24, 7.25].

7.7.1. Recovery of enriched thallium

The CCPE method can be used to recover enriched thallium from partially depleted plating solutions (alkaline EDTA solutions containing thallium metal only) or from recovery solutions (nitric or sulphuric acid or alkaline ammonia nitrate solutions containing copper, thallium and carrier-free ^{65}Zn) obtained after processing of irradiated targets. This electroseparation technique is based on the shift of a metal ion discharge interval and subsequent selective separation, by addition of complexing agents to, and/or pH adjustment of, a solution containing a mixture of metals. The method involves the use of a three electrode set-up: a cylindrical large area copper (or platinum) gauze cathode, a platinum wire anode mounted axially inside the cathode and a reference electrode positioned close to the cathode. The electrode set is immersed in a properly adjusted recovery solution and connected to a potentiostat. This allows fixing the potential of the cathode versus the reference electrode to a value such that one metal is selectively and quantitatively deposited. Upon removal of the metal deposit from the cathode or upon introduction of a new cathode, the composition of the solution and the potential of the cathode are changed such that a second metal can be plated out, and so on. The end of the deposition of a given metal is detected by monitoring the exponential current flowing through the cathode circuitry, current that should approach zero near the end point. The experimental conditions for the separation of copper, thallium and zinc are summarized in Table 7.8. Up to 15 g of enriched ^{203}Tl may be recovered in a single run.

7.7.2. Separation of copper

Copper may be present in the recovery solutions if nitric acid is used to dissolve the thallium layer. If dissolution of the irradiated target material is performed in sulphuric acid, this step may be omitted. This is also the case when thallium is recovered from partially depleted alkaline EDTA solutions. To make the method applicable when the ^{203}Tl/^{201}Pb separation is carried out by co-precipitation of carrier-free ^{201}Pb with $Fe(OH)_3$ in an alkaline ammonia nitrate medium, the procedure starts with the addition of concentrated ammonia to the nitric acid recovery solution.

7.7.3. Separation of thallium

Upon removal of copper, the composition of the recovery solution is altered such that it approaches the plating bath described in Chapter 6. Thallium-203 is selectively plated out on a large area platinum gauze electrode. The thallium can be redissolved in diluted sulphuric acid containing a minor amount of hydrogen peroxide. The peroxide helps to increase the dissolution rate. The solution thus obtained can be used to prepare a new plating bath.

TABLE 7.8. ELECTROSEPARATION OF COPPER, THALLIUM AND ZINC; REFERENCE ELECTRODE: $Hg/HgSO_4$/sat. K_2SO_4 (+412 mV vs NHE)

Element	Solution	pH	Cathode	$E_{cathode}$ vs Ref.
Cu	HNO_3/H_2SO_4	$1.5 < pH < 3$	Cu gauze	–0.630
Tl	EDTA	>12	Pt gauze	–1.650
Zn	NaOH excess	≫12	Cu gauze	Constant current

7.7.4. Separation of zinc

Although it is of no practical concern for radionuclide production itself, ^{65}Zn is plated out on the copper gauze electrode after the addition of a suitable amount of carrier. This is done solely to avoid making a large volume of long lived liquid waste, the disposal of which is very expensive. Pressing together the copper gauze after the zinc plating, less than 1 cm^3 of solid waste can be obtained. As the precious enriched ^{203}Tl has been removed in the preceding step, constant current electroplating at high current density can be applied.

7.8. SYNTHESIS OF ^{11}C COMPOUNDS

For ^{11}C, the molecule that is the most stable in an oxidizing environment is CO_2. In a reducing environment, the most stable molecule is usually methane (CH_4). Either of these two chemical forms are the building blocks of more complex molecules.

7.8.1. Carbon-11 carbon dioxide

Carbon-11 is most commonly produced in a N_2 gas target using the $^{14}N(p, \alpha)^{11}C$ nuclear reaction. A trace of oxygen is added to convert all the ^{11}C into CO_2. Almost all syntheses involving ^{11}C start with CO_2 as the primary product.

A number of other precursor molecules, some of which are shown in Fig. 7.11, are synthesized from labelled CO_2, but all require some synthetic manipulation during or after cyclotron bombardment [7.14, 7.26–7.28].

7.8.2. Commercial modules for synthesis

There are many commercial modules for the preparation of ^{11}C molecules. Excellent reviews have been written that give the characteristics of these synthesis modules [7.29, 7.30]. Although there are a wide variety of designs for automated chemistry systems for PET radiopharmaceuticals, they also share some common characteristics. All of these systems were created using the modular design concept of laboratory unit operations [7.31, 7.32]. Each radiosynthesis can be broken down into a set of common laboratory operations. In radiotracer synthesis, these general purpose operations include manipulations common to the organic chemist, i.e. transferring reagents,

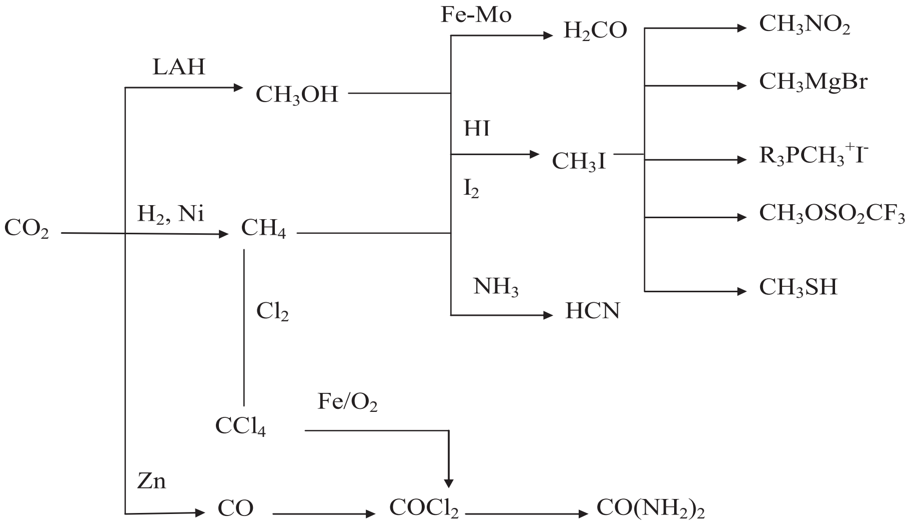

FIG. 7.11. Reaction pathways for the synthesis of ^{11}C precursors.

evaporating solvents, regulating vessel temperature and solid phase extraction (SPE). Unit operations design was first successfully applied to the design of remotely controlled syntheses of several ^{11}C tracers [7.31, 7.33, 7.34]. It is a useful engineering concept that has also been applied successfully to both robot systems [7.35–7.37] and fixed plumbed ‘black box’ automation [7.38]. Structured design techniques facilitate the development of automated systems from manual methods by providing:

(a) Firstly, plumbing building blocks for remotely controlled systems [7.30, 7.39];
(b) Secondly, a framework for both process control system and software design [7.40, 7.41].

7.9. SYNTHESIS OF ^{18}F COMPOUNDS

In the case of ^{18}F, the usual product coming out of the target is either fluoride ions (F^-) or fluorine gas (F_2), depending on the environment in the target during irradiation.

7.9.1. Synthesis of FDG

The most widely used ^{18}F containing compound by far is ^{18}FDG.

Fluorodeoxyglucose was developed in 1976 in a collaborative effort between scientists at the National Institute of Health, the University of Pennsylvania and BNL [7.42]. It was developed for the specific purpose of mapping brain glucose metabolism in living humans, thereby serving as a tool in the basic human neurosciences.

With ^{18}FDG, it was possible for the first time to measure regional glucose metabolism in the brains of living human beings. During that same period, the use of ^{18}FDG for studies of myocardial metabolism and as a tracer for tumour metabolism was reported. After the first synthesis of ^{18}FDG via an electrophilic fluorination with $^{18}F_2$ gas (produced via the ^{20}Ne(d, α)^{18}F reaction), small volume enriched water targets were developed that made it possible to produce large quantities of [^{18}F]fluoride ions via the high yield ^{18}O(p, n)^{18}F reaction. A major advance in the synthesis of ^{18}FDG from [^{18}F]fluoride was reported in 1986 when it was discovered that Kryptofix 222 could be used to increase the reactivity of [^{18}F]fluoride [7.11]. In essence, Kryptofix masks the potassium ions, which are the counter-ions of [^{18}F]fluoride. The reaction of [^{18}F]fluoride with 1,3,4,6-tetra-O-acetyl-2-O-trifluoromethanesulphonyl-2-O-mannopyranose to give 1,3,4,6-tetra-O-acetyl-2-[^{18}F]fluoro-D-gluco-pyranose provides a 95% incorporation of ^{18}F, and the overall synthesis, including purification, proceeds with a yield of about 60%. The synthesis involves two steps: displacement with [^{18}F]fluoride, and deprotection with HCl or NaOH. This new method served an increasing need in the nuclear medicine and neuroscience communities, which were discovering new uses for ^{18}FDG. It is also simple and amenable to automation and, in the 20 years since it was reported, a number of automated synthesis modules have become commercially available.

7.9.2. Synthesis of other fluorine containing compounds

In nucleophilic fluorination, ^{18}F labelled fluoride ions are almost always obtained as an aqueous solution. The fluoride ion is quite unreactive and requires some simple, but very important, manipulations to become a reactive nucleophilic reagent. A great deal of work has gone into developing methods for the preparation of reactive fluoride ions in organic solvents suitable for chemical syntheses. The steps in preparing reactive fluoride are crucial to the success of the labelling reactions, and it is worthwhile to examine the methods commonly being used.

In any aqueous solution, the fluoride ion must be accompanied by a positively charged counter-ion. As the fluoride is removed from the target, the metal ions in the water, which were rinsed off the surface of the target during irradiation, probably serve this purpose. The reactivity of the fluoride is very effectively enhanced by addition of a cationic counter-ion prior to evaporation of the water. Three types of counter-ion have been used:

(1) Large metal ions, such as rubidium or caesium;
(2) Potassium complexed by a cryptand, such as Kryptofix 222 [7.11];
(3) Potassium complexed by tetrabutylammonium salts [7.43].

Most syntheses now utilize the Kryptofix system or tetrabutylammonium salts. The addition of a cation also involves the inclusion of another anion to the reaction mixture. Anions such as hydroxide or carbonate are used, which do not effectively compete with the fluoride ion in nucleophilic displacement reactions. Carbonate is usually the anion of choice, since it is less likely to cause side reactions catalysed by bases.

7.9.2.1. Aliphatic nucleophilic displacements

The reaction of [^{18}F]fluoride ions with various leaving groups is an excellent method for synthesis of aliphatic carbon–fluorine bonds [7.44]. The choice of leaving group will depend on the yield, the stability of its precursors, the ease of subsequent separation of the [^{18}F]fluorinated product from its precursors, reagents and solvents, and the formation of potential side products [7.45].

7.9.2.2. Aromatic nucleophilic substitution

Fluorine substituted aromatic rings are common in many types of biologically active organic molecules. The fluorine atom is similar in size to the hydrogen atom and does not have serious steric effects, but its high electronegativity can significantly alter the electronic characteristics of the aryl ring. Nucleophilic aromatic substitution, where ^{18}F is substituted for a leaving group, has become a method used widely in ^{18}F chemistry [7.46]. The nitro and trimethylammonium groups are the most widely used leaving groups in aromatic substitutions with the [^{18}F]fluoride ion [7.47].

Simple isotopic substitution of [^{18}F]fluoride for [^{19}F]fluoride can be an effective method for synthesis of a new radiotracer. The low SA necessitated by these isotopic substitutions makes this reaction possible only when the SA of the final product is not important.

7.9.2.3. Electrophilic reactions

Various electrophilic fluorinating agents have been developed for use in the synthesis of radiotracers for PET. The first to be used was F_2, derived directly from the irradiation of neon [7.48]. The problem was that fluorine will react with nearly everything and the highly exothermic reactions must be controlled, either with a low temperature or by use of very dilute solutions of fluorine in an inert solvent. The solution to this problem was to convert the fluorine into a slightly less reactive form, such as acetyl hypofluorite [7.49] or xenon difluoride [7.50]. Since all of these reagents must be prepared using the carrier fluorine, the SA of the final product is always low. Despite these drawbacks, electrophilic fluorinations have played a vital role in the development of the radiotracers used for PET. Both FDG and fluoro-DOPA were first prepared using this method. Fluoro-DOPA is still routinely prepared by electrophilic fluorination.

7.9.3. Commercial modules for synthesis

Synthesis of FDG involves the production of [^{18}F]fluoride followed by reaction with mannose triflate and subsequent deblocking of the protected sugar, resulting in the production of [^{18}F]FDG. These steps are generally accomplished using one of several commercially available synthesis systems. The efficiency of the conversion of the label typically varies between 50 and 70%. The cause of this variability is not completely understood. A study was carried out determining the efficiency of [^{18}F]FDG production from three commercially available automated synthesis systems [7.51]. All synthesis systems made use of the method of Hamacher et al. [7.10], where [^{18}F]fluoride (fluoride) displaces the triflate-leaving group and the labelled acetylated FDG is then deblocked using either HCl or NaOH. The yields were determined by comparing the quantity of [^{18}F]fluoride at the start of synthesis and the quantity of FDG produced at the end of synthesis. The synthesis systems used included the CTI-CPCU unit at the PET Scan Centre in Vancouver, British Columbia, the EBCO system at the Vancouver Hospital, also in Vancouver, and the Coincidence Box at the Cross Cancer Centre (CCC) in Edmonton, Alberta, all in Canada. In addition to these studies, another set of studies at the Memorial Sloan–Kettering Cancer Center in New York compared two different GE MicroLab FDG synthesis units.

From these results, it appears that the commercially available synthesis units tested provide similar yields of FDG with comparable qualities of the final products. While the results from Vancouver General Hospital appear a little lower than those at the other two sites, the number of runs is small, and the uncertainties associated with these results certainly overlap with those of the other units.

However, the efficiency of FDG production appears to be dependent upon the source of [^{18}F]fluoride. The yields using the same synthesis system (at PETScan) gave statistically significant different results for the two sources of [^{18}F]fluoride, while the yields on the coincidence box were nearly identical using two different sources of fluoride. However, the target systems for production of fluoride both made use of a niobium target body, although of completely different configurations. The [^{18}F]fluoride produced in the niobium target body provides higher yields than a silver target body. The reason(s) for this difference is not understood. Another possibility is the purity of the target material ($H_2{}^{18}O$) for producing ^{18}F. It should be noted that some commercial manufacturers claim to have yields of more than 65% FDG for in-house production, which implies that the target and water are not the source of the yield problems. Shipping long distances does not appear to affect yields, since the coincidence system's use of fluoride shipped as irradiated $H_2{}^{18}O$ (not loaded on an ion column) from TRIUMF in Vancouver (eight hours from end of bombardment) and that from their own cyclotron, have similar yields.

Table 7.9 provides the decay corrected radiochemical yields of FDG from the various synthesis systems and [^{18}F]fluoride from the different target systems already noted.

The results from the Sloan–Kettering Cancer Centre are shown in Table 7.10 [7.52]. The ^{18}F activity at the start of synthesis is given in this table in per cent.

TABLE 7.9. DECAY CORRECTED RADIOCHEMICAL YIELDS OF FDG FROM THE VARIOUS SYNTHESIS SYSTEMS AND [^{18}F]FLUORIDE FROM DIFFERENT TARGET SYSTEMS AS NOTED IN THE TEXT

Unit	Decay corrected yield ± standard deviation (%)	*n*
CPCU — PETNet fluoride	52.1 ± 7.2	32
CPCU — TRIUMF fluoride	62.0 ± 10.5	17
EBCO — TRIUMF fluoride	57.4 ± 2.8	8
Coincidence — TRIUMF fluoride	65.4 ± 4.4	34
Coincidence — CCC TR19 fluoride	64.7 ± 10.9	64

TABLE 7.10. YIELDS FROM TWO GENERAL ELECTRIC MICROLAB FDG SYNTHESIS BOXES USED IN THE SAME LABORATORY, DEMONSTRATING THE REPEATABILITY OF THE RESULTS

Parameter	Box A	Box B
FDG yield (%)	63.4 ± 5.8	62.9 ± 4.6
Activity left on the reaction column (%)	9.3 ± 3.1	8.4 ± 2.5
Activity left on the alumina column (%)	4.0 ± 0.6	2.6 ± 0.6
Activity left on the ^{18}C column (%)	8.9 ± 1.0	9.5 ± 1.5

7.10. CONCLUSIONS

The processing of the target after irradiation is a critical part of the radioisotope production process. The separation of the product from the target material and the recovery of any enriched isotope target material are critical to the overall success of a facility. The conversion of the chemical for the radioisotope to a useful precursor can be a complex process as in the case of some ^{11}C precursors, or a very simple matter as is the case of fluoride, where the product can be used with almost no further processing.

Electrochemical recovery of solid target material offers several advantages over other methods, and the yields for these recoveries can be very high (>98%). The recovery of the ^{203}Tl given as an example has dramatically simplified the processing that must be done after the plating solution has become depleted.

REFERENCES TO CHAPTER 7

[7.1] FOWLER, J.S., DING, Y.-S., “Chemistry”, Principles and Practice of Positron Emission Tomography (WAHL, R.L., Ed.), Lippincott Williams & Wilkins, Philadelphia, PA (2003) 16–47.

[7.2] DANNALS, R., RAVERT, H.T., WILSON, A.A., WAGNER, H.N., “Special problems associated with the synthesis of high specific activity carbon-11 labeled radiotracers”, New Trends in Radiopharmaceutical Synthesis, Quality Assurance and Regulatory Control (EMRAN, A.M., Ed.), Plenum Press, New York and London (1991) 21–30.

[7.3] HICHWA, R., “Dimensioning of transport lines”, Targetry and Target Chemistry (Proc. 7th Int. Workshop Heidelberg, 1997), TRIUMF, Vancouver (1997) 172, http://trshare.triumf.ca/~buckley/wttc/proceedings.html

[7.4] BEAVER, J., FINN, R.D., HUPF, H., A new method for the production of high concentration oxygen-15 labeled carbon dioxide with protons, Int. J. Appl. Radiat. Isot. **27** (1976) 195–197.

[7.5] TEWSON, T.J., BANKS, W., FRANCESCHINI, M.P., HOFFPAUIR, J., A trap for the removal of oxides of nitrogen from carbon-11 carbon dioxide, Appl. Radiat. Isot. **40** (1989) 765–768.

[7.6] HAMMOND, R.G., RENTON, M.L., MacKAY, D.B., WATERS, S.L., "Design and operation of a krypton-82 gas target for the regular high yield production of rubidium-81 for the preparation of krypton-81m generators", Targetry and Target Chemistry (Proc. 7th Int. Workshop Heidelberg, 1997), TRIUMF, Vancouver (1997) 51–54, http://trshare.triumf.ca/~buckley/wttc/proceedings.html

[7.7] SCHLYER, D.J., BASTOS, M.A., ALEXOFF, D., WOLF, A.P., Separation of [^{18}F]fluoride from [O-18] water using anion exchange resin, Int. J. Appl. Radiat. Isot. **41** (1990) 531–533.

[7.8] MOCK, B.H., VAVREK, M.T., MULHOLLAND, G.K., Back-to-back "one-pot" [^{18}F]FDG syntheses in a single Siemens-CTI chemistry process control unit, Nucl. Med. Biol. **23** (1996) 497–501.

[7.9] PASCALI, C., et al. "A semi-automated system for optimizing the recovery of aqueous [^{18}F]fluoride from target", Targetry and Target Chemistry (Proc. 7th Workshop Heidelberg, 1997), TRIUMF, Vancouver (1997) 60–64, http://trshare.triumf.ca/~buckley/wttc/proceedings.html

[7.10] HAMACHER, K., COENEN, H.H., STOCKLIN, G., Efficient stereospecific synthesis of no-carrier-added 2-[^{18}F]fluoro-2-deoxy-D-glucose using amino-polyether supported nucleophilic substitution, J. Nucl. Med. **27** (1986) 235–238.

[7.11] SCHMITZ, F., et al., "Production of multi Curie [^{18}F]fluoride using a niobium target chamber at small PET cyclotrons", Targetry and Target Chemistry (Proc. 9th Int. Workshop Turku, 2002), TRIUMF, Vancouver (2002) 11 (abstract), http://trshare.triumf.ca/~buckley/wttc/proceedings.html

[7.12] STEEL, C.J., DOWSETT, K., PIKE, V.W., CLARK, J.C., "Ten years experience with a heavily used target for the production of [^{18}F]fluoride by proton bombardment of [^{18}O]water", Targetry and Target Chemistry (Proc. 7th Int. Workshop, Heidelberg, 1997), TRIUMF, Vancouver (1997) 55–59, http://trshare.triumf.ca/~buckley/wttc/proceedings.html

[7.13] SCHUELLER, M.J., Brookhaven Natl Lab., Upton, NY, personal communication, 2005.

[7.14] FERRIERI, R., Brookhaven Natl Lab., Upton, NY, personal communication, 2005.

[7.15] STEVENSON, P.C., HICKS, H.G., Separation techniques used in radiochemistry, Annu. Rev. Nucl. Sci. **3** (1953) 221–234.

[7.16] NAGY, S., KLENCSÁR, Z., "Radiochemical separations by thermochromatography", Handbook of Nuclear Chemistry, Vol. 5, Instrumentation, Separation Techniques, Environmental Issues (VÉRTES, A., NAGY, S., KLENCSÁR, Z., Eds), Kluwer Academic Publishers, Dordrecht (2004) Ch. 7.

[7.17] NAGY, S., KLENCSÁR, Z., “Solvent extraction and ion exchange in radiochemistry”, ibid., Ch. 6.

[7.18] REDDY, A.S., REDDY, M.L.P., Solvent extraction separation of Tl/I/ from Tl/III/ with sulphoxides, J. Radioanal. Nucl. Chem. Lett. **94** (1985) 259–264.

[7.19] ZALUTSKY, M.R., ZHAO, X.-G., ALSTON, K.L., BIGNER, D., High-level production of α-particle emitting ^{211}At and preparation of ^{211}At-labeled antibodies for clinical use, J. Nucl. Med. **42** (2001) 1508–1515.

[7.20] LARSEN, R.H., WIELAND, B.W., ZALUTSKY, M.R., Evaluation of an internal cyclotron target for the production of ^{211}At via the ^{209}Bi(α, 2n)^{211}At reaction, Appl. Radiat. Isot. **47** (1996) 135–143.

[7.21] LEBOWITZ, E., et al., Thallium-201 for medical use, J. Nucl. Med. **16** (1975) 151–155.

[7.22] BRITTO, J.L.Q., BRAGHIROLLI, A.M.S., SILVA, A.G., A new production method for carrier-free ^{201}Tl using IEN’s cyclotron in Rio De Janeiro, J. Radioanal. Nucl. Chem. **96** (1985) 181–186.

[7.23] INTERNATIONAL ATOMIC ENERGY AGENCY, Standardized High Current Solid Targets for Cyclotron Production of Diagnostic and Therapeutic Radionuclides, Technical Reports Series No. 432, IAEA, Vienna (2004).

[7.24] CHAVATTE, K., MERTENS, J., VAN DEN WINKEL, P., Method for effective Tl-201 (III) labelling of diethylenetriamine pentaacetic acid (DTPA) — Functionalized peptides: Radiosynthesis of Tl-201 (III) DTPA — Neurotensin (8-13), J. Labelled Compd. Radiopharm. **43** (2000) 1227.

[7.25] MAKOTO, K., NOBUA, U., HIROAKIA, M., European Patent 0003819, 1982, copies available from European Patent Office, Munich.

[7.26] LANGSTROM, B., LUNDQVIST, H., The preparation of ^{11}C-methyl iodide and its use in the synthesis of ^{11}C-methyl-L-methionine, Int. J. Appl. Radiat. Isot. **27** (1976) 357–363.

[7.27] LANGSTROM, B., et al., Synthesis of compounds of interest for positron emission tomography with particular reference to synthetic strategies for ^{11}C labelling, Acta Radiol., Suppl. **374** (1990) 147–151.

[7.28] FOWLER, J.S., WOLF, A.P., Working against time: Rapid radiotracer synthesis and imaging the human brain, Acc. Chem. Res. **30** (1997) 181–188.

[7.29] ALEXOFF, D.L., “Automation for the synthesis and application of PET radiopharmaceuticals”, Handbook of Radiopharmaceuticals (WELCH, M.J., REDVANLY, C.S., Eds), Wiley, Chichester (2003) 283–305.

[7.30] CROUZEL, C., et al., “Radiochemistry automation for PET”, Radiopharmaceuticals for Positron Emission Tomography: Methodological Aspects (STOCKLIN, G., PIKE, V.W., Eds), Kluwer Academic Publishers, Dordrecht (1993) 45–89.

[7.31] PADGETT, H.C., BARRIO, J.R., MacDONALD, N.S., PHELPS, M.E., The unit operations approach applied to the synthesis of [1-^{11}C]2-deoxy-D-glucose for routine clinical applications, J. Nucl. Med. **23** (1982) 739–744.

[7.32] SEVERNS, M.L., HAWK, G.L., "Medical laboratory automation using robotics", NATO ASI Series on Robotics and Artificial Intelligence (BRADY, M., GERHARDT, L.A., DAVIDISON, H.F., Eds), Springer-Verlag, Berlin (1984) 633–634.

[7.33] BERGER, G., MAZIERE, M., KNIPPER, R., COMAR, D., Automated synthesis of carbon-11 labeled radiopharmaceuticals: Imipramine, chlorpromazine, nicotin and methionine, Int. J. Appl. Radiat. Isot. **30** (1979) 393–399.

[7.34] WELCH, M.J., DENCE, C.S., KILBOURN, M.R., Remote systems for the routine production of some carbon-11 radiopharmaceuticals, J. Labelled Compd. Radiopharm. **19** (1982) 1382.

[7.35] BRODACK, J.W., KILBOURN, M.R., WELCH, M.J., Automated production of several positron-emitting radiopharmaceuticals using a single laboratory robot, Appl. Radiat. Isot. **39** (1988) 689–697.

[7.36] BRIHAYE, C., LEMAIRE, C., LUXEN, A., "Robot assisted synthesis of radiopharmaceuticals labeled with high activity positron emitters", Laboratory Automation and Robotics (Proc. Int. Symp. Hopkinton, 1995), Zymark Corporation, Hopkinton, MA (1996) 644–656.

[7.37] KRASIKOVA, R., Automated synthesis of radiopharmaceuticals for positron emission tomography, Radiochemistry **40** (1998) 364–372.

[7.38] SATYAMURTHY, N., PHELPS, M.E., BARRIO, J.R., Electronic generators for the production of positron-emitter labeled radiopharmaceuticals: Where would PET be without them? Clin. Positron Imag. **2** (1999) 233–253.

[7.39] CLARK, J.C., DOWSETT, K., "Automated carbon-11 radiopharmaceutical production", Targetry and Target Chemistry (Proc. 4th Workshop Villigen, 1992), TRIUMF, Vancouver (1992) 207–209,
http://trshare.triumf.ca/~buckley/wttc/proceedings.html

[7.40] ALEXOFF, D.L., et al., Modular automation in PET tracer manufacturing: Application of an autosynthesizer to the production of 2-deoxy-2-[^{18}F]fluoro-D-glucose, Appl. Radiat. Isot. **37** (1986) 1045–1061.

[7.41] RUSSELL, J.A.G., ALEXOFF, D.L., WOLF, A.P., "Distributed microprocessor automation network for synthesizing radiotracers used in positron emission tomography", NATO ASI Series on Physics and Engineering of Medical Imaging (GUZZARDI, R., Ed.), Martinus Nijhoff, Dordrecht (1987) 765–779.

[7.42] IDO, T., et al., Labeled 2-deoxy-D-glucose analogs, ^{18}F-labeled 2-deoxy-2-fluoro-D-glucose, 2-deoxy-2-fluoro-D-mamrose and ^{14}C-2-deoxy-2-fluoro-S-glucose, J. Labelled Compd. Radiopharm. **14** (1978) 171–183.

[7.43] KIESEWETTER, D.O., ECKELMAN, W.C., COHEN, R.M., FINN, R.D., LARSON, S.M., Syntheses and D_2 receptor affinities of derivatives of spiperone containing aliphatic halogens, Int. J. Appl. Radiat. Isot. **37** (1986) 1181–1188.

[7.44] BLOCK, D., COENEN, H.H., STOCKLIN, G., The NCA nucleophilic ^{18}F fluorination of 1-N-substitutes alkanes as fluoroalkylating agents, J. Labelled Compd. Radiopharm. **24** (1987) 1029–1042.

[7.45] SCHLYER, D.J., PET tracers and radiochemistry, Ann. Acad. Med. Singapore **33** (2004) 146–154.

[7.46] KILBOURN, M.R., Fluorine-18 Labeling of Radiopharmaceuticals, National Academy of Science Nuclear Science Series NAS-NS-3203, National Academy Press, Washington, DC (1990) 1–149 and references therein.

[7.47] DING, Y.-S., SHIUE, C.-Y., FOWLER, J.S., WOLF, A.P., PLENEVAUX, A., No carrier added (NCA) aryl [^{18}F]fluorides via the nucleophilic aromatic substitution of electron-rich aromatic rings, J. Fluorine Chem. **48** (1990) 189–206.

[7.48] CASELLA, V., et al., Anhydrous ^{18}F labeled elemental fluorine for radiopharmaceutical preparation, J. Nucl. Med. **21** (1980) 750–757.

[7.49] SHIUE, C.-Y., SALVADORI, P.A., WOLF, A.P., FOWLER, J.S., MacGREGOR, R.R., A new improved synthesis of 2-deoxy-2-[^{18}F]fluoro-D-glucose from ^{18}F-labeled acetyl hypofluorite, J. Nucl. Med. **23** (1982) 899–903.

[7.50] SOOD, S., FIRNAU, G., GARNETT, E.S., Radiofluorination with xenon difluoride: A new high yield synthesis of [^{18}F]2-fluoro-2-deoxy-D-glucose, Int. J. Appl. Radiat. Isot. **34** (1983) 743–745.

[7.51] RUTH, T.J., TRIUMF, Vancouver, personal communication, 2005.

[7.52] FINN, R., Memorial Sloan–Kettering Cancer Center, New York, personal communication, 2006.

Chapter 8

FUTURE TRENDS

8.1. INTRODUCTION

Ever since the invention of the cyclotron by E. Lawrence, there has been steady progress on various fronts in this field. In this book, cyclotrons, their characteristics, and the theory and practice of producing radioisotopes with cyclotrons, have been reviewed. The important aspects of isotope production including targetry and irradiation of the targets for the most efficient production of isotopes have been discussed. Applications of the radioisotopes produced in a cyclotron are wide ranging, and are limited only by the imagination of the user. As a cyclotron facility embarks upon production of multiple radioisotopes and radiotracers, there is a need to understand the underlying principles so that it becomes possible to design new targets and develop new production and separation procedures that enhance the production of new radioisotopes. The availability of accelerators with ever increasing performance (beam current and energy), the increasing demand for widespread availability of valuable clinical pharmaceuticals, and the pronounced trend towards miniaturization of equipment and electronics, will undoubtedly affect the way in which radionuclides will be produced (automated or manually, on-site or centralized, by nuclide or nuclide generator, etc.).

8.2. TRANSLATIONAL SCIENCE

As in every field of science, radioisotope production is not a static endeavour. The advances in a number of areas will eventually have an impact on the design of accelerators, their targets, the processing of these targets and how the desired radioisotopes are utilized. While it is impossible to foretell future advances and directions of progress, there are a few areas that are likely to have an impact on the field of radioisotope production, either directly or indirectly. For example, the possibility of large scale production of radioisotopes from photons seemed very unlikely a decade ago, while now that possibility seems, at least at the proof-of-principle level, highly probable. Further developments will depend upon the ability to reduce the size of the lasers and increase the frequency of pulse delivery. If this approach proves practical then there will be a concomitant need for new approaches to targetry to take advantage of this technology.

The advances in nanotechnology will have an impact on the way in which radioisotopes will be incorporated into useful chemical entities such as biomarkers and radiotherapeutic agents. If the lab-on-a-chip approach becomes a reality for biomarker production, the miniaturization of the entire process will have a direct impact on how the radioisotopes are produced and delivered. This in turn affects the design of targets and their operation.

8.3. CENTRALIZED RADIOISOTOPE PRODUCTION

In many IAEA Member States, it is likely that there would be only a single or very few accelerator facilities. Considering the necessity of the extensive resources required for such a facility, establishment of a centralized radioisotope production facility fulfilling national needs may be an optimum choice for many Member States. This in turn implies that this facility must keep up with the current state of the art in radioisotope production and radiopharmaceutical development.

It should be understood that distribution of radioisotopes (or radiopharmaceuticals) from a national accelerator facility represents the best use of precious resources. Longer lived radioisotopes are relatively easier to transport to distant locations within a country. Radioisotopes with shorter half-lives present some logistical problems in distribution.

8.4. RADIOISOTOPES FOR GENERATOR PRODUCTION

The Mo/^{99m}Tc generator remains the dominant source for radionuclide incorporation applied to radiopharmaceutical kit formulation when considering clinical applications of radiopharmaceuticals. However, the increasing availability and use of PET radiopharmaceutical agents and the availability of multimodality imaging such as PET and computed tomography (CT) will ensure the continued radiopharmaceutical development of short lived positron-emitting diagnostic agents. Generator systems may offer a solution to centres where there are no readily available sources of short lived PET radioisotopes and for specific applications, including radiotherapy. A list of several accelerator produced generator systems that are currently in use and that may become more widely used in the future is presented in Table 8.1.

TABLE 8.1. EXAMPLES OF GENERATORS YIELDING POSITRON EMITTING DAUGHTER RADIONUCLIDES OF CLINICAL INTEREST

Parent (half-life)	Decay mode (%)	Daughter (half-life)	Decay mode (%)	Characteristic gamma energy (%)
Sr-82 (25 d)	EC (100)	Rb-82 (76 s)	β^+ (96), EC (4)	0.78 MeV (13.5)
Ge-68 (275 d)	EC (100)	Ga-68 (68 min)	β^+ (88), EC (12)	1.078 MeV (3.5)
Zn-62 (9.13 h)	β^+ (18), EC (82)	Cu-62 (9.8 min)	β^+ (98)	1.17 MeV (0.5)
Xe-122 (20.1 h)	EC (100)	I-122 (3.6 min)	β^+ (77), EC (23)	0.56 MeV (18.4)
Ac-225 (10 d)	α (100)	Bi-213 (45.6 min)	β (98) α (2)	0.440 MeV (28.0)
Rn-211 (14.7 h)	EC (74) α (26)	At-211 (7.2 h)	α (42) EC (58)	0.079 MeV (21.3)

In the future, these and other radioisotope generators may become a significant fraction of clinical PET studies and of therapeutic applications.

8.5. HUMAN RESOURCES AND TRAINING

The efficient utilization of an accelerator facility for manufacturing radioisotopes and radiopharmaceuticals requires availability of staff with a variety of qualifications. These qualifications include not only the formal education in a subject appropriate for a particular position, but also practical training directly related to that function.

The rapid growth in this field has resulted in a critical shortage of trained personnel at all levels for the safe and appropriate handling of radioactivity, including a generation gap in leadership. Most university based programmes in nuclear physics and radiochemistry around the world have been phased out. Thus, in most instances, facilities must resort to on-the-job training. Such training should be structured for the maximum benefit to both the trainee and the employer. This training must include experience in quality assurance and QC. Furthermore, an accelerator facility should ensure that its personnel receive continuing education to maintain and improve skills and knowledge as new technology becomes available.

The IAEA has a long record in fostering training in the production, handling and use of radionuclides. The present report will be used for this purpose either as a stand-alone document or in conjunction with a programme that involves scientists coming together to perform collaborative research. It may also be used in advancing a participant's ability to become more involved in independent research into the production and use of radioisotopes.

There will, however, continue to be a need for manuals in specific areas related to many of the topics discussed in this report. While it is self-contained, many of the topics assume a certain level of experience in the field of radioisotope production.

Areas not fully covered in this report that might be considered for further development include the processes whereby a radioisotope is converted into a more useful form, such as a radiotracer or radiopharmaceutical. In addition, while the production of generator radioisotopes has been discussed, their implementation into useful devices for biomedical research or clinical diagnostic utility has not. This area will surely be an important one to pursue, especially for regions not having direct access to an accelerator.

Although in writing this report an attempt has been made to be as comprehensive as reasonably possible, page limitations have imposed constraints. Finally, because of the organic nature of any scientific endeavour the field will continue to evolve, so that updates and revisions will become necessary over time.

8.6. GROWTH AND TRENDS

About 350 of the cyclotrons worldwide are at present involved in some aspect of radionuclide production. There has been approximately an 8% increase in the number of cyclotrons in operation since 2002. The increase has been in developed countries, but even more so in the developing world. Of any single country, the USA has the largest number of cyclotrons. However, taken collectively, the countries of the European Union have more cyclotrons that are used for medical radionuclide production.

The number of institutions that distribute some radiopharmaceuticals and [^{18}F]FDG, in particular, is significant and growing. In a sample of 261 centres taken by the IAEA, 75% of the cyclotrons are being used to produce FDG either for in-house use or for distribution. This is certainly an underestimate as commercial suppliers were under-represented in the survey.

The expansion in the number of cyclotrons during the last ten years has been driven by the advent of advances in medical imaging instrumentation (PET, SPECT and more recently PET/CT), introduction of user-friendly compact medical cyclotrons by several companies, and recent decisions that studies involving some PET radiopharmaceuticals are eligible for reimbursement by government or insurance companies.

There is no doubt that the fastest growing segment of the market is in the commercial distribution of [^{18}F]FDG to local hospitals. Many centres have begun distributing FDG, with at present at least 36% of those centres producing FDG also distributing it. Again, this is a lower limit rather than an accurate assessment.

Over the past few decades, PET studies with radiolabelled drugs have provided new information on drug uptake, distribution and kinetic relationships. The increasing amount of clinically relevant information being obtained with PET has generated a demand for new routes for the widespread and cost effective generation of biological radionuclides and their incorporation into appropriate radiopharmaceuticals.

The trend in the future will most probably follow two complementary directions. On the one hand, further growth of the number of radiopharmaceutical production centres and more widespread distribution of valuable clinical radiopharmaceuticals such as FDG, and, on the other hand, an increasing utilization of PET/CT as the imaging modality, are to be expected. The value of this combination cannot be overemphasized.

On the other hand, a number of radionuclides with nuclear properties satisfying the requirements for application in nuclear medicine are known; however, they are not yet commonly used. The diversity of physical, chemical and biochemical properties of these radionuclides justifies further exploration into this area in order to take advantage of the opportunities offered by such radionuclides. Certain applications, particularly those in oncology, require the tracer kinetics to be followed for periods exceeding the limits of conventional short lived PET radionuclides. This is often necessary for pharmacokinetic studies of radiolabelled anti-cancer drugs and other molecules, such as monoclonal antibodies, where the tissue uptake kinetics far exceeds the limits of short lived PET radionuclides.

The medium half-life PET radiotracers could be applied in the microdosimetry of therapeutic procedures based on radionuclides. Many therapeutic radionuclides are not convenient for SPECT or PET imaging; therefore, their in vivo biodistribution in patients, and consequently the patient specific microdosimetry, cannot be traced during the treatment procedure. Simultaneous administration of the same radiopharmaceutical labelled with a therapeutic radionuclide and its positron-emitting analogue will enable determination of the biodistribution of the therapeutic radionuclide in every patient, as well as calculation of the dose delivered to the tumour and the critical organs.

The high LET and short range of alpha particles allow for very high potency and specificity in alpha endoradiotherapy. The spectrum of malignant diseases that may be treated with alpha emitters includes most common cancers when single cells in circulation or small clusters of cells are the potential target.

With the increasing number of operational radiopharmaceutical production centres, the potential for the required R&D needed for the development of production technologies of these novel radionuclides and the corresponding labelling procedures is also growing. Thus, it is to be expected that the number of clinical applications of novel radionuclides and radiopharmaceuticals will dramatically increase in the near future.

Appendix I

PET CYCLOTRON COMPARISON

Feature	PETrace	MiniTrace	Eclipse HP	Eclipse RD	Cyclone 10/5	Cyclone 18/9	TR-14	TR-19/9	HM-18	HM-12
Manufacturer	GE Healthcare	GE Healthcare	Siemens	Siemens	Ion Beam Applications (IBA)	Ion Beam Applications (IBA)	Advanced Cyclotron Systems	Advanced Cyclotron Systems	Sumitomo Heavy Industries Ltd	Sumitomo Heavy Industries Ltd
Location of headquarters	London, UK	London, UK	Knoxville, TN, USA	Knoxville, TN, USA	Brussels, Belgium	Brussels, Belgium	Vancouver, Canada	Vancouver, Canada	Tokyo, Japan	Tokyo, Japan
Years in operation	24	24	25	25	22	22	15	15	18	18
Origin of technology	Scanditronix (MC-17)	PETrace	Berkeley (TCC)	Berkeley (TCC)	CRC (Louvain)	CRC (Louvain)	TRIUMF (Vancouver)	TRIUMF (Vancouver)	Sumitomo	Sumitomo
Factory location	Uppsala, Sweden	Uppsala, Sweden	Knoxville, TN, USA	Knoxville, TN, USA	Louvain-la-Neuve, Belgium	Louvain-la-Neuve, Belgium	Vancouver, Canada	Vancouver, Canada	Niihama, Japan	Niihama, Japan
Production	Internal	Internal	Internal	Internal	Internal	Internal	Internal	Internal	Internal	Internal
Quality assurance standard	ISO 9001	ISO 9001	ISO 9001:2000 and ISO 13485:2003	ISO 9001:2000 and ISO 13485:2003	ISO 9001	ISO 9001	ISO 9002	ISO 9002	ISO 9001	ISO 9001
Installed base as of 2008	>160	>60	65	93	22	110	3	13	>40	>40
Percentage of sites that meet specification	100	100	100	100	100	100	100	100	100	100
Beam:										
Proton	Yes	Yes	Yes	Yes	Yes	Yes	Yes	Yes	Yes	Yes
Deuteron	Yes	No	No	No	Yes	Yes	No	Yes	Yes	Yes
Proton (MeV)	16.5	9.6	11	11	10	18	14	19.0	18	12
Deuteron (MeV)	8.4	–	–	–	5.0	9.0	–	9.0	10	6
Variable energy extraction	No	No	No	No	No	No	Yes, from 11 to 14	Yes, from 14 to 19.0	No	No

Feature	PETrace	MiniTrace	Eclipse HP	Eclipse RD	Cyclone 10/5	Cyclone 18/9	TR-14	TR-19/9	HM-18	HM-12
Variable current extraction	Yes	Yes	Yes	Yes	Yes, from 1:1 to 1:100	Yes, from 1:1 to 1:100	Yes, from 1:1 to 1: 100	Yes, from 1:1 to 1:100	Yes	Yes
Extracted proton current (μA)	>100	>50	120	80	100	150	>100	>300	>100 >150 (option)	>100 >200 (option)
Extracted deuteron current (μA)	60	–	No	No	50	60	–	>75	40	40
Targets:										
Number of targets	6 (2 × 3)	6 (1 + 5)	8 (2 × 4)	14 (2 × 7)	4 or 8	8	8 (2 × 4)	8 (2 × 4)	8 (2 × 4)	8 (2 × 4)
Position of targets	Together on one side of cyclotron	Together on one side of cyclotron	Dual ports, 180° apart	Dual ports, 180° apart	Evenly spaced inside magnet yoke	Evenly spaced inside magnet yoke	Two ports, four targets	Two ports, four targets	Two ports, four targets	Two ports, four targets
Dual simultaneous irradiation	Yes, targets must be three positions apart	Yes	Yes (right and left hand sides)	Yes (right and left hand sides)	Yes, on opposite targets	Yes, on opposite targets	Yes (right and left hand sides)	Yes (right and left hand sides)	Yes	Yes
Stable beam, dual irradiation	Yes	Yes	Yes	Yes	Yes	Yes	Yes	Yes	Yes	Yes
Number of targets, combed dual irradiation	6	5	16	49	6	6	16	16	16	16
Can target be steered to beam?	Can optimize beam on target by moving beam	Can optimize beam on target by moving beam	Extractor foil rotation for lateral position	Extractor foil rotation for lateral position	Optimize beam by moving stripper foil position	Optimize beam by moving stripper foil position	Yes, both stripper foil positioning and steering target to the beam	Yes, both stripper foil positioning and steering target to the beam	Yes	Yes
Complexity of target system	Low	Low	Medium	Medium	Low	Low	Medium	Medium	Low	Low
Open tank to service target	No	No	No	No	Yes	No	No	No	No	No

Feature	PETrace	MiniTrace	Eclipse HP	Eclipse RD	Cyclone 10/5	Cyclone 18/9	TR-14	TR-19/9	HM-18	HM-12
Time to change target foil and run (min)	~10	~10	~10	~10	~60	~5	~10	~10	~10	~10
Ion source (IS):										
IS type	Internal	Internal	Internal	Internal	Internal, dual	Internal, dual	External	External	Internal	Internal
Source type	Cold cathode, Penning ion gauge	Cold cathode, Penning ion gauge	Cold cathode, Penning ion gauge	Cold cathode, Penning ion gauge	Cold cathode, Penning ion gauge	Cold cathode, Penning ion gauge	Multi-cusp	Multi-cusp	Cold cathode PIG	Cold cathode PIG
IS technology	Scanditronix, 1975	Scanditronix, 1975	Berkeley, 1960	Berkeley, 1960	IBA redesign	IBA redesign	TRIUMF, 1985	TRIUMF, 1985	Sumitomo	Sumitomo
Open tank to service IS	Yes	Yes	Yes	Yes	Yes	Yes	No	No	Yes	Yes
Downtime to service IS	<1 h	<1 h	<1 h	<1 h	<1 h	<1 h	~10 min	~10 min	<1 h	<1 h
Gas load to vacuum tank	Yes	Yes	Yes	Yes	Yes	Yes	No	No	Yes	Yes
Vacuum system:										
Vacuum pumps	One mechanical, one oil diffusion (2600 L/s)	One mechanical, one oil diffusion (2600 L/s)	One mechanical, three oil diffusion (1200 L/s)	One mechanical, three oil diffusion (1200 L/s)	One mechanical, one oil diffusion	One mechanical, four oil diffusion (2500 L/s)	One turbopump, two cryopumps (4000 L/s)	One turbopump, two cryopumps (4000 L/s)	One mechanical, two oil diffusion (6000 L/s)	One mechanical, two oil diffusion (6000 L/s)
Oil in vacuum tank	Limited amount	Limited amount	Limited amount	Limited amount	Limited amount, uses water baffles	Limited amount, uses water baffles	No	No	Limited amount	Limited amount
Operating vacuum (Pa)	5×10^{-6}	5×10^{-6}	1×10^{-5}	1×10^{-5}	3×10^{-6}	3×10^{-6}	2×10^{-7}	2×10^{-7}	1×10^{-5}	1×10^{-5}
Target lock	Yes	Yes	Yes	Yes	Yes	Yes	Yes	Yes	Yes	Yes
Clean vacuum	Yes	Yes	Yes	Yes	Yes	Yes	Yes	Yes	Yes	Yes

Feature	PETrace	MiniTrace	Eclipse HP	Eclipse RD	Cyclone 10/5	Cyclone 18/9	TR-14	TR-19/9	HM-18	HM-12
Main magnet:										
Pole diameter (m)	0.83	0.7	0.9	0.9	0.76	1.08	1.1	1.1	1.08	0.8
Extraction radius (m)	0.42	0.34	0.43	0.43	0.35	0.48	0.4	0.5	0.46	0.33
Number of sectors	3	4	4	4	4	4	4	4	4	4
Symmetric	No		Yes	Yes	Yes	Yes	Yes	Yes	No	No
Shimming	No	No	Trim bars	Trim bars	Edges ground	Edges ground	Hill-edge mounted shims	Hill-edge mounted shims	No	No
Hill field (T)	1.9	2.2	1.9	1.9	1.9	1.9	2.1	2.1	2.0	2.0
Valley field (T)	1.7	0.9	0.14	0.14	0.4	0.35	0.5	0.5	0.5	0.4
Mean field (T)	1.8	1.66	1.2	1.2	1.35	1.3	1.3	1.3	1.46	1.5
Hill:valley ratio	~1	~2	~13	~13	~5	~5	~4	~4	~4	~5
Iron saturation at centre	No	No	Yes	Yes	No	No	No	No	No	No
Ampere turns/ coil	>80 000	75 000	39 000	39 000	112 000	112 000	84 000	84 000	97 200	100 000
Power (kW)	20	10.8	3	3	17	15	22	22	16	16
Coil type	Hollow core, copper	Hollow core, copper	Strip wound, copper	Strip wound, copper	Strip wound, copper	Hollow core, copper	Hollow core, copper	Hollow core, copper	Hollow core, copper	Hollow core, copper
Heat transfer	Direct cooling	Direct cooling	Conduction	Conduction	Conduction	Conduction	Direct cooling	Direct cooling	Direct cooling	Direct cooling
RF system:										
Number of dees	2	2	4	4	2	2	2	2	2	2
Dee angle (°)	75	34	30	30	30	30	44	44	45	45

Feature	PETrace	MiniTrace	Eclipse HP	Eclipse RD	Cyclone 10/5	Cyclone 18/9	TR-14	TR-19/9	HM-18	HM-12
Harmonic mode proton	First	Fourth	Fourth	Fourth	Second	Second	Fourth	Fourth	Second	Second
Frequency (MHz) (proton)	27.2	101	72	72	42	42	74	74	45	45
Harmonic mode deuteron	First	n.a.	n.a.	n.a.	Fourth	Fourth	n.a.	Fourth	Fourth	Fourth
Frequency (MHz) (deuteron)	27.8	n.a.	n.a.	n.a.	42	42	n.a.	37	45	45
Dee voltage (kV)	35	35	37	37	35	38	50	50	30	30
RF power (kW)	13	9	10	10	9	8	~10	~10	15	15
RF stability	Good	Good	Good	Good	Good	Good	Good	Good	Good	Good
Solid dees	Yes	Yes	Yes	Yes	Yes	Yes	Yes	Yes	Yes	Yes
Dee cooling	Direct cooling	Direct cooling	Sector conductively cooled to a squirt tube dee stem	Sector conductively cooled to a squirt tube dee stem	Conduction to the stem tube	Conduction to the stem tube	Direct cooling	Direct cooling	Direct cooling	Direct cooling
RF coupling	Inductive, by coaxial cable	Inductive, by coaxial cable	Inductive, by coaxial cable	Inductive, by coaxial cable	Inductive, by coaxial cable	Inductive, by coaxial cable	Capacitive, 1.625 in. (41 mm) rigid coaxial line	Capacitive, 1.625 in. (41 mm) rigid coaxial line	Capacitive, direct	Inductive, direct
RF matching	Fixed (by coaxial cable)	Fixed (by coaxial cable)	Frequency adjustment	Frequency adjustment	Automatic, variable capacitor	Automatic, variable capacitor	Automatic, closed frequency loop	Automatic, closed frequency loop	Fixed	Fixed
Driving system	Crystal	Crystal	Synthesizer	Synthesizer	Synthesizer	Synthesizer	Synthesizer	Synthesizer	Crystal	Crystal

Feature	PETrace	MiniTrace	Eclipse HP	Eclipse RD	Cyclone 10/5	Cyclone 18/9	TR-14	TR-19/9	HM-18	HM-12
Amplifier location	Away from cyclotron, no radiation hazard	Away from cyclotron, no radiation hazard	Away from cyclotron, no radiation hazard	Away from cyclotron, no radiation hazard	Away from cyclotron, no radiation hazard	Away from cyclotron, no radiation hazard	Away from cyclotron, no radiation hazard	Away from cyclotron, no radiation hazard	On cyclotron	Away from cyclotron
RF technology	Scanditronix, 1990	GE, 1995	TCC, 2005	TCC, 2005	IBA, 2000	IBA, 2000	TRIUMF, 1985	TRIUMF, 1985	Sumitomo	Sumitomo
Yield:										
Carbon-11 (CO_2) (1 Ci = 37 GBq)	30 min, 4500 mCi	30 min, 900 mCi	50 min, 2000 mCi	50 min, 1500 mCi	30 min, 1250 mCi	30 min, 3000 mCi	30 min, 3000 mCi	30 min, 4000 mCi	40 min, 2800 mCi	40 min, 2600 mCi
Carbon-11 (CH_4)	30 min, 1300 mCi	–	–	–	–	25 min, 1200 mCi	30 min, 1200 mCi	30 min, 1200 mCi		
Nitrogen-13 (NH_3)	30 min, 450 mCi	25 min, 75 mCi	10 min, 200 mCi (in target production)	10 min, 100 mCi (in target production)	15 min, 150 mCi (in target production)	15 min, 500 mCi (in target production)	30 min, 500 mCi	30 min, 1500 mCi	30 min, 240 mCi	30 min, 125 mCi
Oxygen-15 (O_2)	6 min, 2000 mCi	10 min, 1000 mCi	10 min, 3000 mCi	10 min, 2000 mCi	2 min, 500 mCi	2 min, 1000 mCi	6 min, 1000 mCi	6 min, 2000 mCi	Continuous, 360 mCi	Continuous, 100 mCi
Fluorine-18 (F_2)			60 min, 750 mCi	60 min, 500 mCi	60 min, 600 mCi	60 min, 1500 mCi 60 min (d), 300 mCi	60 min 1800 mCi	60 min, 1800 mCi 60 min (d), 300 mCi		
Fluorine-18 (F^-), single target	120 min, 6500 mCi	60 min, 1500 mCi	120 min, 3500 mCi	120 min, 2400 mCi	60 min, 1600 mCi	60 min, 7500 mCi	60 min, 3250 mCi	60 min, 9000 mCi	60 min, 7700 mCi	60 min, 6600 mCi
F-18 target type	Niobium	Silver	Tantalum or silver	Silver	Niobium	Niobium	Niobium	Niobium	Niobium	Niobium
Max. beam on F-18 target (μA)	65	50	60	40	50	110	100	150	150	200
Decay corrected yield of FDG (%)	81	81	>65	>65	70	70	65	65	60	60

Feature	PETrace	MiniTrace	Eclipse HP	Eclipse RD	Cyclone 10/5	Cyclone 18/9	TR-14	TR-19/9	HM-18	HM-12
End of synthesis FDG yield (based on 60 min beam, single target) (mCi)	4550	1050	1100	650	1050	4850	1650	4500	4620	3960
Site requirements:										
Dee orientation	Vertical	Vertical	Horizontal	Horizontal	Horizontal	Horizontal	Vertical	Vertical	Horizontal	Vertical
Weight without shield (kg)	22 000	9100	11 000	11 000	12 000	23 000	22 000	22 000	24 000	11 000
Self-shielding option	Yes	Yes, integrated	Yes	Yes	Yes, but vault recommended	Yes, but vault recommended	Yes	Yes	Yes	Yes
Self-shielding material	Boronated water	Composite	Composite	Composite	Concrete	Concrete	Composite	Composite	Composite	Composite
Weight of self-shielding (kg)	47 000	40 000	39 000	39 000	~40 000	-	40 000	40 000	86 000	56 000
Radiation field at 1 m (μSv/h)	10	10	~20	~20	~5	~5	~40	~40	~50	~50
Power requirement	70 kW at 208–480 V	35 kW at 208–480 V	35 kW at 208–480 V	35 kW at 208–480 V	35 kW at 330–480 V	55 kW at 208–330–480 V	60 kW at 208–480 V	65 kW at 208–480 V	55 kW at 200 V	45 kW at 200 V
Acceleration plane	Vertical	Vertical	Horizontal	Horizontal	Horizontal	Horizontal	Vertical	Vertical	Horizontal	Vertical
Computer control system	PC	PC	PC	PC	Step 7 PLC	Step 7 PLC	PC	PC	PC	PC
Computer platform	Linux	Linux	PC Windows XP	PC Windows XP	PC Windows XP	PC Windows XP	PC Windows XP	PC Windows XP	Windows XP	Windows XP
Serviceability	Excellent	Excellent	Excellent	Excellent	Good	Good	Good	Good	Excellent	Excellent
Fault diagnostics	Extensive	Extensive	Extensive	Extensive	Extensive	Extensive	Extensive	Extensive	Extensive	Extensive
Software	.Strong	Strong	Strong	Strong	Strong	Strong	Strong	Strong	Strong	Strong

Appendix II

HIGH ENERGY CYCLOTRON COMPARISON

Feature	Cyclone 30	Cyclone 70	TR-24	TR-30/15
Manufacturer	IBA	IBA	ACS	ACS
Headquarters location	Louvain-la-Neuve, Belgium	Louvain-la-Neuve, Belgium	Richmond, Canada	Richmond, Canada
Origin of technology	University of Louvain	IBA	TRIUMF 1985	TRIUMF 1985
Factory location	Louvain-la-Neuve, Belgium	Louvain-la-Neuve, Belgium	Richmond, Canada	Richmond, Canada
Production	Louvain-la-Neuve, Belgium	Louvain-la-Neuve, Belgium		
Quality assurance standard	ISO 9001	ISO 9001	ISO manufacturing	ISO manufacturing
Installed base as of 2008	23	1	2 pending	5
Percentage of sites that meet specification	100	In development	100	100
Beam:				
Proton	400–750–1200 µA model	Proton 70 MeV	>300 µA	>1000 µA
Deuteron	Option	Yes	n.a.	100 µA
Proton energy (MeV)	15–30	25–70	15–24	15–30
Deuteron energy (MeV)	9–15	15–35	–	7.5–15
Variable energy extraction	Yes	Yes	15–24 MeV	15–30 MeV
Variable current extraction	Yes	Yes	Split ratio 1:100	Split ratio 1:100
Extracted proton current (µA)	400–750–1200 model	350–750 proton	300	>1000
Extracted deuteron current	Option	Yes	–	100
Number of targets	Up to ten per cyclotron		More than eight per cyclotron, configuration dependent	Up to ten per cyclotron
	Up to six beamlines	Up to six beamlines	Up to six beamlines	Up to six beamlines

Feature	Cyclone 30	Cyclone 70	TR-24	TR-30/15
Position of targets	In target bunker	In target bunker	At end of beamline or on target selector	At end of beamline
	SPECT target 250–600 μA	SPECT target 250–600 μA		
	Gas target 100 μA	Gas target 100 μA		
Dual simultaneous irradiation	Yes, standard	Yes, standard	Yes	Yes
Stable beam dual irradiation	Yes, regulated	Yes, regulated	Yes	Yes
Target selector	Switching magnet	Switching magnet	Switching magnet or gimballed selector	Switching magnet
Number of targets, combed dual irradiation	Dependent on configuration	Dependent on configuration	Dependent on configuration	Dependent on configuration
Can target be steered to beam?	Yes	Yes	Yes	Yes
Complexity of target system	Low	Low	Medium or high, depending on target type	High
Open tank to service target	No	No	No	No
Time to service targets	Reduced	Reduced	Automatic insertions and retraction All external target stations	Automatic insertions and retraction All external target stations
Vacuum system:				
Vacuum pumps	Two to four cryopumps	Four cryopumps	One turbomolecularpump, two cryopumps (4000 L/s)	Two cryopumps, two turbomolecular pumps
Oil in vacuum tank	No	No	No	No

Feature	Cyclone 30	Cyclone 70	TR-24	TR-30/15
Operating vacuum (1 torr = 1333.32 Pa)	10^{-7}	10^{-7}	2×10^{-7}	2×10^{-7}
Ion source lock	Yes	Yes	Yes	Yes
Target lock	Yes	Yes	Targets on separate beamline	Targets on separate beamline
Clean vacuum	Yes	Yes	Yes	Yes
Ion source				
Ion source type	Multicusp external	Multicusp external and ECR (alpha)	External	External
Source type	Filament	Filament	Multicusp	Multicusp
Ion source technology	Culham	Culham	TRIUMF 1985, plus continuous development programme	TRIUMF 1985, plus continuous development programme
Open tank to service ion source	No	No	No	No
Main magnet:				
Pole diameter (m)	1.6	2.48	1.1	1.5
Extraction radius (m)	0.5–0.75		0.5	0.66
Number of sectors	4	4	4	4
Symmetric	Yes	Yes	Yes	Yes
Shimming	Edges ground	Edges ground	Hill-edge mounted shims	Hill-edge mounted shims
Hill field (T)	1.7	1.7	2.1	1.9
Valley field (T)	0.12	0.12	0.55	0.55
Mean field (T)	1	1	1.3	1.2

Feature	Cyclone 30	Cyclone 70	TR-24	TR-30/15
Hill:valley ratio	14	14	~4	3.8
Iron saturation at centre	No		No	No
Ampere-turns	60 000	62 000	72 000	72 000
Power (kW)	7.2	60	32	36
Weight (kg)	45 000	120 000	84 000	56 000
Coil type	Hollow copper core	Hollow copper core	Hollow copper core	Hollow copper core
Heat transfer	Direct cooling	Direct cooling	Direct cooling	Direct cooling
RF system:				
Number of dees	2	2	2	2
Dee angle (°)	30	30	40	44
Harmonic mode (proton)	Fourth	Second	Fourth	Fourth
Frequency (MHz) (proton)	66	30	83.5	74
Harmonic mode (deuteron)	4	4	–	4
Frequency (MHz) (deuteron)	Option	30	–	37
Dee voltage (kV)	50	65	50	50
RF power (kW)	40–100 max.	120	25	24–100
RF stability	Excellent	Excellent	Excellent	Excellent
Solid dees	Yes	Yes	Yes	Yes
Dee cooling	Conduction	Direct cooling	Direct cooling	Direct cooling

Feature	Cyclone 30	Cyclone 70	TR-24	TR-30/15
RF coupling	Direct resonant	Inductive	Capacitive	Capacitive
Transmission line	No	Yes, short	1.625 in. (41 mm) rigid coaxial line	6.125 in. (156 mm) rigid coaxial line
RF matching	Variable capacitor	Variable capacitor	Automatic, closed frequency loop	Automatic, closed frequency loop
Driving system	PLL synthesizer	PLL synthesizer	Synthesizer	Synthesizer
Amplifier location	Coupled to cyclotron	Away from cyclotron, no radiation hazard	Away from cyclotron, no radiation hazard	Away from cyclotron, no radiation hazard
RF technology	IBA, resonant cavity design	IBA, resonant cavity design	TRIUMF 1985, plus continuous development programme	TRIUMF 1985, plus continuous development programme
Site requirements:				
Dee			n.a.	n.a.
Orientation	Horizontal	Horizontal	Vertical or horizontal acceleration plane	Horizontal
Radiation field	Bunker shield	Bunker shield	n.a.	n.a.
Power requirements (kW)	100–180	350	80	80–150
Acceleration plane	Horizontal	Horizontal	Horizontal or vertical	Horizontal
Computer control system	Siemens PLC	Siemens PLC		
Computer platform	Windows NT	Windows NT	PC and Allen-Bradley plc	PC and Allen-Bradley plc
Serviceability	Good	Good	Good	Good
Fault diagnostics	Excellent	Excellent	Extensive	Extensive
Software	Strong	Strong	MS-XP and AB PLC programming	MS-XP and AB PLC programming

ANNEXES ON THE ATTACHED CD-ROM[1]

ANNEX I: Detailed calculation of beam heating effects on thallium target

ANNEX II: Optimization of production yields, radionuclidic purity and hot cell shielding of the ^{67}Ga SPECT radionuclide produced by proton irradiation in 30 MeV cyclotrons

ANNEX III: Excel worksheet for calculation of production yields for ^{67}Ga, ^{111}In, ^{201}Pb(^{201}Tl) and ^{18}F radionuclides by (p, xn) reactions, dose rates and lead shielding of hot cells

---

[1] The contents of this CD-ROM have not been edited by the IAEA.

CONTRIBUTORS TO DRAFTING AND REVIEW

DRAFTING

Haji-Saeid, M.	International Atomic Energy Agency
Pillai, M.R.A.	International Atomic Energy Agency
Ruth, T.J.	TRIUMF, Canada
Schlyer, D.J.	Brookhaven National Laboratory, United States of America
Van Den Winkel, P.	Cyclotron Laboratory, Vrije Universiteit Brussel (VUB), Belgium
Vora, M.M.	King Faisal Specialist Hospital and Research Centre, Saudi Arabia

REVIEW

Carroll, L.	Carroll and Ramsey Associates, United States of America
Clark, J.C.	Wolfson Brain Imaging Centre, United Kingdom
Čomor, J.	Vinča Institute of Nuclear Sciences, Serbia
Dehnel, M.	D-Pace, Canada
Ferrieri, R.	Brookhaven National Laboratory, United States of America
Finn, R.D.	Memorial Sloan-Kettering Cancer Center, United States of America
Fowler, J.S.	Brookhaven National Laboratory, United States of America
Schueller, M.J.	Brookhaven National Laboratory, United States of America

IAEA
International Atomic Energy Agency

RELATED PUBLICATIONS

DIRECTORY OF CYCLOTRONS USED FOR RADIONUCLIDE PRODUCTION IN MEMBER STATES

2006 Update

IAEA-DCRP/CD/2006 (2006)
ISBN 92–0–111506–7 Price: €15.00

STANDARDIZED HIGH CURRENT SOLID TARGETS FOR CYCLOTRON PRODUCTION OF DIAGNOSTIC AND THERAPEUTIC RADIONUCLIDES

Technical Reports Series No. 432

STI/DOC/010/432 (71 pp.; 2004)
ISBN 92–0–109304–7 Price: €40.00

MANUAL FOR REACTOR PRODUCED RADIOISOTOPES

IAEA TECDOC Series No. 1340

IAEA-TECDOC-1340 (2003)
ISBN 92–0–101103–2 Price: €15.00

RADIOTRACER APPLICATIONS IN INDUSTRY – A GUIDEBOOK

Technical Reports Series No. 423

STI/DOC/010/423 (281 pp.; 2004)
ISBN 92–0–114503–9 Price: €45.00

www.iaea.org/books

This book provides a comprehensive treatment of cyclotrons, with a special emphasis on production of radionuclides. Individual sections are devoted to accelerator technology, theoretical aspects of nuclear reactions, the technology behind targetry, techniques for preparation of targets, irradiation of targets under high beam currents, target processing and target recovery. This book will appeal to scientists and technologists interested in translating cyclotron technology into practice, as well as postgraduate students in this field.

INTERNATIONAL ATOMIC ENERGY AGENCY
VIENNA
ISBN 978–92–0–100208–2
ISSN 0074–1914